

North Sea Energy 2023-2025

Storylines and blueprints for the integration of three NSE hubs in the future energy system of The Netherlands and the North Sea



North Sea Energy 2023-2025

Storylines and blueprints for the integration of three NSE hubs in the future energy system of The Netherlands and the North Sea.

Prepared by:

TNO

Remco Groenenberg
Javier Fatou Gomez
Femke Janssen
Hamid Yousefi
Gopalan Jayashankar

Alejandro Martín Gil
Aravind Satish
Iratxe González-Aparicio
Harmen Slot
Martin Wevers

Raja Aitazaz
Bart Klootwijk
Jim Rojer
Edwin Bot

Checked by:

New Energy Coalition
Rob van Zoelen

Approved by:

TNO
Madelaine Halter

Table of Contents

Executive summary	3
1. Introduction and research questions	12
2. North Sea Energy hubs	16
2.1 Storylines for development towards 2050	18
2.2 Hub designs	25
2.3 Transport infrastructure scenarios	42
2.4 Hydrogen storage	50
3. Methodology and assumptions	56
3.1 Modelling tools	56
3.2 Modelling assumptions	58
4. Results	63
4.1 Storylines for offshore wind and hydrogen (reference scenarios)	64
4.2 Influence of wake losses on wind farm production (for year 2015)	74
4.3 Grid-connected vs. not grid-connected H ₂ production in Hub North	76
4.4 Offshore solar inclusion	79
4.5 Hydrogen transport scenarios: re-use versus new infrastructure	81
4.6 Hydrogen transport to shore without offshore compression	86
4.7 Influence of offshore hydrogen storage in the NAT re-use storyline	89
4.8 Offshore hydrogen storage: notional designs and cost analysis	97
5. Discussion	109
6. Conclusions and recommendations	114
6.1 Conclusions	114
6.2 Recommendations for future work	118
7. References	120
Appendix A Configuration of the MESIDO framework for the simulations	125
Appendix B Validation of the MESIDO framework for high-pressure H ₂ transport using AURORA	128

Executive summary

Introduction

The aim of the North Sea Energy (NSE) program is to identify and assess opportunities for synergies between low-carbon energy developments offshore (wind energy production, hydrogen production, CCS, and hydrocarbon production) that have the potential to reduce societal cost and help to optimize their spatial integration whilst preserving existing ecological values. Energy hubs are defined by the NSE consortium as areas for offshore energy systems where production, conversion and/or storage of energy commodities (electricity, natural gas, hydrogen) and CO₂ are co-located.

In the previous phase of NSE (NSE 4), three hubs were defined (Hub West, Hub East and Hub North). For each hub, multiple storylines and associated designs were presented, providing detailed insights into techno-economic aspects associated with low-carbon energy developments, while legal, safety, and ecological challenges associated with their spatial integration were highlighted. However, while spatially-explicit, and rooted as best as possible in state-of-art ambitions pertaining to infrastructure development, the storylines and designs are “end-state” visions. In practice, while developing energy hubs, multiple challenges related to the simultaneous deployment and spatial integration of various (future) co-existing use functions must be resolved in time and at the right moment, ranging from technology development and upscaling to regulatory frameworks, and from preserving ecological value to economic viability. It therefore becomes important to define spatial explicit development pathways in time for energy hubs that highlight potential synergies and (spatial) conflicts between use functions, quantify their contribution to meeting the societal needs for the 4 commodities (electricity, hydrogen, natural gas, CO₂), and assess the requirements for infrastructure to transport the commodities to (and from, in the case of CO₂) shore.

Objectives and research questions

The ambition of work package 1 (WP1) of NSE 5 was to refine these “end-state” visions from NSE 4 into incremental 10-year development plans (2025-2035, 2035-2045, and 2045-2050+) for the three offshore energy hubs and their associated transport infrastructure connecting the hubs to shore, and to present them in the form of spatially-explicit blueprints. To guide the work towards realizing this ambition, the following research questions were formulated for this work stream:

- What areas in the hubs are (foreseen to be) developed for wind power, natural gas, hydrogen production and storage and CO₂ storage in the period between 2030-2050, and when?
- How does the limited space in areas to be developed for offshore wind and hydrogen affect the capacities, spatial configuration and energy production of the hubs? How can the hubs be developed in a way that maintains (if not strengthens) the ecological carrying capacity of the North Sea?
- What is the contribution of the hubs towards meeting the demand for electricity, hydrogen, natural gas and CO₂ storage in 2050?
- How do different operational strategies affect the utilization and need for flexibility of the offshore hydrogen production and transport infrastructure to absorb part of the wind power intermittency?

- What is the influence of adding offshore solar on the variability of the electricity production of wind farms?
- How could the infrastructure for transporting electricity and hydrogen from the hubs to shore develop in time, and what role could existing (re-used) pipelines play?
- What is the potential role of offshore hydrogen storage in providing flexibility to maintain a stable and predictable hydrogen supply to shore?

Approach and scope

Two types of research activities were defined to answer these research questions. The first one focused on refining the visions of the three energy hubs from NSE 4 into spatially-explicit blueprints that highlight which activities are to be developed when in time and at which location in the hubs. The blueprints include the locations and capacities of wind farms, electrolysers, and platforms for natural gas production, CO₂ storage and H₂ storage as well as the connecting infrastructure. The second activity focused on the simulation of commodity flows between the hubs (according to their blueprint designs) using digital models, to provide answers to the research questions, regarding energy production, conversion, transport and storage, infrastructure requirements and other constraints when dealing with intermittent supply and demand.

The definition of the spatially-explicit blueprints (designs) required an extensive state-of-the-art study, including looking at previous iterations of the NSE program, studies of other initiatives, such as TYNDP¹, I13050² and NSWPH³, keeping track of progress in spatial planning processes (PH-PNZ⁴, PAWOZ⁵, VAWOZ⁶) for offshore wind energy and hydrogen production, and the required infrastructure. At several moments during the study, partners in the consortium were consulted for guidance. Additionally, the blueprints were developed in close collaboration with the Ecology workstream of NSE5 (nature-inclusive design). Two storylines were defined (named “NSE5-NAT” and “NSE5-DEC”), that are rooted in the I13050 scenarios “National Leadership” (NAT) and “Decentralized Initiatives” (DEC). In NSE-NAT, the North Sea plays a key role in supplying The Netherlands with electricity and hydrogen to reach climate goals, while in NSE-DEC it plays a modest role mainly focused on supplying clean electricity. In addition, a 3-step analysis regarding offshore hydrogen storage was conducted (a screening study to identify potential locations, a notional design study and cost analysis).

For the modelling of the 3 energy hubs, one-year simulations with hourly time steps were performed for the year 2015, considered a higher-than-average wind power production year. Several digital tools were used, described in the Methodology section of this report (Chapter 3). The system was analysed using the MESIDO framework, modelling the geo-spatially explicit components at the individual wind farm, electrolyzer module, transmission cable and hydrogen pipeline levels. The wind supply profiles for the meteorological year 2015 were obtained using a reduced order model fitted in computational fluid dynamics simulations using Farmflow, the hydrogen production used a linearized version of a PyDOLPHYN output

1 Ten-Year Network Development Plan of the European grid operators for electricity and gas (ENTSOG, ENTSO-E, 2022)

2 “Integrale Infrastructuurverkenning 2030-2050” of the Dutch transmission and distribution grid operators (Netbeheer Nederland, 2023)

3 North Sea Wind Power Hub consortium (North Sea Wind Power Hub Programme, 2024)

4 “Partiële Herziening Programma Noordzee 2022-2027” (Ministerie van Infrastructuur en Waterstaat, 2025)

5 “Programma Aansluiting Wind op Zee” (Ministerie van Klimaat en Groene Groei, 2025)

6 “Programma Verbindingen Aanlanding Wind op Zee 2031-2040” (Arcadis, BRO, Delft, & Pondera, 2024)

and the hydrogen transport losses were validated using Aurora. Simulations used power and hydrogen demand profiles from energy system modelling performed in work package 3 of NSE5 (Blom, van Stralen, Eblé, Magan, & Hers, 2025). The system was composed of the three offshore hubs, with additional hydrogen production coming from AquaDuctus imports and out-of-hubs production close to Hub North. Onshore spatially-explicit conditions and other international components were out of scope.

Key findings

We developed designs for the three NSE hubs (Hub West, Hub East and Hub North) and present them as spatial explicit blueprints that show how infrastructure for production, transport and storage of the 4 commodities (electricity, hydrogen, natural gas, and carbon dioxide) could develop in three phases until 2050 (see Figure ES.1). Hub designs have been made for 2 scenarios (NSE5-NAT, NSE5-DEC) that differ in the level of utilization of the Dutch North Sea for producing renewable and low-carbon energy. The two scenarios, and the associated narratives for the phased development of the hubs, which we call “storylines”, can be seen as visions of how the future Dutch energy system, and the role of the hubs in that system, could evolve.

What areas in the hubs are (foreseen to be) developed for wind power, natural gas, hydrogen production and storage and CO₂ storage in the period between 2030-2050 (see Figure ES.1)?

- Our expectation is that **Hub West and Hub East will be fully electrical hubs**, because most of the planned wind farms will be operational well before 2035. GW-scale electrolysis offshore will not mature fast enough to enable investment decisions to be made for installation in the early 2030s, and therefore no hydrogen production is included in the designs of these hubs.
- In contrast, **in our Hub North designs significant hydrogen production capacity is included**, because a) its distance to shore makes transport in the form of molecules more cost-efficient, b) post-2035 the onshore grid and onshore demand will increasingly face difficulty in absorbing all electricity as electricity, and to reduce large-scale curtailment of electricity, conversion to hydrogen could be attractive. Production capacities reach 19.1 GW in NSE5-NAT in 2050 (10 GW in Hub North) and 7.5 GW in NSE5-DEC.
- **Hydrocarbon production will remain relevant until (at least) the period 2045-2050**, with a total potential of $\approx 127 \text{ bcm}^7$ (EBN forecast), of which 60% would come from the 3 hubs (mainly Hub West).

⁷ In the “Sectorakkoord gaswinning in de energietransitie” that was published in April 2025 (Ministerie van Klimaat en Groene Groei, Element NL, and EBN, 2025) the offshore potential is estimated at $\approx 150 \text{ bcm}$.

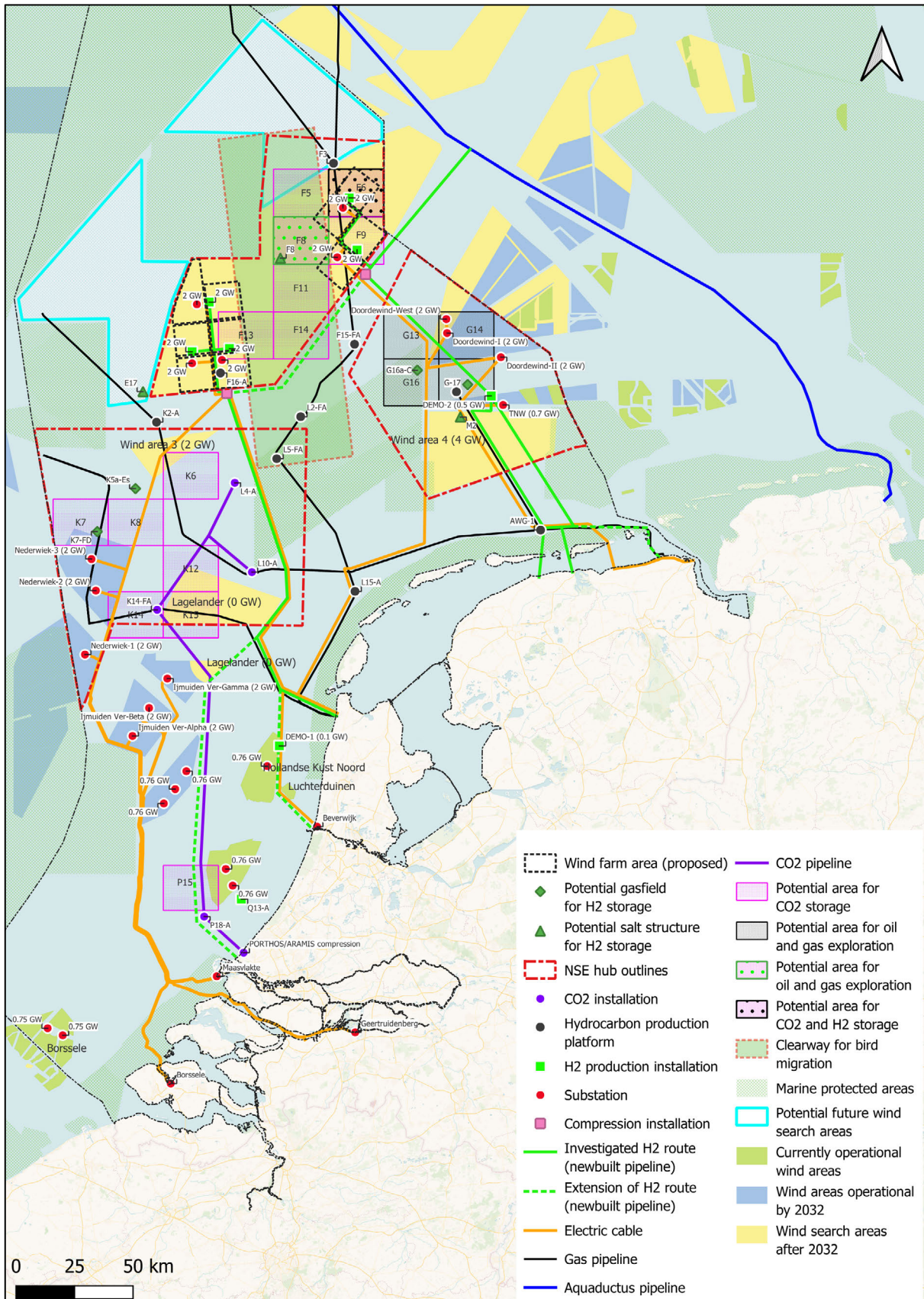


Figure ES.1: Vision of the North Sea in 2050 with blueprints of the 3 NSE hubs according to the ambitious NSE5-NAT scenario with 70 GW offshore wind and 19.1 GW offshore hydrogen production, and transport infrastructure of electricity and hydrogen (all new built).

- **CO₂ storage is expected to reach 22 Mt/yr before 2040 in Hub West**, with potential to increase further towards 40 Mt/yr afterwards by utilizing additional gas fields (Hub West) and/or aquifers for CO₂ storage (Hub North).
- **The ambition of the Dutch government to realize 70 GW of offshore wind by 2050 is becoming more and more challenging.** In our NSE5-NAT storyline meeting this ambition, offshore wind farm capacities would require an unprecedented increase rate: from 12 GW in 2030 to 37 GW in 2040 (2.5 GW/year) and 70 GW in 2050 (3.3 GW/year). These expansion rates are 2-3 times larger than the period 2020-2030. At the same time, the attractiveness of the business case has been declining.

How does the limited space in areas to be developed for offshore wind and hydrogen affect the capacities, spatial configuration and energy production of the hubs? How can they be developed in a way that maintains (if not strengthens) the ecological carrying capacity of the North Sea?

- **Resolving spatial conflicts will be crucial to realize the 70 GW ambition imposed in our NSE5-NAT scenario.** Conflicts exist between offshore wind farm development and mining activities (natural gas production, CO₂ storage) while space must also be reserved for nature to strengthen ecological value. Consequently, **more space must be found** outside of the assigned wind search areas (for 17 GW offshore wind) **to reach this 70 GW target, or ambitions must be down-scaled.**
- By reserving space for nature, there is a reduction of available space in Hub North for wind power and hydrogen production, resulting in a decrease in max. installable wind power capacity from 28 to 20 GW. As space will also have to be reserved for mining activities, the space for offshore wind will further reduce in that region, unless we find innovative solutions that resolve the spatial conflicts.
- **Our “less ambitious” NSE5-DEC scenario reaches 45 GW of wind farm capacities by 2050**, and can probably be realized while reserving space for other uses (both in time and from the perspective of available space).
- Our results for wind power production from clusters of wind farms in Hub North and Hub East with power densities of 10 MW/km² lead to lower full load hours (FLH) compared to studies using lower power density configurations, such as CorRES, for the same meteorological year (2015), up to 10% depending on the conditions (Hub East). This could be due to different wake models used and/or different power densities in the assumptions. Due to **limited space available, power densities of future wind farms** may have to be **significantly higher than current installations** (10-12 MW/km² compared to 7-8 MW/km² for Hollandse Kust wind farms operational and under construction), which will lead to **larger wake losses, reducing their FLH** (and yearly amount of electricity produced).

What is the contribution of the hubs towards meeting the projected demand for electricity and hydrogen in 2050 (see Figure ES.2)?

- In the NSE5-DEC storyline, the installed capacities in the 3 hubs **produce 152 TWh of electricity**, of which 34 TWh is consumed by electrolyzers to **produce 21 TWh of hydrogen**.
- In contrast, in the NSE5-NAT storyline, where installed capacities are higher, in particular in and around Hub North, **187 TWh of electricity is produced in the hubs**, of which 47 TWh is consumed to **produce 30 TWh of hydrogen**.

- In NSE5-DEC, the hubs supply 42% of the yearly electricity demand (364 TWh in I13050-DEC) and 21% of yearly hydrogen demand (102 TWh in I13050-DEC), while in NSE5-NAT, they supply 43% of total electricity demand (433 TWh in I13050-DEC) and 19% of hydrogen demand (159 TWh in I13050-NAT).
- The additional electricity generated by capacity outside of Hub North (in the areas around Klaverbank and Doggerbank) that must be built to reach the 2050 target of 70 GW in NSE5-NAT is almost as large (75 TWh) as the electricity generated inside Hub North (88 TWh), and this accounts for an additional 17% of total yearly electricity demand of I13050-NAT. Of the 75 TWh, 38 TWh is consumed to produce 26 TWh of hydrogen.
- In total, the **installed capacities in and around Hub North produce 60% of the yearly electricity demand of I13050-NAT, and 35% of hydrogen demand of I13050-NAT.**

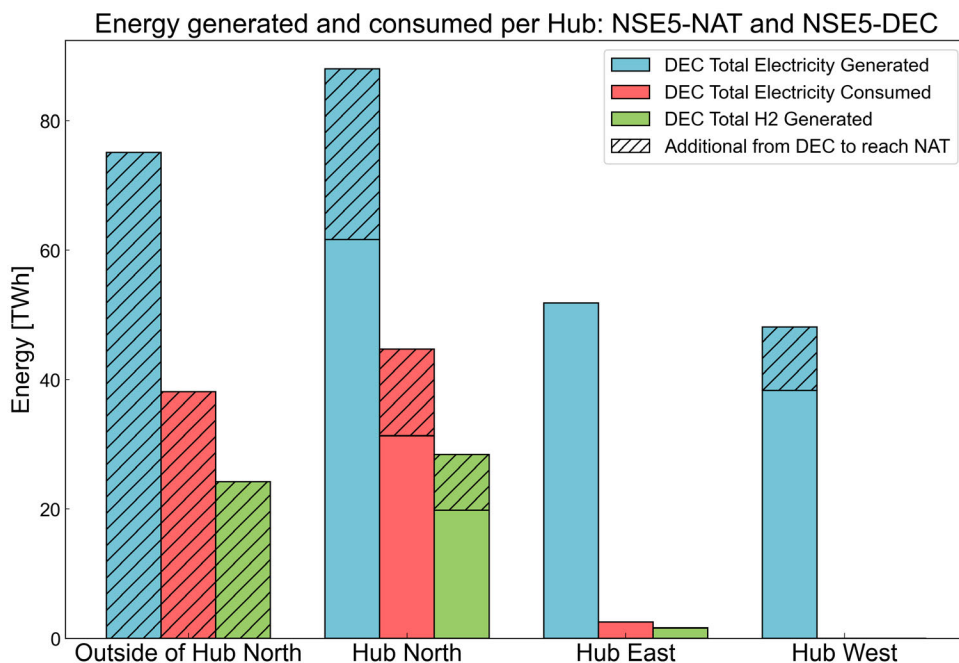


Figure ES.2: Comparison of the energy flows of the NSE5-NAT and NSE5-DEC scenarios on an annual basis. Note that the energy of hydrogen produced is based on the lower heating value of hydrogen.

How do different operational strategies affect the utilization and need for flexibility of the offshore hydrogen production and transport infrastructure to absorb part of the wind power intermittency?

- Using PEM electrolysis with 10% minimum load and a 2:1 ratio of wind to electrolyzer capacity leads to less than 2% use of grid power. Increasing the minimum load to 50% would increase the grid power consumption to around 10%.
- Allowing 10 shutdowns a year for hydrogen production with 10% minimum load and off-grid mode, a power storage system delivering around 15-20 hours of this minimum load would be needed. This may be able to be achieved by short/medium-term power storage methods. However, if zero shutdowns for hydrogen production are allowed, the power storage requirements increase by 5 times.
- **Part of the intermittency of the offshore power production may be able to be absorbed offshore.** Smart operational strategies can increase the number of hours with stable

power delivery to shore, allowing the electrolyzer to dampen some of the wind power fluctuations. More than 1000 additional hours in a year with stable power delivery were obtained by using different parts of the wind curve for minimum/baseload of the electrolyzer compared to always choosing a fixed 1:1 ratio of power to the electrolyzer and export cable to shore.

What is the influence of adding offshore solar on the variability of the electricity production of wind farms?

- The inclusion of offshore solar could potentially result in an increased cable utilization and demand met from the Hubs. However, further research in cost, spatial constraints and other flexibility elements (e.g., power storage) is needed to provide conclusions regarding its suitability and, if so, at which scale.

How could the infrastructure for transporting electricity and hydrogen from the hubs to shore develop in time, and what role could existing (re-used) pipelines play?

- To **transport the hydrogen produced offshore and allow for import** from Denmark, Norway and UK, transport **capacities must reach approximately 18 GW in 2050**. Two designs were realized, landing in the regions of Den Helder and Eemshaven. One design assumes all new 48-inch pipelines while the other one assumes re-use of sections of NGT and NOGAT, with limited new 36-inch pipelines.
- Under the current assumptions, newly built infrastructure for hydrogen transport with 48-inch diameters (versus 36-inch for re-use) provides greater resilience for future energy needs, such as import and production beyond 2050 estimations. For NSE5-NAT, the pressure losses result in around 3 bar for newly built infrastructure, compared to around 50 bar in the re-use case.
- **A combination of reuse and newly built hydrogen pipelines could strike the right** balance between flexibility, resilience, future proofness, and investment cost. This is particularly relevant in the scenarios with higher flowrates (NSE5-NAT), and if additional imports, such as via AquaDuctus, are expected.
- **Offshore compression may be able to be avoided in NSE5-NAT with newly built 48-inches infrastructure** when injecting at 30 bar from the electrolyzer. For the re-use, the potential is more limited: only the NSE5-DEC with no imports from AquaDuctus can be achieved, with NSE5-NAT having unfeasible pressure losses.

What is the potential role of offshore hydrogen storage in providing flexibility to maintain a stable and predictable hydrogen supply to shore?

- **Offshore hydrogen storage** (salt structure or depleted gas field) **may enable a nearly-constant (and predictable) flow to shore** by acting as a buffer to flatten the inherently variable wind-based production, but it **does not necessarily result in reduced pressure fluctuations (or pressure losses) along the offshore network**. Depending on the location of the storage in the network, the **hydrogen may have to take longer pathways to reach the storage**, and this results in **larger pressure losses** overall.
- The pressure stability of the offshore network is largely affected by the control strategy (fixed flowrate versus fixed pressure), the location of the storage and the coordination of the different actors (production, storage and transport). In the simulations performed, an almost constant pressure was achieved at the Eemshaven landing point with a storage in

F8 (Hub North), but in the network overall, the amplitude of the pressure swings increased.

- **Examples of possible candidate salt structures** (in license blocks F8, E17, and M2) and **depleted gas fields** (in license blocks G16, G17, K5 and K7) **in and around Hub North were identified** (see Figure ES.1) where sufficient hydrogen could be stored (3 TWh storage capacity) to transform a variable hydrogen production signal (from 8 GW of electrolyser capacity) into a 3 GW flow to shore year round.
- Notional design studies for an offshore storage facility highlighted that for storage in gas fields, **reservoir properties are very important when selecting candidate fields**. Examples of very important properties are the **well diameter** and the **transmissivity**. The latter is a parameter indicating how easily gas can flow through the reservoir.
- In a (depleted) gas field, **injected hydrogen will mix with residual natural gas** in the reservoir. This **residual gas must be separated** from the hydrogen on withdrawal, and **produces a sizeable tail gas stream** at atmospheric pressure that needs a destination. It can be transported to an offtaker onshore via a pipeline, or reinjected into a nearby reservoir, requiring a very **large tail gas compressor**. The dimensions and weight of **all the topside facilities** for (hydrogen and tail gas) compression and (hydrogen) gas cleaning **may require very large offshore platforms** that are similar in size as the largest known platforms in the world.
- Costs analyses performed for developing offshore storage facilities for the selected use case indicate that the **total investment cost for a facility offshore can be 2-5 times higher than for a similar facility onshore**.

Recommendations for future research

Further alignment of the different stakeholders regarding spatial claims will be required, in order to define spatial configurations that can achieve multiple purposes. This is not limited to the currently designated areas, but also to potentially new areas if the ambitions for installed capacities of wind and hydrogen production remain high.

If space is limited, power densities of wind farms increase and wake losses can become more relevant, as highlighted by this study. A more detailed analysis, including interactions between different areas and the influence for different meteorological years, can provide recommendations over their effect in specific areas.

The international context was simplified in this study. Modelling profiles for the different commodities across different countries in the North Sea would provide a better representation of the supply and demand and what flexibility options are needed.

Aligning with the present and future expected wind tender criteria is relevant to study realistic configurations. This includes conditions such as curtailment in specific time steps or usage of power in specific onshore areas, as seen in the Ijmuiden Ver Gamma tenders.

The influence of different power storage models to tackle short and long-term flexibility has not been studied in detail. This could open the room for more (semi) off-grid strategies for hydrogen production or power delivery (e.g., if ATR85 network code limitations for time-based and time-block transmission rights are present).

Most of the scenarios here explored one main change with respect to a reference. However, as seen in the cases with hydrogen storage, it may be beneficial to explore cases with e.g., multiple storages. Similarly, a combination of newly built and re-use infrastructure could provide a good balance between cost, availability and performance.



1 Introduction and research questions

Europe is working towards a fully climate-neutral society by 2050. This means that the energy system must be climate-neutral before 2050, which requires a major shift in the energy mix. Where fossil energy carriers, and particularly natural gas, (still) form the foundation of the energy system today, electricity will become the backbone of the future energy system. Before 2050, electricity production must become CO₂-free, and the total electricity supply must grow by a factor of two to three. To achieve this, the capacity of solar energy (PV), onshore wind, and offshore wind must increase. Although onshore wind is a very cheap form of renewable energy, its growth potential is limited by the available space and public acceptance. Solar PV (onshore) still has strong growth potential, mainly because of its low costs and easy local integration, but requires a significant simultaneous scaling up of local flexible demand and energy storage. Therefore, countries around the North Sea, like The Netherlands, are strongly focusing on utilizing offshore wind energy production at the North Sea, because it has enormous production potential and can be developed at relatively low costs.

At the same time though, the North Sea region is one of the busiest maritime areas of the world and is surrounded by densely populated, highly industrialised countries (Belgium, Denmark, France, Germany, the Netherlands, Norway and United Kingdom). In the past decades exploration of natural gas and oil reserves has shaped the offshore energy landscape of the North Sea. Today, the North Sea has more than 500 offshore platforms and more than 50.000 km of offshore pipelines run across it. While these existing offshore assets might provide opportunities for offshore energy activities in the future (like CCS and hydrogen production), when no longer needed for hydrocarbon production, today the spatial footprint of their continued operation for hydrocarbon production must be carefully considered in spatial planning processes for new offshore (renewable and low-carbon) energy production, like offshore wind, floating solar, etc.

The aim of the North Sea Energy program is to identify and assess opportunities for synergies between low-carbon energy developments offshore (wind energy production, hydrogen production, CCS, and hydrocarbon production) that have the potential to reduce societal cost and help to optimize their spatial integration whilst preserving existing ecological values. In early phases of NSE (1, 2 and 3), the focus was on generic techno-economic analyses for various system integration options identified. In NSE 4, the focus shifted to more site-specific research with the designation of three regions at the North Sea, termed “energy hubs”, for which designs were conceptually developed. The three hubs, named “Hub West”, “Hub East”, and “Hub North”, take into account the specific offshore environment and stakeholder presence in those regions of the Dutch North Sea, and are considered to become important stepping-stones for large-scale system integration (see Figure 1.1). Hence, they have become one of the central elements in the North Sea Energy programme, and have taken a central place in NSE 5.

Energy hubs are defined by the NSE consortium as areas for offshore energy systems where production, conversion and/or storage of energy commodities (electricity, natural gas, hydrogen) and CO₂ are co-located. Transport of energy commodities and CO₂ to and from shore takes place via national transport corridors and/or via international interconnections.

In this way, energy hubs are search areas for offshore system integration opportunities, i.e., where activities such as electricity production, transport and storage, CO₂ transport and storage, offshore hydrogen production, transport and storage and platform electrification for (greenfield) natural gas production can be combined.

For each of the three mentioned energy hubs, a fit-for-purpose strategy and short-term development plan was presented in NSE 4 in the form of a multitude of storylines to give insights specifically into the techno-economic aspects, but also involving aspects related to legal, safety, and ecological challenges. The final result is presented as conceptual visions of how the three future offshore energy hubs might develop. However, while spatially-explicit, and rooted as best as possible in state-of-art ambitions pertaining to infrastructure visions, the visions are “end-state” visions.

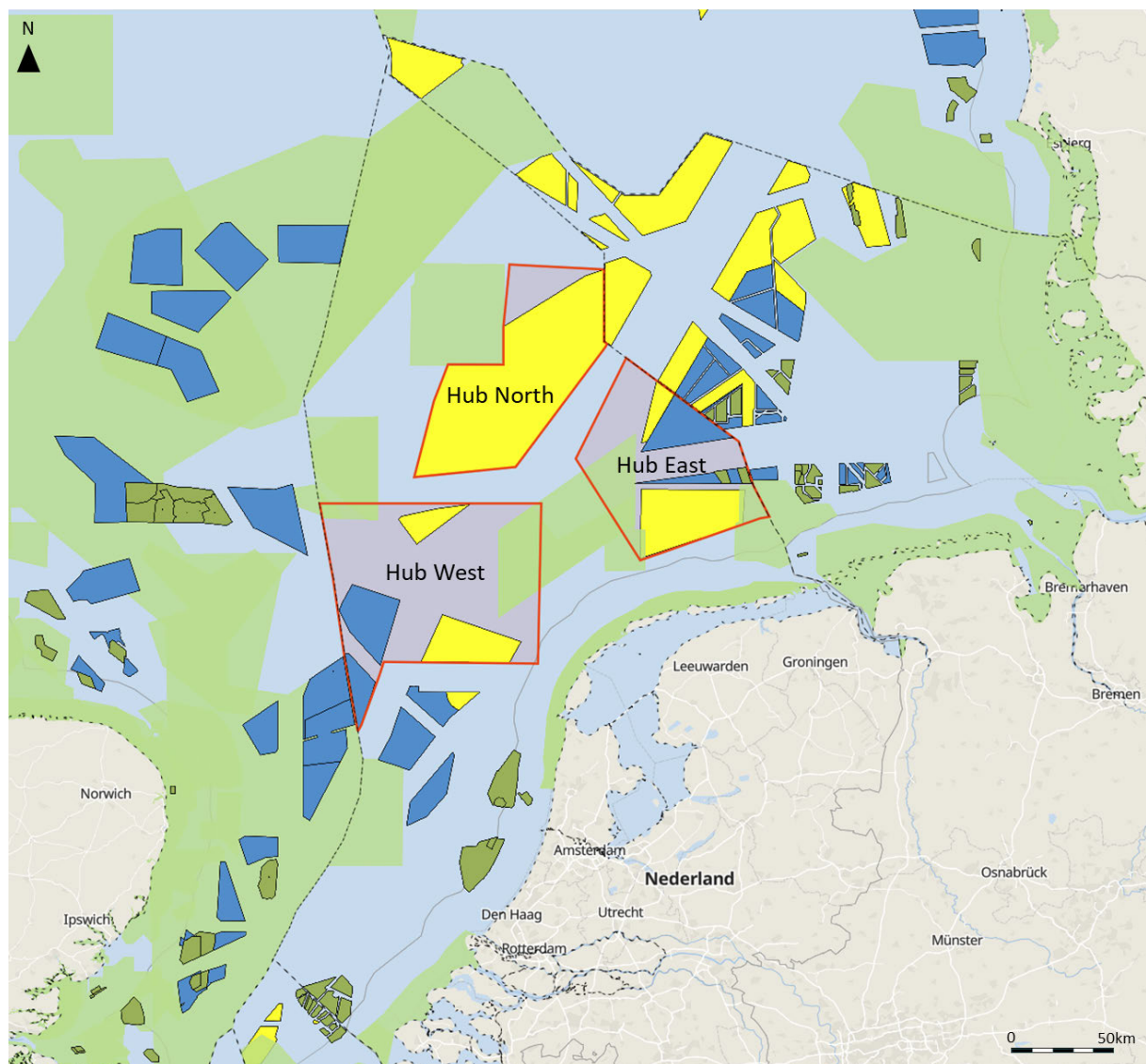


Figure 1.1: Geographic map of the Dutch sector (mainly) of the North Sea with the outlines of the three hubs of NSE (red polygons), in context with operational windfarms (dark green), planned windfarm areas (dark blue), search areas for developing windfarms (yellow), and nature areas (light green).

The ambition for work package 1 (WP1) of NSE 5 was therefore to refine these visions into incremental 10-year development plans (2025-2035, 2035-2045, and 2045-2050+) that are presented in the form of spatially-explicit blueprints for the three offshore energy hubs and their associated transport infrastructure connecting the hubs to shore. In the hub development plans, and in close collaboration with WP 2 to WP 6, key challenges in relation to nature-inclusive design, spatial planning, economics, governance and society were identified and addressed. The specific goals of WP1 were three-fold:

1. To refine the visions of the three energy hubs (west, east, north) as put forward in NSE 4 into spatial explicit blueprints that highlight which activities are to be developed when in time and at which location in the hub area. Together the blue prints constitute hub development plans that define the incremental development of the hubs at 5-10 year intervals. This goal was addressed in the ‘hubs’ workstream of WP1, and is the focus of this report.
2. To perform detailed techno-economic assessments of a number of offshore energy technologies that are expected to become important enablers for future offshore energy hubs: offshore hydrogen production (central, decentral) including direct seawater electrolysis, offshore brine disposal from hydrogen production. This goal was addressed by the ‘Technical Innovations’ workstream, and is addressed in deliverable D1.4 of NSE5 (Buijs, et al., 2025).
3. To define the relevant energy system assets at a generic elementary level for the energy-related activities and parameterize them in an ESDL energy system data repository to be used in integrated energy system modelling studies aimed at simulating flows of energy commodities. This goal was addressed by the ‘Technical Innovations’ workstream, and is addressed in deliverable D1.4 of NSE5.

In this report, the work that was done to achieve the first goal is detailed in Chapter 2, where we present spatial explicit designs (blueprints) for the three hubs and the infrastructure to transport electricity and hydrogen produced in the hubs (and outside) to shore. In detailing the designs, we have indicated when, where and how the hubs could facilitate offshore synergies with CCS and natural gas developments. In Chapters 3 and 4, we detail the methodologies, assumptions and results of integrated modelling studies that were conducted to (partly) answer the following research questions:

- Which configurations are feasible for integrating offshore wind and hydrogen production at offshore hubs?
- How is a hybrid configuration of offshore wind and solar possible w. co-use potential in the hubs?
- What is the optimal mix of offshore electricity, offshore hydrogen production and offshore storage assets (hydrogen and electricity) in the offshore hubs?
- How do we make sure that as much electricity as possible is brought to shore?
- How do we make the hub function as a “baseload” energy supplier (guaranteed baseload capacity) by putting in place sufficient flexibility?

While we initially set out to answer these research questions, they were gradually reformulated during the 2-year project, resulting in new research questions that we provide answers to in this report (in the form of key insights):

- What areas in the hubs are (foreseen to be) developed for wind power, natural gas, hydrogen production and storage and CO₂ storage in the period between 2030-2050?
- How does the limited space in areas to be developed for offshore wind and hydrogen affect the capacities, spatial configuration and energy production of the hubs? How can they be developed in a way that maintains (if not strengthens) the ecological carrying capacity of the North Sea?
- What is the contribution of the hubs towards meeting the demand for electricity, hydrogen, natural gas and CO₂ storage in 2050?
- How do different operational strategies affect the utilization and need for flexibility of the offshore hydrogen production and transport infrastructure to absorb part of the wind power intermittency?
- What is the influence of adding offshore solar on the variability of the electricity production of wind farms?
- How could the infrastructure for transporting electricity and hydrogen from the hubs to shore develop in time, and what role could existing (re-used) pipelines play?
- What is the potential role of offshore hydrogen storage in providing flexibility to maintain a stable and predictable hydrogen supply to shore?

Finally, in Chapters 5 and 6 we discuss the results and highlight the main conclusions of the hubs and transport infrastructure design work of WP 1.

2 North Sea Energy hubs

In this chapter we present the blueprint-like designs for the 3 hubs defined in the context of the NSE programme. Designs have been made for 2 scenarios that differ in the level of utilization of the Dutch North Sea for producing renewable and low-carbon energy. The 2 scenarios, and the associated narratives for the phased development of the hubs, which we call “storylines”, can be seen as visions of how the future Dutch energy system, and the role of the hubs in that system, could evolve. In the following, we will first describe the broader policy context (targets, ambitions), before detailing the storylines.

Our starting point for the storylines is the European ambition to become climate-neutral (net-zero) by 2050, with an intermediate target of 55% reduction of CO₂-emissions (vs. 1990 levels) in 2030 (EU Climate Law). To meet this ambition, commodity-level targets for electricity, hydrogen and CCS have been agreed on at national (excl. CCS) and European level. At national level, the Dutch wind energy roadmap (Noordzeeloket, 2024) aims for 21GW of offshore wind to be installed in 2032. Furthermore, while in a Letter to Parliament of April 2024 (Ministerie van Economische Zaken en Klimaat, 2024) and in the “Notitie Reikwijdte en Detailniveau” of VAWOZ 2031-2040, (Arcadis, BRO, Delft, & Pondera, 2024), the Dutch government confirmed its ambition to have 50GW installed in 2040, the recently published drafted version of the update of the Partiële Herziening Programma Noordzee 2022-2027 (Ministerie van Infrastructuur en Waterstaat, 2025) is planning for 38-42 GW of installed capacity by 2040 (17-21 GW additional capacity in period 2032-2040, on top of the 21 GW of the wind energy roadmap). In an earlier Letter to Parliament from September 2022 (Ministerie van Economische Zaken en Klimaat, 2022), the ambition of 70GW offshore wind installed in 2050 was already confirmed. In our storylines and hub designs, the 2032 target is assumed firm (binding), while the ambitions for 2040 and 2050 are considered “aspirations to strive for”, i.e., they are assumed to be soft (flexible) targets. Internationally, the Dutch ambitions complement the goals for offshore wind set forth in the North Seas Energy Cooperation (NSEC) (European Commission, 2024) NSEC, which unifies Belgium, Denmark, France, Germany, Ireland, Luxembourg, the Netherlands, Norway, and the European Commission, aims to reach at least 260GW of offshore wind energy by 2050, which will represent more than 85% of the EU-wide ambition of reaching at least 300GW by 2050. The 2050 NSEC ambitions are complemented with intermediate targets of at least 76GW by 2030 and 193GW by 2040.

For hydrogen, the European Union’s Green Deal (European Commission, 2019) sets a target of 40GW of electrolyser capacity to be installed by 2030 to produce 10Mt of green hydrogen, and this to be complemented by 10 Mt import of hydrogen from non-European countries (REPowerEU, (European Commission, 2022)). By 2050, renewable hydrogen is to cover around 10% of the EU’s energy needs, significantly decarbonizing energy intensive industrial processes and the transport sector. The Netherlands aims to reach at least 4 GW of green hydrogen production by 2030, with plans to double to 8 GW by 2032, depending on wind power availability, grid capacity and industrial demand. No clear policy-supported targets or ambitions have been communicated for the post 2032-period until 2050. In recent studies published in the context of the “Energy Infrastructure Plan for the North Sea” (EIPN, (Ministerie van Economische Zaken en Klimaat, 2024)) and the pVAWOZ (Arcadis, BRO, Delft, & Pondera, 2024), however, plans are presented for developing infrastructure to transport

energy (in the form of electricity and hydrogen) produced in wind search areas 6 and 7 (Hub North) to shore in the northeastern (Groningen) and western (North-Holland, South-Holland and Zeeland) provinces of the Netherlands. To honour the “Nijbegun” agreement (Ministerie van Economische Zaken en Klimaat, 2024), at least one-third of the energy produced by the additional offshore wind capacity planned at the North Sea beyond the currently operational 4.7 GW must land in Groningen. EIPN assumes that 24 GW of offshore wind can be developed in those search areas in the period from 2032 until the early 2040’s, of which 50% (12 GW) will be electrically connected to shore, and 50% will be connected to production installations for (green) hydrogen (electrolysers). In other words, in the post-2032 period, there is an expectation that up to 12 GW of offshore hydrogen production capacity may be developed, and this expectation has been taken into consideration in developing our storylines and hub designs.

The storylines also acknowledge that CCS is needed to reach achieve net-zero in 2050, and net negative emissions thereafter. CCS amounts needed in The Netherlands vary in scenarios from approximately 10 to 40 megatons (Mt) of CO₂ per year to compensate for residual emissions in various sectors in 2050. The Dutch government anticipates a demand of 20 to 25 Mt/yr of CO₂ in the period 2040-2050 (Ministerie van Klimaat en Groene Groei, 2025). At EU-level, the Net-Zero Industry Act (NZIA, (European Commission, 2024)) that came into effect in June of 2024 introduced a direct obligation on oil and gas producers to collectively realize 50 Mt/yr of CO₂ injection capacity by 2030, whereby the quantity per country and operator is depending on its EU-based oil and gas production in the years 2020-2023. Furthermore, the EU recently released its Industrial Carbon Management (ICM) strategy to accelerate CCS deployment, where it notes that by 2040, approximately 250 Mt/yr of CO₂ injection capacity should be available annually in Europe. A large share of this injection capacity is expected to be developed in the greater North Sea Basin, which requires a significant scaling up of CCS deployment in that region.

For hydrocarbons, the storylines reflect that their production, in particular natural gas, is expected to continue until 2050. In the “Sectorakkoord gaswinning in de energietransitie” that was published in April 2025 (Ministerie van Klimaat en Groene Groei, Element NL, and EBN, 2025), the Dutch government, together with ElementNL and EBN, introduces measures to accelerate the production of natural gas at the North Sea to a) enhance security of gas supply in the Netherlands to compensate for the loss of Russian gas imports, b) reduce dependency on foreign suppliers, and c) reduce the carbon footprint of the Dutch natural gas supply (indigenous production of natural gas has a lower carbon footprint than when supplied from overseas), and d) generate more income for the Dutch state (society).

The ramp-up of production, transport and storage of electricity, hydrogen and CO₂, and the associated infrastructure that is being developed, must go hand-in-hand with other (existing) uses of the North Sea, while for mining activities the geological suitability of the subsurface has to be taken into account. Moreover, in the “Noordzeeakkoord” (Overlegorgaan Fisieke Leefomgeving, 2020), it was agreed between the relevant Dutch stakeholders that the stated energy and climate goals must be achieved without violating the ecological carrying capacity of the North Sea. In developing our hub designs, we have addressed (some of) the spatial integration challenges that are (and will be) encountered, which we did in close cooperation

with work package 4 of NSE 5 on Ecology to ensure that the designs are nature-inclusive (van der Heijden, et al., 2025).

2.1 Storylines for development towards 2050

A storyline is essentially the spine of any narrative, holding together various elements to form a coherent and engaging tale. Here, the tale tells the story of how the offshore energy system at the North Sea, and the three hubs of NSE5 in particular, could evolve until 2050 as part of the broader energy system of northwest Europe, and what role it could play in supplying Europe with clean energy and reaching climate goals. They guide the quantification of the hub design and transport infrastructure scenarios and inform the development process of assumptions and input parameters for model-based performance assessment (see chapters 3 and 4).

Our two storylines, named “NSE5-NAT” and “NSE5-DEC”, are rooted in the “Integrale Infrastructuur Verkenning 2030-2050 editie 2” (I13050-2) (Netbeheer Nederland, 2023) which presents four future scenarios (see Figure 2.1) for realizing a climate-neutral energy supply in 2050, with an associated narrative (also termed “storyline”). Initially we considered using the European-scale scenarios of the Ten-Year-Network-Development-Plan (TYNDP) (ENTSOE, ENTSO-E, 2022) of the European grid operators for electricity and gas, called “Distributed Energy” and “Global Ambition”, however, we found that these 2 scenarios were too limited in differentiating between on- and offshore capacities, and led to hub designs that were too similar in their levels of utilization of the North Sea, and therefore do not represent the experienced uncertain bandwidth of future offshore energy development. Instead, we decided to use the scenarios of I13050-2, because they are well-known, widely accepted, and often referred to by policy makers in the context of infrastructure development planning. Additionally, I13050 has the benefit of providing numbers for (projected) supply and demand for the four commodities (electricity, hydrogen, natural gas and CO₂) considered in NSE, and for four years in the future (2030, 2035, 2040 and 2050). In the next paragraphs, the storylines of the four I13050 scenarios are briefly described. For more detailed information, the reader is referred to the I13050-2 report (Netbeheer Nederland, 2023).

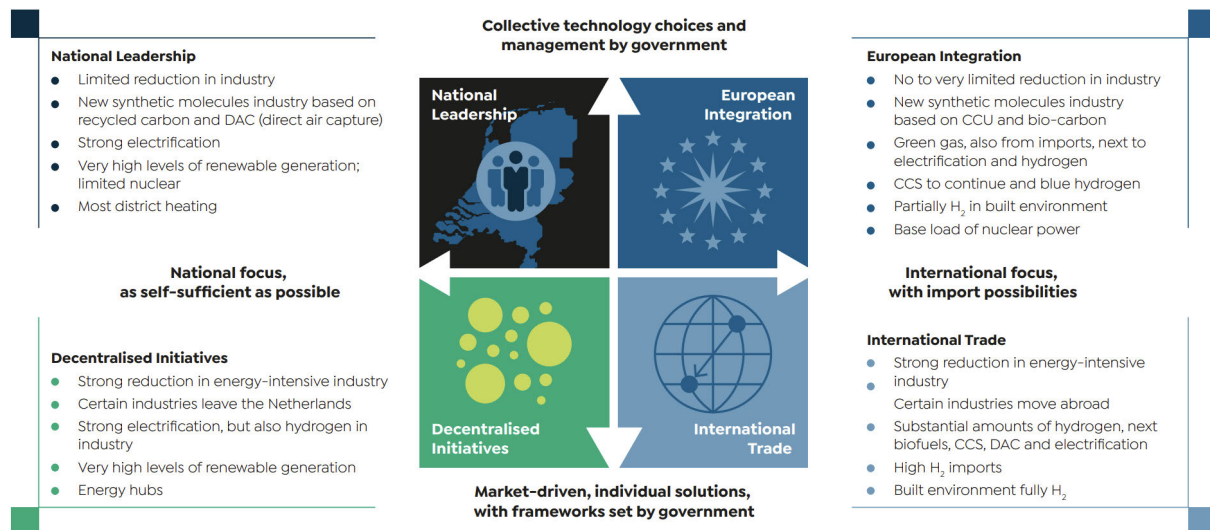


Figure 2.1: II3050-2 scenario framework: the features and assumptions of the four scenarios for climate neutrality. Besides the features listed here, a large number of aspects of the energy system are considered to be changeable. These are specific energy system choices or major uncertainties in terms of demographics, the economy and the environment, social developments, technology and political or governance aspects. For full and extensive details of the scenarios, see the interim report titled “Het energiesysteem van de toekomst: de II3050-scenario’s” (Netbeheer Nederland, 2023).

In the *National Leadership (NAT)* storyline, The Netherlands aims for an energetically efficient system by determining the national energy mix and choosing technologies. The government sets policies, finances key projects, promotes new industries like synthetic fuel production, and incentivizes electrification. In the built environment, district-based coordination develops heat grids using residual heat, geothermal heat, and flexible electrical sources.

In the *Decentralized Initiatives (DEC)* storyline, private-sector climate-neutral technologies are supported, and autonomy is granted to citizens and local communities in the energy transition. Sustainable choices are incentivized through information and financial incentives. Local initiatives utilize available sources, leading to significant growth in onshore solar and wind power. Industry shifts to bio-based and circular feedstocks, with limited acceptance of CCS. Some energy-intensive industries cease operations due to the focus on renewable energy. Heating in buildings uses various local sources like geothermal heat, heat pumps, green hydrogen, and green gas.

In the *European Integration (EUR)* storyline, The Netherlands aims for an integrated European energy system with aligned policies and shared energy sources. Europe seeks independence through joint energy policies, large-scale green gas production, and growth in solar, wind, and nuclear energy. Offshore wind power in the North Sea is maximized through collaboration. Industry becomes sustainable with electrification, biomass, and hydrogen. CCS is widely used for negative emissions, blue hydrogen, and CO₂ capture from fossil sources. Renewable and recycled feedstocks are supplemented with small amounts of fossil feedstocks. CO₂ from neighbouring countries is stored in the Netherlands. Sustainable efforts in the built environment focus on district-based actions and cross-regional heat grids.

Electrification of transport is achieved through expanded charging infrastructure and high-speed rail networks.

In the *International Trade (INT)* storyline, The Netherlands aims to develop its economy by leveraging international energy and feedstock supply chains, seeking the lowest-cost options globally. Free trade is crucial, supported by incentives, subsidies, and CO₂ pricing. Dutch companies contribute to sustainable supply chains. Hydrogen and climate-neutral energy carriers are imported, making the Netherlands a transit hub. The built environment uses hybrid heat supply with hydrogen, while industry focuses on electrification and hydrogen use. Some energy-intensive industries relocate abroad, with more semi-finished products imported for processing. The Netherlands also produces green hydrogen using offshore wind power but relies heavily on energy imports.

We chose the I13050-NAT and I13050-DEC scenarios as the contextual scenarios to nest our hub and transport infrastructure designs into. I13050-NAT was selected because it is the only scenario that meets the ambitions for 70 GW offshore wind in 2050 to support high levels of electrification while also striving for energy independence. A key role for offshore hydrogen production is foreseen in I13050-NAT to produce hydrogen for industry and power generation, and to support the integration of offshore wind. The EIPN studies are also based on I13050-NAT, which can be understood considering the reasoning above. I13050-DEC was selected as the alternative scenario. It is a credible scenario that also aims for a high level of electrification, but assumes a more modest role for offshore wind (45 GW in 2050) and a minor role for offshore hydrogen production, which leads to a more modest utilization of the hubs (and North Sea) for energy production, transport and storage.

When comparing the numbers of NAT and DEC with the scenario of the “Nationaal Plan Energiesysteem” (NPE) (Ministerie van Economische Zaken en Klimaat, 2023) we see that NPE assumes resp. a 30 and 55% higher electricity demand in 2050 vs. NAT and DEC, with half of that demand accounted for by conversion to hydrogen and heat, and losses in the system. Likewise, for hydrogen the NPE assumes resp. a 70% and 165% higher demand (direct end-use, conversion and loss) than NAT and DEC, of which about 75% is assumed to be produced by electrolysis. Similar to I13050, the NPE also assumes that 70 GW offshore wind will have been developed in 2050.

2.1.1 Storyline NSE5-NAT: 70GW offshore wind, key role for offshore P2G

This storyline, named NSE5-NAT, is rooted in the National Leadership scenario of I13050-2. It describes how the three hubs (west, east, north) could develop as an integral part of the offshore energy system in an energy world as envisioned in the I13050-NAT scenario. In that scenario, the North Sea plays a key role in supplying The Netherlands with clean energy to reach climate goals. It assumes that 72 GW offshore wind will be installed in 2050, of which 52 GW is electrically connected to shore, and 20 GW is connected to electrolyzers offshore (off-grid) to produce hydrogen. In developing our NSE5-NAT storyline, and the corresponding hub designs, we aimed to meet those capacities, while being mindful of spatial claims from other activities (e.g., current and future mining-related activities like oil and gas production, CCS, and hydrogen storage, fishery, shipping, etc.) and being nature-inclusive, by reserving space for measures that strengthen the ecological carrying capacity, as proposed in the final report on nature-inclusive energy hubs, deliverable D4.1 of this NSE 5 program (van der Heijden, et al., 2025). On off-grid vs. grid-connected electrolysis, it must be noted that in our

designs we deviate from I13050 by including bi-directional cables (following a study recently published by the NSWPH consortium)(ref) to fulfil a certain minimum load for the electrolyzers. In deliverable D3.4 of NSE 5 (van Zoelen, Mahfoozi, Blom, & González-Aparicio, 2025), the pros and cons of off-grid vs. grid-connected hydrogen production are discussed in more detail.

In Table 2.1, we show the capacity numbers for offshore wind and hydrogen production per hub for the 4 reference years 2030, 2035, 2040 and 2050 in NSE5-NAT. Offshore wind capacity reaches 70.3 GW in 2050, which is in line with the ambition of the Dutch government. Of that 70.3 GW, however, only 40.3 GW can be accommodated by the hubs, and together with 12 GW in planned wind farm areas and known wind search areas outside of the hubs (Noordzeeloket, 2024), space must be found for 17 GW additional offshore wind to meet the 70 GW ambition. In our NSE5-NAT storyline, we assume that the space required for 17 GW of (additional) offshore wind will be allocated in currently “open” areas to the west and northwest of Hub North. Furthermore, we assume that max. 20 GW of offshore wind can be accommodated in Hub North (wind search areas 6 and 7), which is at the low end of the range assumed in the original “Partiële Herziening Programma Noordzee” (20-28 GW) of 2023 (PHPNZ23) (Ministerie van Infrastructuur en Waterstaat, 2023) and less than what is assumed in the EIPN studies (Ministerie van Economische Zaken en Klimaat, 2024). Interestingly, in the recently published drafted version of the update of the “Partiële Herziening Programma Noordzee 2022-2027” of 2025 (PHPNZ25) (Ministerie van Infrastructuur en Waterstaat, 2025), max. 19 GW is assumed (11 GW in the southwestern region of Hub North, and 8 GW in the northeast), which is very close to our assumed 20 GW. Of the 20 GW total capacity, we anticipate that 10 GW will be developed in the period 2030-2040 (the other half in the period 2040-2050), which, together with capacity to be developed in Hub West and Hub East, and outside of the hubs in that period, results in a total installed offshore wind capacity of 37.3 GW in 2040.

Table 2.1: Electricity (wind and solar) and (green) hydrogen supply capacities assumed within and outside the hubs, and onshore, in the NSE5-NAT storyline.

Installed production capacity	Unit	Electricity (wind)				Hydrogen (green)			
		2030	2035	2040	2050	2030	2035	2040	2050
Hub west	GW	2.0	6.0	8.0	10.0	0.0	0.0	0.0	0.0
Hub east	GW	0.6	5.3	7.3	11.3	0.0	0.5	0.5	0.5
Hub north	GW	0.0	0.0	10.0	20.0	0.0	0.0	5.0	10.0
Outside hubs ¹	GW	9.3	12.0	12.0	29.0	0.1	0.1	0.1	8.6
Offshore total	GW	11.9	23.3	37.3	70.3	0.1	0.6	5.6	19.1
Onshore total	GW	9.1	10.6	15.1	20.0	3.0 ²	4.0 ²	17.0 ²	25.0 ²
Total Netherlands	GW	21.0	33.9	52.4	90.3	3.1	4.6	22.6	44.1
Expansion rate offshore	GW/yr	1.0 ³	2.3	2.8	3.3	0.0	0.1	1.0	1.4

1: Includes capacities in operational and planned windfarm areas, unpartitioned wind search areas, and “free” areas in the Dutch sector of the North Sea that have not yet been assigned as wind search areas.

2: In the I13050 study, this capacity is defined as “flexible power-to-gas” without specifying whether it will be developed onshore or offshore.

3: Assumes the offshore wind capacity installed by 2030 to have been built over a 12-year period.

While significantly less than the 2040 ambition of 50GW communicated by the Dutch government, it is very close to the 38-42 GW that is now planned for in the 2025 version of

the PHPNZ (Ministerie van Infrastructuur en Waterstaat, 2025). Consequently, in the period 2040-2050, 29 GW offshore wind capacity must additionally be developed to meet the 70 GW ambition for 2050. The rate at which the capacity must expand increases from 2.3 GW/yr in the period 2030-2035, to 3.3 GW/yr in the period 2040-2050.

Offshore hydrogen production capacity in our NSE5-NAT scenario reaches 19.1 GW, which is 0.9 GW less than the 20 GW assumed in I13050-NAT. Apart from the 0.1 GW (max.) of DEMO-1 (near the Hollandse Kust Noord windfarm), and the 0.5GW of DEMO-2 (near the TNW windfarm in Hub East), we assume that this hydrogen production capacity will be entirely built in and around Hub North, in conjunction with the 37 GW offshore wind capacity developed there. Of the 37 GW, we assume that 50% (18.5 GW) will be connected to electrolysers for hydrogen production, which is in line with studies by NSWPH (North Sea Wind Power Hub Programme, 2024) and for EIPN (Ministerie van Economische Zaken en Klimaat, 2024). The timeline for development of this capacity follows the timeline of offshore wind capacity build-out, i.e., in 2040 5.6 GW of offshore hydrogen production capacity will be operational (~1 GW/yr in period 2036-2040), and adding 13.5 GW in the period 2040-2050 (~1.4 GW/yr) to reach 19.1 GW by 2050. With DEMO-2 expected to become operational in 2033, this gives a 3-year (2032-2034) time window to incorporate learnings from constructing and operating DEMO-2 into the (detailed) design and construction of the first GW-scale hydrogen production in Hub North.

It is relevant to mention that I13050-NAT additionally assumes 20 GW onshore wind and 172 GW photovoltaic capacity to be installed in 2050 that, together with 3 GW of nuclear and 15 GW of hydrogen-fired electricity production capacity, and 18 GW of interconnection, must ensure that the electricity demand (433 TWh/yr) can be met at all times. Furthermore, to meet the assumed hydrogen demand of 159 TWh/yr, 25 GW of flexible (non-dedicated, i.e., grid-connected) hydrogen production is included in 2050, together with 33 TWh blue hydrogen production (~4 GW equivalent capacity at 8000 FLH/yr and requiring CCS) and ~56 TWh import. Interestingly, ~65 TWh/yr of hydrogen is also exported, resulting in a net export of ~9 TWh. Additionally, ~13 TWh hydrogen storage is required in I13050-NAT to match supply and demand and secure supply at all times.

Natural gas production (on- and offshore) in I13050-NAT (and NSE5-DEC) is assumed to decline from 40 TWh/yr in 2030 (~4 bcm/yr) to less than 10 TWh/yr (~1 bcm/yr) in 2040, and to have been completely phased-out in 2050 (see Table 2.2).

Table 2.2: Natural gas production from gas fields offshore, within and outside the hubs (source: EBN). For the period 2019-2023, volumes based on historic production. For the period 2025-2050, volumes are forecasts (Resource Class 1-9) based on the EBN asset list, unrisks (POM) and prospective volumes risks (POS), thus reflecting the full potential of the area (including stranded fields and prospects). No prospective volumes (RC8-9) included “outside” the hubs. Oil volumes are excluded.

Area	Unit	Historic production					Production forecast					
		2019	2020	2021	2022	2023	2025	2030	2035	2040	2045	2050
West ¹	bcm/yr	4.2	3.8	3.6	3.2	2.3	2.5	3.5	2.7	2.5	1.2	0.5
East ¹	bcm/yr	0.6	0.5	0.6	0.5	0.3	0.3	0.2	0.8	0.9	0.8	0.4
North ¹	bcm/yr	0.0	0.0	0.0	0.0	0.0	0.0	0.1	0.3	0.5	0.4	0.2
Outside ¹	bcm/yr	4.8	4.7	4.3	3.5	2.1	3.4	4.0	2.4	1.8	0.7	0.3
Total	bcm/yr	9.6	9.0	8.5	7.2	4.7	6.2	7.8	6.2	5.7	3.1	1.4
II3050 ²	bcm/yr	28.5	-	-	-	-	-	4.2	1.7	0.7	-	0.0

1: Source: EBN

2: Source: II3050, numbers include production onshore and offshore.

Information received from EBN, however, received in the context of NSE 5, and confirmed in the “Sectorakkoord gaswinning” (Ministerie van Klimaat en Groene Groei, Element NL, and EBN, 2025), suggests that production may continue until (at least) the period 2045-2050 and at a faster pace, potentially supplying up to ≈127 bcm⁸ in total in the period 2025-2050. Of that total volume, 60% would be produced from gas fields in the three hubs, mainly Hub West. When comparing the forecasted production of natural gas from offshore fields until 2050 to the declining demand for natural gas assumed in II3050-NAT, we notice that it can potentially fulfil ~30% of demand in 2030, ~40% in 2035, ~70% in 2040, and pretty much the entire (remaining) demand in 2050. This highlights that indigenously produced natural gas from Dutch offshore fields can play a relevant role in the future, in particular by securing supply of natural gas while it is still required (incl. for blue hydrogen production), with the remark that this natural gas will have a lower carbon footprint than when importing it from outside Europe.

For CCS, injection capacities are not explicitly mentioned in II3050. Our interpretation of the information presented in II3050 suggests that by 2030 roughly 20 Mt/yr of CO₂ must be injected in gas fields offshore in both scenarios, initially in the P18 fields (Porthos project, 2.5 Mt/yr for 15 years) (Porthos, 2021) and soon after also in gas fields in Hub West (K and L blocks, facilitated by the pipeline from the Port of Rotterdam to K14 that is developed in the Aramis project) (Aramis, 2021) By 2040, the II3050 scenarios assume that this amount will be halved to 10 Mt/yr, to decline further to (almost) zero by 2050. Here, it is important to note that since the publication of the II3050 scenario report in 2023 (and realizing that the studies probably started a few years earlier), there have been significant developments in CCS, as was already mentioned at the beginning of this chapter. Recently, TNO (Scheepers, Taminiau, Smekens, & Giraldo, 2025) has published a report on carbon removal pathways for The

⁸ In the “Sectorakkoord gaswinning in de energietransitie” that was published in April 2025 (Ministerie van Klimaat en Groene Groei, Element NL, and EBN, 2025) the offshore potential is estimated at ≈150 bcm.

Netherlands in the context of its own scenarios (ADAPT and TRANSFORM) for the future energy system in The Netherlands. In the scenarios, CO₂ injection capacities vary from 11.3-12.7 Mt/yr in 2030, increasing to 12.7-40.0 Mt/yr in 2040, to remain at that level post-2040 (15.0-40.0 Mt/yr), whereby it must be mentioned that these rates are the assumed maximum rates that can be realized by reusing gas fields only. For reference, Porthos and Aramis together could realize 24.5 Mt/yr by 2040. TNO notes that by continuing post-2050 at 40 Mt/yr, the total estimated storage capacity (1700 Mt) will have been used by 2076. For additional injection capacity above 40 Mt/yr, CO₂ storage in aquifers must be developed, for which there is (theoretical) potential in and to the south of Hub West, and in and north of Hub North, or connections must be established to CCS infrastructure of other NS countries (UK, Norway). Clearly, CCS has a big role to play at the North Sea, both in the hubs, and in areas outside the hubs, and its spatial claims must be taken into consideration in spatial planning, especially given that it relies on the 'prefixed' geological suitability of the subsurface.

2.1.2 Storyline NSE5-DEC: 45GW offshore wind, minor role for offshore P2G

This storyline, named NSE5-DEC, is rooted in the Decentralized Initiatives scenario of I13050-2. It describes how the three hubs (west, east, north) could develop as an integral part of the offshore energy system in an energy world as envisioned in the I13050-DEC scenario. In that scenario, the North Sea plays a less prominent role in supplying The Netherlands with clean energy to reach climate goals. It assumes that only 45 GW offshore wind will be installed in 2050, of which 37 GW is electrically connected to shore, and only 8 GW is connected (dedicated, i.e., off-grid) to electrolyzers offshore to produce hydrogen. In developing our NSE5-DEC storyline, and the corresponding hub designs, we aimed to meet those capacities, while being mindful of spatial claims from other activities and being nature-inclusive, which proved to be much easier than for the NSE5-NAT scenario. In Table 2.3, we show the capacity numbers for offshore wind and hydrogen production per hub for the 4 reference years 2030, 2035, 2040 and 2050 in NSE5-DEC.

Table 2.3: Electricity (wind and solar) and (green) hydrogen supply capacities assumed within and outside the hubs, and onshore, in the NSE5-DEC storyline.

Installed production capacity	Unit	Electricity (wind)				Hydrogen (green)			
		2030	2035	2040	2050	2030	2035	2040	2050
Hub west	GW	2.0	6.0	6.0	8.0	0.0	0.0	0.0	0.0
Hub east	GW	0.6	5.3	7.3	11.3	0.0	0.5	0.5	0.5
Hub north	GW	0.0	0.0	6.0	14.0	0.0	0.0	3.0	7.0
Outside hubs ¹	GW	9.3	12.0	12.0	12.0	0.1	0.1	0.1	0.1
Offshore total	GW	11.9	23.3	31.3	45.3	0.1	0.6	3.6	7.6
Onshore total	GW	9.1	10.6	12.1	15.0	3.0 ²	4.0 ²	14.5 ²	25.0 ²
Total Netherlands	GW	21.0	33.9	43.4	60.3	3.1	4.6	18.1	32.6
Expansion rate offshore	GW/yr	1.0 ³	2.3	1.6	1.4	0.0	0.1	0.6	0.4

1: Includes capacities in operational and planned windfarm areas, unpartitioned wind search areas, and “free” areas in the Dutch sector of the North Sea that have not yet been assigned as wind search areas.

2: In the I13050 study, this capacity is defined as “flexible power-to-gas” without specifying whether it will be developed onshore or offshore.

3: Assumes the offshore wind capacity installed by 2030 to have been built over a 12-year period.

Offshore wind capacity reaches 45.3 GW in 2050, which is significantly less than the ambition of the Dutch government. Of that 45.3 GW, 33.3 GW can be accommodated by the hubs, which, together with 12 GW in planned windfarm areas and known wind search areas (Ministerie van Infrastructuur en Waterstaat, 2025) meets the 45 GW from I13050-DEC. In our NSE5-DEC storyline, we see that only 14 GW of offshore wind must be accommodated in Hub North (wind search areas 6 and 7), which is significantly less than the max. 19 GW assumed possible in the PHPNZ25 (Ministerie van Infrastructuur en Waterstaat, 2025). Of the 14 GW total capacity, we anticipate that 6 GW will be developed in the period 2030-2040, and the other 8 GW in the period 2040-2050. The rate at which the capacity must expand decreases from 2.3 GW/yr in the period 2030-2035, to 1.4 GW/yr in the period 2040-2050.

Offshore hydrogen production capacity in our NSE5-DEC scenario reaches 7.6 GW in 2050, which is 0.4 GW less than the 8 GW assumed in I13050-DEC. Apart from the 0.1 GW (max.) of DEMO-1 (near the Hollandse Kust Noord windfarm), and the 0.5 GW of DEMO-2 (near the TNW windfarm in Hub East), we assume that this hydrogen production capacity will be entirely built in and around Hub North, in conjunction with the 14 GW offshore wind capacity developed there. Of the 14 GW, we again assume that 50% (7 GW) will be connected to electrolysers for hydrogen production. The timeline for development of this capacity follows the timeline of offshore wind capacity build-out, i.e., in 2040 3.6 GW of offshore hydrogen production capacity will be operational (0.6 GW/yr in period 2036-2040), and adding 4 GW in the period 2040-2050 (~0.4 GW/yr) to reach 7.6 GW by 2050.

It is relevant to mention that I13050-DEC additionally assumes 15 GW onshore wind and 183 GW photovoltaic capacity to be installed in 2050 that, together with 20 GW of hydrogen-fired electricity production capacity (no nuclear), and 19 GW of interconnection, must ensure that the electricity demand (364 TWh/yr, 20% less than I13050-NAT) can be met at all times. Furthermore, to meet the assumed hydrogen demand of 102 TWh/yr, 25 GW of flexible (non-dedicated, i.e., grid-connected) hydrogen production is included in 2050, together with 20 TWh blue hydrogen production (~2 GW equivalent capacity at 8000 FLH/yr and requiring CCS) and ~50 TWh import. Interestingly, ~57 TWh/yr of hydrogen is also exported, resulting in a net export of ~7 TWh. Additionally, ~21 TWh hydrogen storage is required in I13050-DEC to match supply and demand and secure supply at all times.

For natural gas production and CCS, the anticipated volumes and foreseen injection capacities are the same for both storylines, and have already been discussed above, as part of the NSE5-NAT storyline.

2.2 Hub designs

For the 2 storylines NSE5-NAT and NSE5-DEC, we defined (spatial explicit) designs (blueprints) per hub for the year 2050. These designs meet the capacity targets for wind and hydrogen as laid down in the 2 storylines (see Table 2.1 and Table 2.3). For all hubs we (initially) focused on the electricity-hydrogen system, defining capacities (and locations) of wind and hydrogen production installations per hub, and calculating how much of each is produced when and where (hourly basis) to quantify transport capacities required (how much must be transported where and how). In the next sections, for each hub, we present the designs for the NSE5-NAT and NSE5-DEC storylines, with focus on assets and infrastructure for production (electricity, natural gas), conversion (hydrogen), and storage of

CO₂. In section 2.3 we detail the transport infrastructure designs for electricity (cables) and hydrogen (pipelines), with focus on hydrogen, and in sections 2.4 and 4.8 we summarize the findings of an exploratory study on the role, potential and feasibility of offshore hydrogen storage.

2.2.1 Hub West

The Hub West designs for the NSE5-NAT and NSE5-DEC storylines (see Figure 2.2) are (almost) the same, except for the fact that in the design of NSE5-DEC, the Lagelander windfarm area is not included. Our expectation is that Hub West will be an electrical hub (capacity ratio electrons: molecules 100:0), because most of the planned wind farms will be operational well before 2035.

GW-scale electrolysis offshore will not mature fast enough to enable investment decisions to be made for installation in the early 2030's, and therefore no hydrogen production is foreseen. In the next sections, for the four commodities (electricity, hydrogen, CO₂ and natural gas), and by period (2025-2035, 2035-2045, and > 2045), we describe in more detail what is included in the design, and explain what information the design choices are based on.

2.2.1.1 Electricity

According to the latest letter to parliament (Ministerie van Economische Zaken en Klimaat, 2024) regarding the offshore wind energy roadmap (Noordzeeloket, 2024), in 2030, the windfarm of Nederwiek 1 (Zuid) should be operational (2 GW, split into NDW 1-A and NDW 1B of 1 GW each). In the period 2031-2035, Nederwiek 2 and 3 (Noord, 4 GW) will become operational. In fact, Nederwiek (NDW) 1, 2, 3 will all be operational by 2032, and spatial planning alignment is currently ongoing. Between 2035-2040 Lagelander (2 GW) might be added, and therefore it is included in the spatial planning process for offshore wind deployment in the period 2031-2040 (PHPNZ25) (Ministerie van Infrastructuur en Waterstaat, 2025) After 2040, WA-3 (2 GW, partly in hub) is planned to be built. In total, the hub design for the NSE5-NAT storyline therefore includes 10 GW offshore wind capacity to be deployed by 2050, all connected electrically to shore (5 x 2 GW HVDC cable). The hub design for the NSE5-DEC storyline excludes the 2 GW offshore wind of Lagelander, hence a total of 8 GW of offshore wind capacity to be deployed by 2050. For the NDW and Lagelander windfarms spatial conflicts with current and future mining activities (natural gas, CO₂, H₂) must be resolved (see also under 2.2.1.3 and 2.2.1.4).

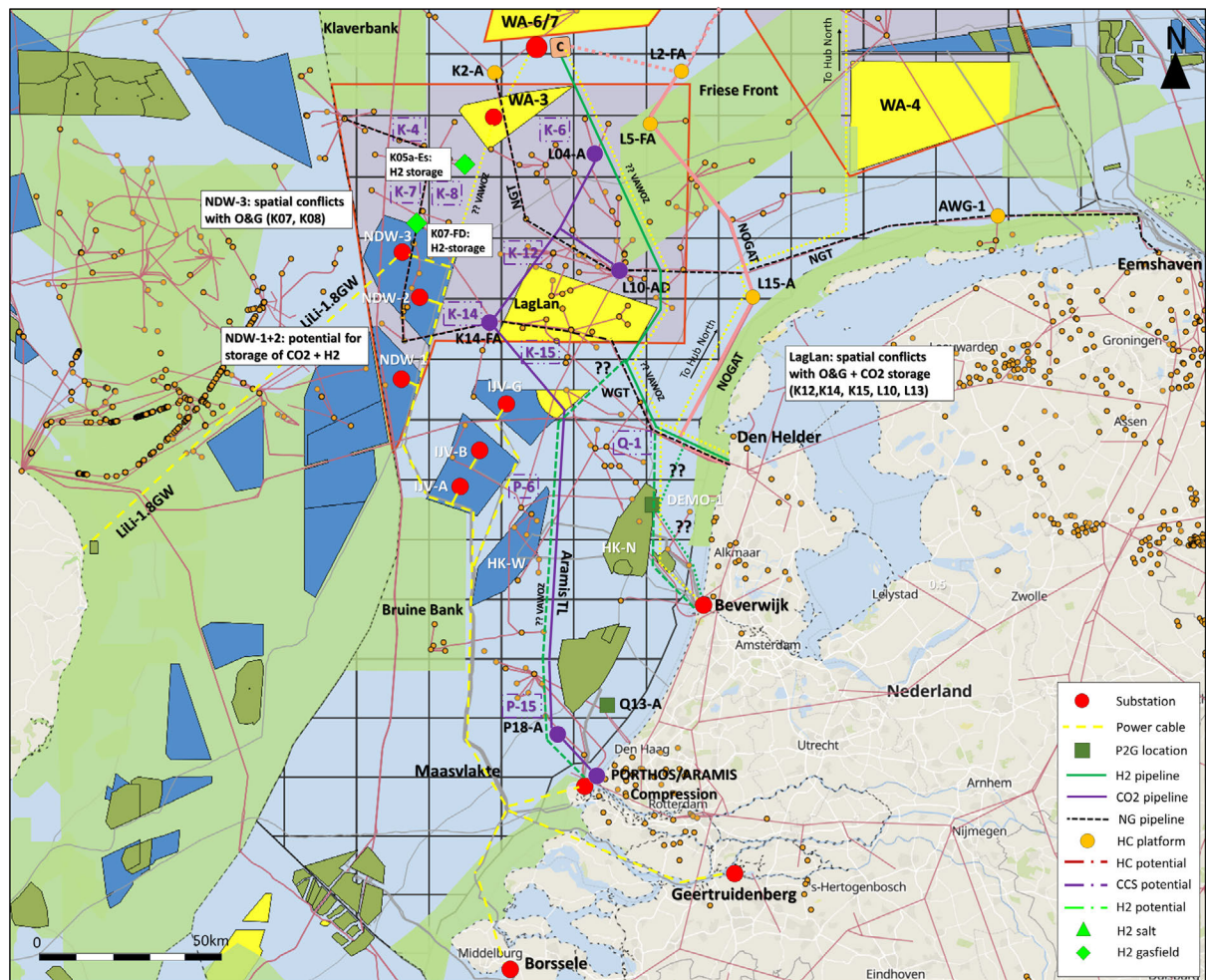


Figure 2.2: Geographic map of the NSE5-NAT design of Hub West. The NSE5-DEC is almost the same, only the Lagelander windfarm is omitted in that design.

The electricity produced will be transported to shore via substations and (bundles of) HVDC cables having 2 GW total capacity (per windfarm), and that land at Borssele (NDW-2), Maasvlakte (NDW-1) and Geertruidenberg (NDW-3). The connection of Lagelander to shore is in scope of the pVAWOZ 2031-2040 program (Arcadis, BRO, Delft, & Pondera, 2024). Additionally, the NDW-3 windfarm will be connected to the UK via the LionLink cable (1.8 GW), and possibly to Belgium (2GW) according to the whitepaper on offshore TSO collaboration of TenneT (TenneT, 2022). Additional flexibility measures will probably be required in a 100 % electrons scenario, hence there may be scope for offshore solar and (electricity) storage at the hub (next to onshore flexibility). However, also for these flexibility measures it may be argued that realizing those before the (early) 2030's may be challenging. Learnings from the planned projects on floating solar in HK-W (5 MWp) and IJVER (50 MWp – Zeevank II), offshore energy storage (HK-W), and the baseload power hub (BLPH) pilot of CrossWind could play an important role in this. In Chapter 4, the impact of including offshore solar and (electricity) storage on the aggregate electricity production profile of the hub is further explored, and in deliverable D3.3 of NSE 5 (van Zoelen, Rob; Boer, Dina; Mahfoofi, Salar, 2025) the economics are quantified. In deliverable D6.3 (Uritsky & Mohanan Nair, 2025), the logistics are further explored.

2.2.1.2 Hydrogen

In our current design, we have not included any hydrogen production in the hub itself because GW-scale electrolysis offshore will not mature fast enough to enable investment decisions to be made for installation in the early 2030's. An alternative design could include green hydrogen production at/near Lageland (and/or WA3), should windfarms be built there in the period between 2032 and 2040 (or beyond), however, to date no plans for this have been publicly communicated. Furthermore, it is worth mentioning that these wind farms will probably be repowered in the period 2045-2055, which would provide an excellent opportunity to integrate (then) technologically mature offshore hydrogen production.

While not within the hub, a relevant development to be mentioned in the area of the Hollandse Kust Noord (HK-N) windfarm, closer to the coast, is the 30-50 MW offshore P2G-H2 demonstration project (DEMO-1), that is planned to be operational towards the end of this decade (2028-2029). The DEMO-1 installation will likely be connected to the HK-N substation for power, and the produced hydrogen will be transported to shore either via an existing pipeline (Gasunie, 2025) or via a new to build pipeline. Furthermore, it is relevant to mention that at Q13A the PosHYdon 1 MW P2G-H2 pilot is sited (also outside of the hub).

Furthermore, the routing of potential future offshore (electricity and) hydrogen transport infrastructure to transport (electricity and) hydrogen from Hub North (wind search areas 6 and 7) to West-NL may run through Hub West (see Fig. 2.2, map of Hub West). Two possible scenarios have been depicted in Fig. 2.2: one that assumes new to build pipelines (36 inch) running southward from the compression station on the south side of Hub North to PoDH, PoA, and POR ("midden" route in pVAWOZ), and another that assumes reuse of NOGAT (36-inch) from L2-FA to PoDH post-2045, when the production of natural gas from gas fields in and around Hub North is expected to have ceased. The two scenarios are described in more detail in section 2.3.

Finally, there may be potential for hydrogen storage in selected gas fields in the hub, for example in fields K05a-Es (TotalEnergies) and K07-FD (Tenaz Energy), requiring a pipeline connecting the field to the hydrogen transport infrastructure. While the distances from K05a-Es (50 km) and K07-FD (70km) to the SW compression station in Hub North (logical tie-in point) is quite large, adding complexity and cost, some of the alternatives for the hydrogen pipeline route in pVAWOZ run much closer to the fields. In our design we have chosen to include the easternmost route of pVAWOZ, because it is the shortest route to Den Helder, however, it runs farthest from the fields. In section 2.4, the potential for hydrogen storage is further detailed, and in section 4.8 notional designs are presented for developing hydrogen storage in salt caverns and reservoirs in and around Hub North and along the hydrogen pipeline routes presented in section 2.3.

2.2.1.3 CCS

The Aramis project is a key project in Hub West (see Fig. 2.2 map of Hub West). The Aramis project (Royal HaskoningDHV, 2024) aims to develop a pipeline for transport (trunkline) of up to 22 Mt/yr of (dense phase) CO₂ from the compression hub at the Port of Rotterdam to a distribution hub (D-HUBN) at K14-FA (Shell Global Solutions) in Hub West. The trunkline route runs from the Tweede Maasvlakte northward, passing west of the windfarm area Hollandse Kust Zuid, east of Hollandse Kust West, and again east of IJmuiden-Ver Gamma, before diverting northwest to K14-FA. At the K14-FA hub, the CO₂ is distributed over several

(depleted) gas fields, owned and operated by Shell (K14-FA, 34-43 Mt capacity), TotalEnergies (L04-A, 34 Mt capacity) and Eni (L10-ADLE, 96 Mt capacity), and for which operator-specific projects are ongoing to develop the fields for CO₂ storage. While the potential for reuse of depleted gas fields is clear, the reuse of platforms and wells is quite limited in the current plans of the operators. Electrification of CCS platforms via the offshore electricity grid is also not foreseen. For platforms without heating equipment for CO₂, the power demand is low (5-10 kW), and alternative solutions (small windmills, solar panels, batteries, back-up generator) are preferred to provide that power. For platforms with heating equipment, the power demand is large (potentially 10s of MW), but very short-lived, and gas-fired heaters are considered the best solution to deliver that power. In the first years of operation of Aramis, until 2030, up to 5.4 Mt/yr of CO₂ is expected to be injected in K14 and L04. After 2030, when L10 is added, this increases to 14Mt/yr, with further potential to increase to the full capacity of the trunkline of 22 Mt/yr by adding more fields. Together with the injection capacity of Porthos of 2.5 Mt/yr (in the P18 fields, 20km from the coast at Rotterdam), this amounts to ≈ 8 Mt/yr by 2030, potentially increasing to ≈ 25 Mt/yr by 2040. Spatial conflicts will arise between potential future CCS developments and the appointed wind area Lagelander, where 2-4 GW of wind capacity is foreseen to be developed. Lagelander coincides with a region with large storage potential, the Aramis CCS infrastructure will be developed (partly) in this region, and there is large potential for CO₂ storage in aquifers.

2.2.1.4 Natural gas

The production of natural gas from Hub West is expected to continue until 2050. EBN forecasts continued production to be between 2-4 bcm/yr until 2030, decline slightly to 2-3 bcm/yr in period 2030-2040, and then decline further to less than 1 bcm/yr in period 2040-2050. Cumulative production from Hub West until 2050 is expected to be ≈ 55 bcm. It must be noted though that these numbers are optimistic forecasts, reflecting the full potential of the area incl. stranded fields and prospects, and that they do not yet include the scenarios in the acceleration plan for natural gas production (“sectorakkoord aardgaswinning”, (Ministerie van Klimaat en Groene Groei, Element NL, and EBN, 2025)). There is a lot of existing infrastructure for natural gas production and transport, and while the expectation is that this infrastructure will be gradually dismantled and removed as production declines, there currently are spatial conflicts with the windfarm areas of Nederwiek that are to be operational by 2032 (EBN, 2023) and similar conflicts exist for the windfarm areas of Lagelander (EBN, 2024) (see Figure 2.3). Lagelander overlaps with one of the historical core areas for natural gas production in the Dutch North Sea.

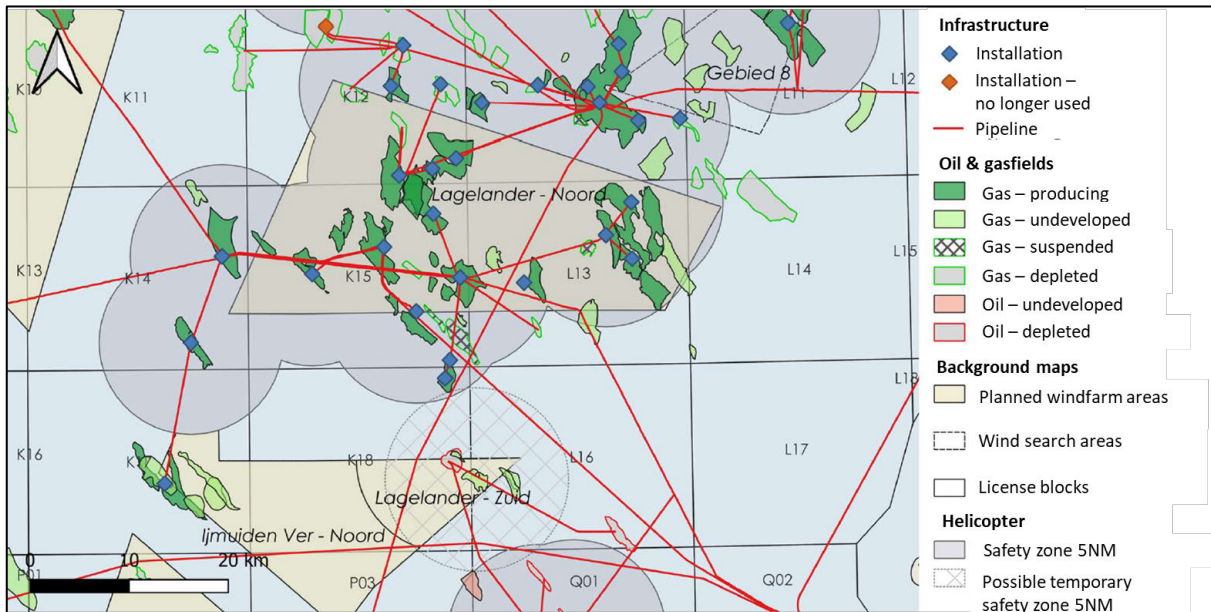


Figure 2.3: Overview of oil and gas activities in and around Lagelander, including an illustrative safety radius of 5 NM around platforms with a helicopter deck (EBN, 2024).

Within the various licensed blocks or parts of blocks within the Lagelander area, there are twenty-eight producing gas fields (resource class 1), half of which can continue to produce until 2050. For six of these assets, EBN expects activities to increase gas production in the next 8 years (resources classes 2 to 5). Furthermore, there are also more than forty stranded assets (resource classes 6 and 7) and many prospects (resource classes 8 and 9) in the Lagelander area, some of which are actively studied by oil & gas operators and could be drilled before 2050 (ref). Solutions to resolve the spatial conflicts that are currently being investigated include reducing the helicopter safety zone to 2.5 NM, and defining a dedicated narrow approach corridor.

2.2.2 Hub East

For Hub East, only one design was developed that applies to both storylines (see Figure 2.4). Our expectation is that the energy produced in Hub East will be mainly transported to shore in the form of electrons, because a) GW-scale electrolysis offshore will not mature fast enough to enable investment decisions to be made for installation in the first half of the 2030s, and b) the 4 GW capacity to be developed post-2040 in wind area 4 is close to nature and multi-use areas, and due to its proximity to shore (40-60 km) transport of the electricity via cable will be more cost-effective⁹. Hence, Hub East is also foreseen to become an electrical hub, but with “demo-scale” P2G, capacity ratio electrons: molecules $\approx 96:4$. In the next sections, for the four commodities (electricity, hydrogen, CO₂ and natural gas), and by period (2025-2035, 2035-2045, and > 2045), we describe in more detail what is included in the design, and explain what information the design choices are based on.

⁹ Interestingly, OPERA-model-based optimization led to cost-optimal offshore hydrogen capacities in Hub East by 2040 (see Figure 3.5 of deliverable D3.1) in the order of 0-1.5 GW by 2040 with median at 0.7 GW.

2.2.2.1 Electricity

In 2030, 0.6 GW offshore wind capacity will be operational, the windfarm Gemini. In the period 2031-2035, Ten Noorden van de Wadden (TNW, 0.7 GW) and Doordewind I+II (DDW-I, DDW-II, 2 x 2 GW) will have been deployed. In the period 2036-2040, an additional 2 GW is planned to be developed (DDW-West), and between 2041-2050 there is potential for (at least) another 4 GW in wind area 4 (WA-4). In total, the Hub East design for the NAT and DEC storylines includes 11.3 GW offshore wind capacity to be deployed by 2050, all connected electrically to shore via HVDC cables.

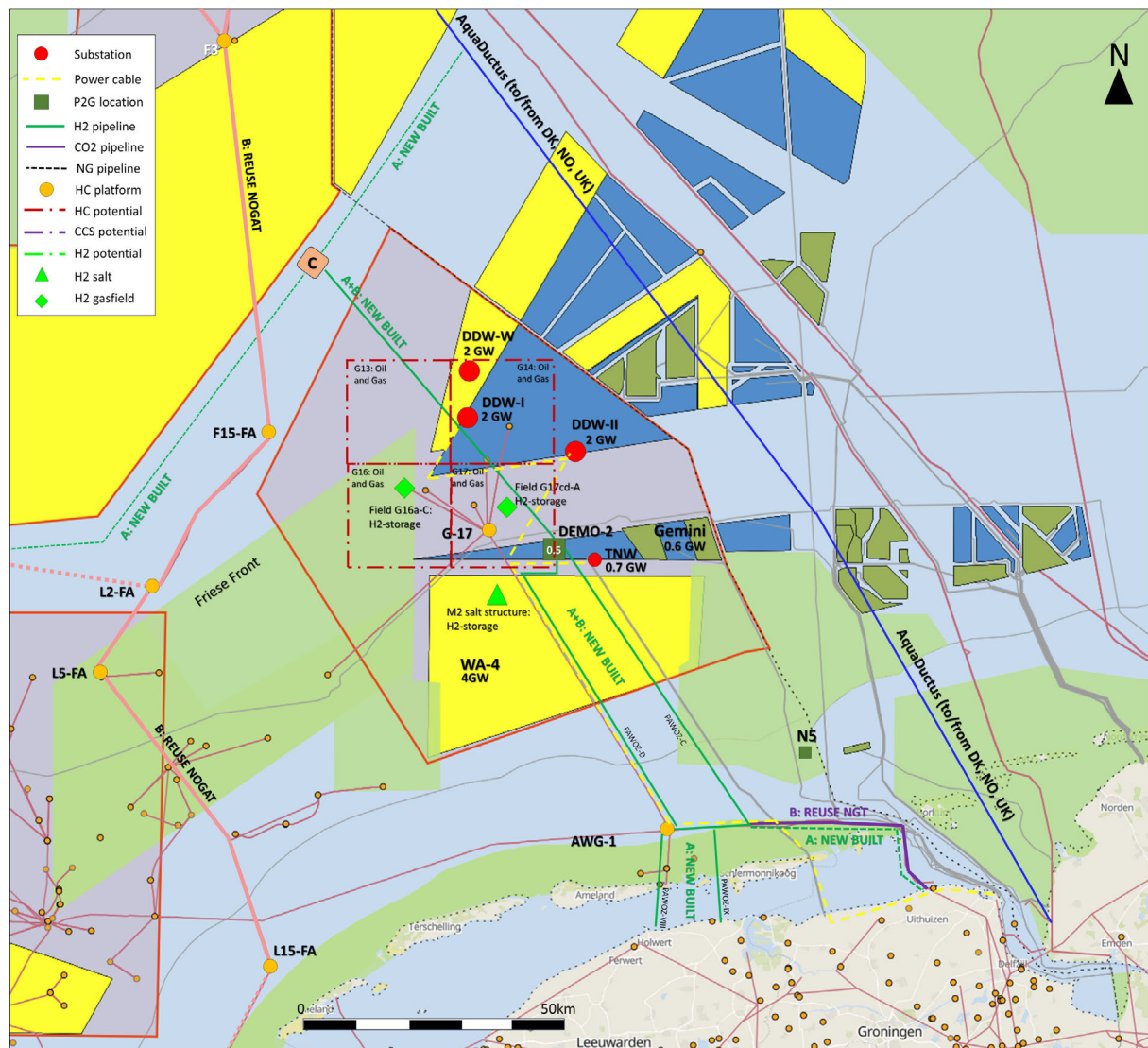


Figure 2.4: Geographic map of the design of Hub West (for NSE5-NAT + NSE5-DEC).

TNW, DDW-I and DDW-2 are planned to be operational in 2033 (in scope of PAWOZ spatial planning process) (Ministerie van Klimaat en Groene Groei, 2025). DDW-W is in the spatial planning consultation (PHPNZ25) for period 2032-2040. It is uncertain whether a windfarm can be economically built there, primarily because the assigned area has an unfavourably narrow, elongated geometry that limits the room for optimizing placement of the wind turbines. WA-4 (4 GW, (ENTSO-E, 2024)) is planned for period after 2040. The electricity produced will be transported to shore via substations and (bundles of) HVDC cables having 2 GW total capacity (per windfarm), and that land at Eemshaven. To optimize cable utilization,

additional flexibility measures may be required, hence there may be scope for adding offshore solar and (electricity) storage in this hub (next to onshore flexibility). In February 2025, a design for the preferred routing for the cables (2 x 2 GW HVDC) from DDW-I and DDW-II substations to shore was published in the context of the PAWOZ programme (Ministerie van Klimaat en Groene Groei, 2025). The routing between the 2 substations runs along the SW-outskirts of the DDW area, and then from the DDW-II substation to the westernmost tip of TNW, from where the cable route runs along an existing pipeline for natural gas from the G17-d platform to the AWG-1 platform close to Ameland. From AWG-1 it then runs east along the NGT pipeline to cross the Wadden Sea via a tunnel under Schiermonnikoog to land onshore at Kloosterburen. From Kloosterburen it then runs further east to Eemshaven.

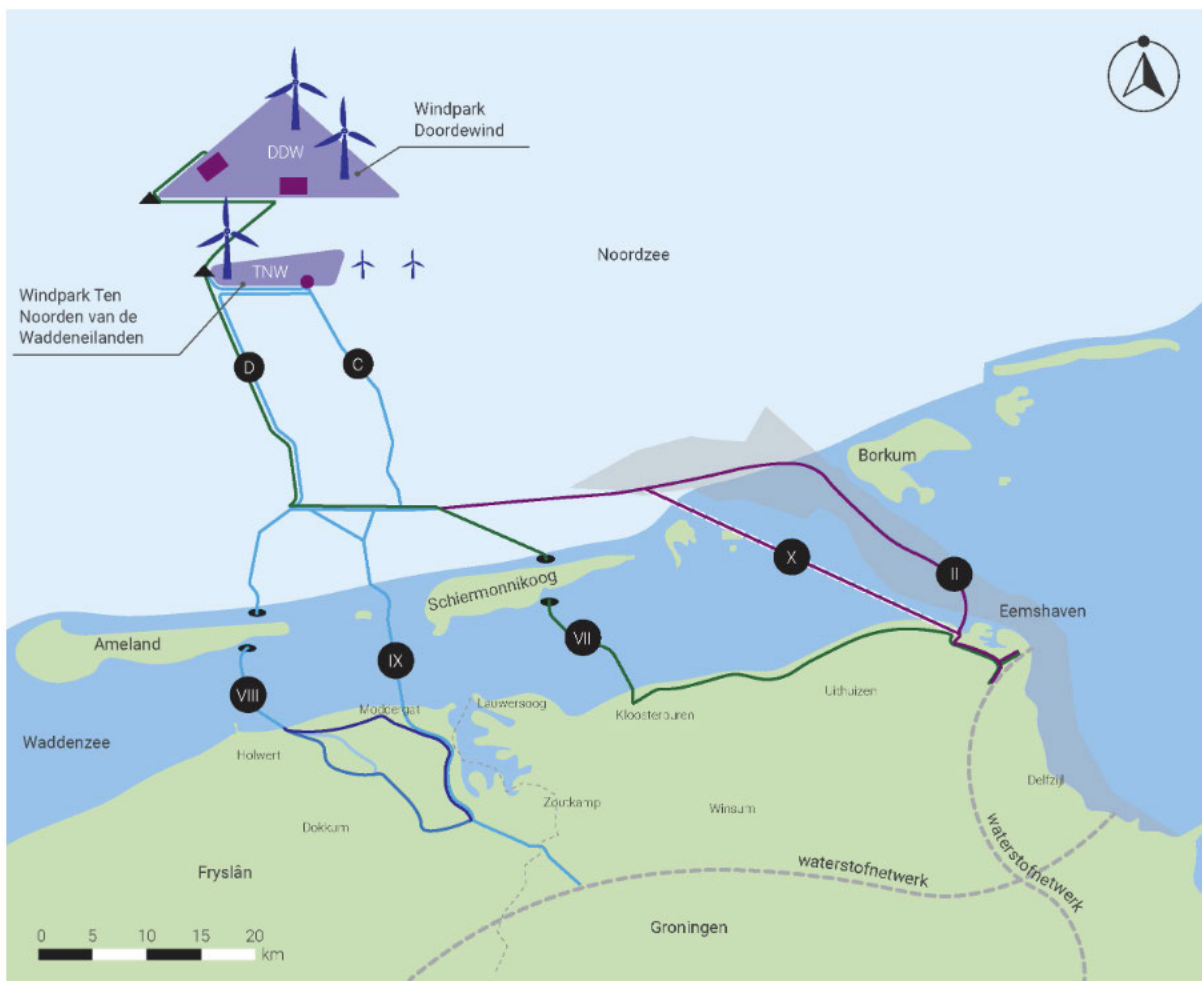


Figure 2.5: Preferred routes for transport of electricity from the Doordewind windfarm areas (DDW, in green, labelled D and VII) and hydrogen produced at DEMO-2 near the Ten Noorden van de Wadden wind farm area (TNW, in light blue, labelled C, D, VIII and IX) to shore. Purple lines (labelled II and X) indicate cable routes for future windfarms beyond TNW and DDW, e.g., in and around Hub North.

It is yet undecided what capacity the TNW grid connection will get, this relates to the plans for DEMO-2 (see below). In the recent letter to Parliament (Ministerie van Economische Zaken en Klimaat, 2024) about the demos, a 200 MW connection of TNW to a substation of

DDW is mentioned. For the TNW and DDW windfarms (EBN, 2023) spatial conflicts with current and future mining activities (natural gas, CCS, hydrogen) are yet to be resolved.

2.2.2.2 Hydrogen

In our NAT and DEC designs for Hub East we have included only 0.5 GW of hydrogen production in the hub, this is the announced demonstration project at TNW (DEMO-2) that is planned to be operational in 2033. DEMO-2 will connect to TNW, and TNW will have a 200 MW cable connection to a DDW substation (in scope of PAWOZ). No offshore hydrogen production is included at DDW-West, because its (commercial-scale) deployment, together with the windfarm itself (in period 2032-2040 according to pVAWOZ), would have to follow too soon after DEMO-2 becomes operational to properly include the learnings from DEMO-2. Moreover, it is uncertain whether the DDW-W windfarm itself will be built (see section 2.2.2.1). No offshore hydrogen production is included for WA 4 either, due to closeness to shore and restrictions imposed by presence of nature and multi-use areas.

In February 2025, two preferred alternatives for transport of hydrogen from DEMO-2 to shore via a new to build pipeline (48") were communicated (Ministerie van Klimaat en Groene Groei, 2025) (see Fig. 2.5). One route runs along an existing pipeline for natural gas from the G17-d platform (near the western tip of TNW) to the AWG-1 platform close to Ameland, while the other follows a "new" route from the TNW substation SSE to a location along the NGT pipeline above the western tip of Schiermonnikoog. From those two locations, there are two routes to cross the Waddensea, one that tunnels under Ameland to land near Holwerth, and another that runs just west of Schiermonnikoog to land near Moddergat. From these onshore locations, the routes connect to the onshore hydrogen pipeline further south. It must be noted that besides these routes for a new to build pipeline, there is also a third option for crossing the Wadden Sea that is being investigated, one that would use the NGT pipeline section running between AWG-1 and Eemshaven (36 inch). Furthermore, in our designs we have assumed that the pipeline from DEMO-2 to a landing point at or close to Eemshaven will ultimately be extended from DEMO-2 towards the northwest to connect to offshore hydrogen production facilities that would be developed in Hub North. The transport routes as described above have been included in the designs of the transport infrastructure that are described in more detail in section 2.3.

Finally, there may be potential for hydrogen storage in salt structures and selected gas fields in the hub, for example in salt structure M2, and in G16a-C and G17Cd-A (Eni), requiring a pipeline connecting the caverns or gasfield(s) to the hydrogen transport infrastructure. The two fields and the salt structure all lie close to the hydrogen pipeline route included in our design, i.e., less than 20km away, and quite close to DEMO-2 and the TNW and DDW substations for power, making them interesting candidates. In section 2.4, the potential for hydrogen storage is further detailed, and notional designs are presented for developing hydrogen storage in salt caverns and reservoirs in and around Hub North and along the hydrogen pipeline routes presented in section 2.3.

2.2.2.3 CCS

In and around Hub East there are currently no active CO₂ storage projects. It is possible that storage potential in empty gas fields will be identified in the future, in particular in the G14-

A&B fields, with the platforms (including helicopter approach routes) possibly being reused (EBN, 2023).

2.2.2.4 Natural gas

The production of natural gas from Hub East is expected to continue until 2050. EBN forecasts continued production to be between 0.2-0.3 bcm/yr until 2030, increasing to 0.5-1.0 bcm/yr in period 2030-2040, and then decline again to less than 0.5 bcm/yr in period 2040-2050. Cumulative production from Hub East until 2050 is expected to be ≈ 15 bcm. It must be noted though that these numbers are optimistic forecasts, reflecting the full potential of the area incl. stranded fields and prospects, and that they do not yet include the scenarios in the plans for accelerating natural gas production. There is existing infrastructure for NG production and transport, and while the expectation is that this infrastructure will be gradually dismantled and removed as production declines, there currently are spatial conflicts with the windfarm areas of Doordewind (DDW-I, DDW-II, DDW-West) that are to be operational in the period 2031-2035. Studies are being run to solve these conflicts.

2.2.3 Hub North

This section describes the nature-inclusive designs for NAT and DEC, which are quite different (see Figure 2.6 and Figure 2.7). Hub North includes the wind (search) areas 6 and 7 and the area in-between, with a potential for deployment of offshore wind of 18-28 GW according to the PHPNZ23 (Ministerie van Infrastructuur en Waterstaat, 2023) No decisions have yet been communicated though regarding the allotment of these areas for wind farm development. Our expectation is that in Hub North a significant hydrogen production capacity will be deployed, because a) its distance to shore makes transport in the form of molecules more cost-efficient, b) post-2035 the onshore grid and onshore demand will increasingly face difficulty in absorbing all electricity as electricity, and to reduce large-scale curtailment of electricity, conversion to hydrogen could be attractive¹⁰. In the ongoing pVAWOZ 2031-2040 planning process, 6-7 cable connections of 2 GW each are considered, confirming that at least 12-14 GW of wind capacity is expected to be electrically connected to shore. Our NAT design of Hub North includes 20 GW of wind capacity and 10 GW hydrogen production capacity, while our DEC design includes 14 GW wind capacity and 7 GW hydrogen production capacity.

¹⁰ This expectation is confirmed by system modelling performed in WP 3 (see (Blom, van Stralen, Eblé, Magan, & Hers, 2025) report).

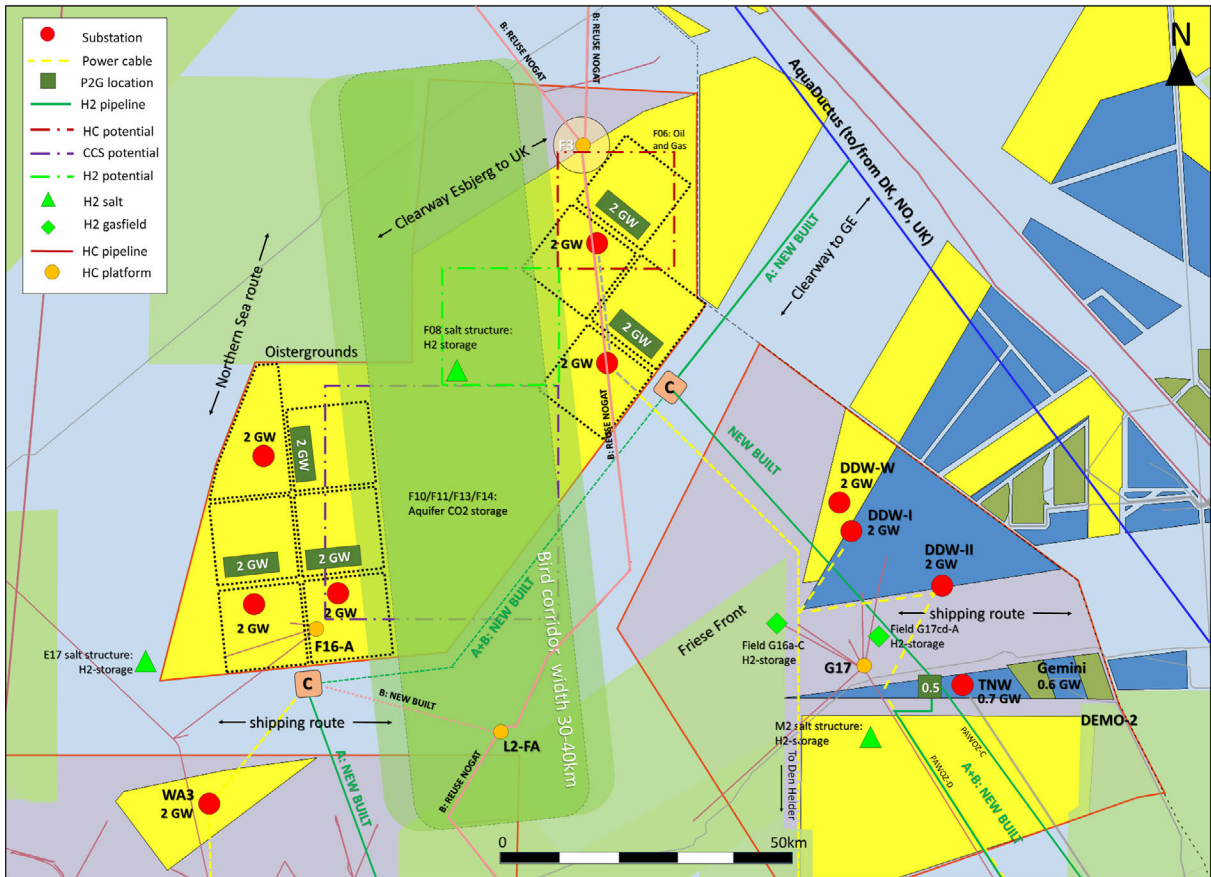


Figure 2.6: Geographic map of the design of Hub North for storyline NSE5-NAT.

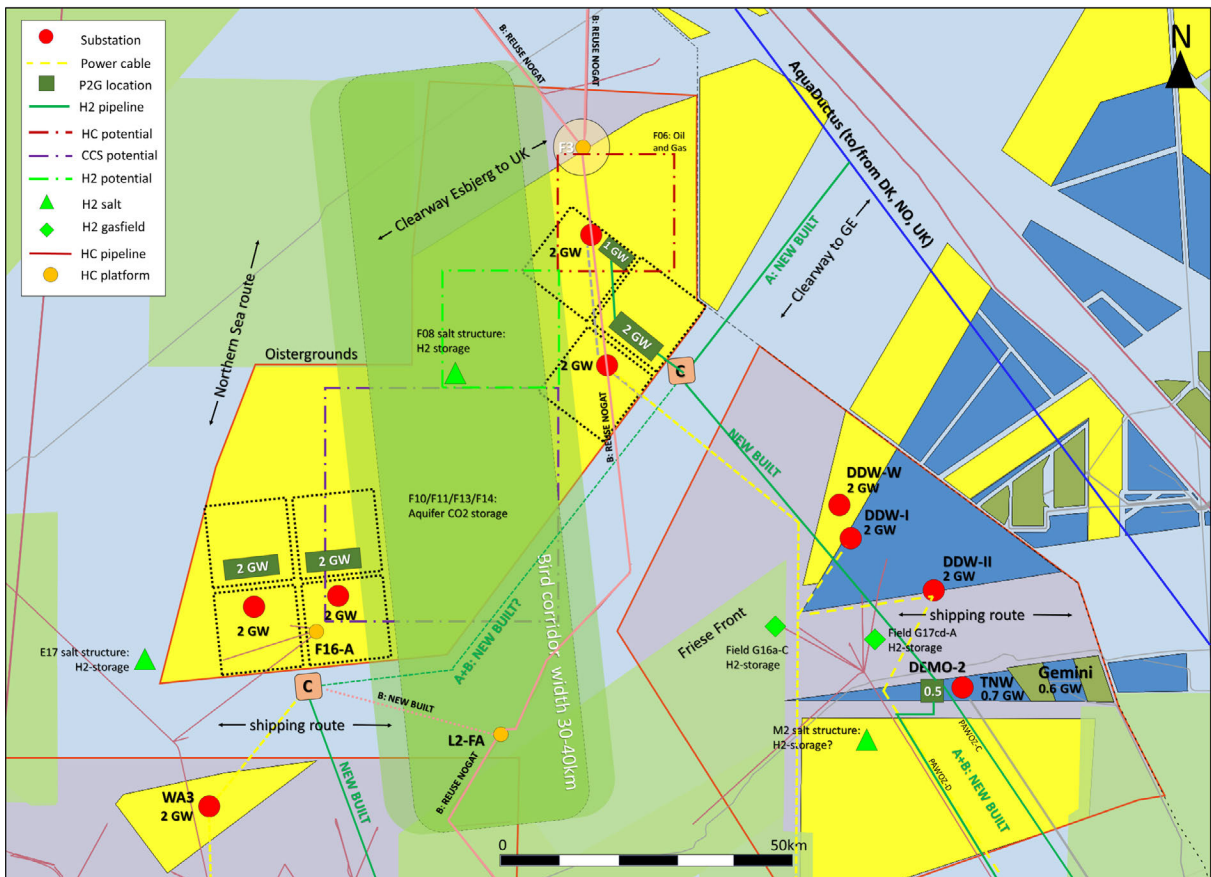


Figure 2.7: Geographic map of the design of Hub North for storyline NSE5-DEC.

Our NAT design of Hub North includes 20 GW of wind capacity and 10 GW hydrogen production capacity, while our DEC design includes 14 GW wind capacity and 7 GW hydrogen production capacity. A key feature of the designs is the ecology corridor. This SE-NW running corridor should have a width of 30-40km to enable (water)birds and mobile species (pelagic species and marine mammals) to pass safely from coastal areas to the open seas beyond the EEZ . It connects the nature area Friese Front, lying southeast of the hub, with the nature area Oistergrounds, lying northwest of the hub.

With assumptions as stated, 20 GW wind capacity requires 10 plots of 200 km², amounting to 2000 km² in total, which is ≈ 50% of the available space in the hub (≈ 4200 km²). Each plot should house not only the 96 wind turbines and electrical infrastructure (e.g., a substation, cabling), but also the required installations and infrastructure for hydrogen production.

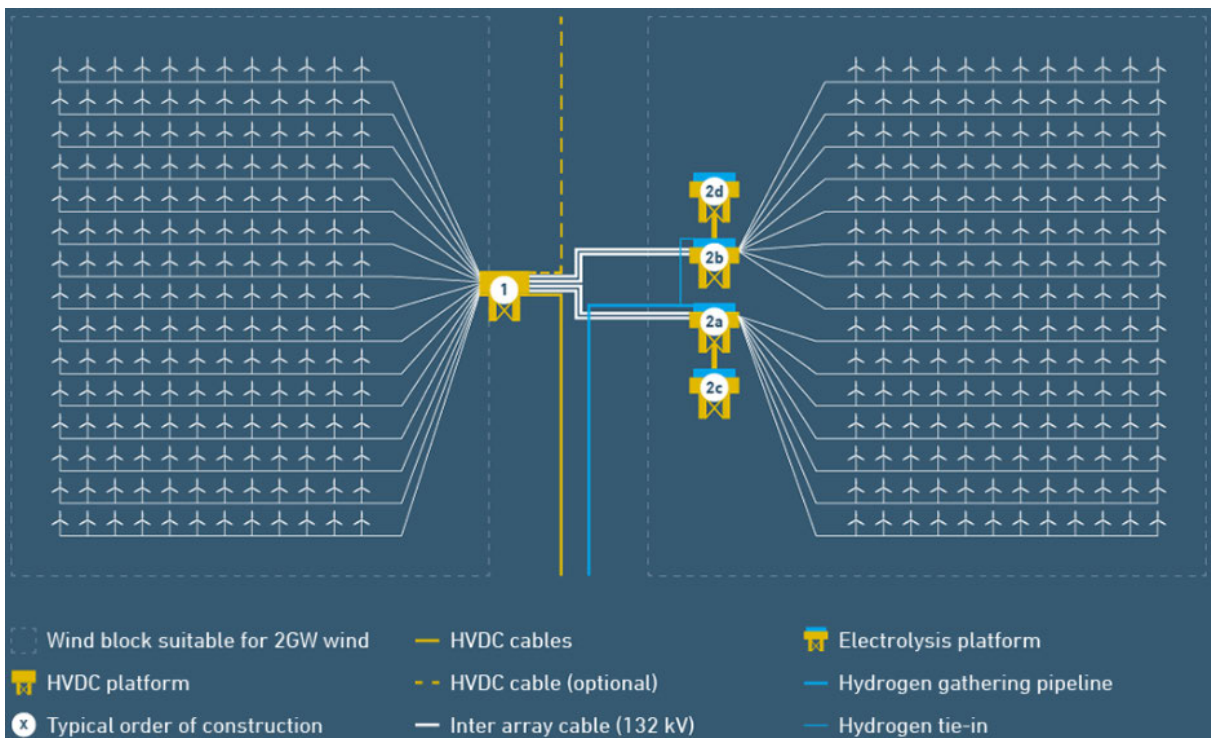


Figure 2.8: Blueprint of 4GW module that includes 2 windfarms of 2 GW capacity and 2 GW of centralized (platform-based) hydrogen production (North Sea Wind Power Hub Programme, 2024)

The NSWPH consortium has published (blueprint) designs for hydrogen production integrated within windfarms (North Sea Wind Power Hub Programme, 2024). One of the designs is for a 4 GW module that includes 2 windfarms of 2 GW capacity and 2 GW of centralized (platform-based) hydrogen production (see Figure 2.8). Each 4GW module consists of wind turbines (192 in our case, assuming 21MW turbines and 4 hydrogen production platforms of 500MW connected capacity each (of which 475 MW is directly used by the electrolyser, remaining 25MW is for BOP). The wind turbines of one of the two wind farms are connected to a substation of 2 GW (HVDC) with 132 kV interarray cables, while the wind turbines of the other wind farm are connected to the hydrogen production platforms with 132 kV interarray cables. Furthermore, the hydrogen production platforms are connected to the substation to receive electricity from shore should this be required, i.e., the substation is connected to shore with a bi-directional cable. Finally, to transport the

produced hydrogen, platform tie-ins and a gathering pipeline are included that run from the platforms to the offshore hydrogen grid, possibly via a compression platform where it is first compressed to grid pressure.

In our designs we have taken the 4GW module of NSWPH as a building block. To reach the desired capacity of 20GW wind capacity and 10GW hydrogen production capacity, we need to place 5 modules in the “free” area that remains to the SW and NE of the ecology corridor. NSWPH proposes a 12 GW hub (blueprint) design (North Sea Wind Power Hub Programme, 2024), consisting of 3 modules of 4 GW each and one compression platform with a capacity to compress an amount of hydrogen that is produced from 5.2 GW of wind at peak production capacity (see Figure 2.9). This 12 GW hub we have placed in the SW area of the hub, and would be connected to landing points onshore in/near the ports of Den Helder and/or Amsterdam and/or Rotterdam (to be decided as part of pVAWOZ 2031-2040) with 3 bidirectional HVDC cables of 2GW capacity each, and 1 hydrogen pipeline landing near Den Helder to connect to the onshore hydrogen grid. For the remaining 8GW, 2 modules of 4 GW and a 3.5 GW capacity compression platform would be required, which we have placed in the NE area of the hub. This capacity would be connected electrically to the West-NL shore with 2 HVDC cables of 2 GW capacity each, and with a hydrogen pipeline connecting to Eemshaven via DEMO-2. Spatially this configuration appears to be possible, when assuming that there is a certain degree of freedom in optimizing the geometry and position of the wind farm plots to the space available. A more detailed spatial analysis on the basis of design studies for the wind farms to be built can confirm this, however this was outside of the scope of NSE5.

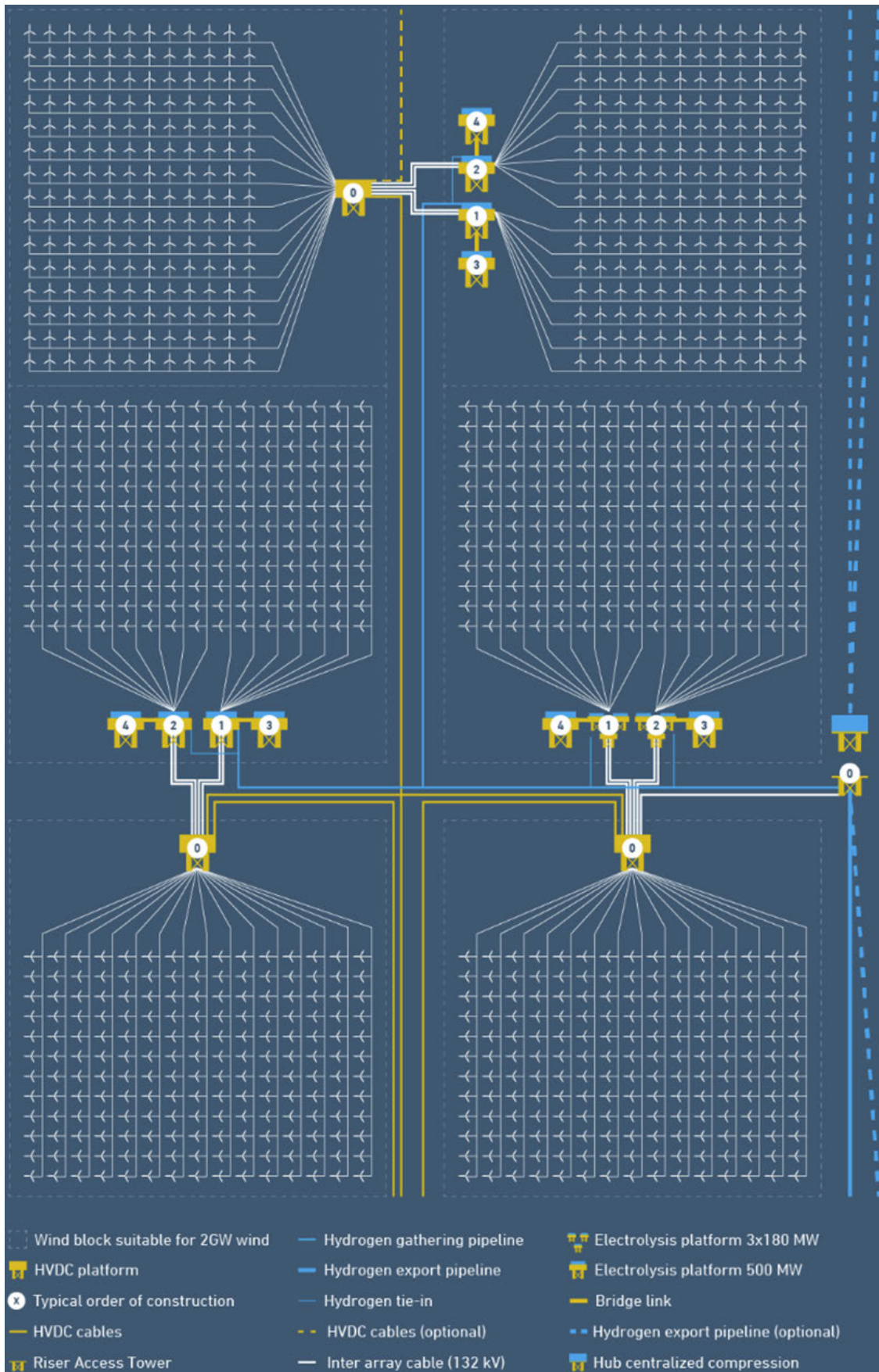


Figure 2.9: Blueprint of 12GW hub consisting of 3 modules of 4 GW each and one hub-centralized compression platform (North Sea Wind Power Hub Programme, 2024)

The DEC design (Figure 2.7) includes 14 GW wind capacity and 7 GW hydrogen production capacity. With the same assumptions for the wind farm design, that result in a power density of 10 MW/km², the required space amounts to 1400 km², which is ≈ 33% of the total available space in the hub. Taking again the 4 GW module of the NSWPH consortium as a building block, 3 modules plus 1 additional 2 GW windfarm with 1 GW hydrogen production are needed to reach the desired capacity (14 GW wind, 7GW hydrogen production). In our DEC design of Hub North, we have placed 2 modules of 4 GW plus a 3.5 GW compression platform in the SW area of the hub that would require 2 HVDC cables of 2 GW capacity and 1 hydrogen pipeline to transport electricity and hydrogen to landing points onshore in West-NL. The remainder (1 module, the single 2 GW windfarm with 1 GW hydrogen production, and a 3 GW capacity compression platform, and requiring 2 HVDC cables and a pipeline for transport to the West-NL shore) we have placed in the NE area, leaving the ecology corridor unmodified. Alternatively, a design that places all capacity to the SW of the ecology corridor would be possible (ref. map of alternative DEC design, see Figure 2.10), with the advantage of concentrating all activity in one area while leaving the area to the NE of the corridor undisturbed, where summer stratification is strongest (van der Heijden, et al., 2025).

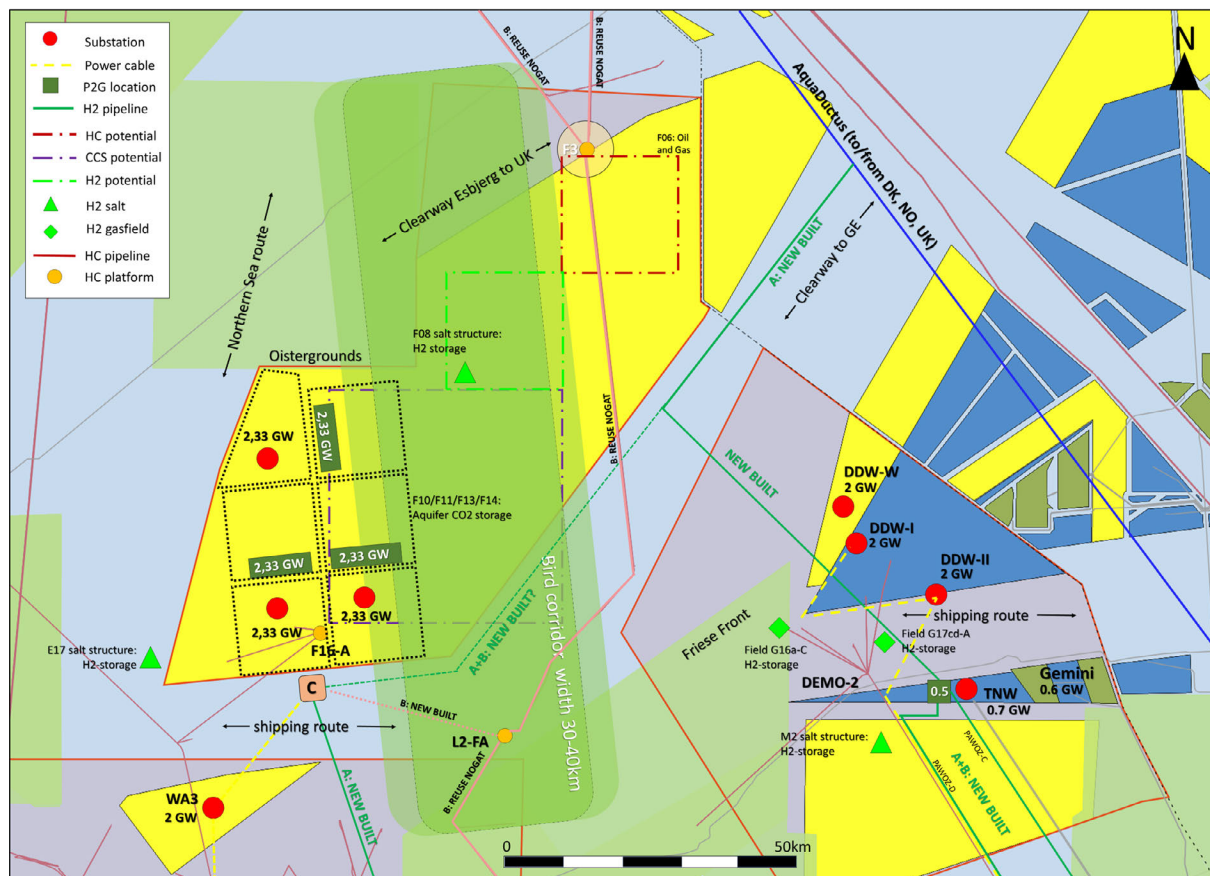


Figure 2.10: Geographic map of the alternative design of hub north for storyline NSE5-DEC.

To fit all capacity in the SW area of the hub the plot size can be increased to 233 km², this would require that the ecology corridor is shifted ≈ 5-10 km to the east. Alternatively, the “standard” 12 GW hub (blueprint) design of NSWPH (with 3 modules of 4 GW) would have to be modified by allowing 0.33 GW overplanting in the 2 GW wind farm plots (increasing the power density to 11.7 MW/km²) and increasing the hydrogen production capacity in each of

the 3 modules by 0.33 GW. However, increasing the power density will attenuate wake effects, resulting in a lower wind farm yield (see also Section 0).

2.2.3.1 Hydrogen

In our NAT design, we have included 10 GW of hydrogen production capacity, while in the DEC design, only 7GW is included. In the previous section, the (modular) NSWPH (blueprint) design(s) of the integrated wind-hydrogen assets that we use as building blocks for our hub designs was already detailed (see Figure 2.8 and Figure 2.9). Here, it is worth mentioning that the NSWPH consortium published designs not only for platform-based hydrogen production, but also for island-based and turbine-based hydrogen production (North Sea Wind Power Hub Programme, 2024). Designs are presented for an island with 10 GW of wind capacity connected and 6GW of hydrogen production capacity as well as for a 4 GW windfarm with 2 GW turbine-based hydrogen production capacity. For our hub designs, we decided to assume 500 MW sized platform-based hydrogen production, because it is expected to (ultimately) become the standard. It includes 475 MW electrolyser capacity (PEM), producing hydrogen at 30 bar pressure, a desalination unit (reverse osmosis or thermal), and sea water cooling. The platform requires a plot space of 70 m x 110 m, is 40 m high (3 decks), and weighs 24,000 tons. Two smaller-scale platform solutions are also presented, with capacities of 30-50 MW (intended size of DEMO-1) and 180 MW. Especially the 180 MW-size platform is considered an interesting intermediate size, e.g. for demonstration projects (e.g., DEMO-2) or during scale-up, because among others it is suitable for converting power from two inter-array cables supplying 90 MW each, it can be installed with float-over as well as dual crane heavy lift vessel, it has a process design like 500 MW platform design, and it has reasonable costs and is weight effective, compared to 500 MW (North Sea Wind Power Hub Programme, 2024).

For the transport of the hydrogen produced in the hub (and in yet unassigned areas to the west and north of the hub, in the NSE5-NAT storyline), pipeline routes are included in the design that connect the 2 compression stations in the SW and NE of the hub to landing points at Eemshaven and Den Helder. One transport scenario assumes new to build pipelines (48 inch) for the routes, while the other scenario assumes reuse of 36-inch sections of NGT and NOGAT post-2045, when the production of natural gas from gas fields in and around the hub is expected to have ceased. Furthermore, connections are also proposed between the 2 compression stations to close the “ring”, and to AquaDuctus, for import of hydrogen from Norway and Denmark. The two scenarios are described in more detail in section 2.3.

Finally, there may be potential for hydrogen storage in salt structures and selected gas fields in and around the hub, for example in salt structures F08, E17, and M2, and in fields G16a-C (Eni) and G17Cd-A (Eni) in Hub East, and fields K05A-Es and K07-FD in Hub West, requiring a pipeline connecting the caverns or gasfield(s) to the hydrogen transport infrastructure. For the two fields and the M2 salt structure that lie in Hub East, and for the 2 fields that lie in Hub West, this was already discussed in sections 2.2.1. and 2.2.2. For the salt structures E17 and F08, distances to the nearest compression station are \approx 50km, where compression capacity and power is available. In section 2.4, the potential for hydrogen storage is further detailed, and in section 4.8 notional designs are presented for developing hydrogen storage in salt caverns and reservoirs in and around hub north and along the hydrogen pipeline routes presented in section 2.3.

2.2.3.2 CCS

CO₂ storage potential is being explored in this hub. EBN expects that this activity will mostly take place in deep saline aquifers. An initial screening shows that the geological formations of the Triassic have high potential for CO₂ storage, notably in blocks F10, F11, F13 and F14 and in blocks F07 and F08. The highest potential is just outside of the hub on the north side. While the timeline for the development of CO₂ storage in this hub is uncertain, and may only start post-2040, the spatial claim it may have must be taken into consideration in the spatial planning of the hub. In its memo (EBN, 2023), EBN shows two spatial planning scenarios for future mining activities that mainly differ in the spatial claim of CCS activities, in particular platforms that, under current regulations, require a 5 nautical mile safety zone for helicopter approach. As can be seen, future CCS (and oil & gas production) activities mainly impact the northeastern region of Hub North.

2.2.3.3 Natural gas

The production of natural gas from Hub North is expected to continue until 2050. EBN forecasts continued production to be about 0.1 bcm/yr until 2030, increasing to 0.4 bcm/yr in period 2030-2040, and then decline again to 0.3 bcm/yr in period 2040-2050. Cumulative production from Hub North until 2050 is expected to be ≈ 7 bcm. It must be noted though that these numbers are optimistic forecasts, reflecting the full potential of the area incl. stranded fields and prospects, and that they do not yet include the scenarios in the plans for accelerating natural gas production. Furthermore, in various licensed blocks or parts of blocks within the hub, oil and gas activities are planned, incl. fields expected to be developed in the short term (before 2030) and prospects (not yet proven hydrocarbon occurrences) that can be drilled in the future. If hydrocarbons are proven in the prospects (economically recoverable volumes), they might be developed. While there is existing infrastructure for natural gas production and transport in the hub, in the form of platforms and pipelines, most of it will be dismantled before the first windfarm will be developed (platforms E18-A and F16-A on the south side of the hub) by the early 2030s. Only platform F3-FB will likely remain in operation and the spatial claim for helicopter approach is therefore accounted for in the hub design. Furthermore, there is prospectivity in blocks F06 and F09 (and in F02, F03 just north of the hub), and the associated potential spatial claim also impacts mainly the northeastern region of Hub North (see Figure 2.11).

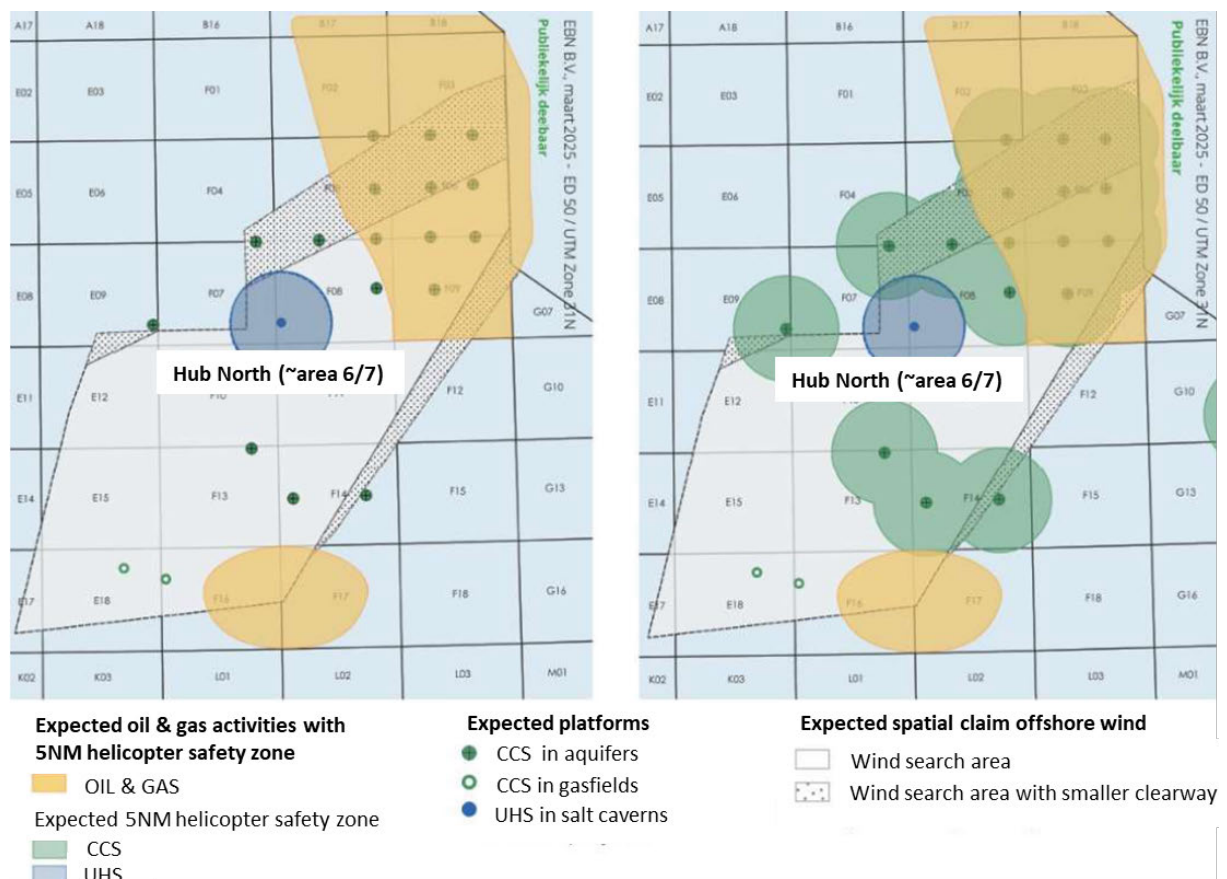


Figure 2.11: Two concept scenario's for the development of the technical mining potential of Hub North (oil & gas, CO₂ en H₂ storage). The amount of platforms for CO₂-storage in aquifers is roughly estimated based on the technical potential of the aquifer. The positioning of the platforms is also conceptual. Based on the current knowledge, a cluster of platforms is required to develop the storage of hydrogen in the salt cavern. This cluster is on the figure displayed as one platform for the sake of clarity. Obstacle free zone are kept to 5NM, in agreement with current practices in the Netherlands. Future development might lead to a reduction of this obstacle free zone. Source: EBN (EBN, 2023).

2.3 Transport infrastructure scenarios

All the energy that is produced in the hubs, and not used by assets in and around the hubs, must be transported to shore, either in the Netherlands, or to other countries around the North Sea. Electricity is transported most efficiently over long distances with (525 kV) HVDC cables. While windfarms built in the past were connected via HVAC (closer to shore, lower capacity), for the windfarms that are yet to be developed in the hubs, with capacities of 1 GW or more, and located at significant distances from shore, HVDC will be the standard. As the TSO for electricity in The Netherlands, TenneT is (also) the responsible party for developing the offshore infrastructure. In recent years, TenneT has constructed the infrastructure for the windfarms that are now operational (Egmond aan Zee, Gemini, Borssele, Hollandse Kust), consisting of substations, where the (interarray) cables that transport the electricity from the turbines at 66 kV (AC) come together and where the voltage is increased to 220 kV (AC), and HVAC cables (220 kV), which transport the electricity to shore (see Fig. 2.12) (TenneT, 2025).

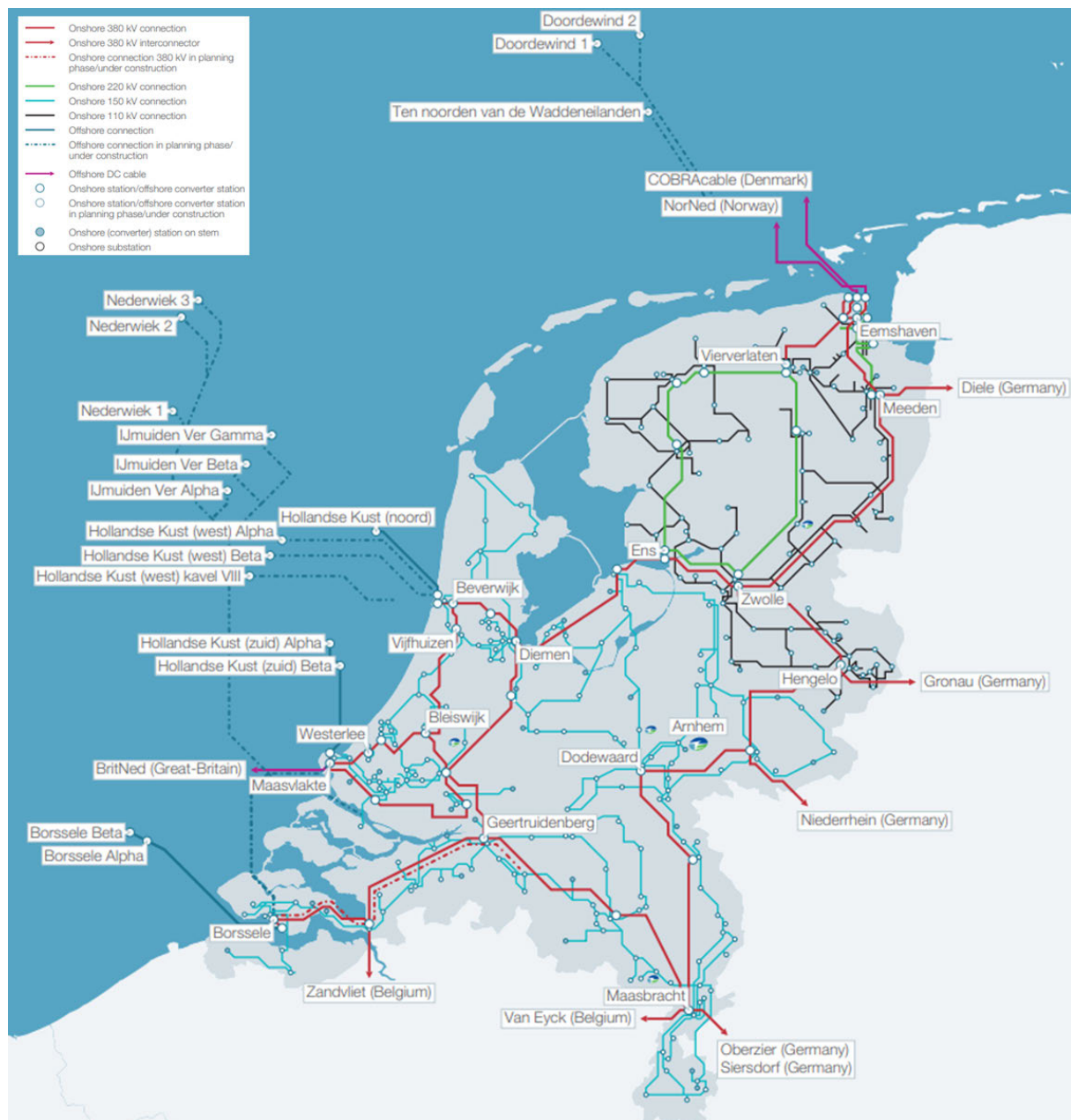


Figure 2.12: TenneT grid map displaying operational and planned (routes of) cables connecting offshore windfarms to the onshore grid (source: (TenneT, 2025)).

For the windfarms that are to be built in the period until 2032 as part of the Dutch offshore wind energy roadmap, and that have a capacity of 1 GW or more ((IJmuiden Ver, Nederwiek, Doordewind), TenneT has developed a standardized design for a 2 GW (converter) substation and (bidirectional?) cable with 2 GW capacity to transport electricity to shore over long distance. All these connections are either in the planning or construction phase, and their exact routing is (mostly) known (see Figure 2.12) (TenneT, 2025), hence they have been included in the maps with the hub designs as such, together with already operational connections. Most recently, a design for the preferred routing for the cables (2 x 2 GW HVDC) from DDW-I and DDW-II substations to shore in the Eemshaven region was published in the context of the PAWOZ programme (Ministerie van Klimaat en Groene Groei, 2025) (see also 2.2.2.1).

For wind search areas that are to be developed post-2032 (Lagelander in Hub West, DDW-West in Hub East, and wind search areas 6 and 7 in Hub North), a public consultation process will open in May 2025: the VAWOZ programme (Arcadis, BRO, Delft, & Pondera, 2024). pVAWOZ proposes different routings, locations and landing points for electrical infrastructure (HVDC cables, substations) to transport electricity from wind search areas 6 and 7 in hub north to shore in West-NL (see Figure 2.13), and for pVAWOZ foresees that 6-7 2 GW HVDC cable connections will be required. In our designs of Hub West and hub north, we have drawn the most western cable route for transport of electricity from to be developed windfarms in the SW area of hub north, i.e., the route that runs via wind search area 3 to the Nederwiek-3 windfarm, and from there follows the chosen cable routing to Rotterdam and Zeeland regions. However, it is expected that additional routes proposed in pVAWOZ that run through or just east of Lagelander may also be required to transport electricity to the Amsterdam/IJmuiden and Den Helder regions.

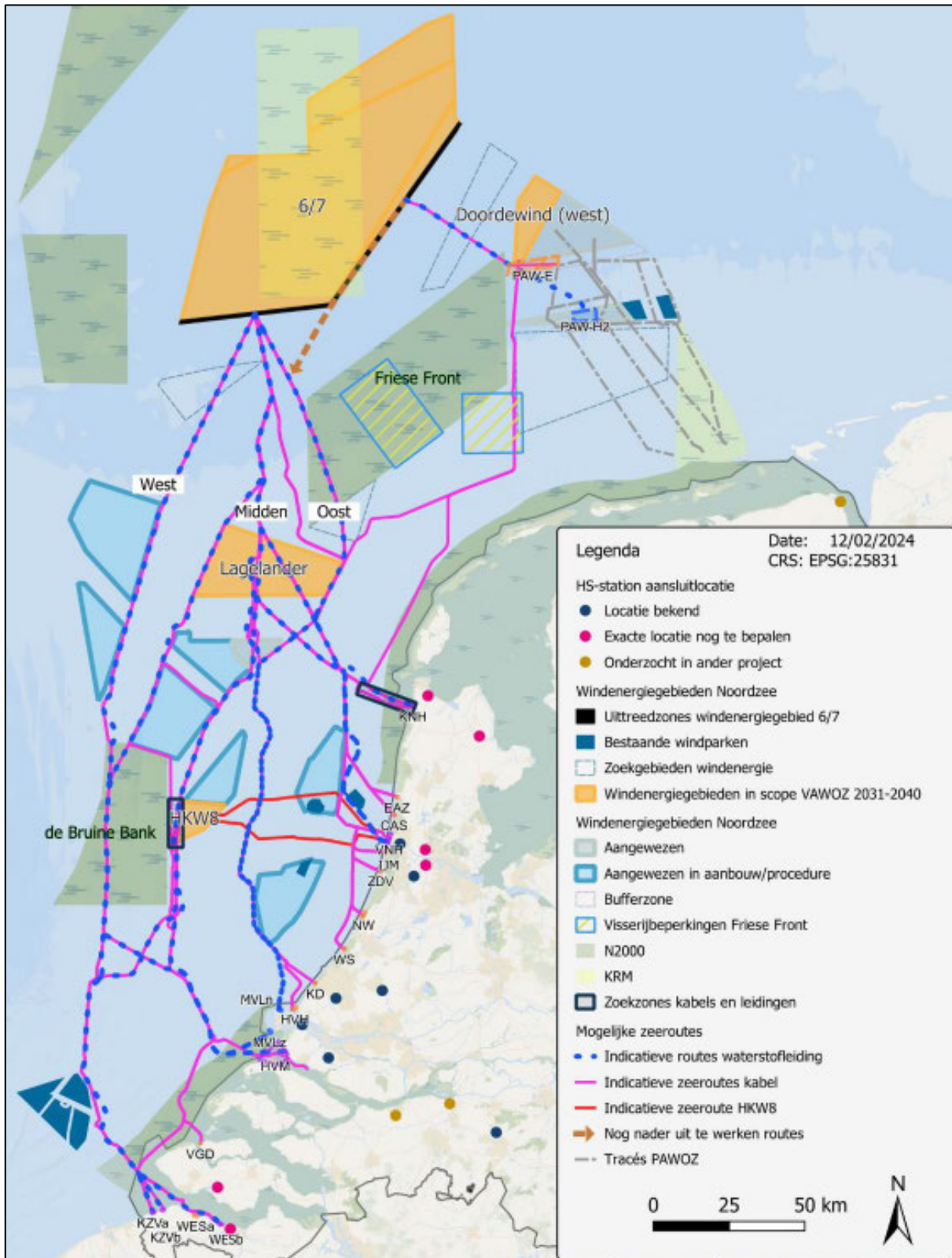


Figure 2.13: Possible routes for transport of electricity (pink lines) and H₂ (blue dashed lines) from Hub North (wind search areas 6 and 7) to landing points in the northwest coastal regions of The Netherlands (Arcadis, BRO, Delft, & Pondera, 2024). Although not in scope of VAWOZ, the PAWOZ routes for transport of electricity and H₂ from Hub East (TNW and DDW windfarms) to the northeast of The Netherlands are also shown on this map in dashed grey lines for context.

Additionally, pVAWOZ proposes a route for cables to transport electricity from to be developed windfarms in the NE area of hub north to the Den Helder region, and this route has been included in the maps with the designs of the hubs. Finally, it is important to note that the 6-7 cable connections that are foreseen for hub north would probably be sufficient for the 14 GW wind capacity of the NSE5-DEC storyline, when taking into account that a part of the electricity will be used to produce hydrogen (7GW capacity). However, for the 20 GW wind (and 10 GW hydrogen production) capacity of the NSE5-NAT storyline, additional cables will likely be required.

On international cable connections between countries around the North Sea, the Offshore TSO Collaboration published a 3rd expert paper in April 2025 (Offshore TSO Collaboration, 2025). In the paper, a set of promising cross-border interconnectors is presented (see Fig 2.14) to advance offshore network infrastructure development in line with the aims of the Esbjerg and Ostend declarations. Apart from the already planned interconnectors, e.g., the 1.8 GW LionLink interconnector between the Netherlands and the UK (in Hub West, see Section 2.2.1.1 and Figure 2.2), it proposes interconnectors (3 x 2 GW) between clusters with offshore wind in the Dutch (hubs west and north) and a) the German part (license areas further from shore, with numbers N14 and higher) of the North Sea, b) the eastern UK cluster off the coast of Newcastle, and c) the Antwerp region in the northwest of Belgium.



Figure 2.14: OTC electricity grid map 2025, displaying planned and promising cross-border (interconnector) projects until 2040 (source: [OTC expert paper III](#)).

For the transport of hydrogen produced offshore in hub north (wind search areas 6 and 7, and potentially in areas to the west and north), an offshore hydrogen grid must be developed that connects to the onshore hydrogen grid. Gasunie, the HNO (Hydrogen Network Operator) for the offshore grid, is currently executing a design study for the offshore hydrogen grid, however at the time of writing of this report no results have been made public, i.e., no firm information is available about the exact routing of the future offshore grid. For our designs we therefore based ourselves on publicly available information (Ministerie van Economische Zaken en Klimaat, 2024) (NGT, NOGAT, 2023), and developed 2 designs for a future offshore hydrogen grid to transport the amounts of hydrogen produced in our storylines to landing points at Eemshaven and Den Helder.

Table 2.4 displays the transport requirements for the designs. The (peak) transport capacities for the two scenarios for the years 2030, 2035, 2040 and 2050 were calculated by taking the total (peak) hydrogen production capacities installed offshore (in Hub West, hub north and in “free” areas west and northwest of hub north) multiplied by a 0.7 efficiency (LHV) for the year 2050. Additionally, a capacity requirement for import of hydrogen from Denmark and Norway, via the connection to AquaDuctus, was added based on system-level scenario modelling work in WP3 of NSE5 (Blom, van Stralen, Eblé, Magan, & Hers, 2025). However, because hydrogen import from those countries via offshore connections is not explicitly modelled in WP 3, we decided to calculate this capacity requirement for import by averaging the hourly amounts (= capacities in GW) of hydrogen imported onshore from Germany into the Netherlands, assuming import from Norway and Denmark via the onshore grid through Germany. This resulted in an additional capacity requirement for import of 4.3 GW for NSE5-NAT and 5.4 GW for NSE5-DEC. Together with the requirements from offshore hydrogen production this results in a total required transport capacity of 17.7 GW for NSE5-NAT in 2050, and of 10.65 GW for NSE5-DEC in 2050. In comparison with the capacity requirements in EIPN (Ministerie van Economische Zaken en Klimaat, 2024), our NSE5-NAT transport capacity is slightly lower than their mid-level design scenario of 22 GW, and our NSE5-DEC transport capacity is slightly higher than their low-level design scenario of 8 GW.

Table 2.4: Hydrogen transport capacity requirements for the 2 infrastructure designs from NSE5-NAT and NSE5-DEC storylines, and the EIPN design requirements (Ministerie van Economische Zaken en Klimaat, 2024) for comparison.

Year	Unit	NSE5-NAT			NSE5-DEC			EIPN		
		Hubs	Import	Total	Hubs	Import	Total	Low	Mid	High
2030	GW	0.0	0.0	0.0	0,0	0.0	0.0	0.0	0.0	0.3
2035	GW	0.35	0.0	0.35	0.35	0.0	0.35	1.0	1.0	2.0
2040	GW	3.85	0.0	3.85	2.45	0.0	2.45	6.0	10.5	13.0
2050	GW	13.30	4.30	17.6	5.25	5.40	10.65	8.0	22.0	35.0

Other requirements (boundary conditions) for our designs stem from the PAWOZ and VAWOZ planning processes, e.g., to have a connection to DEMO-2 before 2033 to transport the hydrogen produced to shore in the northeast of the country, and to establish connections to the Eemshaven and northwest Netherlands region (Den Helder/IJmuiden/Amsterdam) before 2040 to transport hydrogen produced in hub north (wind search areas 6 and/or 7) to

shore. Other boundary conditions include the pressure range of the onshore hydrogen network (30-66 bar), and a maximum flow velocity of 25 m/s.

We developed 2 designs for the offshore hydrogen grid, one that assumes that it will be built completely with new pipelines, and another that assumes that a significant part of it will reuse existing pipeline sections of NGT and NOGAT. The design with only new pipelines is our reference scenario (see Figure 2.15). It assumes pipelines with a 48 inch diameter everywhere, and consists of two routes: 1) an easterly route that runs from the northeast region of Hub North to (ultimately) a landing point near Eemshaven where it connects to the onshore grid, passing through Hub East via DEMO-2, and 2) a westerly route that runs from the southwest region of Hub North to a landing point near Den Helder (along one of the VAWOZ routes, see also the Hub West design (section 2.2.1.2) where it connects to the onshore grid. Construction of the easterly route of the reference scenario (only new pipelines) is assumed to take place in three phases: 1) construction of the PAWOZ preferred route before 2033 to transport hydrogen produced by DEMO-2 to shore between Ameland and Schiermonnikoog (as included in the design of Hub East, see section 2.2.2.2), 2) extension of the route from DEMO-2 to the compression platform in the northeast region of Hub North to transport hydrogen produced in that region (and imported via AquaDuctus) to the landing point near Eemshaven, and 3) connecting the compression platform the compression platform in the southwest region of Hub North. Phase 2 should be executed in the period 2033-2040 to make sure that any hydrogen produced in the northeast (in the mid-2040s) and southwest of hub north (starting in late-2030s) can be transported to shore. Construction of the westerly route could then be delayed (vs. current plans of pVAWOZ to have it ready before 2040) until the mid-to-late 2040s when the full hydrogen production capacity in Hub North and the connection to AquaDuctus have been realized, and plans may have firmed up for additional hydrogen production capacity to the west and northwest of Hub North.

The design with reuse of sections of NGT and NOGAT is our alternative scenario (see Figure 2.16). It assumes pipelines with a 36-inch diameter everywhere, except for the NOGAT section from platform L2 northward, and also consists of two routes: 1) an easterly route that runs from the northeast region of Hub North to a landing point near Eemshaven, passing through Hub East via DEMO-2, and reusing part of the NGT pipeline, and 2) a westerly route that runs from the southwest region of Hub North to a landing point near Den Helder via platform L2 and reusing part of the NOGAT pipeline. The easterly route reuses the 36-inch NGT pipeline between a point 10 km east of the AWG-1 platform and the landing point near Eemshaven, which has the advantage of crossing the Waddensea with minimal environmental impact. From (roughly) AWG-1, a new 36-inch pipeline then connects to DEMO-2, and this to be in place before 2033 when DEMO-2 starts producing hydrogen. In the period 2033-2040, the extension from DEMO-2 to a compression station in the northeast region of Hub North (36-inch new pipeline) must (again) be executed to transport hydrogen produced in that region to the landing point near Eemshaven.

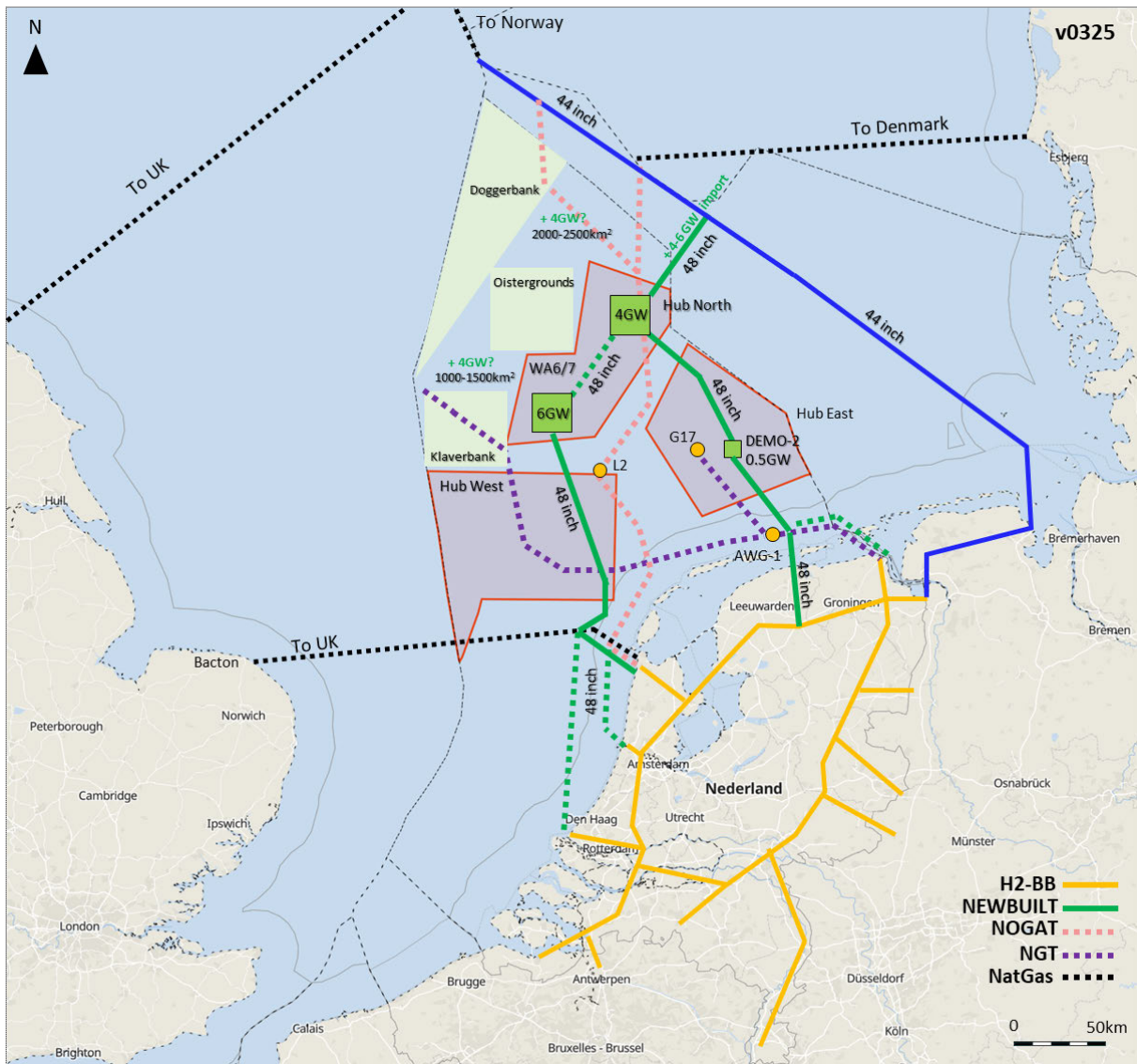


Figure 2.15: Routing of potential future offshore hydrogen grid assuming new pipelines only.

Additionally, by connecting the compression station in the southwest region of hub north to the extension by the late-2030s, the hydrogen produced in that region can also be transported to shore via the easterly route. Construction of the westerly route, connecting the southwest region via platform L2 and NOGAT to shore in Den Helder, could then be delayed (vs. current plans of pVAWOZ to have it ready before 2040) until the mid-to-late 2040s when the full hydrogen production capacity in hub north and the connection to AquaDuctus have been realized, and plans may have firmed up for additional hydrogen production capacity to the west and northwest of hub north. In this alternative design, this delay is actually a prerequisite because the expectation is that NOGAT (and the section of NGT from AWG-1 westward to L10) will have to stay in use for transporting natural gas from fields in hub north and Hub East until the mid-2040s. Furthermore, in this alternative design, the connection to AquaDuctus for import of hydrogen is realized by reusing the 24 inch section NOGAT from platform L2 northward, earliest from 2045. In section 4.5, we detail the results of model-based performance analyses of the two storylines, whereby we quantify pressure variations in the pipelines for a low-pressure (30-10 bar) regime without offshore compression, and a high-pressure (100-66 bar) regime with offshore compression. Furthermore, in a separate report titled “Overview of Subsea Pipeline

Connection Options for Hydrogen Supply in the North Sea (Clark & Varma, 2025), Subsea7 (one of the partners of NSE5, D1.3a) details the results of a study into the connections and crossings that must be realized in the construction of the 2 designs, and the associated costs, which are further detailed for the designs in deliverable D3.3 (van Zoelen, Rob; Boer, Dina; Mahfoozi, Salar, 2025).

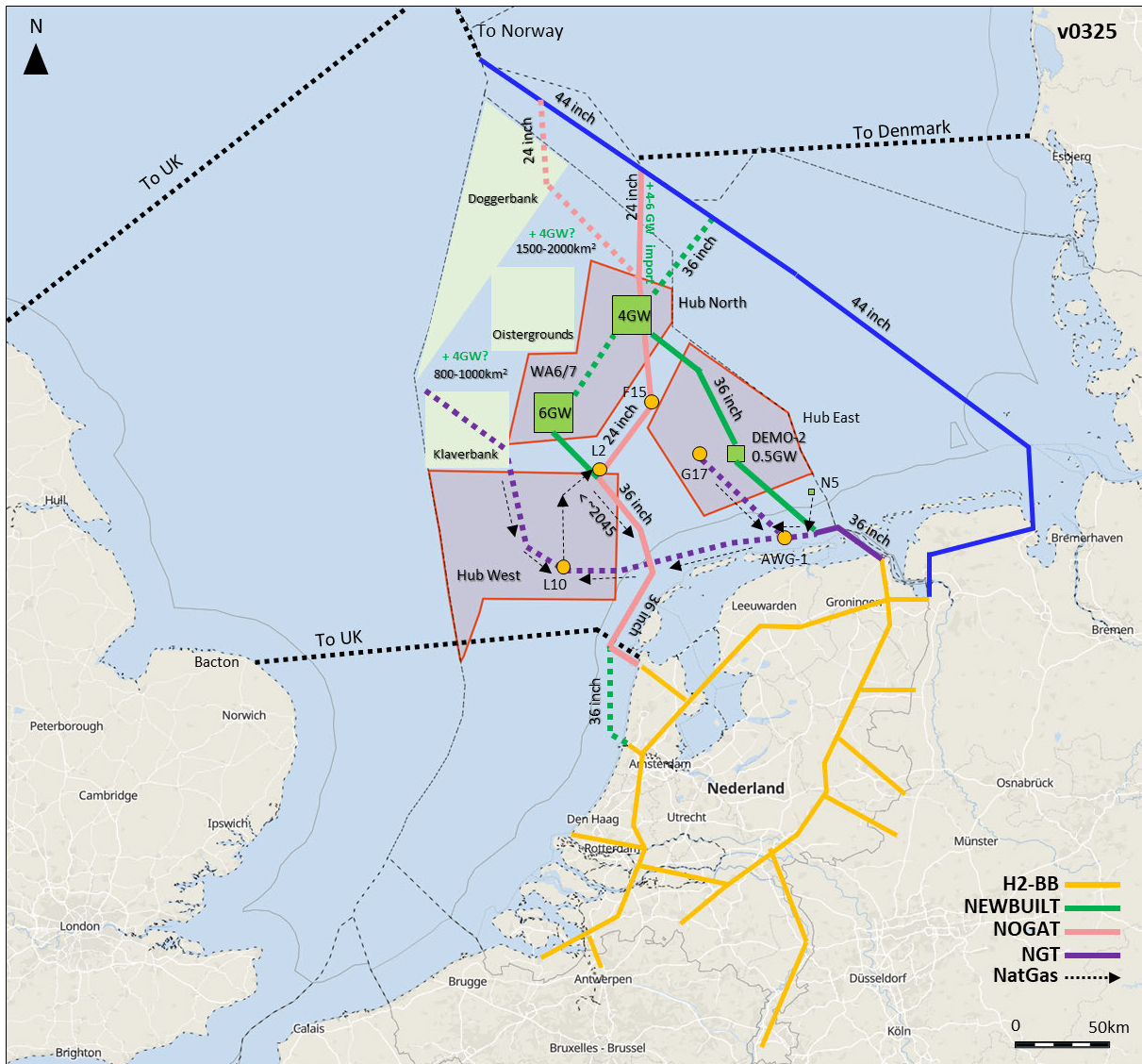


Figure 2.16: Routing of a potential future offshore hydrogen grid assuming (partly) reuse of NGT and NOGAT

2.4 Hydrogen storage

Underground hydrogen storage (UHS) has the potential to play a crucial role in the future energy system. It can balance the mismatch between intermittent supply and variable demand for both short-term fluctuations (grid balancing) and seasonal variations (seasonal storage), secure supply, and increase independence (strategic storage). Additionally, it enables high levels of renewables (wind, solar) integration into the grid, by providing flexibility to an integrated electricity-hydrogen energy system.

In this section, we present the results of studies on developing offshore UHS at the North Sea. Offshore UHS can play an important role in managing pressure fluctuations in the offshore hydrogen network. By offering a buffer to absorb (large amplitude, high frequency) fluctuations in the rate hydrogen production from wind, transport to shore can happen at a predictable, constant rate, and this greatly improves the durability of pipelines, especially reused pipelines that have been in operation for natural gas for decades. In NSE5, as part of the activities in the workstreams on the hub designs and the technical innovations, we therefore carried out research aimed at improving our technical understanding of the challenges of developing hydrogen storage offshore for this specific purpose (use case), by identifying suitable offshore areas for storage, defining the design requirements, developing (high-level) designs of offshore storage facilities, and estimating the costs of offshore UHS. Our approach consisted of three steps, whereby in each step we aimed to answer a specific research question:

1. **Screening:** Where can hydrogen be stored underground in the Dutch sector of the North Sea? Outcomes of this step are presented in section 2.4.1 of this report.
2. **Notional design:** What are the technical design requirements for offshore UHS, and what would an UHS facility offshore look like in terms of installations, size, weight, etc.? Outcomes of this step are presented in in section 4.8.1 of this report.
3. **Costing:** What would it cost to develop UHS offshore, and how does this compare to onshore UHS? Outcomes of this step are presented in section 4.8.2 of this report.

To address the first question, the study focused on salt structures and gas fields¹¹ in Hub North and nearby fields. A screening process was conducted on a broad portfolio of gas fields, supplemented by previous study on offshore salt structure screening (van Gessel, et al., 2022). The screening was carried out in two stages: the first stage utilized mainly public data, while the second stage incorporated data provided by operators to shortlist gas fields with good potential for offshore hydrogen storage.

The second question (see section 4.8.1) examined the subsurface and surface requirements for UHS. The design parameters assume that storage will serve as a buffer for 8 GW of Power-to-Hydrogen in wind search area 7 in Hub North, ensuring a constant hydrogen throughput via pipeline to shore. The analysis focuses on the performance of the reservoir/cavern and well(s), as well as on requirements for the surface facilities for compression and gas cleaning, including space and weight considerations on offshore platforms.

To answer the third question (see section 4.8.2), a costing model from Hystories project (Bourgeois, Duclercq, Jannel, & Reveillere, 2022) was used to calculate the investment and operational costs for the notional designs that were developed for offshore UHS in salt caverns and in a gasfield in step 2. A more detailed cost analysis was performed for constructing and operating an offshore UHS in a salt structure (by Shell and Gasunie, see below).

It is important to mention that a part of the research was carried out by the partners Shell, Gasunie and EBN, and contributed in-kind. It concerns a design study and associated factsheet for developing salt cavern storage in a salt structure in license block E17 near the

¹¹ Oil fields were excluded from the screening due to the higher complexity of hydrogen storage compared to gas fields, and because seals of oil fields are not proven to hold gas.

southwest corner of hub north (Shell, included in deliverable D1.4 on Technical Innovations, (Buijs, et al., 2025)), a factsheet on salt cavern storage in a salt structure in license block F08 (EBN, included in deliverable D1.4 on Technical Innovations), and a study into the costs of developing UHS offshore in a salt structure in license block M2, near DEMO-2 in license block G17, deliverable D1.3b of NSE5 (de Borst, Looijer, Duff, Kuperus, & Vink, 2025). Moreover, in deliverable D3.3 of NSE5 (van Zoelen, Rob; Boer, Dina; Mahfoozi, Salar, 2025), the investment and operational cost found in this study were used to calculate the levelized storage costs in order to indicate the relative size of these compared to other costs in the offshore hydrogen value chain.

2.4.1 Screening

Only gas fields in Hub North itself and in a region 40–60 km from its boundary were included in the screening.

Our reasoning for this is two-fold:

1. If the storage connects to a compression station in or around hub north, which could be considered logical, because a) these are the collection points for hydrogen produced in the hub, and b) are the farthest from shore, and c) compression power is already available that could elevate pressure towards storage pressure, then the distance from the field to that compression station must be bridged by a pipeline. Cost increases with every km, as do pressure losses, and here we consider 40-60 km to be the limit;
2. If the storage connects to the offshore grid more downstream of the compression stations, then with increasing distance, the value of the storage in managing grid pressures to increase the durability of the pipelines is expected to reduce.

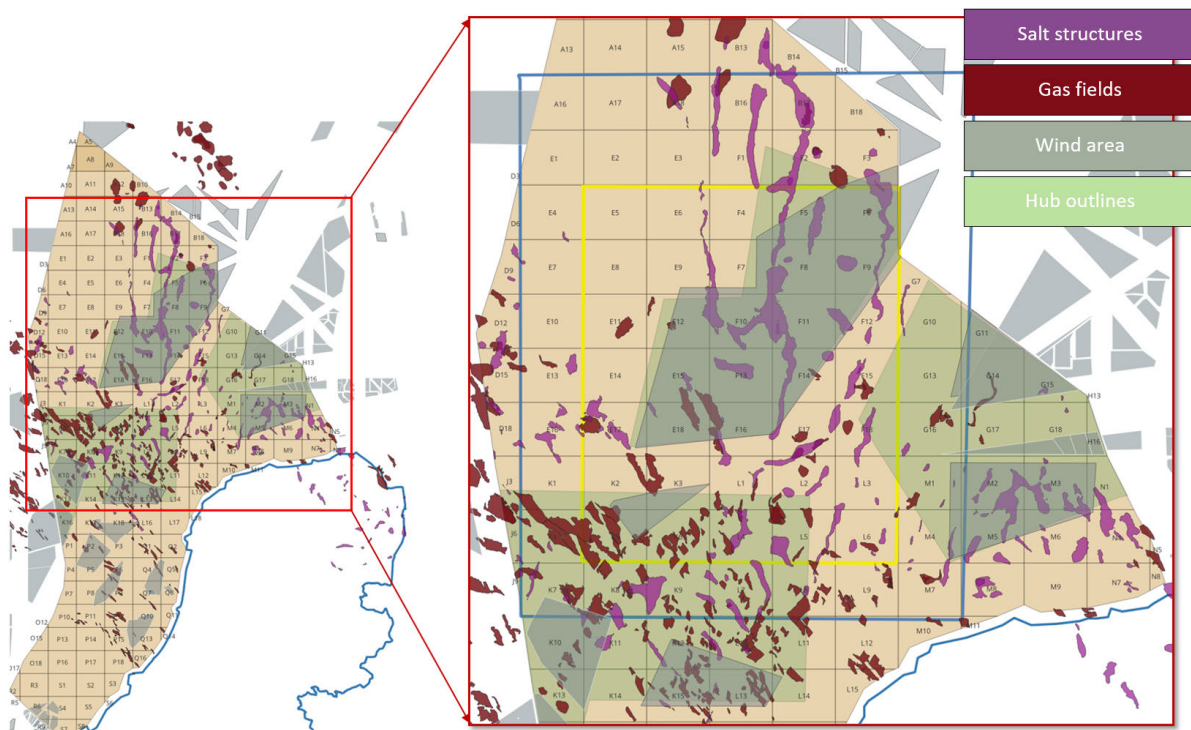


Figure 2.17: Screening area focused on Hub North and nearby salt structures and fields. The yellow rectangle marks areas ~40 km from the boundary, and the blue rectangle covers areas ~60 km from the boundary.

Figure 2.17 (right) displays two regions: one defined by the yellow rectangle (~40 km from the hub boundary) and one defined by the blue rectangle (~60 km from the hub boundary). The total number of gas fields within the yellow and blue regions is 48 and 122, respectively.

The screening process was conducted in two steps (see Figure 2.18):

- **1st screening step:** This step used key parameters available in public databases. These parameters, listed in Table 2.5, include lifecycle phase, surface restrictions, and reservoir volume (GIIP).
- **2nd screening step:** In this step, the longlist of fields from the first screening was further narrowed to a shortlist using additional parameters provided by operators and considered important for assessment. These parameters include transmissivity (permeability * net thickness), gas composition, and the presence of faults penetrating shaly caprocks (see Table 2.5).

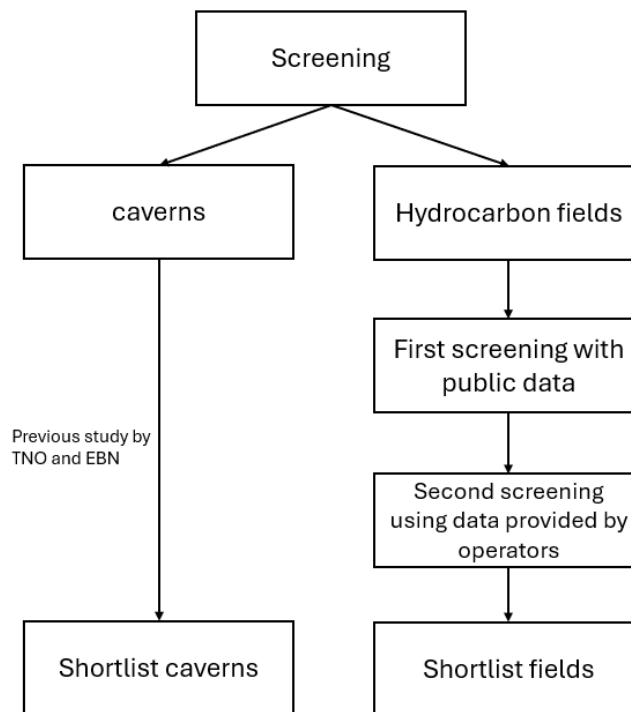


Figure 2.18: Screening workflow for selection of suitable gas fields and salt structures.

Table 2.5: Screening parameters applied to gas fields in the current study.

Step	Parameter(s)	Exclusion criteria
1	Lifecycle phase	Abandoned fields, undeveloped fields, prospects
	Surface restrictions	Excl. shipping zones, ecological (protected) areas and defense areas.
	Reservoir volume, GIIP	Very large (> 5 bcm) and very small (<0.5 bcm) reservoirs
2	Transmissivity (K*h) [mD.m]	< 500 mD.m
	Gas composition	Containing H2S >30 ppm
	Presence of faults	Faults penetrating (into) shaly caprock

Regarding the second screening step, the transmissivity (Kh, defined as permeability * thickness) plays an important role in the subsurface performance of the reservoir. It is a measure for injectivity and productivity, and greatly influences the number of wells needed for injection and withdrawal. It is also preferable that the original gas contains no or little H₂S (30 ppm limit assumed), because high(er) values require H₂S-resistant well materials and

additional purification, which impact risk and economics. Furthermore, if existing faults penetrate the shaly caprock, they could create potential pathways for hydrogen leakage, which is undesirable. Note that additional parameters may also be relevant and could be incorporated in future studies involving more detailed screening, depending on the specific requirements of each case.

2.4.1.1 Results

After the first screening step, based on public data, 47 fields out of the initial 122 in the blue region remained as candidates (see Figure 2.19, left map). Most fields were excluded due to reservoir size (either too large or too small) or lifecycle phase. Naturally, adjustment of the screening parameters would affect the results.

In the second screening step, additional criteria were applied, narrowing the selection to 9 fields, primarily due to many fields having too low Kh values. Figure 2.19 (right map) shows the locations of the gas fields that remain after the second screening step, along with the operators of these fields, highlighting that:

- In Hub North, no reservoirs meet the screening criteria. Of the 9 remaining fields, 4 are located in Hub West, and 5 are in the G16/17 blocks in Hub East.
- The fields in the G16/17 blocks (operated by Eni) are near the DEMO-2 project, and will probably not be far from the offshore hydrogen grid that may well run past DEMO-2 to GW-scale hydrogen production sites in Hub North. These reservoirs have favorable Kh values and are shallower compared to those in Hub West, making them more suitable from a technical perspective.

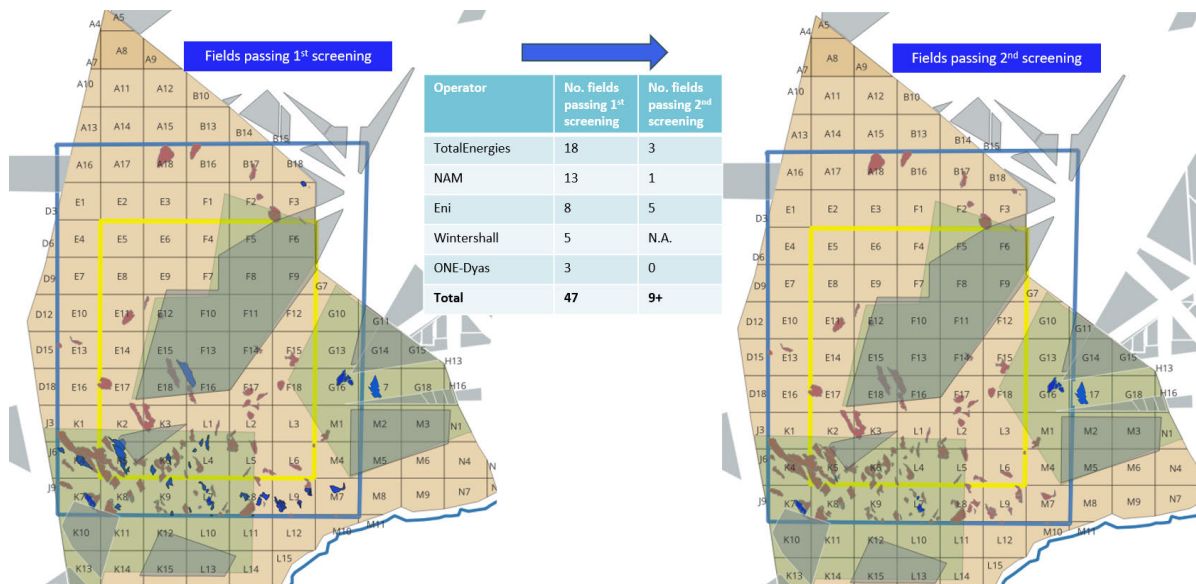


Figure 2.19: Results of the first and second screening of gas fields. Only blue fields meet the screening criteria.

The screening of salt structures suitable for developing caverns for store was not within the scope of NSE5. Instead, results were used from a study by TNO and EBN (van Gessel, et al., 2022). In the study, contours of salt structures in the Zechstein salt at 1000 m and 1500 m depth were mapped to assess how many caverns could be developed in the structures. Promising salt structures include those in the F8 block (within Hub North, 35 caverns, ~9

TWh storage capacity) and the M2 block (near the G17 block in Hub East, 16 caverns, ~4 TWh storage capacity).

Figure 2.20 displays the locations of the nine “suitable” gas fields (that passed the screening) and the identified salt structures in the screening area, together with possible routes of a future offshore hydrogen grid as presented in the previous section (2.3). A promising region is in Hub East, where the gas fields in the G16/G17 blocks and the salt structure in the M2 block are in proximity to the DEMO-2 project and (possibly) to the future offshore hydrogen grid.

The screening conducted in this study is high-level, and the identified gas fields and salt structures must be seen as examples with potential for hydrogen storage in and around Hub North. A more detailed study is needed to confirm their suitability. Additionally, it is recommended to include gas fields and salt structures in other areas in the screening for underground hydrogen storage locations, in particular areas in a zone around the future offshore hydrogen grid (once more firm) and nearshore of the provinces of North Holland and South Holland, to gain a comprehensive understanding of the entire area.

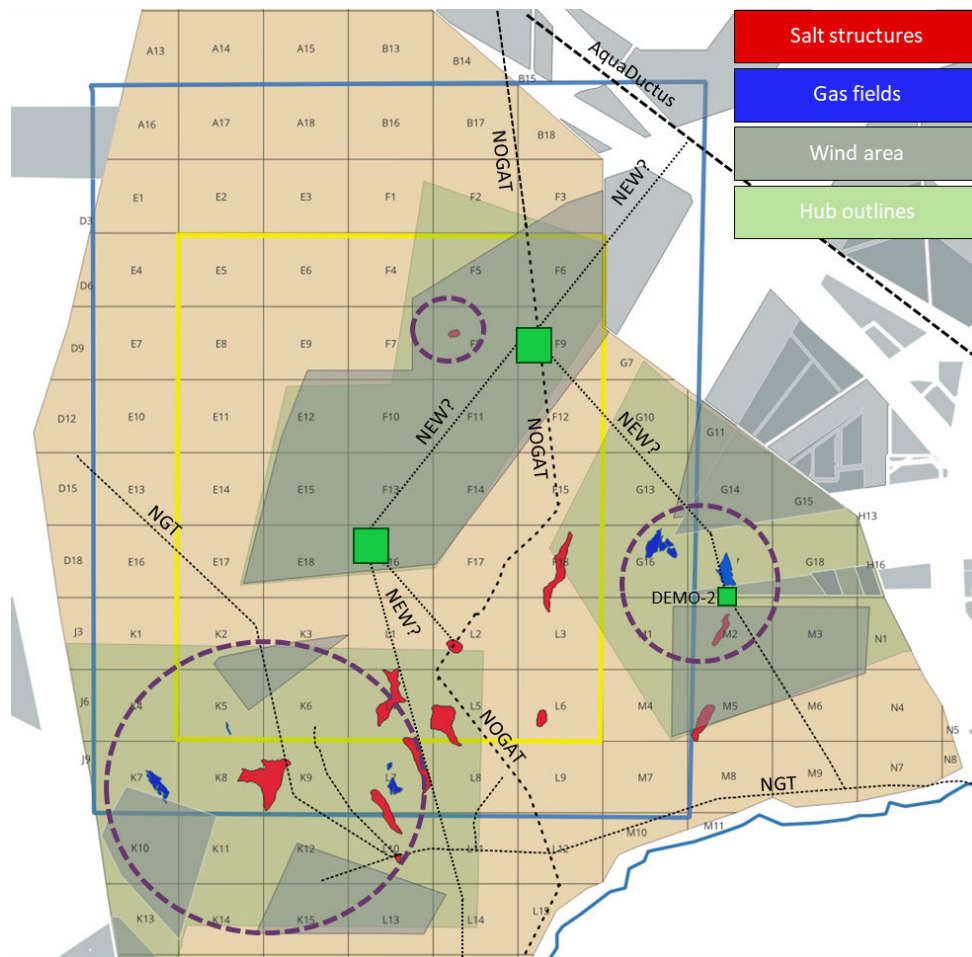


Figure 2.202.21 Combined map of screened gas fields and salt caverns. Three regions are highlighted with circles: the F8 salt structure, the Hub East region with a combination of caverns and gas fields near the DEMO-2 project, and a large area in Hub West. The dotted black lines represent possible hydrogen pipeline routes (see section 2.3). The green squares indicate areas where hydrogen production is foreseen, with compression nearby (depending on infrastructure design) to inject into the network.

3 Methodology and assumptions

3.1 Modelling tools

3.1.1 Energy System Description Language

Energy System Description Language (ESDL, (ESDL, 2019)) is a geo-explicit language that is created to describe the energy assets in a system and relations (connections) between them. This description contains the relevant asset parameters that allow the models to perform the simulations. The assets are split in a few generic groups (Production, Consumption, Transport, Storage and Conversion) from which more detailed assets can be picked. In the context of this project, the offshore energy system designs with the three NSE hubs at the North Sea presented in Chapter 2 are modelled, including the transport network (cables and pipelines), production assets in the form of windfarms with their respective power profiles, conversion assets in the form of electrolyzers and assets that consume electricity and hydrogen at the landing points. The ESDL models allow for exchange of the system description between several models and thereby also serve as input and output of the models. MESIDO and Aurora use ESDL models as input for their simulation and optimization purposes, where MESIDO can also provide information back in an ESDL model. The wake surrogate model calculates the windfarm profile based on the geometries and other wind turbine information is provided through an ESDL.

3.1.2 MESIDO

MESIDO (Rojer, Janssen, van der Klauw, & van Rooyen, 2024) is an open-source python code developed by TNO for the modelling and optimization of energy systems, with a focus on physical modelling of energy networks. It can model full networks and multiple commodities, gaseous (e.g. hydrogen, natural gas, etc.), electricity and heat, as a Mixed Integer Linear Problem (MILP), where the relevant physical detail can be chosen depending on the questions that one wants to answer. The linearization of the problem allows for big (multi-commodity) networks to be optimized within reasonable time, while losing only little accuracy. The code is fully ESDL compatible, allowing one to geo-explicitly draw all the energy system's relevant assets and connections and provide the required asset parameters along. Typically techno-economic design and operation optimization are done using MESIDO, however in the context of this work, it has been utilized as a simulator, such that one can assign the operational strategy upfront by providing priorities to different assets and/or partial asset capacities. The code supports different time step sizes and horizons as well as a non-uniform timeline, however in this context all simulations were done for a full year with hourly timesteps.

3.1.3 AURORA and MOLE

Aurora is a proprietary in-house tooling that facilitates modelling and simulations of gas network flows (van der Linden, Octaviano, Bokland, & Busking, 2021). The backbone of Aurora is built on the physics that describe a compressible fluid flow through a pipe, by applying the principles of mass balance, momentum balance and the equation of state. Given a topology of network model consisting pipes at a transmission or a distribution level (defined by an energy system descriptive model, such as the ESDL language) the model translates it into components with design and physical parameters. This in turn, forms a

system of PDE's that are numerically solved for pressure, flow, and gas quality. The solver can run both quasi-steady state and in a transient fashion depending on the required level of detail. Aurora is also coupled with a numerical underground hydrogen storage simulator called "MOLE" (Model for Large-Scale Energy Storage) (Yousefi, 2023), which solves flow equations for storage (reservoirs or salt caverns), wells and compressors using nodal analysis. MOLE allows the user to specify several parameters such as storage volume, geological properties, well properties and surface facilities (compressors, heat sinks, turbines) for each storage unit in a network, which comprises a single underground storage facility. Since the tool runs a detailed physics-based model, the relevance of it in this study comes as a validation equipment for the simulations run with MESIDO. Thus, the linearisations from MESIDO to compute the pressures in the network are validated against Aurora – MOLE to quantify the difference in degree of approximations.

3.1.4 PyDOLPHYN

PyDOLPHYN (Fatou Gómez, Martín-Gil, & Dussi, 2025) is a TNO modelling tool for dynamic simulations and optimization of multi-energy assets. It can provide a more detailed representation of the energy components compared to MESIDO and AURORA, allowing for complex non-linear behaviours, such as transient or thermal effects. It was previously used in North Sea Energy 4 to calculate configurations of wind and hydrogen production (Dighe, Fatou Gómez, Dussi, Poort, & Shoeibi Omrani, 2022). In the context of this work, it has been utilized for two purposes. Firstly, the PEM electrolyzer model used in MESIDO uses a PyDOLPHYN-based curve for its linearization. Secondly, a comparison of the effects of different operational strategies regarding prioritizing power delivery or hydrogen production was performed.

3.1.5 Farmflow

Farmflow (Bot & Kanev, 2020) is a parabolised 3D Reynolds-Averaged Navier-Stokes solver. It is used for the wake modelling of wind farms, and can compute a single wake power deficit or an array power deficit. This allows to compute different wind farm layouts and solve power deficits given different conditions, such as wind speed and direction. In the context of this work, a set of simulations was performed, to compute energy production for different layouts and power densities. The results were used to fit a reduced order model (wake surrogate), as explained in the following section.

3.1.6 Wake surrogate model

The wind power curves for the different farms were generated using a surrogate model that was fitted using FarmFlow data. This surrogate model was trained using the following parameters:

- Parametrized wake losses for a 20 MW wind turbine with a rotor diameter of 252.3 m (resulting in a rotor power density of 400 W/m²).
- The results of the model are only accurate for this turbine type, and for wind farm layouts with a homogeneous wind farm power density between 4 and 15 MW/km².
- The parametrization of the wake losses is based on FarmFlow output. The wake model of FarmFlow is primarily a 3D parabolized Navier-Stokes code including a $k - \epsilon$ turbulence model.
- The tool was implemented in the Map Editor toolbox of the North Sea Energy program.

- At every hour, it uses the wind speed and direction to characterize the production. An additional 5% is added when using turbines larger than 15 MW, and an extra loss of 5% is added due to non-aerodynamic losses within the farm (e.g., cabling).
- Only the effects of a single wind farm/area are considered, no interactions with other wind farms are part of the model.

Figure 3.1 shows an example of a wind farm layout. The calculated production with the surrogate model has around 0.2% differences with respect to FarmFlow in this case, while providing a computational time in the order of seconds, compared to the c.a. 120 hours of the original model. This allows to test different layout configurations. A comparison of the wind farm production for the different farms will be made in Section 0. The surrogate model was implemented in the Map Editor that can visualize and edit ESDLs, which was updated by WP5 of NSE5.

3.2 Modelling assumptions

The system modelled comprises only the 3 offshore Hubs, which are modelled using different nodes at wind farm/electrolyzer levels for production and cable/pipeline segment for the transmission of power and hydrogen. The system boundaries are at the landing points, with the supply/demand matching done at a central node (see Figure 3.2). The only contributions explicitly modelled include hydrogen import from AquaDuctus and, for the NSE5-NAT scenario, additional wind power contributions on the North-West side out of Hub North.

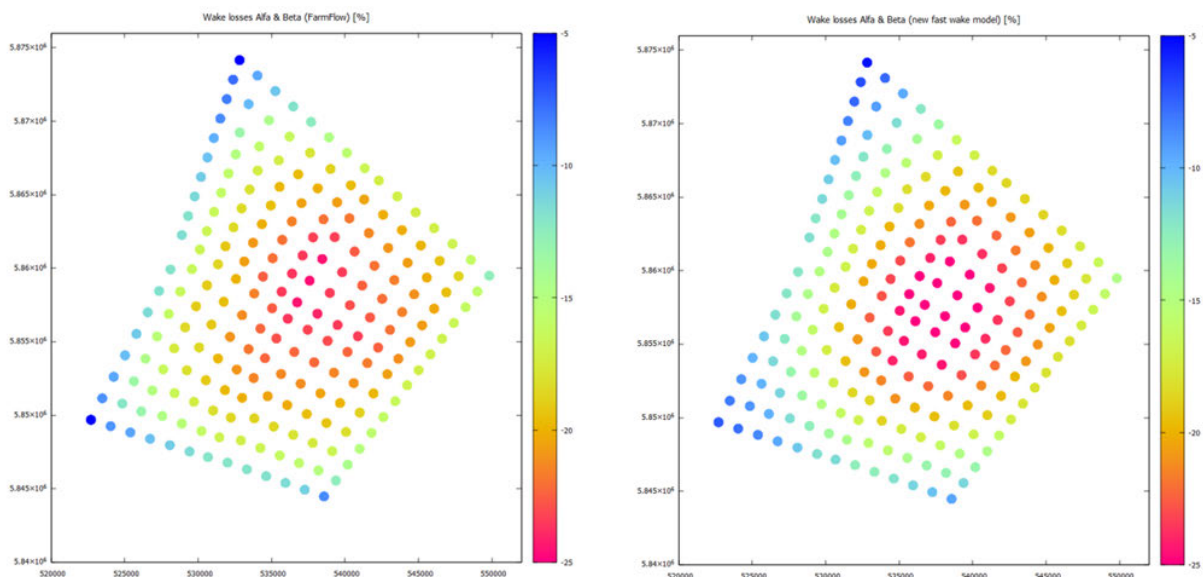


Figure 3.1: Comparison between the Farmflow results and the fitted model for a specific wind farm layout.

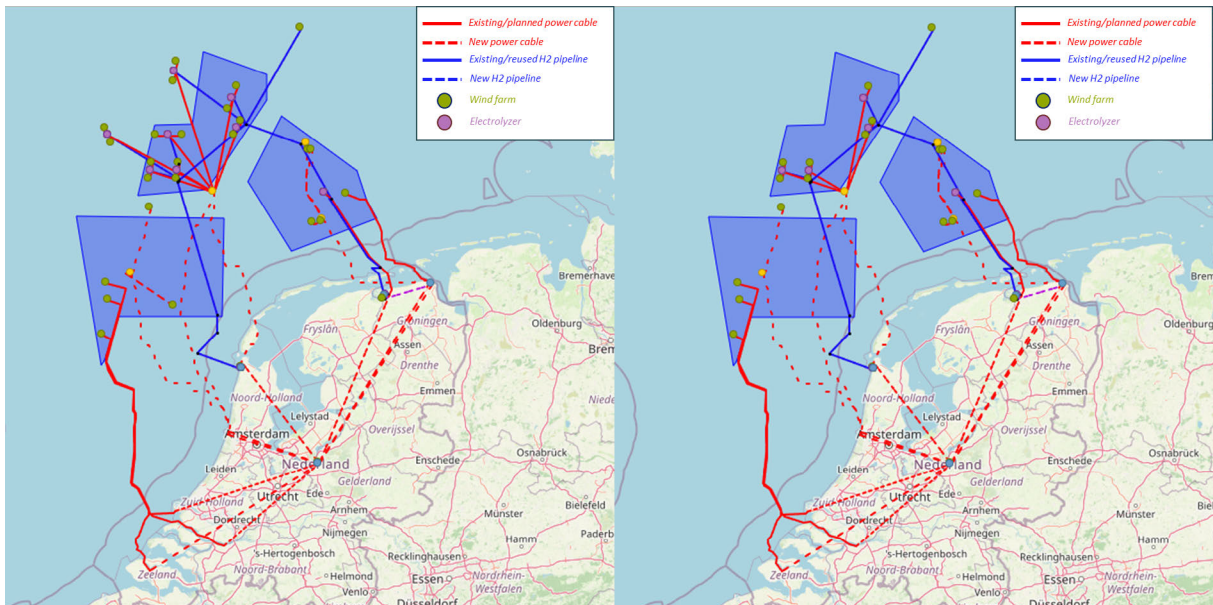


Figure 3.2: Modelling setup in ESDL Map Editor for NSE5-NAT (left) and NSE5-DEC (right) reference scenarios.

3.2.1 Supply and demand

3.2.1.1 Wind profiles

The wind power profiles used correspond to the year 2015, using the Dutch Offshore Wind Atlas dataset (Wijnant, et al., 2019). The choice of the meteorological year can result in significant differences in the wind power production, demand mismatch and other quantities associated with it, such as cable utilization and storage needed. An assessment of differences between different meteorological years with respect to wind farm power output was made at the start of the work. The year 2015 was a year with above-average production. In comparison, for years such as 2009 and 2010, which had a lower production, the wind farm production measured in TWh along the year were around 6% and 14% lower than 2015, respectively. This means that the energy flows obtained in this work may also be slightly optimistic if considering the average of historical data. The reasoning for choosing 2015 as the meteorological year was made to be consistent with work presented in deliverable D3.1 of WP 3 of NSE5 (Blom, van Stralen, Eblé, Magan, & Hers, 2025). This WP acquired international data at a different level of granularity than WP1. This data was available with the required level of quality for 2015, Hence, consistency across work packages was prioritised, as certain demand data is an input from D3.1. It should be noted that the variability of these profiles, and not only their average production, can be very relevant for long-term storage.

3.2.1.2 Power and hydrogen demand and import flows

The power and hydrogen demand profiles used in the simulations correspond to results from NSE5, D3.1. The demand profile used are generated for the NAT- and DEC-based scenarios. The electricity demand profile is the sum of all electricity demand profiles for the Netherlands. This is similarly applied to the hydrogen demand, however a split between the different landing points of the offshore network is required. The numbers from the different onshore clusters for the hydrogen demand from D3.1 were used to distribute the mass

flowrates transported offshore to the two landing points. Due to the different granularity levels of both works, a 1:1 match between this activity and D3.1 could not be made. The results after the assessment was that 44% of the offshore hydrogen will go through Eemshaven (EEM in subsequent graphs) while 56% will flow through Den Helder (DEN). The resulting national demand profiles for the first 100 hours of 2015 are shown 1.27 below in Figure 3.3.

Besides the wind profiles and the national demand profiles, another major influence on capacities and dynamics is caused by the import hydrogen. The focus for this study is the offshore network and thereby, the offshore import of hydrogen on the network is modelled. The AquaDuctus pipeline provides significant potential transport capacity for cross-country hydrogen flow. The timeseries of all cross-country import to NL calculated in D3.1, is averaged over all nonzero values, to represent a ‘filled’ pipeline as well as to remove the highly fluctuating dynamics of the import as a result of the market modelling, which we want to prevent in the offshore system. This results in a constant import through AquaDuctus of 4.3 GW hydrogen for the NAT scenario and 5.4GW hydrogen for the DEC scenario. Thereby this allows for an assessment the suitability of infrastructure to deal with these larger hydrogen transport scenarios.

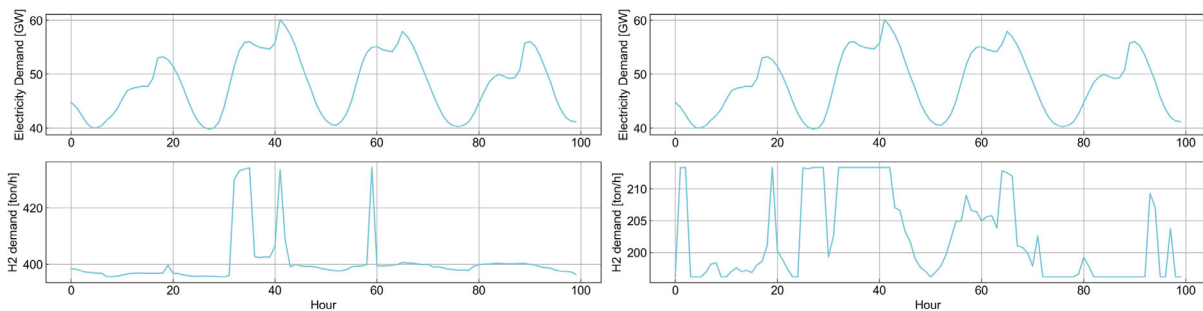


Figure 3.3: Demand profiles for the first 100 hours of the year, for NAT (left) and DEC (right).

3.2.2 Operational strategy for an NSWPH block and electrolyzer assumptions

The basic modelling block used for hydrogen production can be observed in Figure 3.4. It has a ratio of 2:1 in the capacities of wind farm and electrolyzer, and the cable capacity to shore (2 GW) matches the maximum output that can be provided by the wind subtracting the contribution towards hydrogen production (2 GW). It should be noted that there is one exception in the scenarios tested. This is DEMO 2 in Hub East, which is a 500 MW unit powered by a 700 MW wind farm in Ten Noorden van de Wadden (TNW). A simplification made in the assumptions is that both the electrolyzer and the wind farm operate as a single unit. This is particularly relevant for the electrolyzer, as the different modules operate uniformly, and the minimum load is the combined minimum load of the different modules. In practice, there may exist a possibility of independent control strategies for each of the modules. This can lower the minimum load factor of the combined system, reducing the requirements from either the grid or an auxiliary power system if no shutdowns are allowed. The effect of this has not been explored in this work.

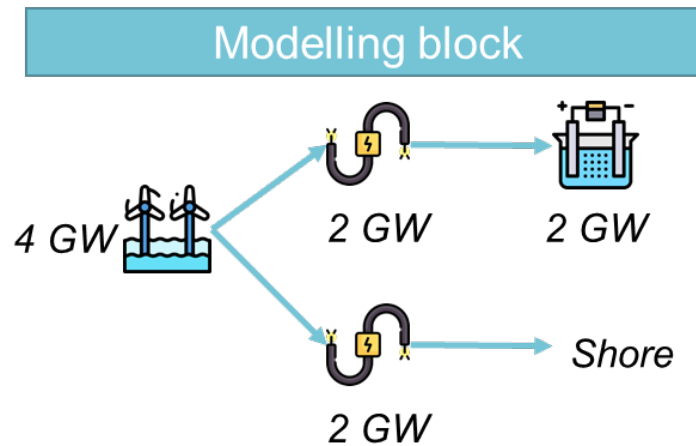


Figure 3.4: Schematic diagram of NSWPH 4GW module used for the hydrogen production in Hub North. Due to the matching cable capacities to the maximum capacity of the wind farm, no curtailment occurs in the main set of scenarios.

Table 3.1: Electrolyzer assumptions. For details of electrolyzer performance see the model linearization appendix.

Electrolyzer assumptions	Value
Technology	PEM
Minimum load	10%
Specific energy consumed [kWh/kg H2]	55 at nominal load, efficiency curve depending on load
Degradation rate	N/A
Operational hours	No maintenance, can operate at any time
Ramp-up/ramp-down constraints	0-100% in one hourly time step

Table 3.1 shows the main assumptions regarding the electrolyzer configuration. The PEM technology assumes that all the ramp-up and ramp-downs can be performed with the prescribed operation, and no transient or thermal effects are considered. The specific energy consumption uses as a reference the factsheet from deliverable D1.4 of the Technical Innovations workstream of WP 1 (Buijs, et al., 2025), and accounts for:

- Certain amount of averaged degradation. In offshore conditions, with intermittent power, the performance degradation is likely to be more than 1% per year.
- Extra energy for certain Balance of Plant components.
- Any other extra energy necessary on maintenance operations, etc., is not taken into account in this number.

An overview of the performance curve of the model can be seen in the Appendix regarding the model linearization with MESIDO (see Appendix A).

With respect to the operational strategy, a balance between sending power to shore and ensuring a reasonably stable load on the electrolyzers has been chosen (labelled as NSE5 strategy in the rest of the document). For the 4 GW blocks, the priority was set as:

- Aim to fulfil a baseload of 50% for the electrolyzer from wind power (first 1 GW of the wind power capacity).

- If this is not possible, aim to fulfil up to 50% (baseload) but at least 10% (minimum load) of the capacity of the electrolyzer from wind.
- If the 10% of minimum load cannot be achieved, add enough power from the grid
- The second part of the wind power (1-3 GW), is used to send power to shore.
- The last part of the wind power (3-4 GW), is used for additional load for the electrolyzer.

The reasoning over using another strategy (such as using equal power at all times for the electrolyzer and the cable export) was to dampen some of the fluctuations in the offshore system using the hydrogen production facility, enabling a more stable power delivery. The consequences of this strategy can be seen in Section 4.3.

3.2.3 Operational strategy for the offshore system evaluated

The overall system is operated in a supply/demand matching strategy, with hourly time steps and for a 1-year simulation time. In certain parts of the offshore system considered, there is a choice to be made every time step regarding prioritizing power delivery to shore or hydrogen production offshore. This determines the infrastructure (cable, pipeline) utilization, and ultimately can pose constraints on it. This choice is in practice a multi-stakeholder decision, as it depends on contractual agreements between power/hydrogen producers and off-takers, but also on infrastructure limitations at particular time steps, such as grid congestion onshore. An example of this can be seen in the tenders for Ijmuiden Ver Gamma at the moment of writing this document. There, one of the eligibility criteria includes the possibility of curtailing up to 25% of the wind farm capacity for 15% of the time (RVO, 2025).

4 Results

This chapter presents an overview of the main results obtained with the different simulations, using the methodology outlined in the previous chapter. The order of the following sections follows a similar ordering to the original research questions.

The first set of simulations (Section 4.1) allowed to obtain the wind power and hydrogen production of the NSE5-NAT and NSE5-DEC storylines, in addition to the pressure losses of the newly-built hydrogen transport infrastructure. Focusing in Hub North, and regarding wind power production and limited space, the influence of the wake losses for different power density configurations is discussed in Section 4.2. A comparison of two different operational strategies for Hub North and NSWPH-like wind + hydrogen blocks is discussed in Section 4.3. A discussion on the addition of offshore solar is included in Section 4.4.

The following two sections comprise a discussion on different transport scenarios. The first one (Section 4.5) compares newly built with mostly re-used infrastructure. Afterwards, a discussion on cases without mechanical compression offshore is performed in Section 4.6.

The last two sections comprise the role of hydrogen storage. Section 4.7 models the system with two different storage locations, from the one screened in Section 2.4. Afterwards, an assessment on notional designs and cost analysis regarding offshore hydrogen storage is described in Section 4.8.

For all the sections regarding the full-system simulations, Table 4.1 shows a comparison of the different parameters and storylines taken. The rest of the sections that are not in this table model differ from these main system simulations, either by providing qualitative insights (offshore solar), or by taking a look at parts of the system (grid-connected versus non-grid connected electrolysis and hydrogen storage notional design and cost analysis).

Table 4.1: List of scenarios run for the full system. Other simulations comprise part of the system, such as the single-storage analysis and grid-connected versus non-grid connected electrolysis production in Hub North. These simulations are not included in this table, and are covered in their respective subsections.

Section	Case name	Storyline	Storage	Transport infrastructure	Reference pressure [bar]	Import AquaDuctus	Others
Main storylines (Section 4.1)	REF-NAT	NAT	No	Newly built	100	Yes	
	REF-DEC	DEC	No	Newly built	100	Yes	
Transport scenarios (Section 4.5)	TR-NAT	NAT	No	Re-use	100	Yes	Compared with REF-NAT
	TR-DEC	DEC	No	Re-use	100	Yes	Compared with REF-DEC
	TR-DEC-2	DEC	No	Re-use	30	No	Compared with REF-DEC and TR-DEC
Offshore-onshore compression (Section 4.6)	P30-NAT	NAT	No	Newly built	30	Yes	Compared with REF-NAT
Hydrogen storage (Section 4.7)	STOR-F8	NAT	Yes, at F8	Re-use	100	Yes	Compared with TR-NAT
	STOR-G17	NAT	Yes, at G17	Re-use	100	Yes	Compared with TR-NAT

4.1 Storylines for offshore wind and hydrogen (reference scenarios)

As mentioned in Section 3.2, the two storylines defined in Chapter 2 (NSE5-NAT and NSE5-DEC) were adapted to the year 2050 using ESDL and MESIDO. They contain wind power and hydrogen production and transport. Then, they were simulated for a given set of reference boundary conditions, as outlined in Table 4.1. In particular, the operational strategy was to perform supply/demand matching with the demand profiles. These two simulations will be used as a reference in the rest of the report, and compared with the different sensitivities. The main set of scenario-dependent assumptions, apart from the ones outlined in the Methodology (Section 3.2) are:

- Newly built hydrogen transport infrastructure.
- Reference pressure in the hydrogen network set at 100 bar at the connection with AquaDuctus.
- Diameter of 48 inches for newly built hydrogen pipelines.
- Hub North with a corridor with no wind farms or electrolysers, resulting in a wind power density of around 10.0-10.5 MW/km² due to the space limitations.
- Additional capacities outside of Hub North (to reach 70GW by 2050) included in analysis to provide more realistic pipeline and cable utilizations of relevant infrastructure.
- Meteorological year used: 2015.
- No hydrogen storage offshore.

Figure 4.1 shows a comparison regarding different energy flows at hub level for the two storylines. In the NSE5-DEC storyline, the installed capacities in the 3 hubs produce 152 TWh of electricity, of which 34 TWh is consumed by electrolyzers to produce 21 TWh of hydrogen. In contrast, in the NSE5-NAT storyline, where installed capacities are higher, in particular in and around Hub North, 187 TWh of electricity is produced in the hubs, of which 47 TWh is consumed to produce 30 TWh of hydrogen. In NSE5-DEC, the hubs supply 42% of the yearly electricity demand (364 TWh in I13050-DEC) and 21% of yearly hydrogen demand (102 TWh in I13050-DEC), while in NSE5-NAT, they supply 43% of total electricity demand (433 TWh in I13050-NAT) and 19% of hydrogen demand (159 TWh in I13050-NAT). Furthermore, it can be observed that the additional electricity generated by capacity outside of Hub North (in the areas around Klaverbank and Doggerbank) that must be built to reach the 2050 target of 70 GW in NSE5-NAT is almost as large (75 TWh) as the electricity generated inside Hub North (88 TWh), and this accounts for an additional 17% of total yearly electricity demand of I13050-NAT. Of the 75 TWh, 38 TWh is consumed to produce 26 TWh of hydrogen (16% of I13050-NAT demand). In total, the installed capacities in and around Hub North produce 60% of the yearly electricity demand of I13050-NAT, and 35% of hydrogen demand.

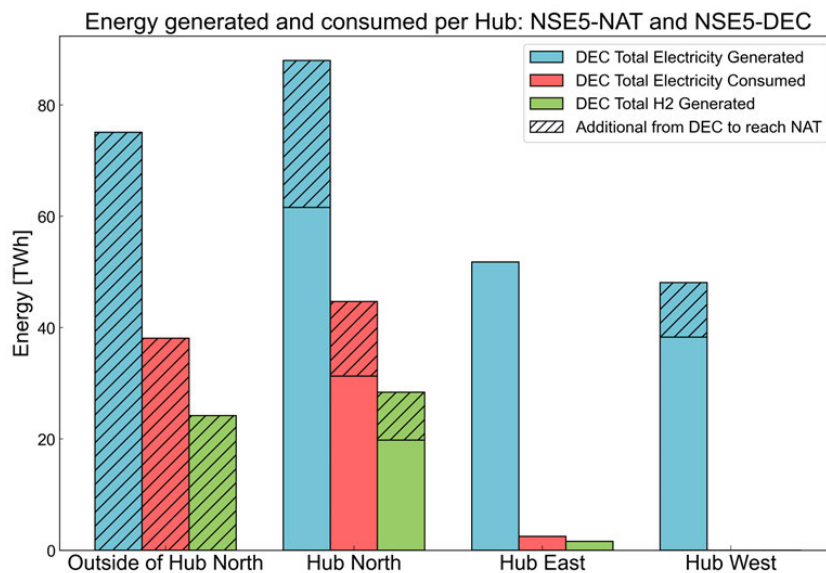


Figure 4.1: Comparison between NAT (left) and DEC (right) storylines on energy flows (TWh/yr) per hub on annual basis. In the rest of the plots in the report regarding supply/demand matching, the capacities outside of Hub North are not included. Energy consumed for hydrogen production is based on lower heating value.

For both storylines, as explained in Section 3.2.1, the power and hydrogen demand to be fulfilled at every hour was set the same. Figure 4.2 shows that the profiles regarding supply/demand mismatch on a monthly basis, while sharing similarities due to have been computed for the same meteorological year, also have some differences. In particular, both share certain months with very low wind power provided compared to the power demand, such as October, but in the NAT scenario there are certain months, such as December, where almost all of the demand can be fulfilled just by the Hubs. This demand, as explained in the Methodology section, was scaled from the national demand. Thus, there are certain months where, considering the rest of the offshore system outside the scope of this study, a large part of the national demand could be fulfilled with the NAT capacities. These results follow a slightly different trend for the hydrogen demand. Figure 4.3 shows that in the DEC scenario.

The effect of the operational strategy of the electrolyzers can be observed in Figure 4.4, which shows the correlation between the electricity and the hydrogen that is required from outside the hubs.

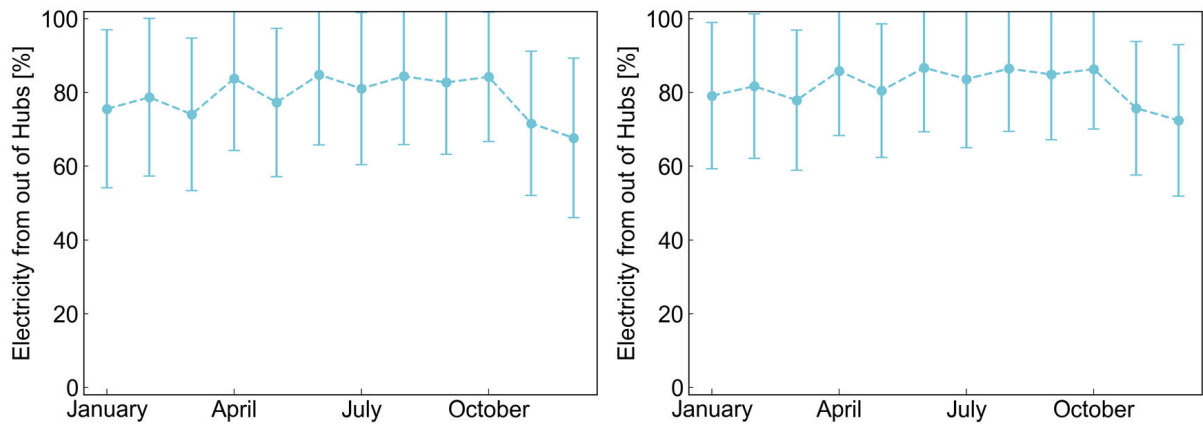


Figure 4.2: Electricity demand that cannot fulfilled by the hubs for NAT (left) and DEC (right) storylines. The scatter circles show mean, while the bars show the standard deviation of the monthly values.

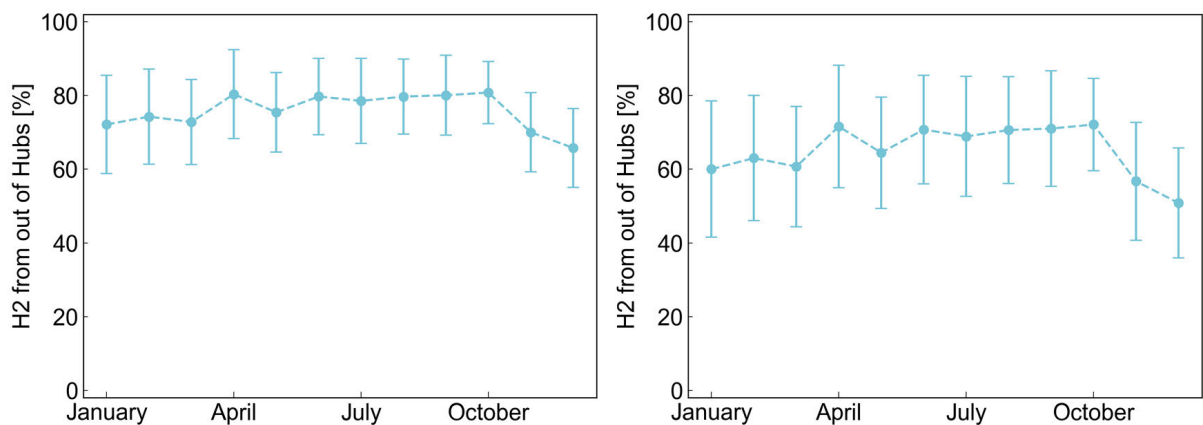


Figure 4.3: Hydrogen demand that cannot fulfilled by the hubs for NAT (left) and DEC (right) storylines. The scatter circles show mean, while the bars show the standard deviation of the monthly values.

The electrolyzers are not allowed to be shut down and have a minimum load of about 10% of their capacity, resulting in a maximum of 93% of the total demand being fulfilled by sources outside of the hubs, even when all electricity demand needs to be fulfilled by other sources than the wind parks in the hubs. The first 50% of electrolyser capacity is prioritised over the electricity transport to shore, indicated by the top right conglomerate of dots, after which all electricity is transported to shore, identified by the almost vertical line, after which the last 50% of the electrolyser is used for any electricity exceeding cable capacity, e.g. the lower left conglomerate. The NAT and DEC scenario show similar profiles, however the hubs in DEC can provide a larger percentage of the total hydrogen demand as the hydrogen demand is smaller for the DEC scenario.

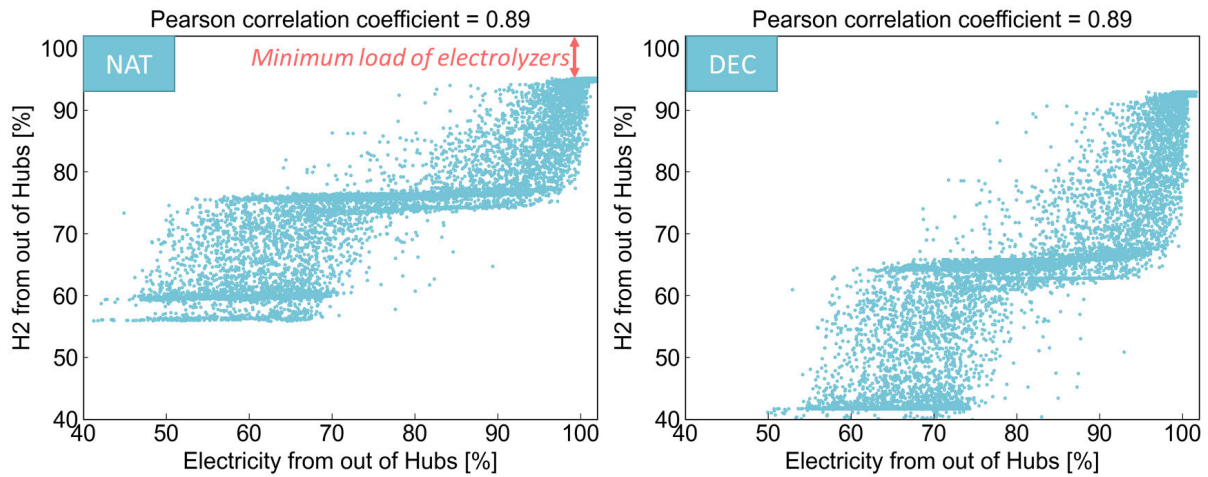


Figure 4.4: Hourly mismatch of electricity and hydrogen for NAT (left) and DEC (right) scenarios. These graphs show the electricity and hydrogen that are not fulfilled by the 3 Hubs (supply/demand mismatch).

The fluctuations in the power and hydrogen production in the hubs (Figure 4.5) originate from the power profile which is a result of the wind speed and from the operational strategy of the electrolyzers. The power gradient for production spreads evenly, while the power demand gradient reaches larger values for ramp up than for ramp down. For the power supply and demand, the histograms are relatively similar. This suggests that short-term power storage solutions may be able to accommodate part of these fluctuations. Conversely, we can observe a clear difference between the dynamics for the demand and the production of hydrogen. As the bandwidth of the hydrogen demand gradient is much smaller than that of the hydrogen being produced, it indicates fewer fluctuations for demand versus production. This shows that the dynamics of the hydrogen production and demand are not properly matched and that other strategies or assets might be used to align both. Potential solutions would be short-term storages near the electrolyzers, to stabilize the production outflow, to change the operational strategy, or to add long-term subsurface storage for an (almost) constant hydrogen flow to the shore. Power storage solutions could also be beneficial for this match. However, to match supply and demand curves for hydrogen, large amounts of power storage would be necessary, leading to medium/long-term energy storage solutions and not only small-duration battery storage.

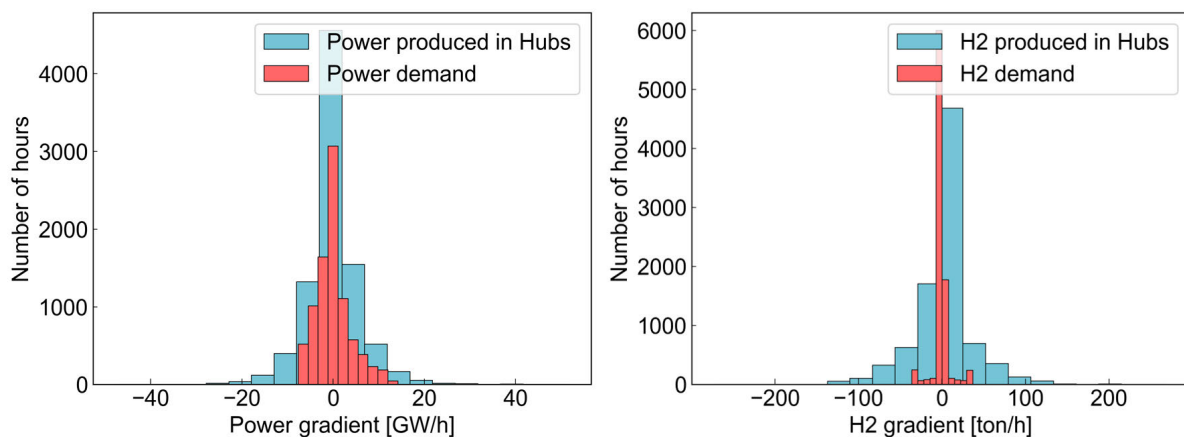


Figure 4.5: Hourly gradients of power and hydrogen supply from the Hubs and demand for NAT reference scenario.

4.1.1 Scenario NAT

This section contains the results regarding the NAT reference scenario for the newly built infrastructure. Figure 4.6 shows the pressure fluctuations along the whole network for this scenario on a daily basis. It is observed that the fluctuations are mostly contained within a 3-bar range. When looking at specific pipes (right graph), similar results are observed.

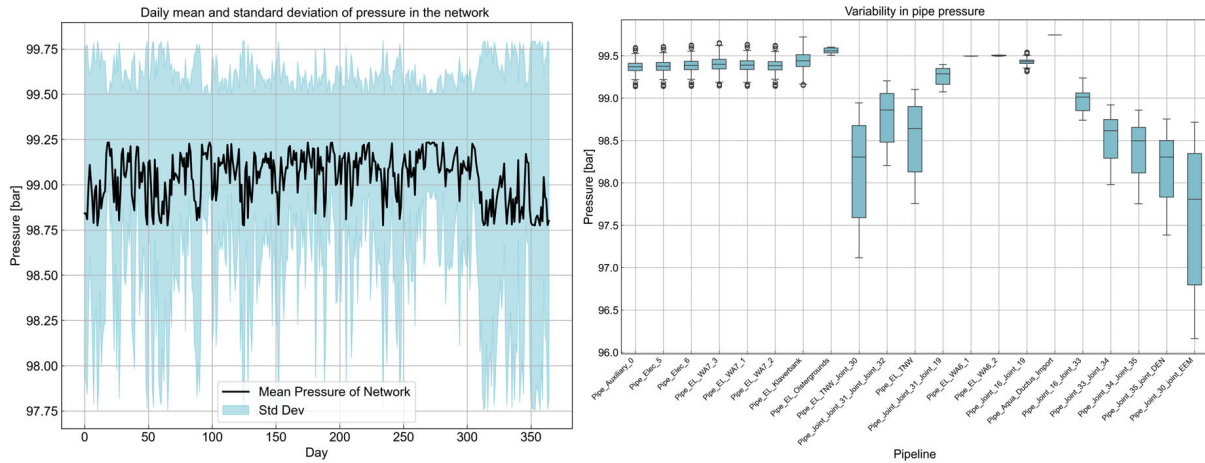


Figure 4.6: Network daily average/standard deviation (left) and single pipe pressures (right) for the NAT reference scenario.

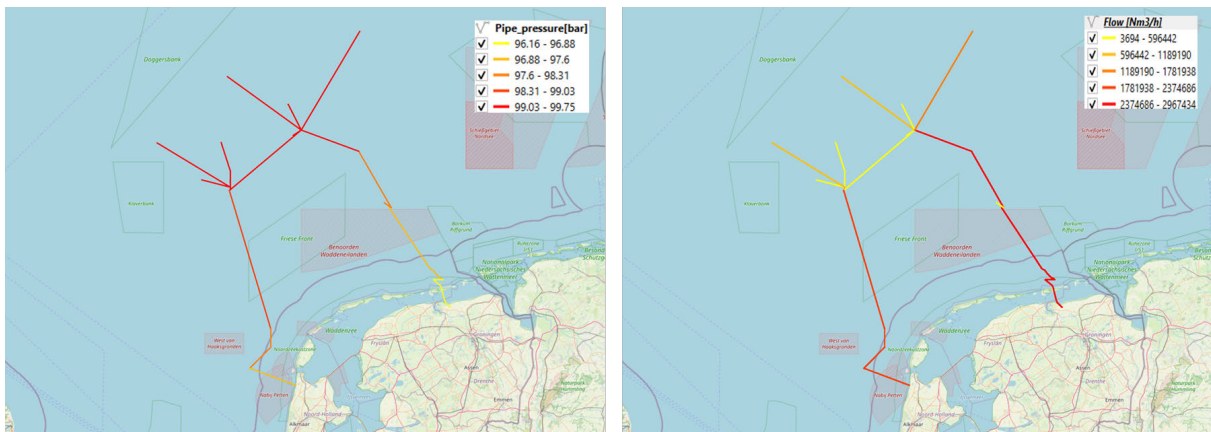


Figure 4.7: Pressure [bar] (left) and Flow [Nm³/h] (right) at the event of maximum flow in the network. Note that the legend in the pressure distribution map shows the average pressure in the pipeline computed between the inlet and outlet pressure of the pipeline.

The pipelines close to the electrolyzers have a variability of less than 1 bar, with the pressures at the landing points having slightly higher deviations, resulting (partially) from higher flowrates when combining different production sources and import.

Figure 4.7 shows the pressure and flow distribution in the network at an instance (event) of maximum flow in the network. The maximum flow occurs in an hourly interval where the total mass present in the network is found to be maximum, and this is when the largest pressure drops are also expected. This variability in flowrates occurs due to the dynamic production of hydrogen from the electrolyzers. During this event, a total of 3.85 bar pressure loss is estimated across the network. As indicated in the previous sections, the newly-built scenario consists of landing points in Den Helder and another location closer to Eemshaven,

between Ameland and Schiermonnikoog. For simplicity, the latter is referred to as the Eemshaven landing point. Highest pressures, close to 100 bar, in the grid are experienced in the pipeline connecting to the AquaDuctus import. This is due to the fact that we have a fixed import of hydrogen through AquaDuctus at 100 bar pressure (see Figure 4.8). Due to the 48-inch diameter of the pipeline, a constant throughput of 4.3 GW hydrogen (import) leads to minimal pressure loss in this pipeline. This makes the pressures in the Hub North relatively close to the pressures in this pipeline, thus requiring all the produced hydrogen in Hub North (both in wind areas 6 and 7) to be injected into the network at this pressure level. However, pressure losses occur as hydrogen is transported to shore. Pressures at Eemshaven are lower than Den Helder due to the difference in the flow rates.

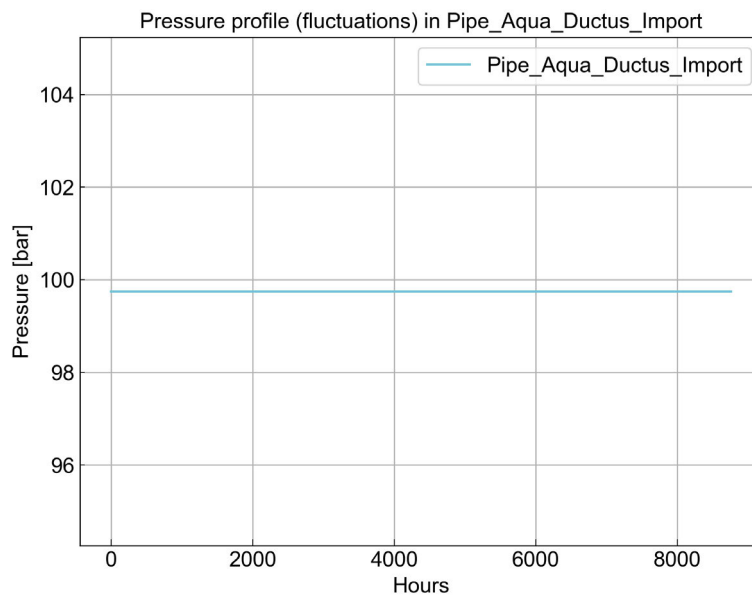


Figure 4.8: Average pressure [bar] in the pipeline connecting to AquaDuctus Import

Flow rates at Eemshaven are set (as a boundary condition) 1.27 times higher than in Den Helder (see Figure 4.9). The flow distribution in the network is trivial in this case, having two distinctive routes, with one link running from WA6 to landing point at Den Helder and another running between WA6 and Eemshaven. The demand at the landing point in Eemshaven is met by production in WA6, import from AquaDuctus and DEMO-2, whereas production in WA7 along with additional flow from AquaDuctus Import is routed by the pipe between WA6 and WA7, utilized for consumption at Den Helder.



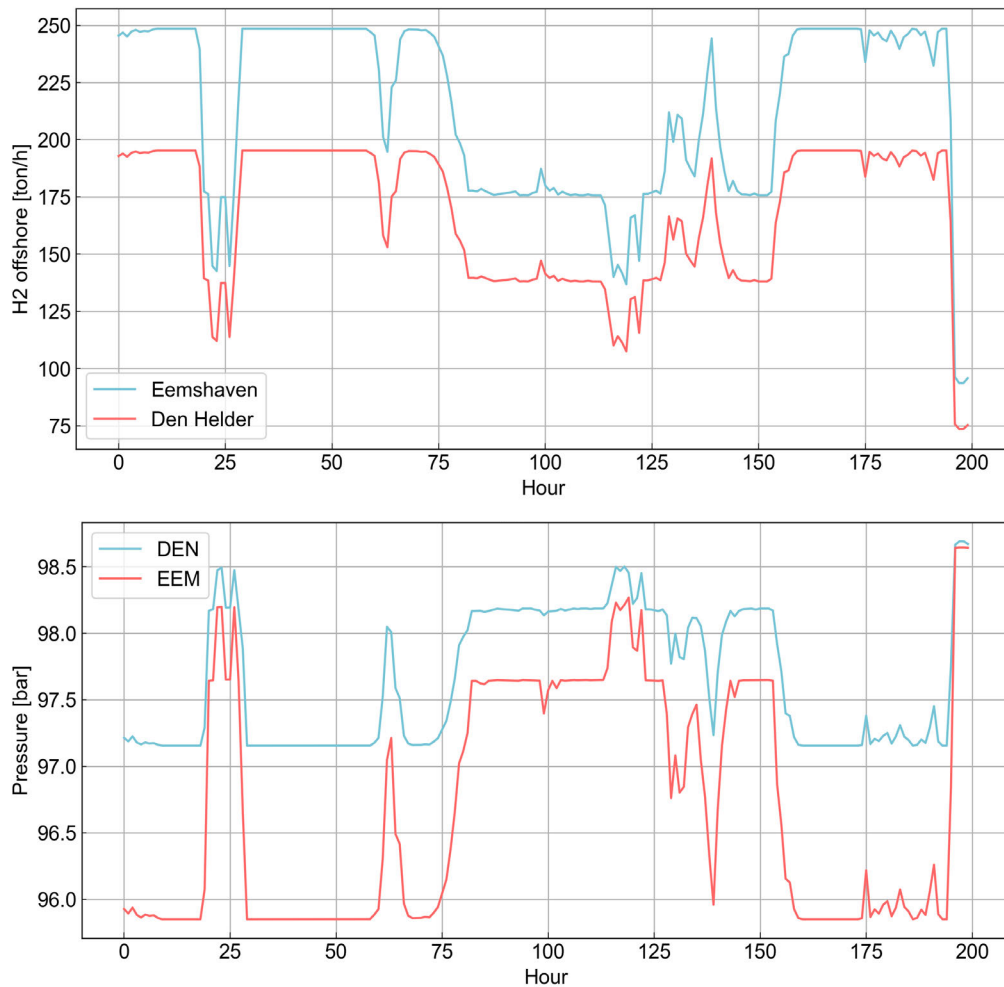


Figure 4.9: Snippet of flow rates [ton/h] at Eemshaven and Den Helder landing points (top) and the corresponding pressure [bar] (bottom). Note that the plots correspond to the first 200 hours of the simulated year.

Figure 4.10 shows the utilization of such links/branches in the network. The pipe running between WA6 and WA7 (henceforth addressed as West-East connection in this section) carries approximately 11 TWh hydrogen annually, roughly 20-30% of what is carried in the west and east connections, bringing out the importance of an interconnected network. The load duration curve of its flowrate also indicates that its utilization looks similar to a piecewise constant curve, with several hours (around 800-1000) transporting similar flowrates.

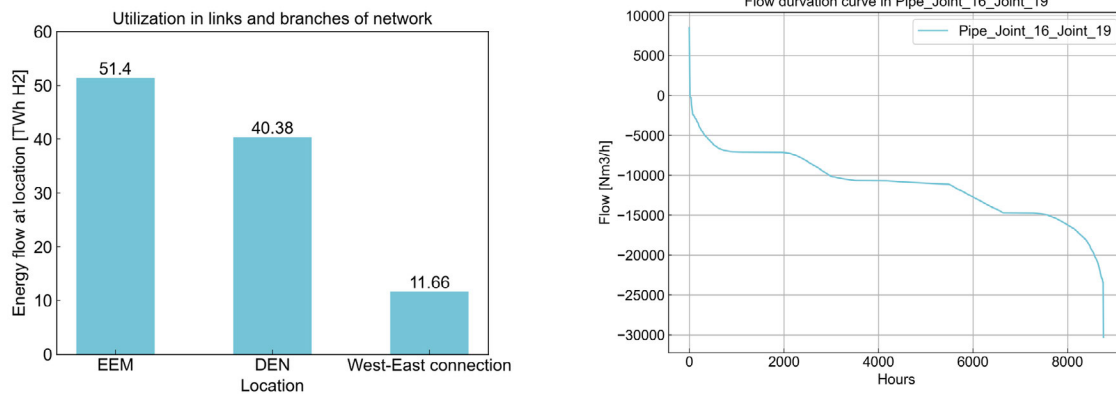


Figure 4.10: Utilization of links/branches [TWh] in the network (left), and flow duration curve in the West-East link (right) [Nm3/h]. Note that 'Pipe_Joint_16_Joint_19' is the pipe addressed as West-East link. Negative and positive flow rates are shown to address the direction of flow. Negative flow indicates direction from WA6 to WA7.

Figure 4.11 shows the pressure drop in the network. Generally, we see low pressure drops occurring in the network, with a maximum pressure drop of 2 Pa/m in the pipeline connecting to the landing point at Eemshaven. These lower pressure drops are in fact due to the choice of the large pipeline sizes of 48 inch, which indicate the low utilization of the capacity in this case. The figure on the right also shows the standard deviations of pressure in the pipeline, which imply and quantify the fluctuations that occur through the year. The fluctuations in the pressures arise from transporting hydrogen in varying flow rates, with most of it occurring in the pipeline that also experiences the maximum pressure drops. Thus both the design and the physical parameters contribute to the fluctuations occurring in this pipeline. Although only a deviation of 1% from the mean pressure (in this pipeline) is observed.

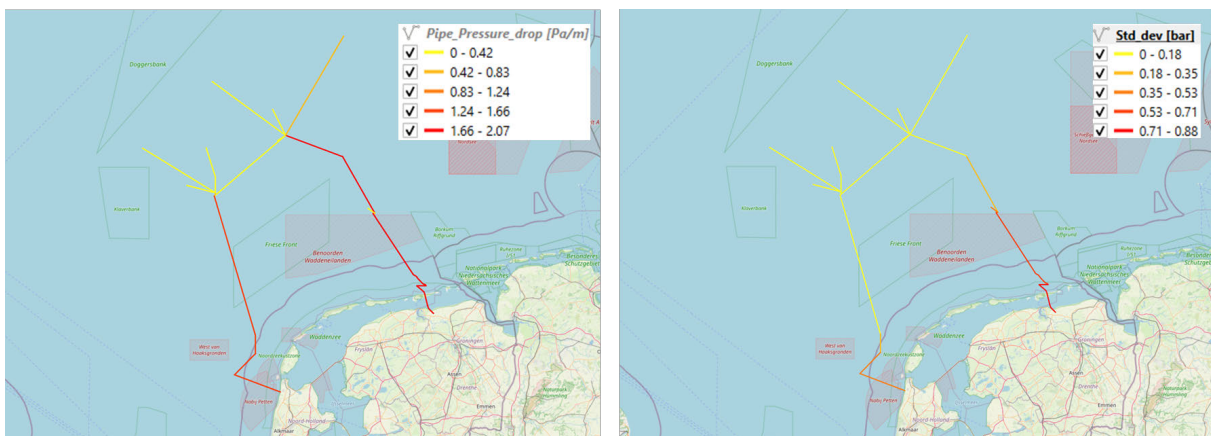


Figure 4.11: Pressure drop [Pa/m] in each pipe at the hour of maximum flow in the network (left). Standard deviation of pressure [bar] in the network.

The top part of Figure 4.12 shows the variability in pipe pressure in a box plot. Generally, the network consists of pipes that undergo different levels of pressure variability. Pipes with high variability (wider boxes) are in this case closer to the shore than the pipes with low variability. Pipes with high variability are exposed to larger pressure fluctuations, but are well

contained within the 25th – 75th percentile, whereas pipes with low variability (narrower boxes) have fluctuations (outliers) outside their quartile ranges. This occurs due to the variability in the production of hydrogen in the offshore area, which requires injection of hydrogen into the grid at a wider range of pressures. It indicates that the network is relatively less stable in terms of fluctuations in the offshore area compared to pipes near the onshore location.

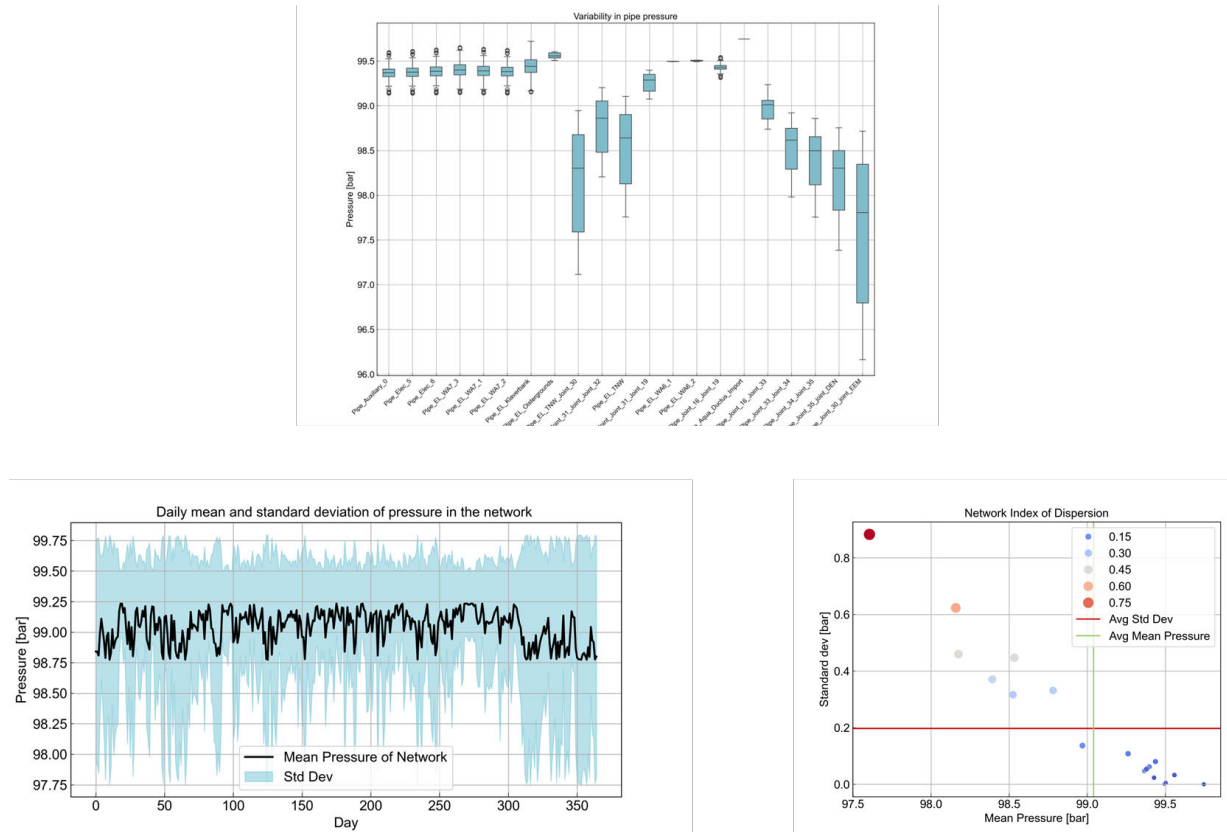


Figure 4.12: Statistics on the network. Variability in pipe pressure (top), daily mean pressure in the network (bottom left) and Index of dispersion (bottom right)

The figure on the bottom right of Figure 4.12 shows the index of dispersion in the network, essentially a scatter plot of standard deviations of the pressures in the pipes against their mean pressures. Pipes with higher mean pressures (closer to the offshore production area), have lower deviations, whereas pipes with lower mean pressures (closer to shore) have higher deviations, and indicate different levels of stability, and supports the map shown in Figure 4.11. The plot on the bottom left shows the average pressure in the network at a daily interval. No seasonal variations are observed due to the dynamic nature of production from various sources, but in the network average pressure fluctuates around 99 bar, with max-to-max occurring in the 0.5 bar range.

4.1.2 Scenario DEC

Similarly to the NAT scenario, the results to the NSE5-DEC reference scenario are presented in this section (newly built infrastructure, no hydrogen storage, reference pressure of 100 bar, import from AquaDuctus). Figure 4.13 shows the pressure and the flow distribution similar to the maps in the previous section at the interval specific to the maximum flow hour. In this case, a lower pressure difference across the network is seen. Since the scenario DEC is designed with lower capacities of P2G in the hubs, the hourly production is much lower compared to the NAT scenario. With lower flow rates in the pipeline, pressure losses in the

pipelines are minimal. A maximum of 2 bar of pressure difference across the network is seen. In order to compensate for lower production from the hubs, the AquaDuctus import ramps up to 5.4 GW. Although, this leads to only additional pressure drop of 0.08 bar (not shown). Even though the flow rates at Eemshaven and Den Helder are retained with the same ratio as indicated in the previous section, the network delivers hydrogen to the shore at similar pressure levels. The pressure at Eemshaven now is only 0.3 bar lower than in Den Helder.

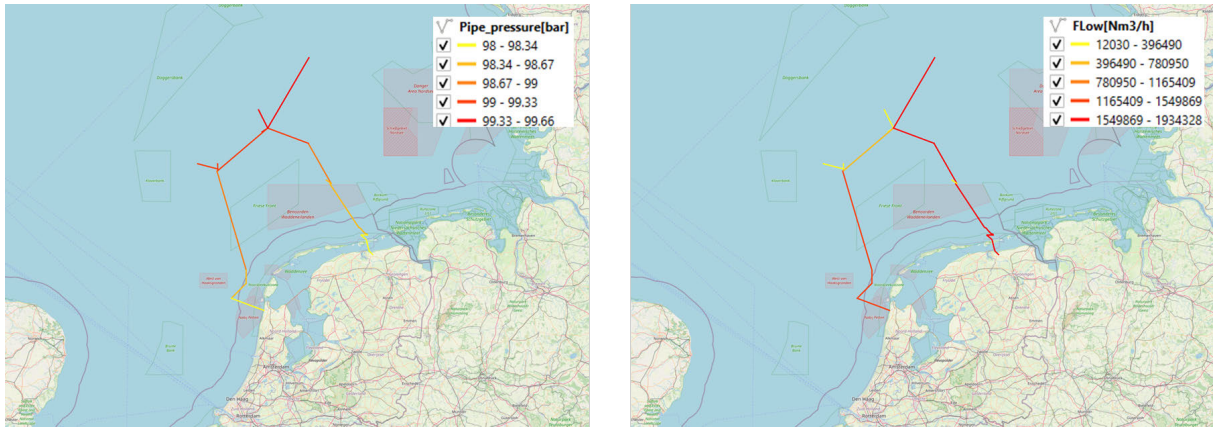


Figure 4.13: Pressure [bar] (left) and Flow [Nm³/h] (right) at the event of maximum flow in the network. Note that the legend in the pressure distribution map shows the average pressure in the pipeline computed between the inlet and outlet pressure of the pipeline.

Figure 4.14 shows the pressure drop in each part of the network at the maximum flow interval. The pressure drops in this scenario are only as much as 40% of the maximum pressure drops experienced in the NAT scenario in the same pipelines. The pressure drop is more or less uniform along the west and the east sides of the network. The deviations (shown in right) show the same trend as the NAT case, where high magnitudes (with a maximum of 0.15% coefficient of variation) are experienced in the pipelines closer to shore whereas low deviations occur more in the offshore region.

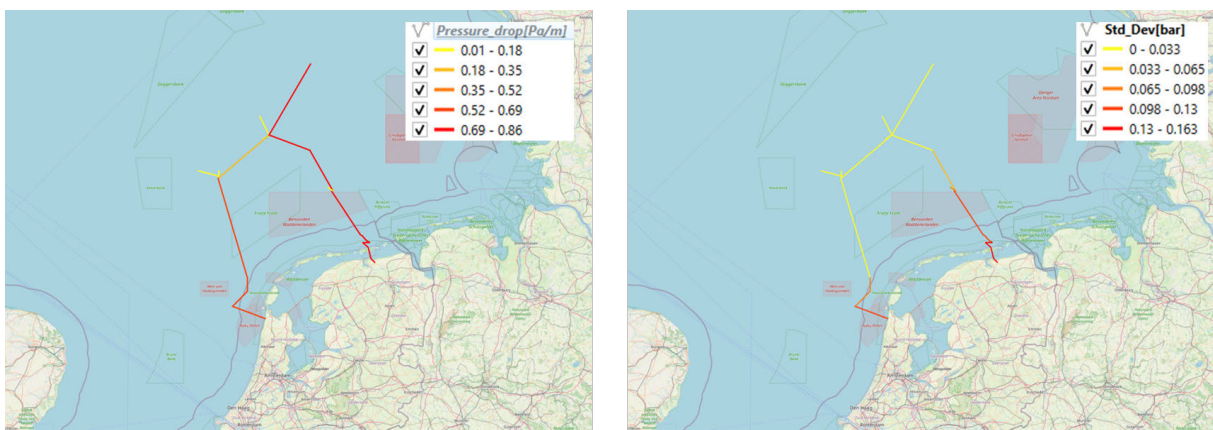


Figure 4.14: Pressure drop [Pa/m] in each pipe at the hour of maximum flow in the network (left). Standard deviation of pressure [bar] in the network.

4.1.3 Learnings from the reference scenarios

Overall, the NAT scenarios are designed with higher ambitions for production and consumption of hydrogen (see Figure 4.1). Generally, high transport capacities (rates) lead to

more hydrogen throughput in the grid resulting in larger pressure drops while transporting it to the shore. However, in the new-built scenario the network is sized with 48-inch pipes, which results in large transport capacities, and this reduces pressure losses for hydrogen to be safely transported. The maximum utilization of the network reaches only 40% of its nominal capacity at 100 bar. The (nominal) capacity of the network is around 6.7 kton at 100 bar, whereas the maximum mass present during moments of maximum flow is 2.7 kton, leaving room for much more injection of hydrogen into the grid. At the intervals of maximum expected pressure drop, NAT and DEC experience pressure drops of around 3.85 and 2 bar respectively. Daily variations are also contained within the 0.5 bar pressure range. In both cases, highest swings are expected near the landing points, in the range of 0.5 – 2.5 bar.

4.2 Influence of wake losses on wind farm production (for year 2015)

The modelling of the wake losses in the production of the wind farms can have a large effect in the outcome of the results. Using single turbine power curves can result in overpredictions of the power production compared to the production of a complete wind farm. It is out of scope of this project to model the whole North Sea with high-fidelity models, such as large-eddy simulation (LES), due to its high computational cost. However, efforts to achieve a more accurate representation than purely analytical models has been attempted by constructing a surrogate model fitted with FarmFlow CFD simulations, as explained in Section 3.1.6. This section highlights the main differences found in a comparison with other approaches.

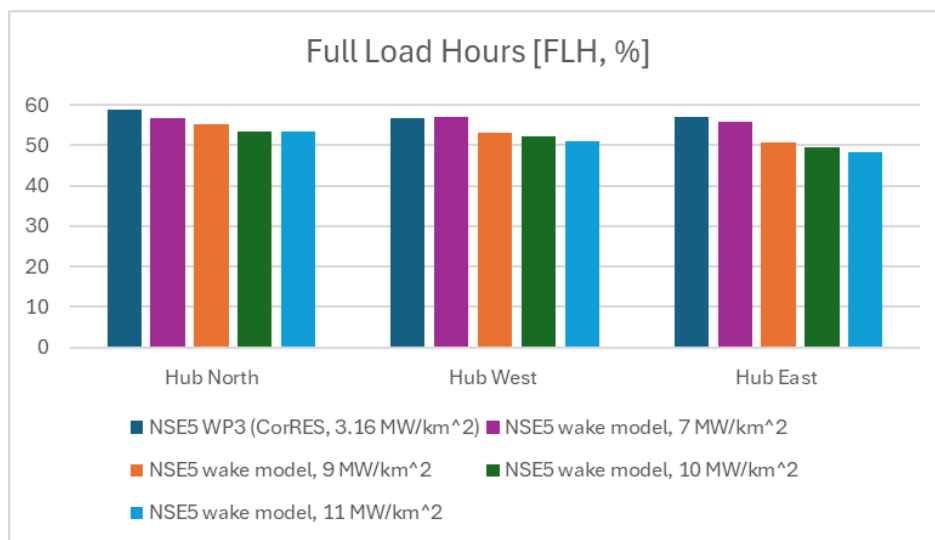


Figure 4.15: Comparison of full load hours of different wind farms for the 3 Hubs for a the NSE5 wake model and CorRES dataset used in deliverable D3.1. In bold, the value for 10MW/km² which has been approximately used in the different wind farms.

Figure 4.15 shows a comparison of full load hours of different approaches. The first one corresponds to a wake model that covers a wider area with potentially multiple wind farms: Area 6 for Hub North, Nederwiek Noord for Hub West and Area 4 for Hub East. The other method contains the values used in D3.1 of this program (Blom, van Stralen, Eblé, Magan, & Hers, 2025), with the input data provided by CorRES (Murcia, et al., 2022) at 3.16 MW/km² and 155 m of Hub height (Koivisto & Murcia Leon, Offshore wind generation time series for technology SP316 HH155 (PECD 2021 update), 2022). It can be seen that the differences in

values between the CorRES results and the wake model for 10 MW/km² are significant, with around 10% variations. This could be due to, between other factors, smaller power densities considered in CorRES. As a comparison, in 2022, the average power density in offshore wind farm in the Netherlands was around 7 MW/km² (Taminiau & van der Zwaan, 2022).

In fact, when using the value of 7 MW/km² as a power density, the production for three Hubs is much closer to the CorRES dataset). However, this does not explain all of the differences observed, as the NSE5 wake model in Hub West has slightly higher production at 7 MW/km² compared to the CorRES dataset at 3.16 MW/km². These remaining differences could be due to the specific type of wind turbine and exact location chosen. In fact, CorRES also includes a dataset with existing installations (Koivisto & Murcia Leon, Existing offshore wind generation time series (PECD 2021 update), 2022), which includes Hub East for 2015. This data has a full load hours percentage of 48.8, comparable to the 10-11 MW/km² cases from the NSE5 wake model. It can furthermore be observed that the effect of considering these wake losses for a larger area is quite different depending on the location considered. For Hub North, there is a distinct loss of production when increasing the power density, almost plateauing beyond 10 MW/km². For Hub West and Hub East, there are larger differences between the wind farm and area levels, and a consistent decrease in power production with higher power densities.

In all of the cases considered, the power production obtained is below the values used in Work Package 3. These differences are the largest in Hub East, with 13% less production in the case of this work compared to the CorRES dataset for a power density of 3.16 MW/km² and 155 m of hub height. Some of the differences may be related to the wake effects, while other may be due to different geographical locations, specific wind turbine model/power curve used and other aspects, such as inter-array losses. In particular for CorRES, in (Murcia, et al., Validation of European-scale simulated wind speed and wind generation time series, 2022) it is mentioned that a generic wake model was used for the dataset due to the lack of information of specific layouts, with significantly lower power densities than the ones present in our work. To add to these differences, in the NSE5 WP1 results, no interactions between different wind areas were taken into account in this model, so the decrease in production may be larger in practice than the values outlined here. The effects of the higher power densities on the wind farm production depend on the conditions of the particular year, and analyses with multiple years of data should be done to determine conclusions regarding the operational envelope of a wind farm for its lifetime.

Link to the research questions:

How does the limited space in areas to be developed for offshore wind and hydrogen affect the capacities, spatial configuration and energy production of the hubs?

- The results from this section show that densely-populated wind farm areas will result in a significant decrease of the energy production at the hubs, in some occasions beyond 10% compared to the average power density of 7 MW/km² of offshore wind farms in the Netherlands in 2022. This should be taken into account when considering supply/demand matching scenarios and when considering even higher power densities, such as in designs with significant overplanting.

4.3 Grid-connected vs. not grid-connected H₂ production in Hub North

For the simulations performed in this work package, a balance between sending power to shore and ensuring a reasonably stable load on the electrolyzers has been chosen. For the 4 GW blocks, corresponding to 4 GW of wind power with 2 GW of cables and 2 GW of electrolyzers, the priority was set as:

- Aim to fulfil a baseload of 50% for the electrolyzer with electricity produced from the first (1 GW) tranche of wind power (0-1 GW). If this is not possible, aim to fulfil less than 50% but at least 10% of the capacity of the electrolyzer (minimum load), preferably from wind, and otherwise from the grid, as a bidirectional connection is assumed.
- Send the electricity from the second tranche of the wind power (1-3 GW) to shore.
- Use the electricity from the third tranche of wind power (3-4 GW) for additional load of the electrolyzer.

Figure 4.16 shows the differences between the NSE5 operational strategy and using equal power to the electrolyzer and the cable to shore. Both strategies have a similar utilization factor of the electrolyzer and the export cable, with a near-identical utilization of both components in both cases. However, there is a clear difference seen in the power delivery to shore (middle graphs). In the load duration curves, it is observed that there are more than 1000 extra hours where the cable to shore is fully used with the NSE5 strategy. This is a very significant reduction, that is the result of allowing the electrolyzer to dampen some of the fluctuations of the wind energy production. This can also intuitively be seen in the left graphs, when looking at the top part of the orange components (wind to grid). There, more “flat” parts are observed, compared to the higher amount of fluctuations with an equal power strategy. A visual comparison between 10 and 50% minimum load for the NSE5 operational strategy is shown in Figure 4.17, where its effect is observed for a period of high wind power (top) and low wind power (bottom).

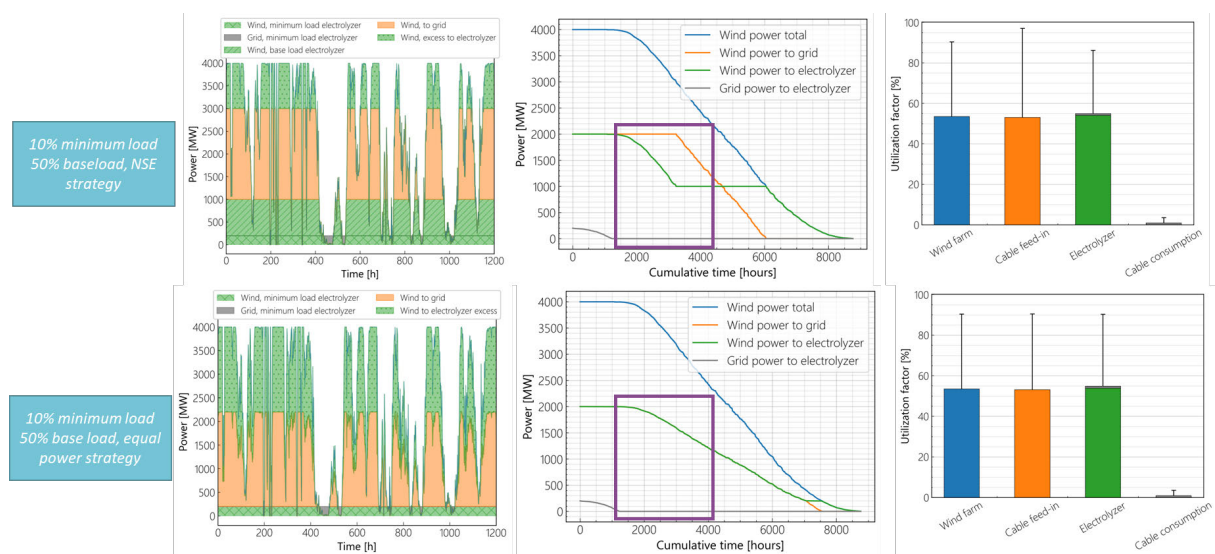


Figure 4.16: Comparison between the strategy used in this work and a strategy sending equal wind power at all time steps to both the cable and the electrolyzer.

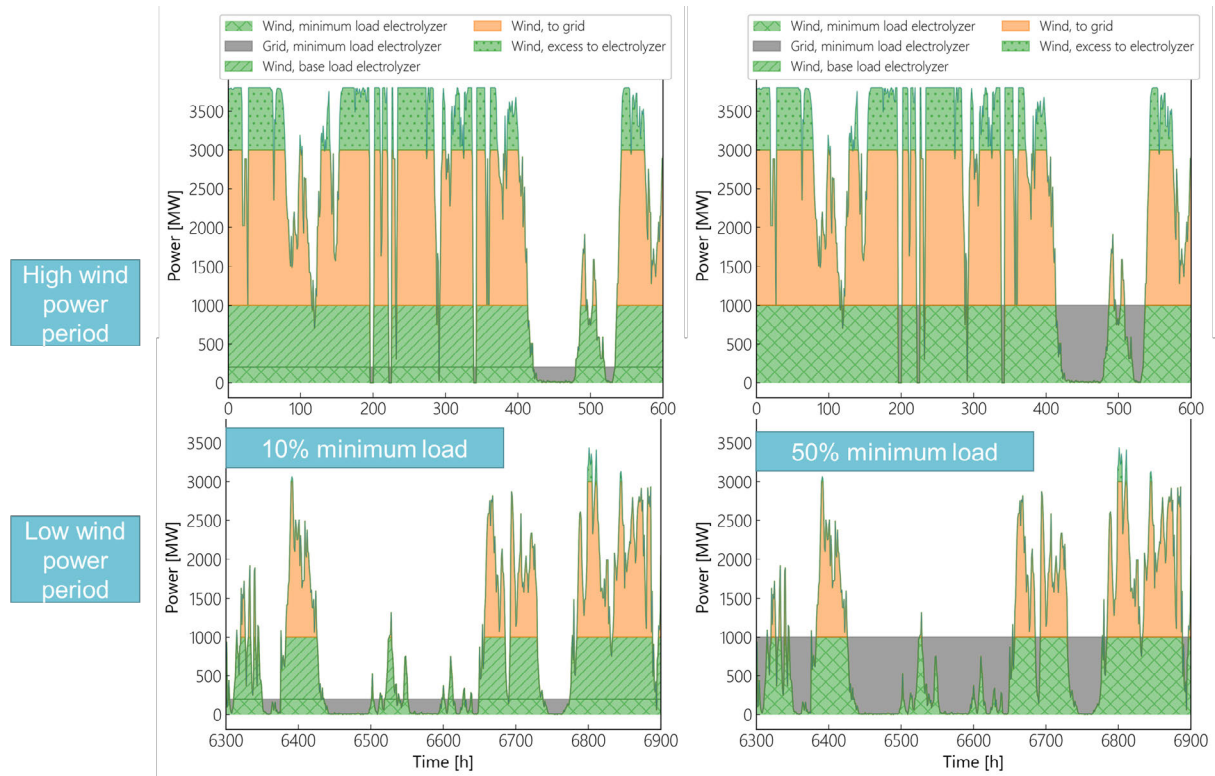


Figure 4.17: Illustration of periods with high and low wind power for 10% (left) and 50% (right) minimum load of the electrolyzer.

Figure 4.18 shows the increase of the full load hours using grid power for different levels of minimum load. It can be observed that, for 10% of minimum load, only a 1% of grid power is necessary. This increases to around 10% for 50% minimum load. These modest amounts are a consequence of the oversizing of the wind farm in the block compared to the electrolyzer (2:1 ratio). Even if the overall energy used is relatively small, the number of hours using grid power is significant: from almost 1300 hours to almost 2900 hours at 10-50% minimum load, respectively. The number at 10% minimum load is around 15% of the hours in a year. This highlights that if fully continuous operation is required, a certain level of grid connection or power storage is necessary.

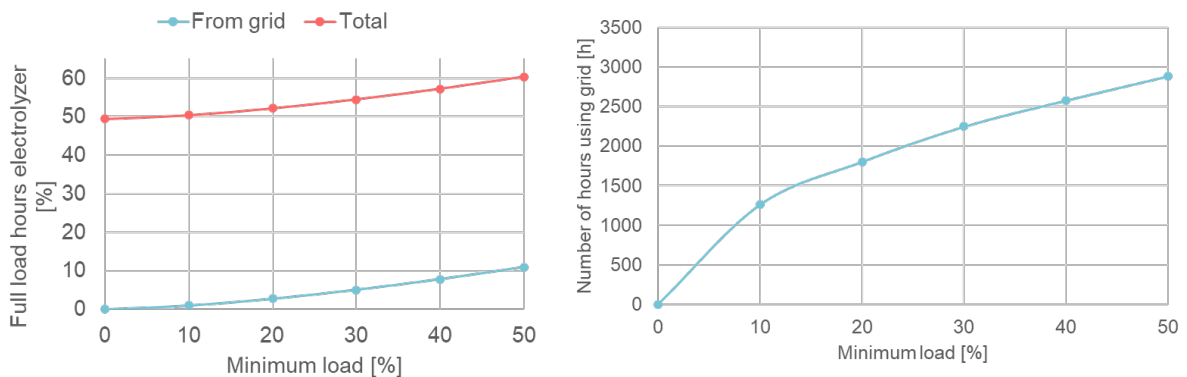


Figure 4.18: Full load hours of the electrolyzer for different amounts of minimum load (left) and nr. of hours using grid power (right).

To quantify potential grid/storage power requirements, Figure 4.19 shows the energy used in each of the cycles when not enough wind power is available. Each cycle is defined as a period ranging from 1 to multiple hours when auxiliary power is needed to meet the minimum load.

The cycle ends once enough wind power is available. It can be observed that, for the case with 10% minimum load, the majority of the cycles correspond to energy requirements of around 1-2 times the capacity of the electrolyzer (less than 4 GWh for a 2 GW electrolyzer). The case of 50% minimum load roughly multiplies these requirements by an order of magnitude. If fully continuous operation is required, there are some outliers during the year that can increment the grid/storage energy requirements by 5 times.

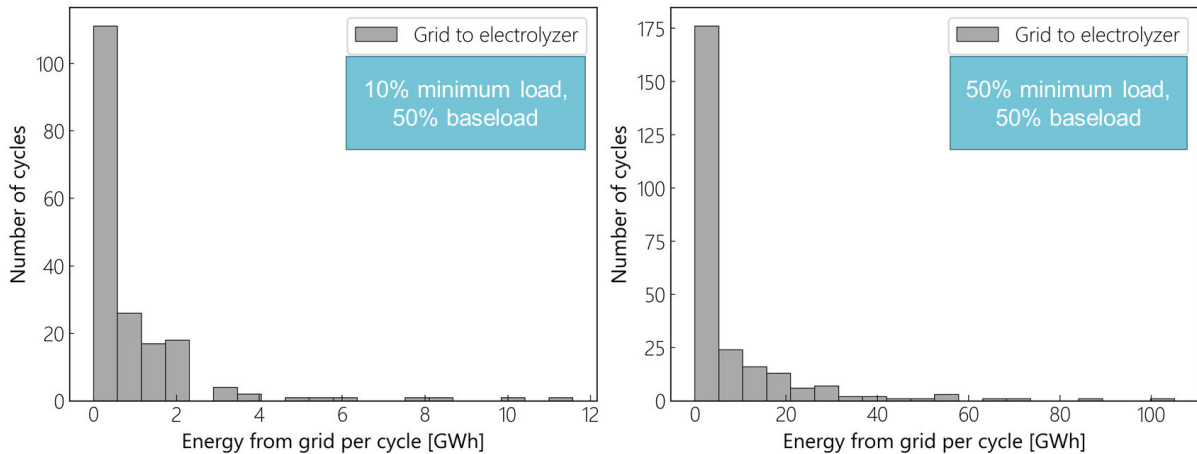


Figure 4.19: Comparison of grid utilization/ cycle for cases of 10 and 50% minimum load, used to estimate auxiliary battery capacity.

This is also observed in Figure 4.20, where the 5 largest cycles of the year are depicted. If only a small number of shutdowns were allowed, then the storage requirements can be significantly smaller (50% reduction for 5 shutdowns in a year). The compromise between the number of yearly shutdowns allowed in a year compared to the capacity of this auxiliary power system or grid power required is depicted in Figure 4.21. For 10% of minimum load, allowing 10 shutdowns in a year resulted in an energy required of around 3 GWh. 20 shutdowns lead to 2 GWh, and at around 60 shutdowns this decreases to 1 GWh. For 50% of minimum load, the trend is similar, but with energy requirements around 8-10 times larger.

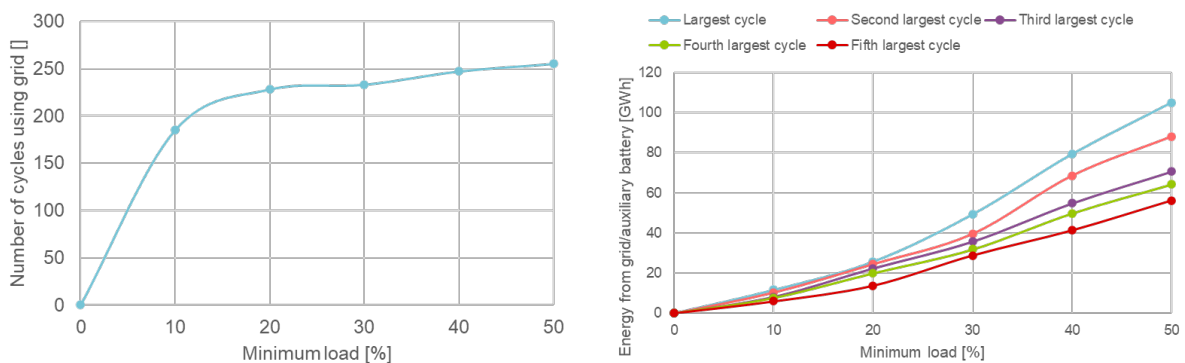


Figure 4.20: Number of cycles using grid (left) and energy required from grid or an auxiliary power storage system (right). A cycle is defined as a period with not enough wind power available.

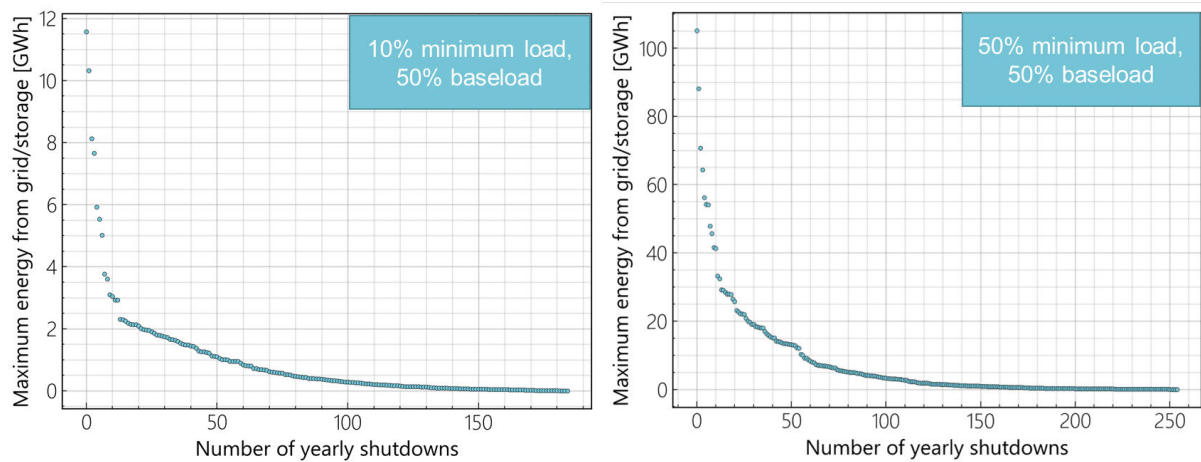


Figure 4.21: Number of yearly shutdowns compared to the maximum energy required for a cycle from grid/power storage in a year for different levels of minimum load.

Link to the research questions:

How do different operational strategies affect the utilization and need for flexibility of the offshore hydrogen production and transport infrastructure to absorb part of the wind power intermittency?

- Using PEM electrolysis with 10% minimum load and a 2:1 ratio of wind to electrolyzer capacity leads to less than 2% use of grid power. Increasing the minimum load to 50% would increase the grid power consumption to around 10%.
- Allowing 10 shutdowns a year for hydrogen production with 10% minimum load and off-grid mode, a power storage system delivering around 15-20 hours of this minimum load would be needed. This may be able to be achieved by short/medium-term power storage methods. However, if zero shutdowns for hydrogen production are allowed, the power storage requirements increase by 5 times.
- Smart operational strategies can increase the number of hours with peak power delivery to shore, allowing the electrolyzer to dampen some of the wind power fluctuations. More than 1000 additional yearly hours were obtained by using different parts of the wind curve for minimum/baseload compared to a 1:1 ratio of power to the electrolyzer and export cable to shore.

4.4 Offshore solar inclusion

In this section, the inclusion of offshore solar is explored at a high level. A test was performed by adding offshore solar in an extreme case. This case is based on the reference, NAT-based configuration, but with a slightly altered operational strategy. An example of the basic modelling block used is shown in Figure 4.22. This augments the NSWPH-like block with the addition of 4 GW of offshore solar. The export cable to shore is still set at 2 GW, which forces the system to curtail when the combined solar and wind production exceeds 2 GW. This particular case study was performed at an earlier stage of the work. Hence, some of the assumptions (e.g., wake model, transport infrastructure) do not fully represent the final configurations, and the conclusions of this section should be taken as qualitative.

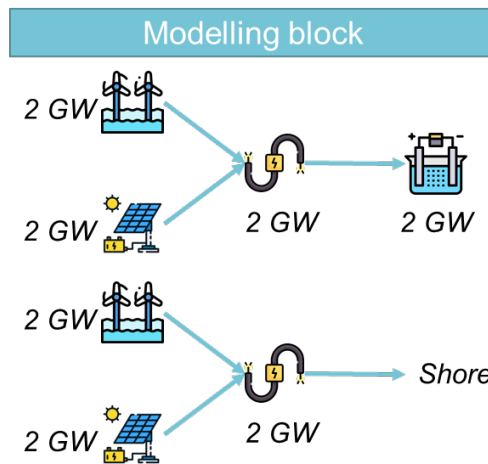


Figure 4.22: Structure of a modelling block for the case regarding the inclusion of offshore solar.

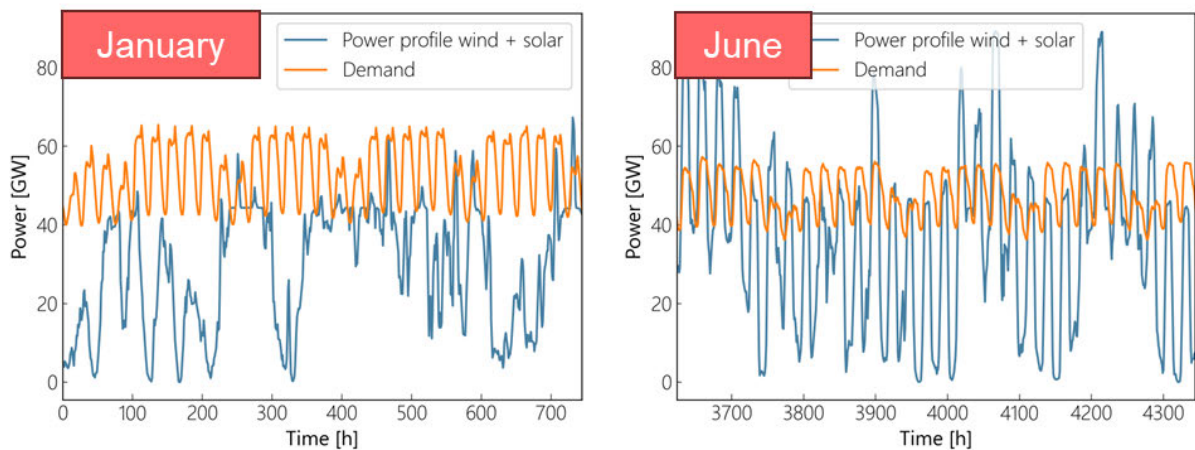


Figure 4.23: Profiles of power supply and demand when including offshore solar for January and June (of meteo year 2015).

The profiles of supply and demand when including offshore solar for two of the months can be observed in Figure 4.23. For the month of January, the profile looks similar to the offshore wind profile alone: demand can rarely be met with the supply of wind power available. For June, the two profiles look significantly better matched. There are multiple instances where supply exceeds demand. With storage solutions, such as batteries or other longer-term technologies, such as pumped hydro or flow batteries, there could be significant benefits when considering only the complementarity and availability of energy sources. In the summer months, the power that can be delivered to shore could reach 8-10 GW on average. The curtailment of the system in this heavily transport-limited scenario was in the order of 30 TWh. This is similar to the production of around 7 GW of installed capacity of an offshore wind farm.

This exploratory scenario is not meant to provide a comprehensive overview of advantages and drawbacks of offshore solar, as there are several limitations such as the absence of techno-economic calculations, flexibility options or land availability estimations. A business case assessment can be found in D3.3 (van Zoelen, Rob; Boer, Dina; Mahfoozi, Salar, 2025). Instead, this work provides a qualitative overview of potential benefits of supply/demand

matching for the three hubs considering the current boundary conditions, to be further explored. Other initiatives, such as the ongoing SENSE-Hub (Oceans of Energy; NWO-NIOZ; Deltares; Primo Marine; New Ground Law; Advanced Electromagnetics BV; TNO, 2025), explore in detail specific configurations and business case for the Dutch North Sea.

Link to the research questions:

What is the influence of adding offshore solar on the variability of the electricity production of wind farms?

- Offshore solar can provide an additional source of power to complement offshore wind and increase the utilization of export cables, reaching the maximum capacities at several moments, leading to excess power curtailed of 30 TWh. However, the simplicity of the calculations made in this study limit the applicability of further conclusions regarding its suitability, as other factors such as energy storage and infrastructure should be considered.

4.5 Hydrogen transport scenarios: re-use versus new infrastructure

4.5.1 NAT scenario, re-use infrastructure, 100 bar

Figure 4.24 shows the pressure distribution (left) and the flow distribution (right) at the event of maximum flow under the NAT scenario. The pressure losses experienced by the re-used infrastructure are much higher for transporting the same amount of gas compared to the new-built infrastructure. A total pressure difference across the network is a maximum of 50.3 bar, which is 16 times higher than the pressure difference seen in the newbuild infrastructure. Importing 4.3 GW of hydrogen from AquaDuctus (which is a constant throughput, resulting in constant pressure drop) results in approximately 20 bar pressure drop through the section of NOGAT connecting to the AquaDuctus pipeline, and an additional pressure drop of 10 bar in the consequent pipeline.

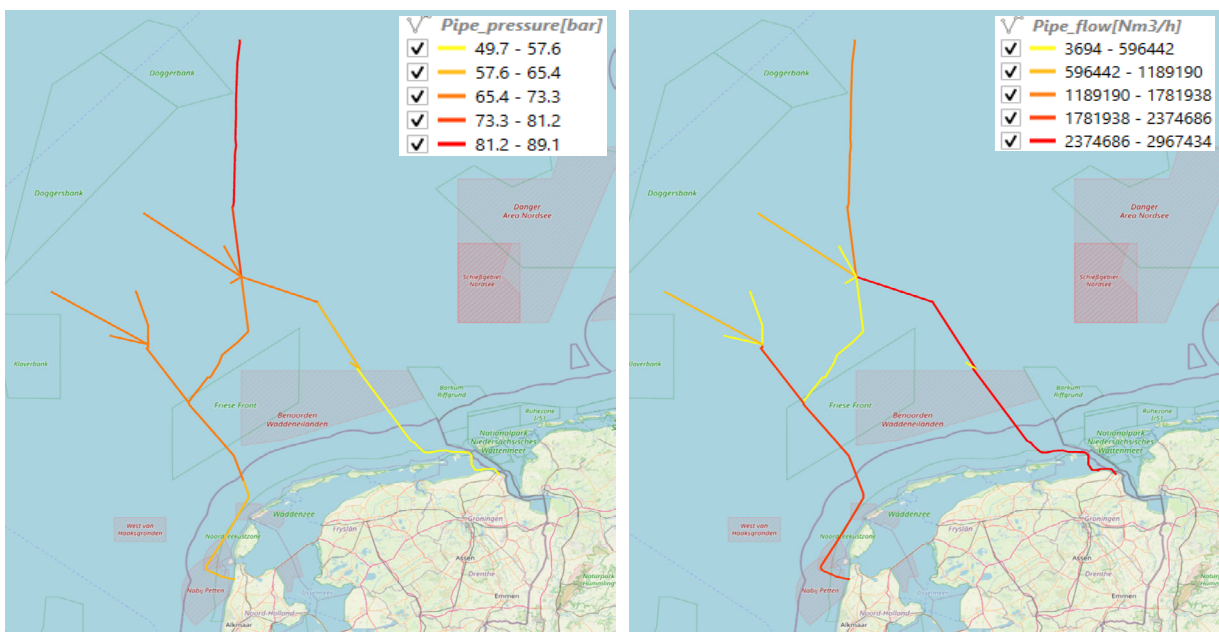


Figure 4.24: Pressure [bar] (left) and Flow [Nm3/h] (right) at the event of maximum flow in the network. Note that the legend in the pressure distribution map shows the average pressure in the pipeline computed between the inlet and outlet pressure of the pipeline.

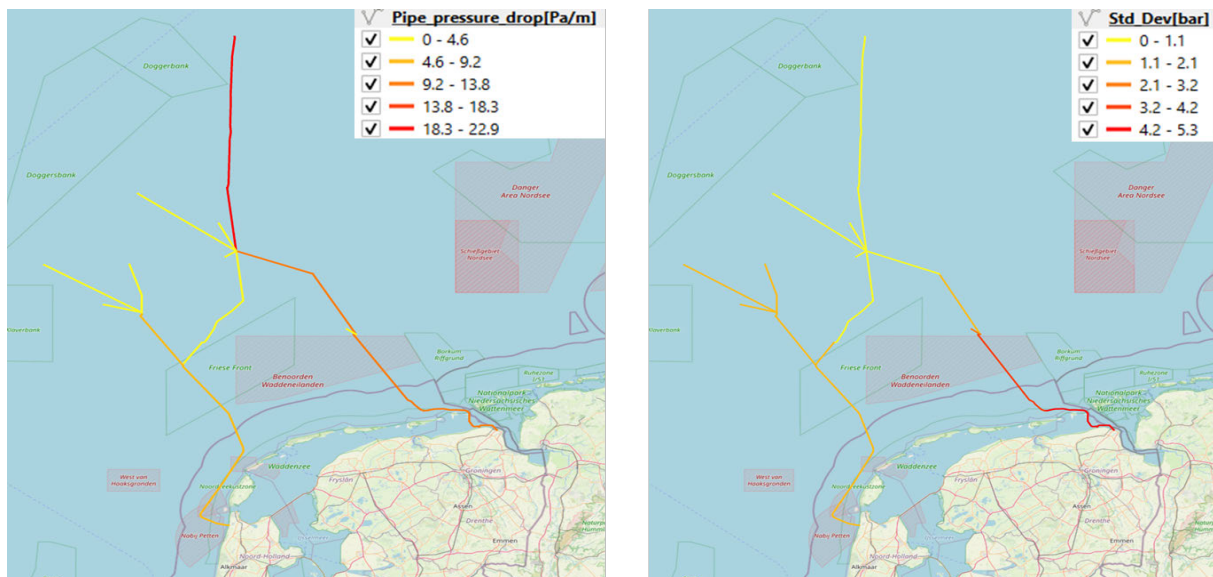


Figure 4.25: Pressure drop [Pa/m] in each pipe at the hour of maximum flow in the network (left). Standard deviation of pressure [bar] in the network.

This results in an entry pressure of hydrogen into Hub North of 70 bar. Even at an instance of minimum flow interval (lowest flow present in the network), the pressure difference in the grid is 35 bar, with 30 bar in the NOGAT pipe until the point of entry into Hub North alone making it critical. These high pressure losses are very well related to the dimensioning of the re-use infrastructure utilizing pipes that are sized between 24 inch and 36 inch. Thus the capacity of the network is reduced. By operating in a re-used infrastructure, only 50% of newbuild’s infrastructural capacity is available.

The highest pressure drops occur in the section of NOGAT connecting to the AquaDuctus import, with 23 Pa/m (Figure 4.25). Other sections of NOGAT show relatively low pressure drops. The section connecting to the landing point at Den Helder has pressure drops in the range of 9 – 14 Pa/m, whereas the middle section (also addressed as the west-east link) shows one of the lowest pressure drops in the network. The standard deviations of pressure are higher as expected in this network due to large pressure losses. Since the capacity of the network is lower, we see large pressure drops making the pressure near the shore region lower. Due to the properties of hydrogen (density, compressibility) pressure losses are higher at lower pressure levels. This in combination with the dynamic nature of demand, induces large fluctuations in the pipeline. Highest deviations are seen in the NGT section landing at Eemshaven with up to 9% from the mean, with mean pressure of 58 bar. With the deviation of 5.3 bar, the maximum pressure that hydrogen lands with is 63 bar, and the lowest to 53 bar. Landing point of Den Helder shows lower deviations, with 3% from the mean pressure. Low flow rates at Den Helder leads to higher mean pressures realized in the region, making the fluctuations not as high as compared to Eemshaven.

Figure 4.26 shows the hourly and daily variations of pressure in the network. Within the two scenarios, the mean pressure in the network in the re-use scenario is much lower, due to its capacity. The peak-to-peak fluctuations of both hourly and daily intervals are higher in the re-use case than the newbuild case. Additionally, the spread of the fluctuations around the mean pressure of the network is also higher in the re-use case. The re-use infrastructure seems to have generally a higher variability in operating conditions due to its dimensionality (in design) of the network.

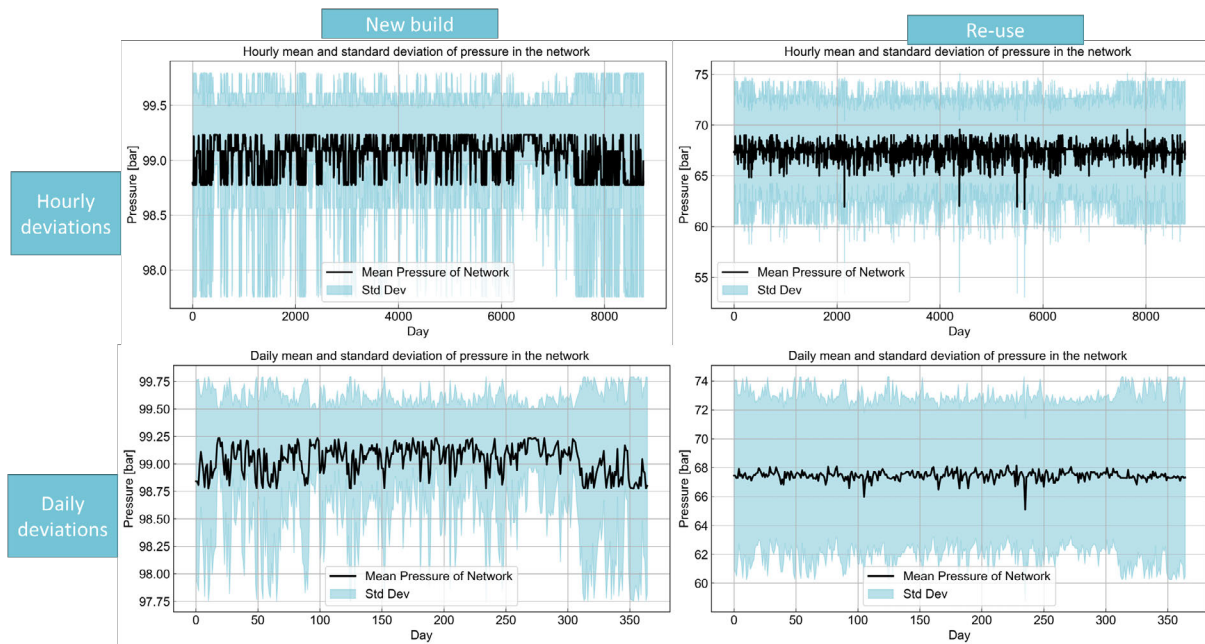


Figure 4.26: Hourly and daily deviations for NAT new-built and re-use scenarios. Note: different scale in y-axis for two cases.

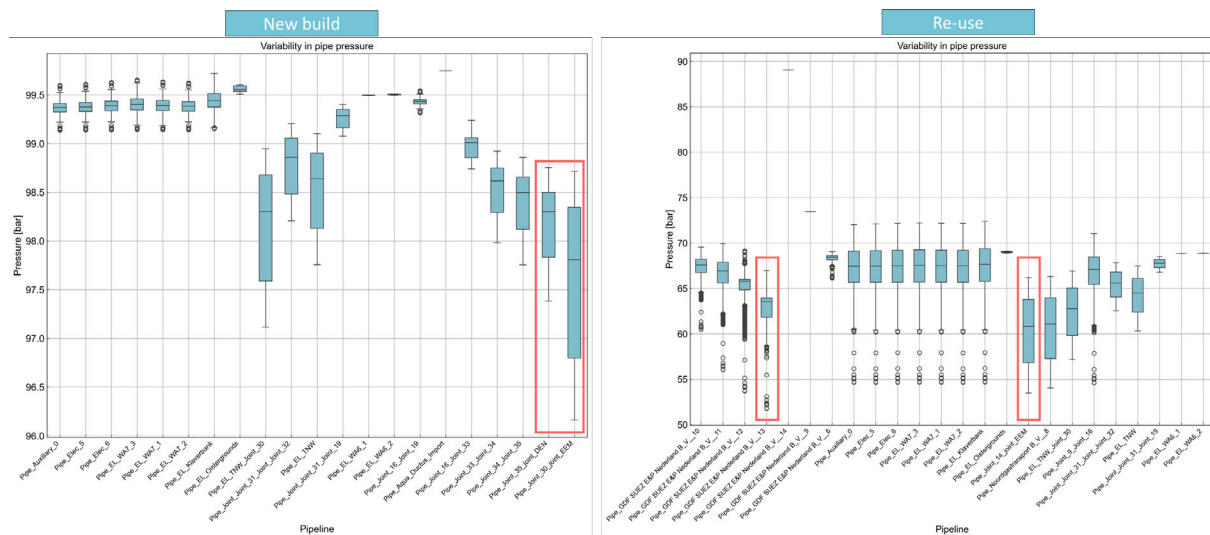


Figure 4.27: Comparison of pressures (new build vs. reuse) in each of the pipe sections. Pipes connected to landing points in coral outline.

Figure 4.27 shows the variability in the pressure range in each of the pipeline. As seen in the sections before, the highest variability occurs in the pipes connected to the landing point in Eemshaven. Highlighted in red are the pressure regimes in the pipes connected to the landing points. In Eemshaven, the fluctuations are spread more, but does not contain fluctuations outside their quartile ranges, but the pipes section of NOGAT connecting to the landing point of Den Helder has many outlying points compared to the new-built case, and thus contains pressure fluctuations which are far from the typical spread of fluctuations in that region. Although this does not occur in this pipe alone, but in almost all pipes in the network in the re-use case. This generally shows the regions of stability in the two networks. The production areas in both the cases contain high fluctuations, and additionally in the re-use infrastructure, most regions of the network (including one of the landing points) show

more fluctuations. It can be observed on the right side of the graph how the two sections closest to AquaDuctus incur in significant pressure losses, lowering the pressure of the rest of the system below 70 bar on average.

4.5.2 DEC scenario, re-use infrastructure, 100 bar

Similar to the NAT re-use scenario, the pressure drops have increased significantly in the DEC re-use scenario, up to a maximum of 68 bar. The NOGAT pipe section connecting the AquaDuctus to the remainder of the offshore network is about 135 km long while the connection in the newbuilt scenario is only 78 km which already would increase the pressure drop over that section by a factor of 1.7. Furthermore the capacity of the NOGAT pipes is smaller as the diameter is 24 inch instead of 48 inch in the newbuilt scenario. Thereby the pressure drop would increase by at least another factor of 16, a total factor of 27 already just referring to the import pipes. The fluid properties of 100 bar are therefore no longer valid, therefore the pressure drop will increase further. This results in a total pressure drop of almost 50 bar over these NOGAT pipe sections. This correlates well with the pressure drop in the NAT re-use scenario above, which states 30 bar for 4.3 GW import, while DEC imports 5.4 GW hydrogen and thus should result in an factor 1.6 for the pressure drop over the NOGAT pipe section connecting AquaDuctus.

Figure 4.28 shows the variability in the pressure range for every pipe. All pipes besides the pipes connecting AquaDuctus, are operated at pressure on or below 50 bar. This also indicates that the hydrogen feed in pressures required at the electrolyzers only reach up to the 50 bar instead of the almost 100bar in the new built scenario. The pressures at the landing points vary between 32 and 45 bar, where typically Den Helder has a lower landing point pressure. Whereas the re-use network shows significant pressures drops over the entire network, the new built network shows relatively small pressure drops and reaches the shore with unnecessary high pressures.

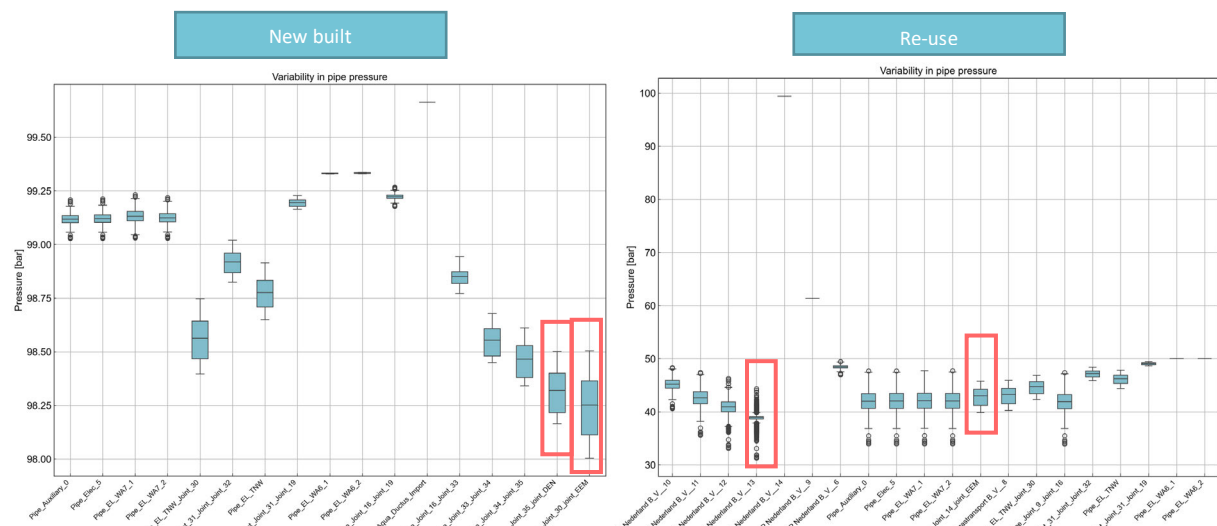


Figure 4.28: Comparison of new build and re-use pressures at each of the pipelines. In coral, outlined the pipelines connected to the landing points.

Figure 4.29 shows a mean pressure of about 48 bar in the network, with a standard deviation of about 15 bar. While this standard deviation seems large, it can again mostly be explained by the import through the AquaDuctus connection. Excluding the importing pipes, Figure 4.29 (right), provides smaller standard deviations, in the order of 3 to 4 bar.

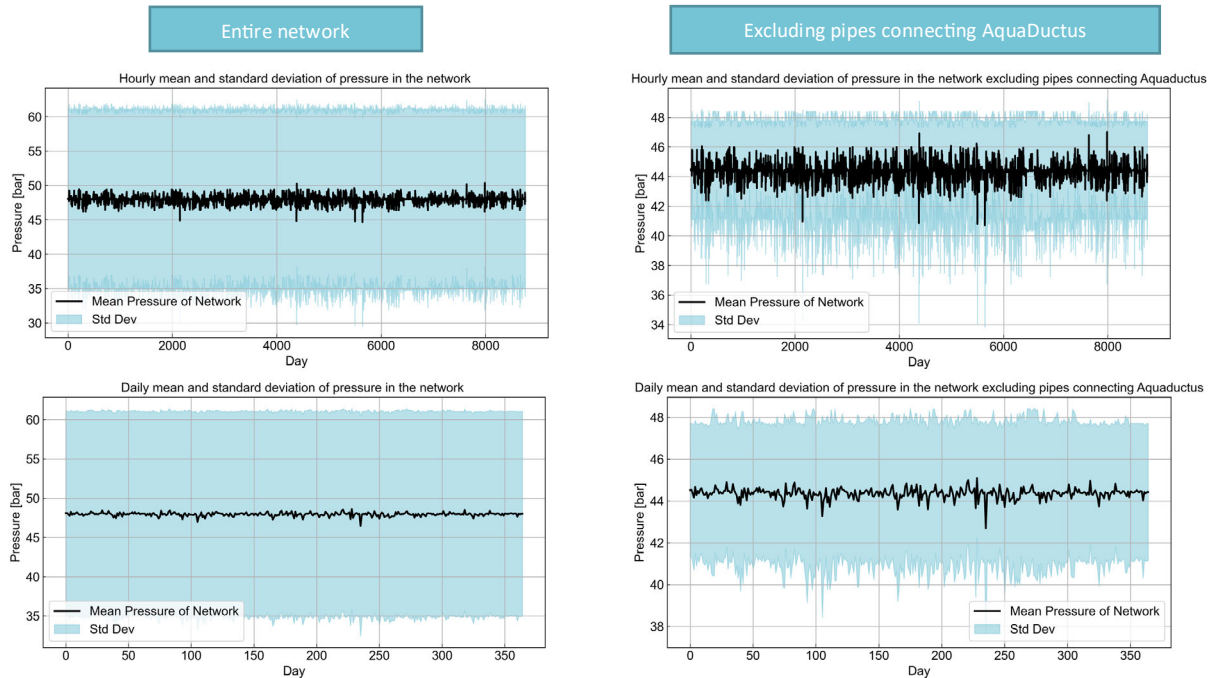


Figure 4.29: The mean pressure and the standard deviation across the entire network (left) and across the part of the network excluding the AquaDuctus connection (right).

Link to the research questions:

How could the infrastructure for transporting electricity and hydrogen from the hubs to shore develop in time, and what role could existing (re-used) pipelines play? What capacities would be required, what design choices must be made, and how do they affect, e.g., the requirement for compression offshore?

- This section shows that the usage of re-used infrastructure for hydrogen transport poses challenges in its resilience towards future uses and potential compression requirements onshore. Under the current assumptions, newly built infrastructure for hydrogen transport with 48-inch diameters (versus 36-inch for re-use) provides greater resilience for future energy needs, such as import and production beyond 2050 estimations. For NSE5-NAT, the pressure losses result in around 3 bar for newly built infrastructure, compared to around 50 bar in the re-use case.
- A combination of reuse and newly built hydrogen pipelines could strike the right balance between flexibility, resilience, future proofness, and investment cost. This is particularly relevant in the scenarios with higher flowrates (NSE5-NAT), and if additional imports, such as AquaDuctus, are expected.

4.6 Hydrogen transport to shore without offshore compression

4.6.1 NAT, newly built infrastructure and imports from AquaDuctus

This scenario entails operating the network with same flow rates but at a different pressure level in order to exclude mechanical compression from electrolyzer feed-in locations. As noted in deliverable D3.3 (van Zoelen, Rob; Boer, Dina; Mahfoozi, Salar, 2025), compression can result in a large share of the offshore hydrogen network costs. Thus we enforce the entry point of the pipe from AquaDuctus import to feed into the network in Hub north at 30 bar. To be able to have a setpoint of 30 bar at this entry, AquaDuctus import requires to feed in at a pressure 1.3 bar higher, as this happens to be the pressure loss along this line. As the network is operated with lower pressure levels, the pressure drops are higher (see Figure 4.30). At the instance of maximum flow in the network, a pressure difference of 11 bar is experienced across the network for the same amount of flow transported. Although it's good to note that the pressure drop is not too much compared to its maximum pressure, and a maximum of is 35% loss is seen across the network. The largest pressure drops are still experienced along the east line running from WA7 to WA6, with the highest of 6 Pa/m occurring in the pipe connecting to the landing point of Eemshaven 7 (see Figure 4.30).

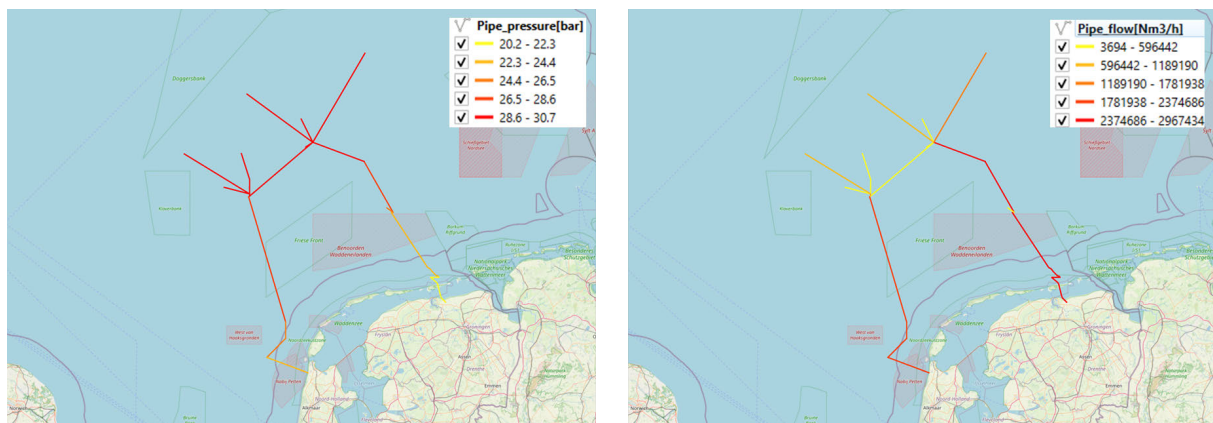


Figure 4.30: Pressure [bar] (left) and Flow [Nm³/h] (right) at the event of maximum flow in the network. Note that the legend in the pressure distribution map shows the average pressure in the pipeline computed between the inlet and outlet pressure of the pipeline.

With the lower pressure regimes, the pressure swings in the pipes are slightly higher than compared to the case when operated with 100 bar, for the same reason discussed above (see Figure 4.31 and Figure 4.32). The same trend is still observed when operating with lower pressures as well.

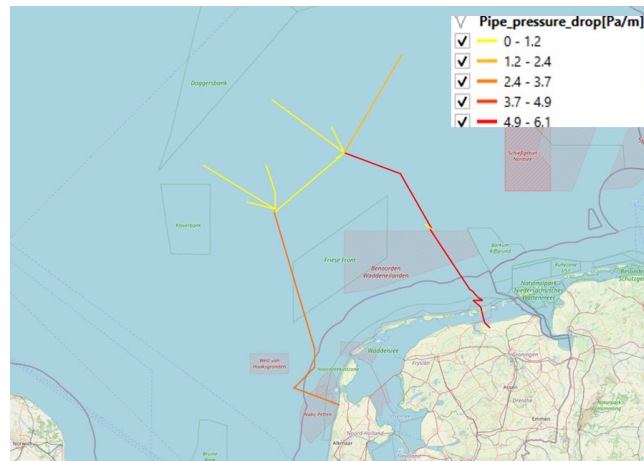


Figure 4.31: Pressure drop [Pa/m] in each pipe at the hour of maximum flow in the network (left). Standard deviation of pressure [bar] in the network.

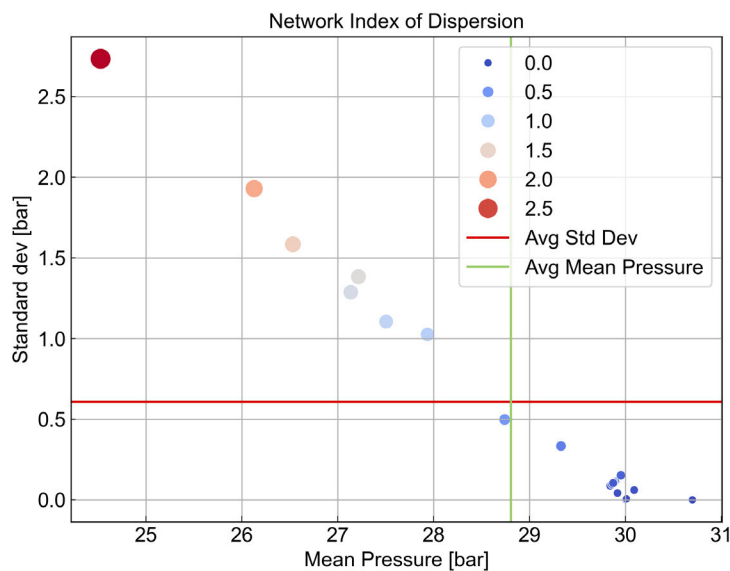


Figure 4.32: Network index of dispersion for the NAT case with no offshore compression.

Pipelines closer to the production locations have lower standard deviations and operates are typically higher pressures, whereas the standard deviations in the pipes connecting to the shore have deviations that are now three times higher. A limitation in the scope of the study is that the AquaDuctus connection has always been used for import. If used for export as well, there may exist the need to pressurize up to a certain extent offshore, depending on the pressure of its connection.

4.6.2 DEC, re-use infrastructure and no imports from AquaDuctus

This scenario shows a case where a lack of mechanical compression offshore could be achieved in the DEC scenario. In this case, this is done by not having any imports from AquaDuctus. Since the previous scenarios assessed have shown large pressure drops across the AquaDuctus pipe, which possibly poses a requirement of offshore compression, this scenario tests the possibility of safe transport of hydrogen without large pressure drops using the capacities assigned to DEC. Figure 4.33 shows the resulting pressure distribution across the network, at the event of maximum flows. The maximum pressure difference across the network is 6.3 bar. The pressure at the junction where the middle and the top section of

NOGAT meets is set to 30 bar (as a boundary condition). To be able to meet this pressure setpoint, electrolyzers in WA7 need to inject into the grid at slightly higher pressure of 34 bar. Within a 3 bar pressure drop, the re-use infrastructure is able to transport hydrogen onshore onto the Eemshaven landing point and similarly to the Den Helder landing point. Since the setpoint pressures in the west side of the network are higher, the landing point pressures in Den Helder are typically higher than in Eemshaven.

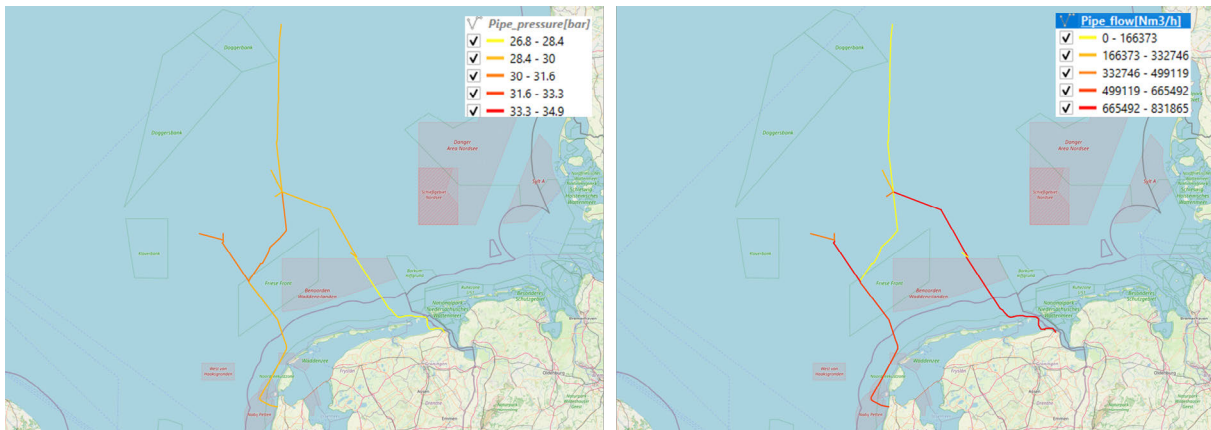


Figure 4.33: Pressure [bar] (left) and Flow [Nm³/h] (right) at the event of maximum flow in the network. Note that the legend in the pressure distribution map shows the average pressure in the pipeline computed between the inlet and outlet pressure of the pipeline

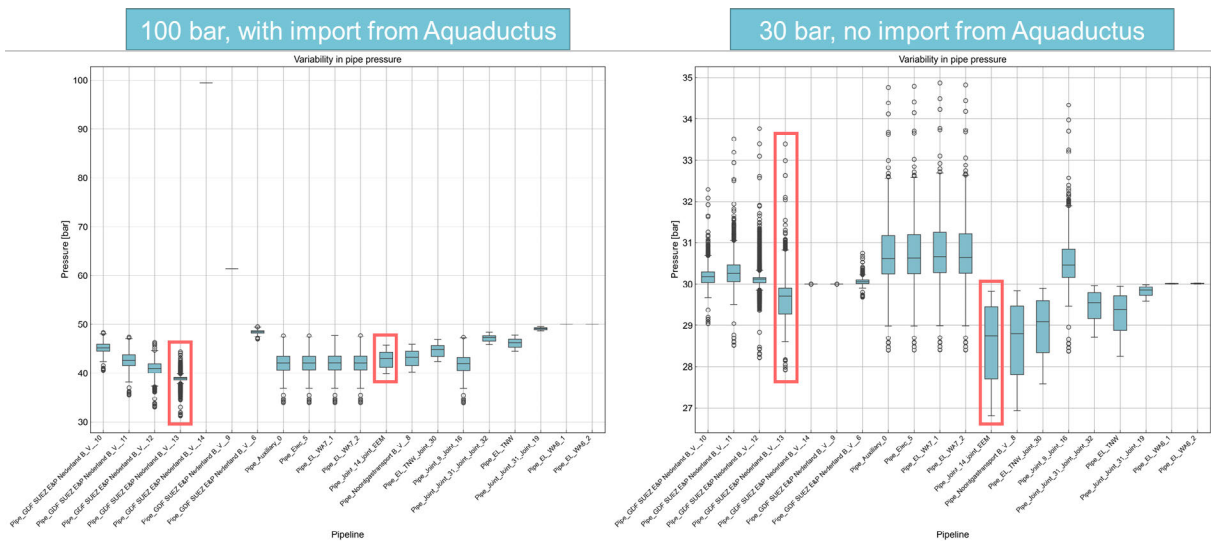


Figure 4.34: Box plot of pressure distribution over the different pipelines for the DEC, re-use scenarios with 100 bar and import from AquaDuctus (left) and 30 bar without this import (right). The two landing points are highlighted in coral colour.

Figure 4.34 shows the pressure distribution over the different pipelines in a box plot. It can be observed that, in this case, the pressure at the two landing points usually has a pressure loss below 3 bar. This is the result of the significantly lower flowrate in the DEC scenario without the AquaDuctus import, that makes this case mathematically feasible. For both landing points the pressure remains above 25 bar, which would allow for onshore compression to the backbone to be feasible, in a not very dissimilar manner as with an onshore electrolyzer at 30 bar. Hence, it can be expressed that, for this case, the system could feasibly be operated.

A result of the boundary conditions set (mathematical artifact) can be observed in the Den Helder landing point. In some time steps, the pressure goes beyond 30 bar. This is due to the way the system is solved: there is a constraint on the *mass flowrate* to be delivered at the landing point, but there is no constraint regarding pressures along the system. This means that in order to have a mathematically allowed solution, pressure increases along the system, particularly in the areas on the west side (e.g., areas 6 and 7). The solver assumes that there is a mechanism that increases this pressure, but it does *not* explain how (e.g., by intermediate boosting). In reality, this could result in at least two outcomes. The first one is that the electrolysers could inject at c.a. 35 bar in certain time steps, to allow for the boundary condition to be met. This is expected to be a reasonable pressure for PEM electrolysers operating in 2050, as there are already systems that can operate beyond this pressure with relatively small penalties in efficiency or operating range (Hancke, Bujlo, Holm, & Ulleberg, 2024). The second way would be to keep the electrolysers at 30 bar and reducing the overall pressure in the system, leading to lower pressures at the landing points. The quantitative calculation of these strategies is non-linear and was beyond the scope of this study. However, as the differences are smaller than 5 bars in this overpressures in only particular time steps, it can be hypothesized that this could likely be a realistic operational strategy.

Link to the research questions:

How could the infrastructure for transporting electricity and hydrogen from the hubs to shore develop in time, and what role could existing (re-used) pipelines play?

- Offshore compression may be avoided to transport the hydrogen amounts produced in the NSE5-NAT scenario when using newly built 48-inches infrastructure and injecting at 30 bar from the electrolyzer.
- For the design with re-use, the potential is more limited: only the hydrogen amounts produced in the NSE5-DEC storyline without imports from AquaDuctus can be realistically transported, while the (much) larger amounts of hydrogen of the NSE5-NAT storyline result in too high pressure losses to be feasible.
- In deliverable D3.3 of NSE5 (van Zoelen, Rob; Boer, Dina; Mahfoozi, Salar, 2025), it was observed that compression represents a largest share of offshore hydrogen network costs. This supports the relevance of establishing further research in different compression and transport configurations.

4.7 Influence of offshore hydrogen storage in the NAT re-use storyline

Offshore UHS can play an important role in managing pressure fluctuations in the offshore hydrogen network. By offering a buffer to absorb (large amplitude, high frequency) fluctuations in the rate hydrogen production from wind, transport to shore can happen at a predictable, constant rate, and this greatly improves the durability of pipelines, especially reused pipelines that have been in operation for natural gas for decades.

To explore this hypothesis, this section presents two cases with hydrogen storage incorporated into the storylines. When we look at the hydrogen mass flowrate reaching Eemshaven (EEM) and Den Helder (DEN) for the scenarios run in the storylines, we can check that there is a high variation in the hourly amount of gas reaching the shore. For instance,

Figure 4.35 shows the number of hours when the amount of hydrogen reaching EEM and DEN is different than the hourly mean (obtained for one year simulation), for the storyline NAT re-use 100 bar, which will be used as the reference case to analyse the influence of offshore hydrogen storage. From the set of simulations, this choice was motivated due to being a challenging case in terms of pressure losses and fluctuations, as seen in Section 4.5.1, with 20 GW of electrolyzer capacities in Hub North and outside of the Hub North areas. As depicted in the histogram, the number of hours for which the mass flowrate at the landing point is outside the $\pm 5\%$ deviation is quite significant: 6039 hours, which accounts for more than 8 months. Besides, the number of hours outside the $\pm 40\%$ interval is 2675 (ca. 4 months). Thus, the usage of offshore hydrogen storage to allow for a constant landing mass flowrate seems to be of interest. Even though the histogram for both landing points is identical, the hourly mean mass flowrate is different: 48.9kg/s for EEM and 38.4kg/s for DEN.

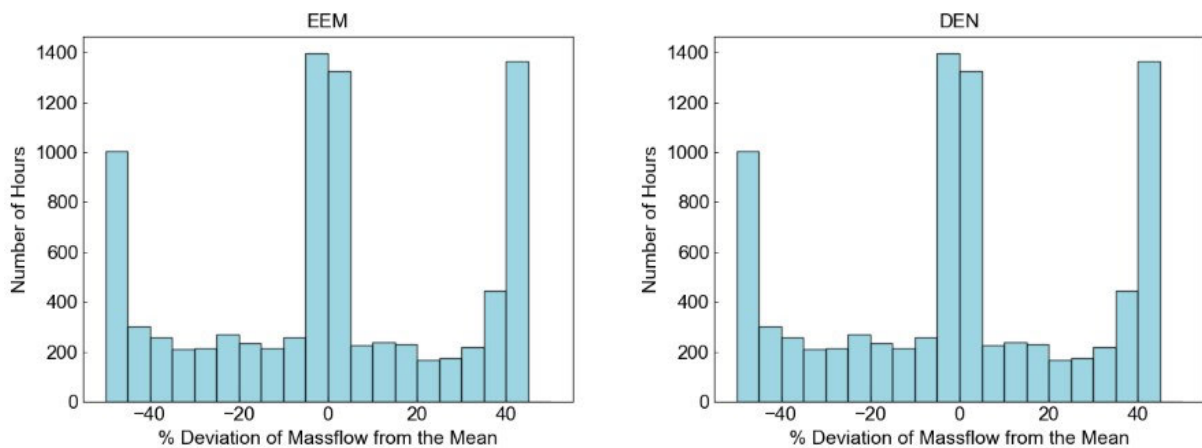


Figure 4.35: Histogram of the percentage deviation of mass flowrate from the (yearly) mean mass flowrate reaching landing ports EEM and DEN, for the storyline NAT reuse. Each bin accounts for a 5% deviation.

Two potential storage locations are considered in the analysis, as depicted in Figure 4.36, that were identified during the screening (section 2.4.1): two depleted gas fields (G16/G17), with a capacity of roughly 1000 million Sm^3 each; and a cluster of salt caverns (F8), with a capacity of 85 million Sm^3 per cavern. For the current analysis, we do not include both storages at the same time, as this would include complexity in the solver. With the current operational strategy (fixed flowrate), we can perform the analysis with a single storage. However, should we want to fix the pressure at the landing point (different operational strategy), then we would most likely require more than one storage in the network.

Figure 4.37 shows the evolution of the F8 storage cluster level as a function of time, for a year simulation. Besides, it shows the input and output mass flowrate from the storage. Note that the result for G16/G17 would be the same, so it is not shown in here. According to these results, a total of 150 kt (1.65 billion Sm^3) storage capacity would be required to ensure a constant mass flowrate at the landing points, for a 1-year simulation.

Table 4.2 gathers the simulation output for the scenario with G16/G17 storage and the scenario with F8 storage. A total of 2 gas depleted fields would be required in the G16/G17 cluster or a total of 21 salt caverns would be required in the F8 cluster.

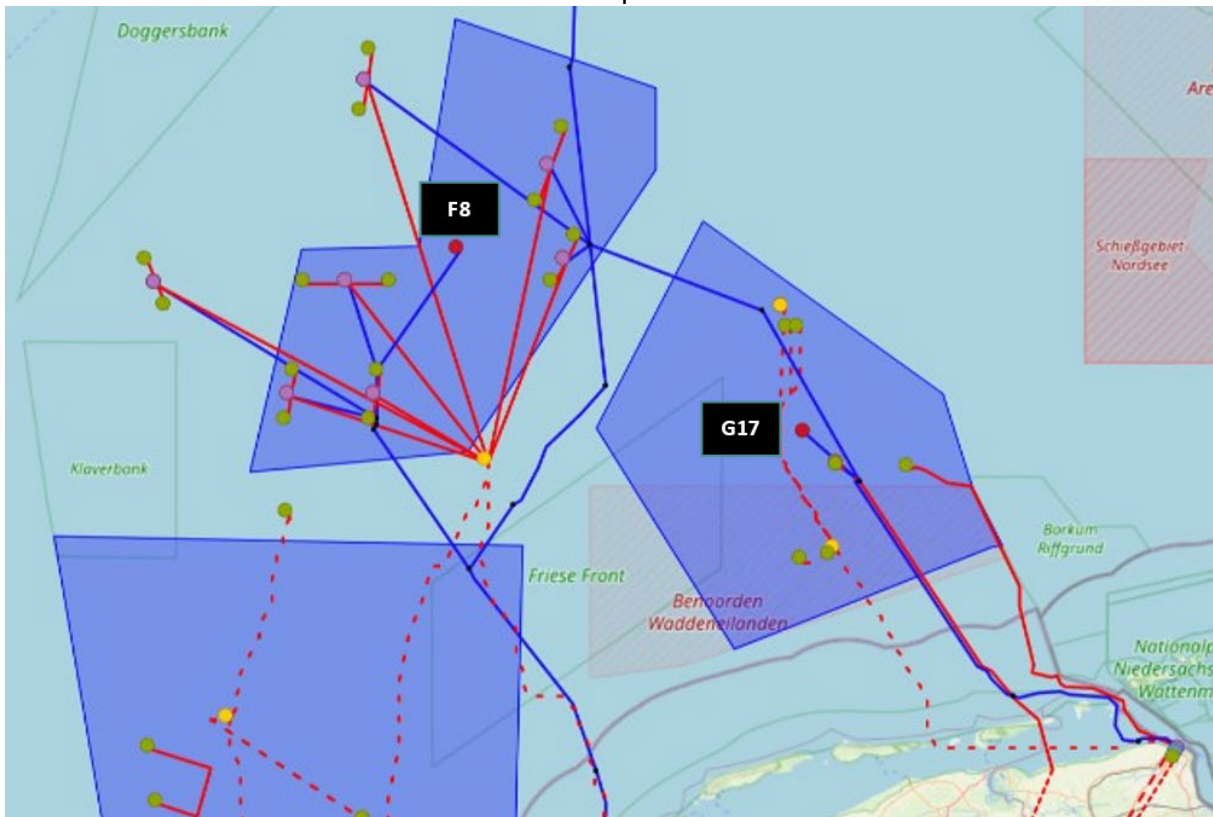


Figure 4.36: Location of the depleted gas field cluster (G16/G17) and salt cavern cluster (F8) simulated in this section. Each storage location is indicated with a red dot.

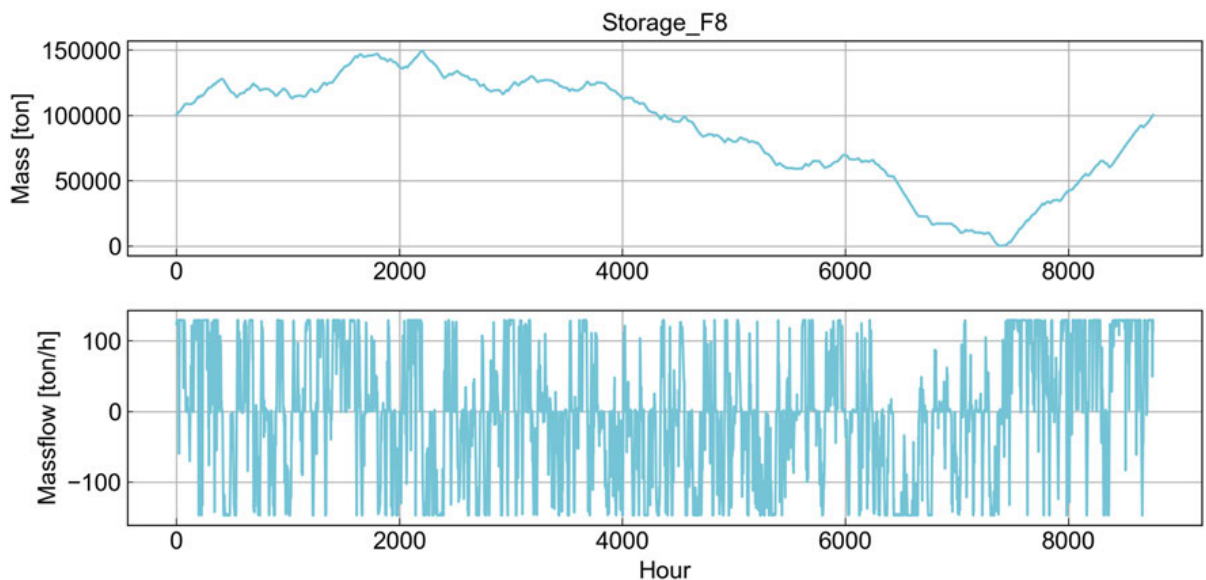


Figure 4.37: Evolution of the F8 storage level and mass flowrate as a function of time.

Table 4.2: Simulation results for both G16/G17 and F8 storage clusters.

Location	Capacity required [kton]	# Gas fields or caverns required	Max. withdrawal rate [in million Sm ³ /day] per salt cavern/gasfield	Max. injection rate [in million Sm ³ /day] per salt cavern/gasfield
G17	150 (1.65 billion Sm ³)		1.78 (2)	23.61
F8	150		21	2

As storage is an ambidextrous asset acting as both supply and demand based on the hourly mismatch, its presence influences the pressure in the grid. Figure 4.38 shows the pressure distribution at the event of maximum flow in both the storage scenarios, comparing it to the reference case (here, NAT re-use). The snapshot is showcased at an interval of maximum flow, which happens to be a case when the mismatch between supply and demand requires the storage to be charging. As the locations of the storages vary in the grid, the routing and the direction of flow from and to storages differ. As a consequence, this locally affects the pressure in the part of the network. Without operating with any of the storages, the west-east link carries flow from WA6 to WA7, thus having a direction of flow from east to west. When F8 is charging, the additional demand posed by the storage, requires large flows through the west-east link (the middle section of NOGAT) making the pressures already lower, in turn lowering the pressures at Den Helder compared to the pressures in Eemshaven.

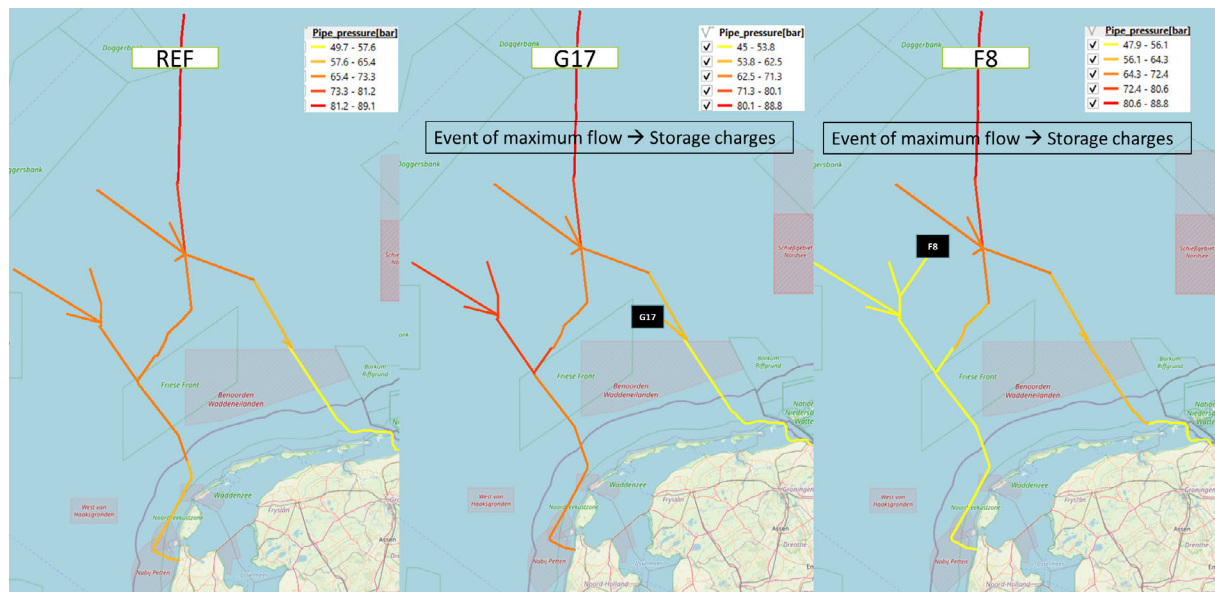


Figure 4.38: Pressure distribution [bar] in the network in NAT re-use case (left; also considered as the reference here), storage at G17 (middle), and storage at F8 (right)

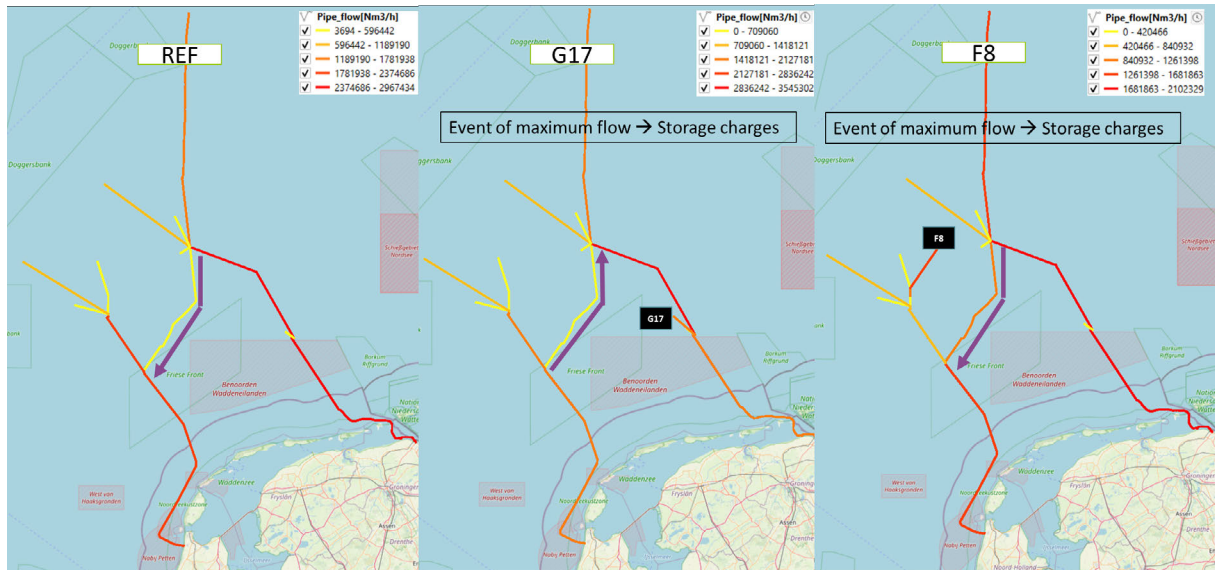


Figure 4.39: Flow distribution [Nm³/h] in the network in NAT reuse case (left; also considered as the reference here), storage at G17 (middle), and storage at F8 (right)

Contrastingly, when G17 poses an additional demand (when charging) the flow direction in the west-east link reverses. This makes the pressures at WA7 higher, and requires flow to be transported from WA7 to the east link, lowering the pressure along the line. This makes the pressures at Eemshaven lower than in Den Helder. Since the storages are located in either sides of the network (F8 in west and G17 in east), apart from the flow direction, the utilization of the west-east link changes, making the interconnection crucial. With addition of storages, the utilization of the line increases by 3-4 TWh (see Figure 4.40). Additionally, there is a significant shift in the load duration in this line. Negative flow rates indicate direction from west-to-east whereas positive indicates vice-versa. For most part of the year we require flow in the direction from east-to-west (see reference case), apart during the intervals when G17 charges and F8 discharges that requires flow direction to be reversed in these lines. Interestingly, in the case of F8 operating, the load duration curve resembles the duration curve of pipes connected to electrolyzers.

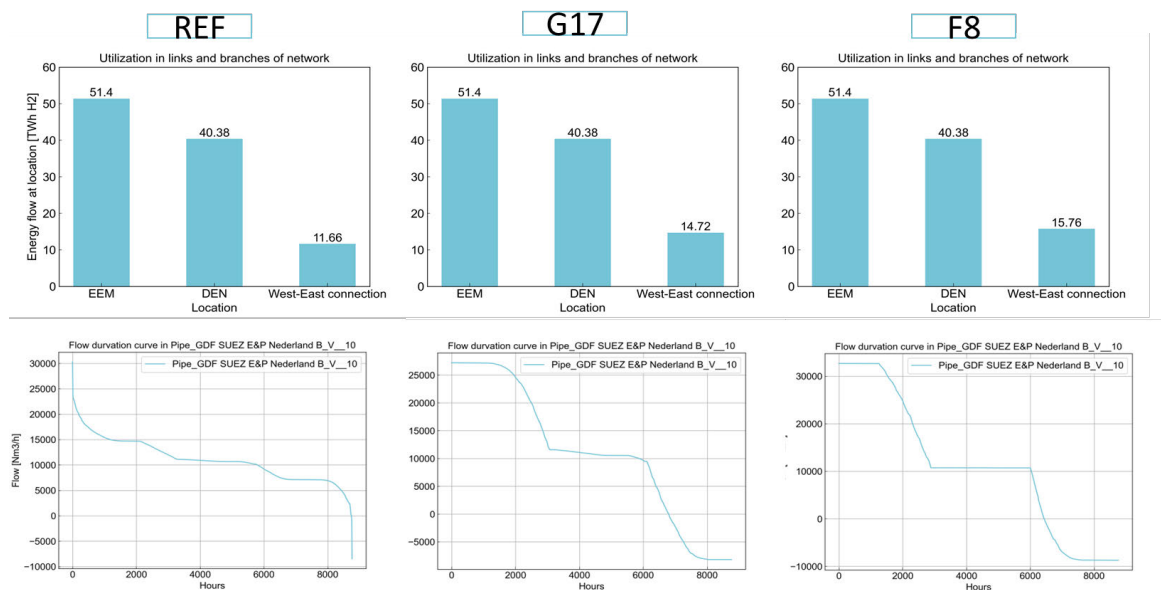


Figure 4.40: Utilization of the west-east link (middle section of NOGAT) across different scenarios compared to the reference case. G17 = gasfield; F8 = salt structure.

Table 4.3 compiles the maximum pressure difference across the network when operating with storages. Introducing storage introduces additional flow in local part of the network, making the pressure levels shift. Since the location plays an important role, and it’s relative position to other supply and demands, the pressure distribution varies. Comparing with the reference case, introducing any of the addressed storage increases the pressure losses in the grid. At the event of maximum flow the storage charges, and at the event of minimum flow, the storage discharges. When G17 charges, pressure losses are higher compared to F8, whereas when it discharges, the behaviour is vice versa.

Table 4.3: Pressure drop (bar) at events of max. and min. flows across reference (NAT reuse) and storage cases

Event/Case	Reference	Storage G16/G17	Storage F8
Event of maximum flow	50	57	54
Event of minimum flow	35	45	47

This is because, the pressures at the junction between the middle and the last section of NOGAT experiences wide range of fluctuations, arising from the flow direction at that junction. The pressure level at the location is determined either by F8’s flow rates based on charging or discharging events. This in turn affects the rest of the pipes along the west line, making it fluctuate based on the charging and discharging events. An opposite behaviour at this landing point is experienced when G17 is operating. A similar behaviour is experienced in the opposite end of the middle section of the NOGAT line, leading to pressure fluctuations as seen as in the figure.

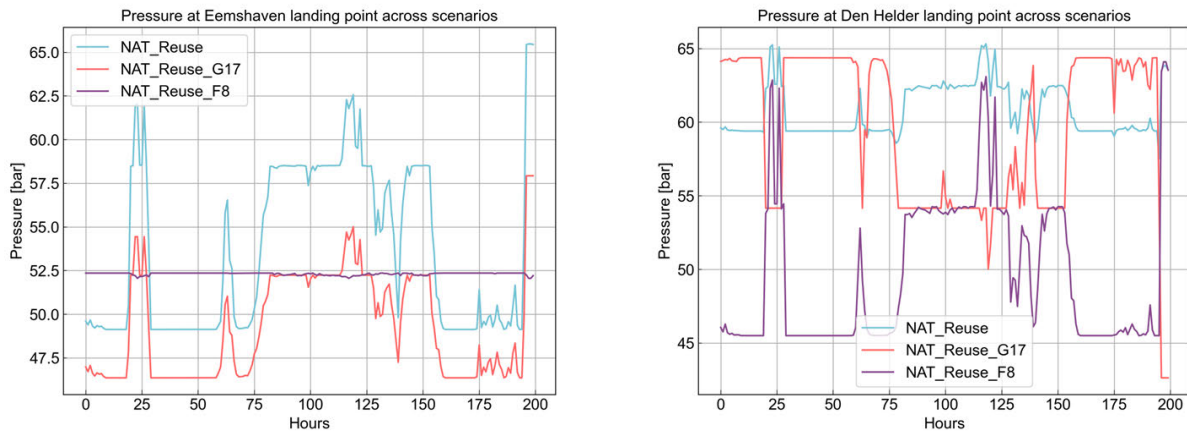


Figure 4.41: Pressures at landing points Eemshaven and Den Helder across reference, and both storage cases

Another difference between the results for the scenario G17 and F8 lies on the pressure oscillations within the network. When we take a look at Figure 4.42, we can check that the addition of storage increases the mean oscillations in the network (greater for G17 than F8) and decreases the mean pressure (lower for F8 than G17). The overall pressure decrease and increase of pressure oscillations with the addition of storage was somewhat expected, as a greater fluid redistribution is needed in order to satisfy a constant demand.

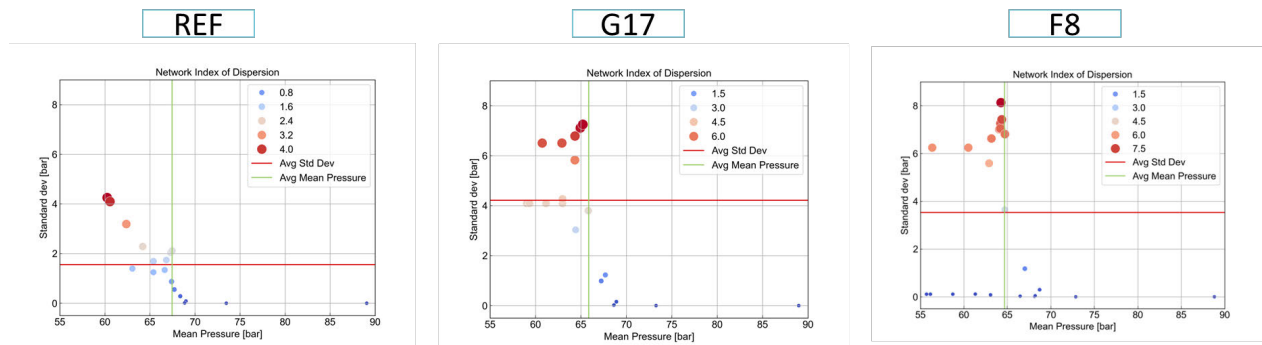


Figure 4.42: Scatter plot of each pipeline mean and standard deviation of the whole hydrogen network. Point size is a function of the value of the standard deviation of the pipe. Lines for the average mean pressure and average standard deviation is also depicted. G17 = gasfield; F8 = salt structure.

Figure 4.42 depicts the pressure variation for each of the pipes of the network, comparing the reference case with the G17 and F8 cases. Interestingly, it can be checked that the pressure variations for all the pipes leading to EEM for the case with F8 storage are very little when compared to the reference and the G17 case. For instance, the pressure variations at the landing point EEM are as little as 0.1bar. This group of pipes with lower pressure variations was already hinted in Figure 4.43, as we check there are more pipes closer to 0 standard deviation than for the rest of cases. The storage charging/discharging profile for G17 and F8 are similar, however G17 is closer to EEM, resulting in more flow through the pipes from Wind Area 6 and 7 towards G17 when charging, which in turn results in larger pressure drops. In this case, these larger fluctuations in flowrates and pressure drops between G17 and wind search areas 6 and 7 continued towards EEM as the pressure where G17 connects to the pipes of NGT fluctuated significantly. Furthermore, the location of the connection of F8 compared to the location of the compressor station can have a large influence on the pressure fluctuations. In the current case, the flow direction near the compressor station is reverted at some timesteps, when there is almost no hydrogen production and F8 is discharged compared to when it F8 is charged. This results in higher pressure required at the output of the storage which are transported through the network.

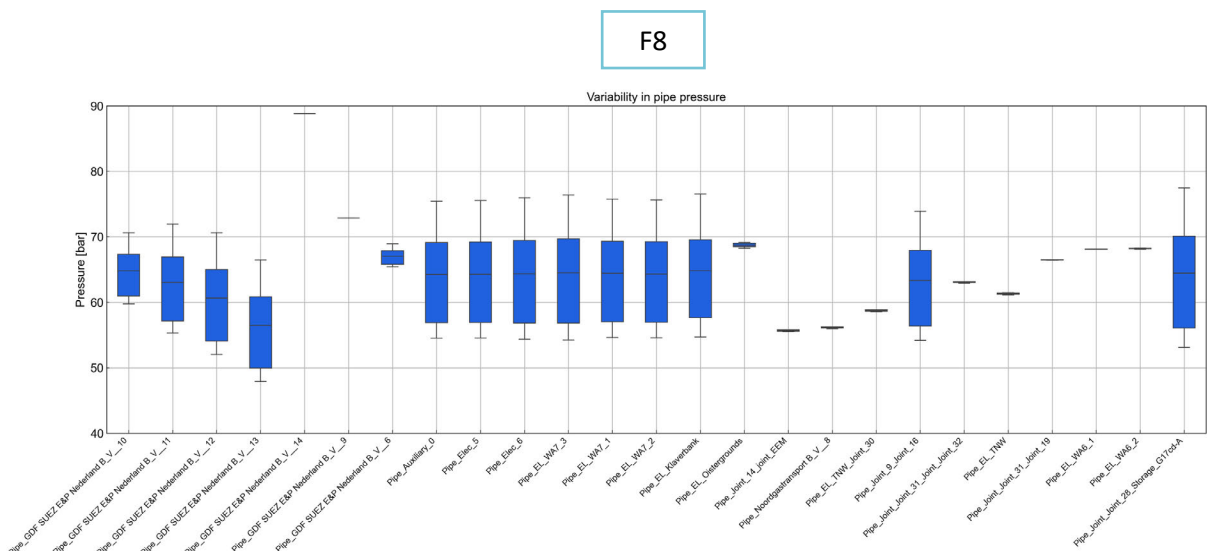
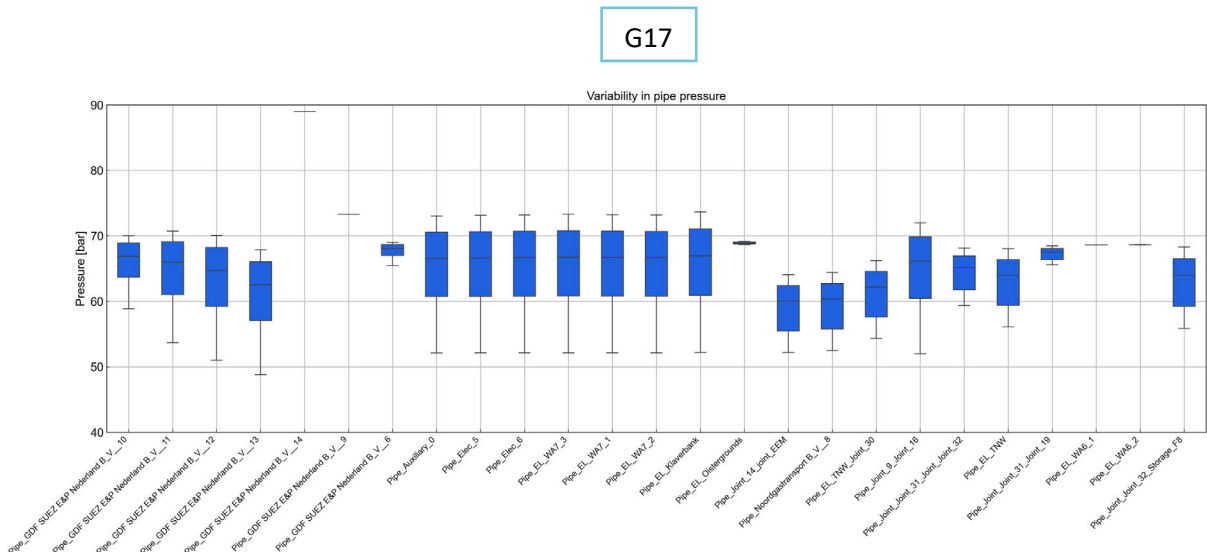
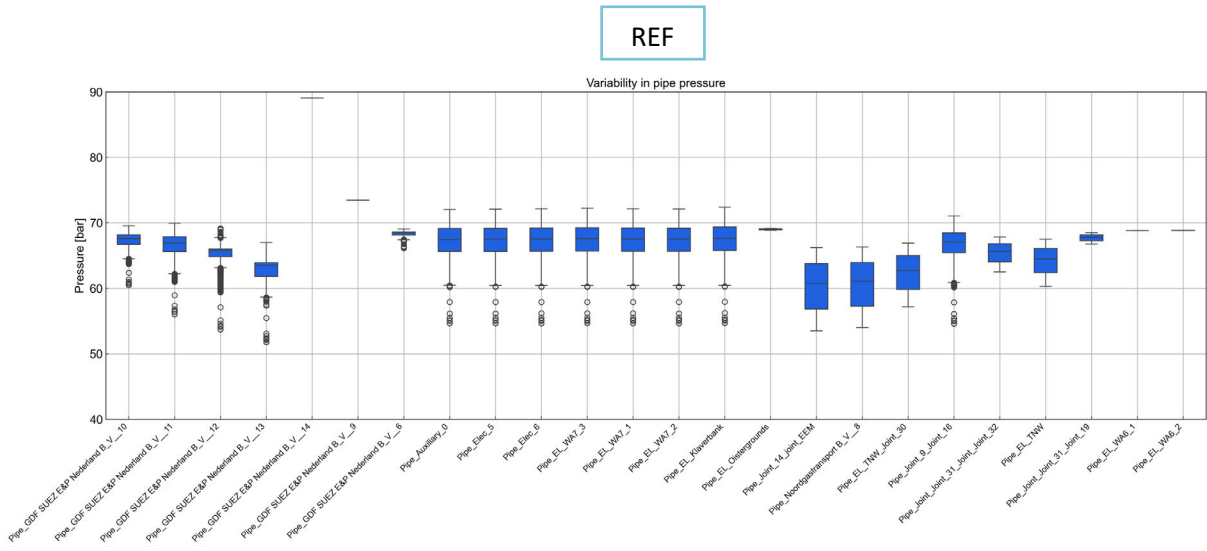


Figure 4.43: Box plot showing the distribution of pressure across pipes. The box represents the interquartile range (IQR), the central line indicates the median, whiskers extend up to 1.5×IQR, and outliers are shown as individual points. G17 = gasfield; F8 = salt structure.

On the whole, it is shown that with storage, a constant mass flowrate to the shore can be fulfilled in the two options explored. However, this may have a detrimental effect on the pressures of the network. Generally, more fluctuations are seen when operating with storage. The deviations of pressures in the pipelines are higher in order to compensate for more dynamic flow from/to storages. Additionally, the proximity of a storage location with respect to a demand location plays a role in how the pressure at the landing points look like. The further the storage, the larger the pressure drop, but *could* ensure a more stable pressure profile at the landing point, and the closer a storage, the lower the pressure drop, but more dynamic pressure profiles can be expected. This is specific to the case designed, and thus may differ and become more complex when multiple storages are involved, or may change based upon different strategies, such as fixing the pressure instead of flow. An operational strategy focused in minimizing pressure fluctuations was out of the scope of this study, and could be an activity of further research.

Link to the research questions:

What is the potential role of offshore hydrogen storage in providing flexibility to maintain a stable and predictable hydrogen supply to shore?

- Including an offshore hydrogen storage of 150 kton/5 TWh (in salt caverns or depleted gas fields) may enable a nearly-constant flow to shore, but it does not necessarily result in reduced pressure fluctuations or pressure losses along the offshore network. Adding storage can lead to the hydrogen flowing in longer paths for the injection/depletion cycles, leading to larger pressure losses overall.
- The pressure stability of the offshore network is largely affected by the control strategy (fixed flowrate versus fixed pressure) and the coordination of the different actors (production, storage and transport). In the simulations performed, the Eemshaven landing point could achieve an almost constant pressure with a storage in F8 (Hub North). However, the peak-to-peak amplitude in pressure increased when adding storage.
- No intermediate cases with a different operational strategy (e.g., minimize pressure fluctuations), smaller storage capacities or a mix of multiple locations have been explored, which could enhance the ability to control the pressure/flow fluctuations along the network more efficiently.

4.8 Offshore hydrogen storage: notional designs and cost analysis

4.8.1 Notional designs

The main objective of this section is to evaluate the requirements for hydrogen storage in connection with 8 GW electrolysis capacity in Hub North to produce hydrogen. The storage is intended to function as a buffer, enabling a stable and continuous flow of hydrogen to shore. Assuming an electrolyser efficiency of 68%, the max. hydrogen production at peak production of the wind farms is 5.44 GW. To estimate the required storage capacity, we considered three representative wind years: a high wind year (2015), a medium wind year (2009), and a low wind year (2010), and calculated how much hydrogen can be continuously delivered to shore. The base case for this analysis is the high wind year, 2015.

The results for the three different weather years are summarized in Table 4.4, which indicate that:

- The required storage capacity ranges from 1.5 to 3 TWh, which corresponds to either one depleted gas field or approximately 6–12 salt caverns, depending on design parameters.
- To maintain a stable hydrogen supply to shore, the storage capacity should be 6% to 12% of the total annual hydrogen production (ratio storage : production in Section 4.1).

Table 4.4: Storage requirements (capacity, rates) for different weather (wind) conditions.

Parameter	Unit	High wind year (2015)	Medium wind year (2009)	Low wind year (2010)
Average load factor (wind search area 7)	[-]	0.56	0.52	0.47
Total hydrogen production	TWh/year	26.6	24.8	22.3
Sustainable throughput	GW	3.04	2.83	2.55
Storage capacity required	TWh	3.11	1.46	2.62
Ratio storage : production	[-]	12%	6%	12%
Max production rate	GW	3.0 (1.0 mln m ³ /h)	2.8 (0.94 mln m ³ /h)	2.6 (0.85 mln m ³ /h)

The storage volume profile generated from the analysis for the high wind year scenario is shown in Figure 4.44, which indicates that a storage capacity of 3.11 TWh is required to cover the full range of wind conditions.



Figure 4.44: Annual storage volume profile. Positive values represent injection, while negative values indicate withdrawal. The total required storage capacity is 3.11 TWh.

4.8.1.1 Use case definition for depleted gas fields and salt caverns

Three scenarios can be considered for offshore UHS to fulfil the capacity and performance requirements posed by the defined use case:

1. Storage in depleted gas fields only
2. Storage in salt caverns only
3. A combined approach using a depleted gas field and salt cavern

Here we focus only on the combined storage scenario (Nr. 3), as it is considered the most realistic option. Since the storage profile is highly dependent on hourly weather variations, in a scenario using only depleted gas fields, wells cannot effectively manage the required hourly operational switching. Gas reservoirs are more suitable for long-term storage rather than peak shaving. A scenario based only on salt caverns would require up to 12 caverns, which is potentially technically achievable but may not be feasible to develop within the next 10-15 years. To take advantage of the strategic, long-duration capacity of depleted gas fields and the high flexibility of salt caverns, the combined scenario is considered more practical. This approach is also more complex from an engineering point of view, as it would likely involve two offshore platforms—one for the gasfield and one for the caverns. In this configuration, the depleted gas field would be used for storing a more stable, slower-varying hydrogen

profile (daily to weekly), while the salt caverns would handle short-term variations, acting as smaller and faster buffer storage.

4.8.1.2 Well performance

Focusing on the combined scenario, Table 4.5 summarizes the main design parameters for salt caverns and depleted gas fields, based on the factsheets that were developed in the context of the Technical Innovations workstream in this WP1. It is assumed that each salt cavern has one well, which is sufficient for its injection and withdrawal operations. In contrast, the number of wells required for depleted gas fields depends on reservoir transmissivity (Kh), well diameter, and maximum erosional velocity.

Table 4.5: Key design parameters for both salt caverns and depleted gas fields. Bold values indicate the base case assumptions for each parameter.

Parameters	Unit	Depleted gas fields	Salt caverns
Working pressure range	bar	150-250	95-200
Subsurface temperature	°C	100	45
Kh	mD.m	500, 1000, 2500	---
Working volume	Twh/bcm	3.11 / 1.04	
Max erosional velocity	m/s	25 , 50, 100	
Internal tubing diameter	inch	5 , 7, 9	9
Max pressure depletion	bar/day	---	10
Abandonment pressure	bar	50	---
Original gas composition	%	CH ₄ (88), C ₂ H ₆ (4), C ₃ H ₈ (1), CO ₂ (1), and N ₂ (6)	---

Figure 4.45 presents a sensitivity analysis of the maximum flow rate for a single well, considering different assumptions for well diameter, transmissivity (Kh), and maximum allowable velocity. It clearly illustrates how these parameters influence the flow rate. When reservoir transmissivity is (too) low (Kh<500 mD·m), the well diameter has no impact on production, i.e., the flow rate is limited by transmissivity. However, at higher transmissivity values, a larger well diameter significantly increases the production rate. The analysis estimates the highest flow rate that can be sustained for at least 90 days. In contrast to the seasonal trend typically seen in gas storage, the storage profile shown in Figure 4.44 likely does not require this assumption (90-day constant flow).

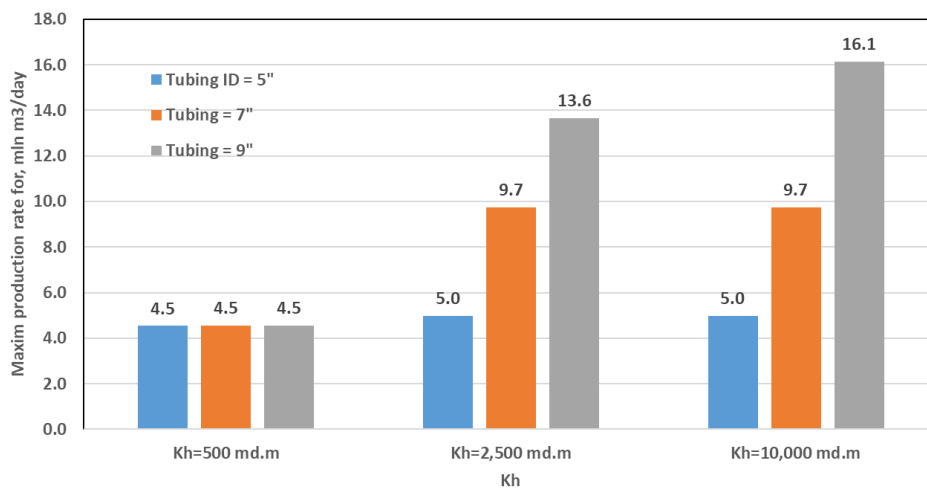


Figure 4.45: Maximum production flow rate for different well diameters and Kh values. A maximum erosional velocity of 100 m/s is assumed, with an emptying period of 90 days.

Kh [md.m]	Max V [m/s]	Number of wells		
500	25	11	9	8
500	50	9	8	7
500	100	8	7	5
1000	25	8	7	5
1000	50	6	6	5
1000	100	5	4	4
2500	25	7	5	3
2500	50	4	3	3
2500	100	3	2	2
		5	7	9
		Diameter [inch]		

Figure 4.46: Number of wells required for the gas reservoir based on Kh, maximum velocity in the wellbore, and well diameter.

This analysis is followed by an estimate of the number of wells required for the storage reservoir. In the best-case and worst-case scenarios, 2 and 11 wells are needed, respectively (see Figure 4.46). Note that many offshore gas reservoirs have a Kh value around 500 mD·m and typically use 5-inch tubing. Some fields may have higher Kh values. Assuming a conservative erosional velocity limit of 25 m/s, reservoirs with Kh > 1000 mD·m may require between 5 and 8 wells, depending on tubing diameter (5–7 inches).

4.8.1.3 Pressure profile in the system

To understand the overall pressure profile in the system, the waterfall plot in Figure 4.47 illustrates the pressure range for each component of the storage facility. It is assumed that the electrolysis (output) pressure is around 30 bar, which is then compressed to approximately 210 bar for caverns and 290 bar for gas fields. The main difference between caverns and reservoirs lies in well performance. Due to the smaller well size, higher depth of the reservoir, and lower transmissivity compared to caverns, the pressure depletion in the well and near the wellbore is higher in gas reservoirs. After hydrogen is withdrawn, it is exported via pipeline to the shore, where it will enter the onshore grid at a pressure above 50 (or 66) bar.

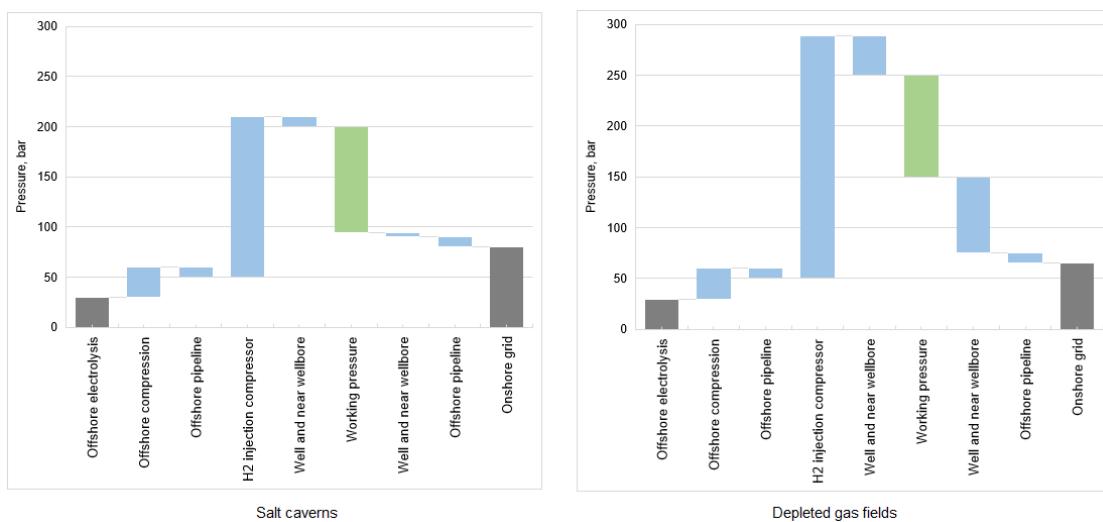


Figure 4.47: Pressure profile for offshore hydrogen storage in salt caverns (left) and depleted gas fields (right). Gray bars represent elements outside the storage system, blue bars represent injection and withdrawal modes, and green bars indicate the working storage pressure limits.

4.8.1.4 Surface facility design

In our evaluation of the surface facility design, the main objective is to determine the size and weight of the equipment to understand whether it can be realistically located on an offshore platform. The main equipment includes compression (for both salt caverns and gas fields) and gas cleaning (separation for gas fields, dehydration only for salt caverns). In the scenario where both salt caverns and gas fields are used, we assume the gasfield operates at a constant daily rate, while the salt cavern storage manages the fluctuations (the delta). The main characteristics of this setup are presented in Table 4.6. The sizing parameters (footprint and weight) are based on a recent study used as a reference (Westerhout , 2024). For gas separation, it is assumed that pressure swing adsorption (PSA) is used to separate hydrogen from the residual gas present in the reservoir. The recovery factor of PSA unit is assumed at 90%. The fractions of hydrogen and residual gas in the withdrawn stream are case-dependent and depend on the abandonment pressure and the composition of the residual gas. The stream from the well is processed through the PSA unit, resulting in a high-pressure purified hydrogen stream and a tail gas stream (containing residual gas and some hydrogen) at near atmospheric pressure. The purified hydrogen is directed to the hydrogen pipeline, while the tail gas must be managed. This can be done by either reinjecting it into the reservoir, disposing of it in other gas fields, or exporting it to shore. All three options require a large compressor to boost the pressure from 1 absolute bar to either 300 bar (for reinjection and disposal) or 50 bar (for export).

Table 4.6: Surface facility sizing for caverns and gas fields, including only compression and gas separation units (excluding all other equipment and systems on the platform).

Type of storage	Characteristics	Surface facility	Area [m ²]	Weight [tonnes]
Depleted gas fields	Max Inj. rate = 2.3 GW (≈ 18.4 million Sm ³ /day) Max discharge pressure = 290 bar	Hydrogen compressor (30 MW)	500	2,000
		Tail gas compressor (19 MW) – export to shore (5 stages)	9,100	10,600
		PSA	3,100	6,100
Salt caverns	Max Inj. rate = 4.6 GW (≈ 36.8 million Sm ³ /hr) Max working pressure = 210 bar	Hydrogen compressor (78 MW)	1,200	5,100

Figure 4.48 illustrates the flow rate of the withdrawal stream as well as the flow rate and composition of the tail gas stream based on the abandonment pressure and gas composition listed in Table 4.5. In this scenario, the tail gas stream can reach up to 3.5 million sm³/day, with approximately 1 million sm³/day consisting of natural gas impurities; the remainder is hydrogen. Variations in abandonment pressure or the use of a cushion gas other than pure hydrogen would affect both the volume and composition of the tail gas. Due to the large compressors and PSA units required for hydrogen storage in depleted gas fields, a large offshore platform with a topside weight of at least 20,000 tonnes is needed, excluding other necessary equipment. When additional equipment are included, the total weight and size of the platform could double or even triple, meaning that a very large platform would be required. This poses a major challenge, as only a few existing platforms in the world might be suitable for this scale. The Pioneering Spirit, the world's largest lifting vessel with a capacity of up to 48,000 tonnes, is among the few capable of handling such heavy topsides.

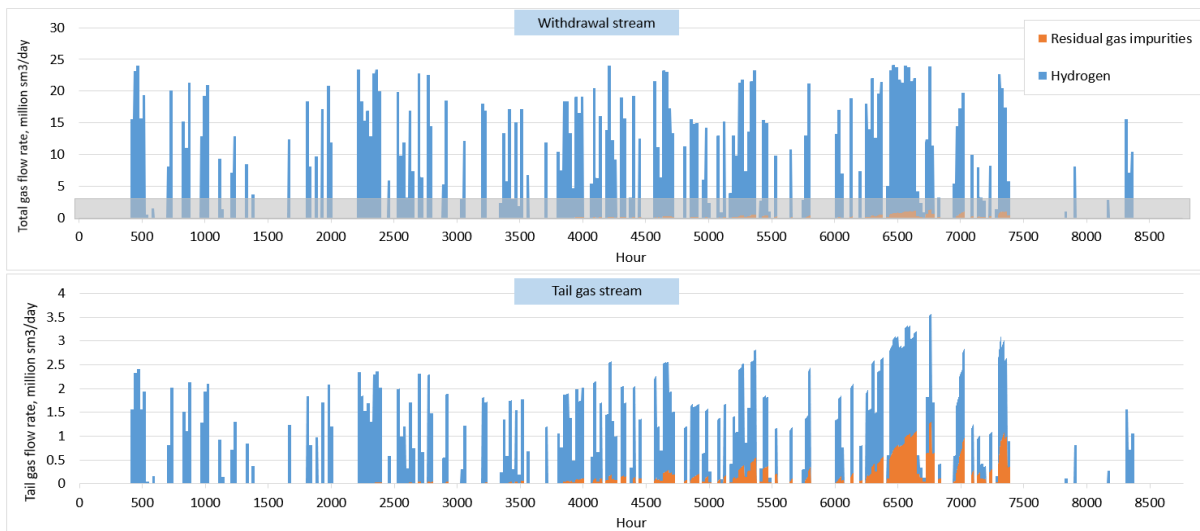


Figure 4.48: Total gas withdrawal stream (top) and tail gas stream (flow rate and composition) from the PSA unit (bottom) over one year of operation. The grey-shaded area in the top plot shows the part of the withdrawal stream that is considered tail gas.

Globally, only a limited number of platforms have operated in this topside weight range. Notable examples in the North Sea include [Sleipner A](#) with a topside of approximately 57,000 tonnes, [Gullfaks C](#) at 49,000 tonnes, and [Statfjord B](#) at 42,500 tonnes¹². As such, the development of a new and very large offshore platform would be essential for hydrogen storage at this scale. In contrast, salt caverns do not require tail gas compressors or gas separation units, making them a more practical option in terms of surface facilities and platform footprint. Given the challenges related to offshore platforms, particularly for depleted gas fields, an alternative could be nearshore storage, where the surface facilities are placed onshore.

4.8.2 Cost analysis

Estimating the cost of offshore underground hydrogen storage (UHS) in gas reservoirs and salt caverns is complex due to significant uncertainties, particularly concerning various cost components at sea. In this section, cost estimates are based on data from the Hystories project (Bourgeois, Duclercq, Janel, & Reveillere, 2022). The reference values are taken from onshore storage, and based on literature and private communications, a multiplier of 3 has been applied to approximate offshore conditions. For comparison, the analysis considers using either salt caverns or depleted gas fields individually, rather than a combination of both, to examine how storage type affects overall cost. The main assumptions used in this assessment are summarized in Table 4.7.

¹² Troll A is another possible example, with an overall height of 470 m and a total weight of 680,000 tonnes, though the exact topside weight is not found in public data.

Table 4.7: Assumptions for the cost analysis of offshore UHS in salt caverns and depleted gas fields.

Assumptions	Unit	Depleted gas fields	Salt caverns
Number of wells	[-]	5 (injection/production) + 1 (observation)	12 caverns (1 well per cavern)
Depth	m	3000	1000
Storage capacity	TWh	3.11 (1 bcm)	
Maximum withdrawal flow rate	GW	3.0 (24 Million sm ³ /day)	
Maximum injection flow rate	GW	2.3 (18 Million sm ³ /day)	
Hydrogen cost for cushion gas	€/kg	5	
Electricity cost	€/MWh	60	
Contingency costs	[-]	20% of CAPEX	

Figure 4.49 presents the CAPEX and OPEX estimates for both storage types. The total CAPEX for salt caverns is estimated at approximately €M 5,100, while for depleted gas fields it is around €M 5,800. For gas fields, about 80% of the CAPEX is attributed to surface infrastructure, mainly due to hydrogen purification and compression units. In contrast, salt caverns have a more balanced cost allocation between surface and subsurface components. The key cost drivers for caverns include leaching operations on the subsurface side and compression and drying facilities on the surface. The annual OPEX for both options is largely driven by surface facility requirements, particularly related to operation and maintenance. Based on the mass of stored hydrogen, the CAPEX cost per working volume for both systems is slightly above €60/kg.

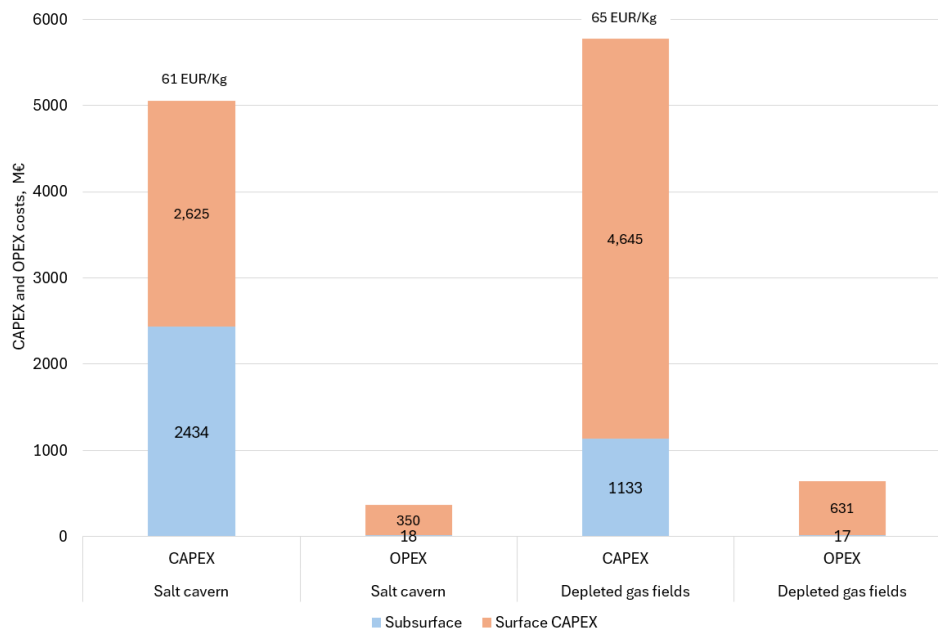


Figure 4.49: CAPEX and annual OPEX costs for offshore UHS.

4.8.2.1 Case study offshore salt structure

As an in-kind contribution, Shell and Gasunie conducted a more detailed cost analysis for the development of offshore salt caverns in Hub East. It is important to note that the assumptions and design parameters for their analysis were independently defined and differ from those used for the screening and notional design studies presented before. The study assessed stand-alone solutions which do not rely on any other offshore hydrogen infrastructure and could be realized in the medium-term in the 2030s. It turned out that salt

structures of sufficient extent and quality for cavern construction are quite limited near-shore. Out of two candidates identified, a salt structure in the M2 block (near the G17 block) was chosen which is located, 70 km offshore along the existing pipeline corridor from Eemshaven via platform AWG-1 (see Figure 4.50 and Figure 2.4).



Figure 4.50: Location of offshore salt cavern in the M2 block (near the G17 block) for the case study conducted by Shell and Gasunie.

Table 4.8: Design parameters for on- and offshore UHS in salt caverns for case study by Shell and Gasunie.

Parameters	Unit	Onshore	Offshore
Top depth	m	1000	2000
Storage capacity	million Nm ³	100 (9000 tonnes)	
Injection rate	million Nm ³ /day	1 (4 tonnes/h)	
Withdrawal rate	million Nm ³ /day	2 (8 tonnes/h)	
Pressure range	bar	56-185	240-369
Temperature	°C	45	75
Cushion gas (CG) volume	million Nm ³	25	90
Working gas (WG) volume	million Nm ³	52 (33+19)	40 (25+15)
CG/WG ratio	[-]	48%	225%
Number of caverns needed	[-]	3	4

A location along on existing pipeline corridor was considered important to avoid challenges and delays that would be associated with permitting for new pipeline corridors particularly when crossing the Natura 2000 areas in the Waddenzee. The top depth of the caverns is 2,000m, i.e., deeper than typical onshore salt caverns, which was accepted as no shallower salt is available in near-shore locations. The design assumptions for the offshore caverns are displayed in Table 4.8, and compared to a typical onshore cavern at a depth of 1,000 m. Note that the lower pressure limit at greater depths, initially set at 24% of lithostatic pressure, was adjusted to 52% to counteract the higher fluidity of salt at deeper levels that accelerates cavern convergence. Further research is needed to determine whether caverns can be economically operated at such high depths which fall outside the current operational experience and what a suitable pressure limit may be to avoid excessive convergence. The

adjustment of the lower working pressure limit leads to the need for four caverns instead of two.

Cost estimates were based (also) on the HyStories model (Bourgeois, Duclercq, Jannel, & Reveillere, 2022) for onshore caverns in combination with Shell-internal cost estimates and cost benchmarking data as well as cost escalation factors for the offshore scope and cost. The cost estimates exclude financing costs and inflation. To separate the cost impact of going offshore, going to higher depth, and of increasing the lower working pressure limit, respectively, three offshore cases were considered next to the onshore reference case:

- Onshore salt cavern at a depth of 1,000 m
- (Hypothetical) offshore salt cavern at a depth of 1,000 m
- (Hypothetical) offshore salt cavern at a depth of 2,000 m but with the same lower working pressure limit in terms of lithostatic pressure as the shallower cavern (24%)
- Offshore salt cavern at a depth of 2,000 m with increased lower working pressure limit of 52% of lithostatic pressure.

Key findings for the four designs considered are summarized below:

1. The investment cost for storage facility with salt caverns at a depth of 1,000 m was estimated at 290M€, based on the HyStories model. This corresponds to a unit CAPEX cost of 30 €/kg storage capacity.
2. For a facility offshore with salt caverns at the same depth (1,000 m), the total cost increases approximately fourfold to 1,158M€, resulting in a unit CAPEX cost of 130 €/kg storage capacity. This increase is primarily caused by higher construction and connection costs, as well as by the complexity and novelty of offshore cavern development that necessitates higher contingency.
3. For a (hypothetical) offshore cavern at a depth of 2,000 m, assuming the same lower pressure limit of 24% of lithostatic pressure, the unit cost remains approximately the same. Extra costs for deeper wells are compensated by reduced costs due to needing one cavern less to realize the same storage capacity due to the higher pressures at larger depth.
4. For the case at a depth of 2,000 m offshore, with the lower pressure limit increased to 52% of lithostatic pressure (compared to 24% in previous cases), the total CAPEX rises to 1,777M€. This corresponds to a unit cost of 200 €/kg storage capacity. The 1.5-fold increase is mainly due to reduced storage capacity per cavern and higher cushion gas requirements to prevent excessive creep closure at greater depths.
5. In order of importance, key cost drivers are (i) location on/offshore, (ii) depth resulting in the need to increase the minimum pressure limit, (iii) store size (storage capacity), and (iv) storage speed (injection and withdrawal capacity) In case that very high rates need to be realized, the storage speed could overtake the store size in terms of cost driver ranking.

Figure 4.51 shows how various cost components contribute to the increase in unit CAPEX from 30 €/kg for an onshore cavern to 200 €/kg for an offshore cavern. Due to the novelty of offshore cavern construction, the contingency was increased from 20% (onshore) to 50% (offshore). Next to cost, time is a key challenge which is further aggravated in an offshore setting. It is expected that the construction of the cavern and the plant will take at least 10

years, This means that first revenues will only be generated at the earliest 10 years after taking FID, which may block investment by commercial entities.

4.8.3 Summary

In this section, we summarize the results of the screening and notional design study for offshore UHS in the Dutch sector of the North Sea. The screening was limited to Hub North and surrounding area extending up to 60 km away from its border. Figure 4.52 displays the gas fields and salt structures that are identified as good examples of potential candidates, along with key characteristics such as depth, working pressure range, and proximity to Hub North and possible route(s) of a future offshore hydrogen grid. More in-depth site-specific investigation is required to confirm their suitability for hydrogen storage. Additionally, gas fields in the Q-blocks (light blue circle) are indicated on the map because they could be interesting candidates for nearshore development. Please note though that they were not evaluated in this study.

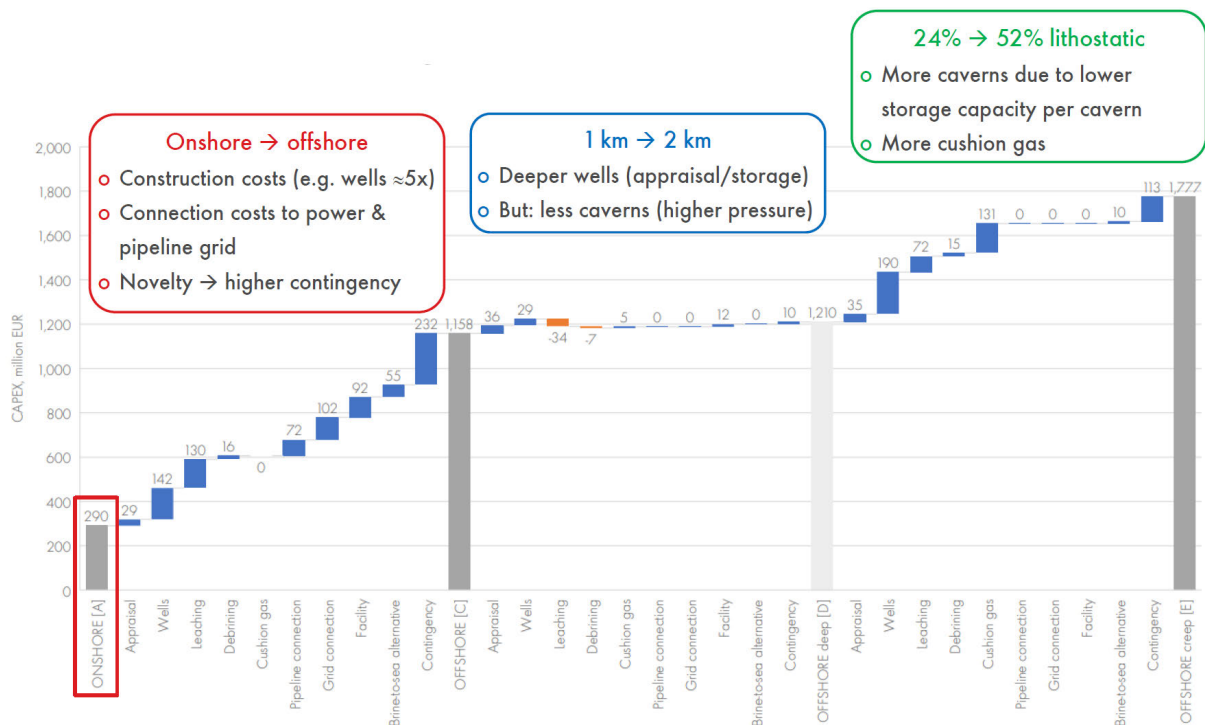


Figure 4.51: Impact of different parameters on the cost increase from onshore to offshore salt cavern development. The total CAPEX estimate rises from €M 290 to €M 1,777, a sixfold increase.

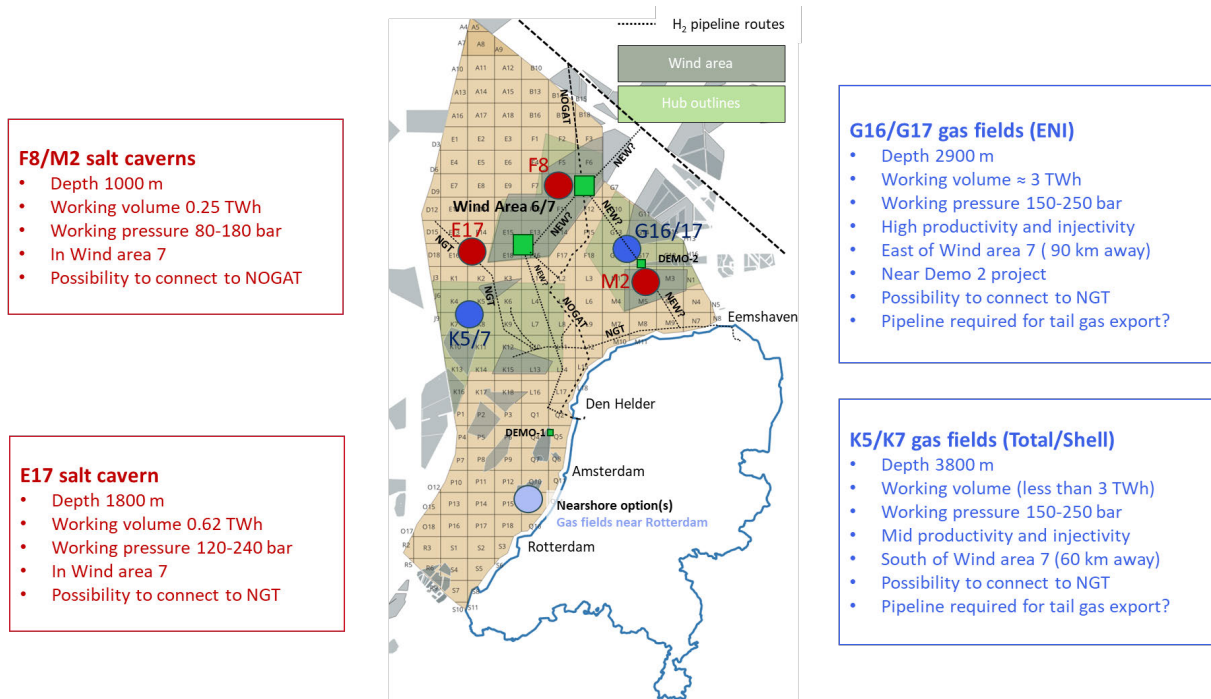


Figure 4.52: Examples of candidate gas fields and salt structures for offshore hydrogen storage. Dark blue circles indicate gas fields offshore, dark red circles indicate salt structures offshore, and the light blue circle indicates possible nearshore options for storage in gas fields. The dotted black lines represent possible hydrogen pipeline routes (see section 2.3). The green squares indicate areas where hydrogen production (and compression, if required) is foreseen.

Following the screening, a notional design of UHS facilities was conducted, addressing both subsurface and surface infrastructure requirements for storage in salt caverns and gas reservoirs. The main conclusions are summarized below:

- A combination of both reservoir storage (high volume, slow response) and cavern storage (low volume, fast response) may offer the benefits of both long-term energy buffering and operational flexibility.
- A key subsurface challenge for gas reservoirs is the need for multiple wells, driven by typically low Kh values in the hub North region. Most existing reservoirs currently have only one or two wells designed for natural gas production.
- On the surface, the primary challenges are the limitations of offshore platform space and weight capacity. Gas reservoirs require large hydrogen compressors, PSA unit, and compressor for tail gas handling. The tail gas stream for the PSA unit, can reach volumes of several million sm^3/day . It is discontinuous and variable in composition, requiring appropriate solutions such as reinjection, export, or disposal.

A schematic design for hydrogen storage using a combination of gas reservoirs and salt caverns is shown in Figure 4.53. This conceptual layout assumes an 8 GW offshore wind farm fully dedicated to hydrogen production, with a continuous 3.0 GW hydrogen flow transported to shore via pipeline. The schematic includes indicative numbers for the flow rates and storage capacity.

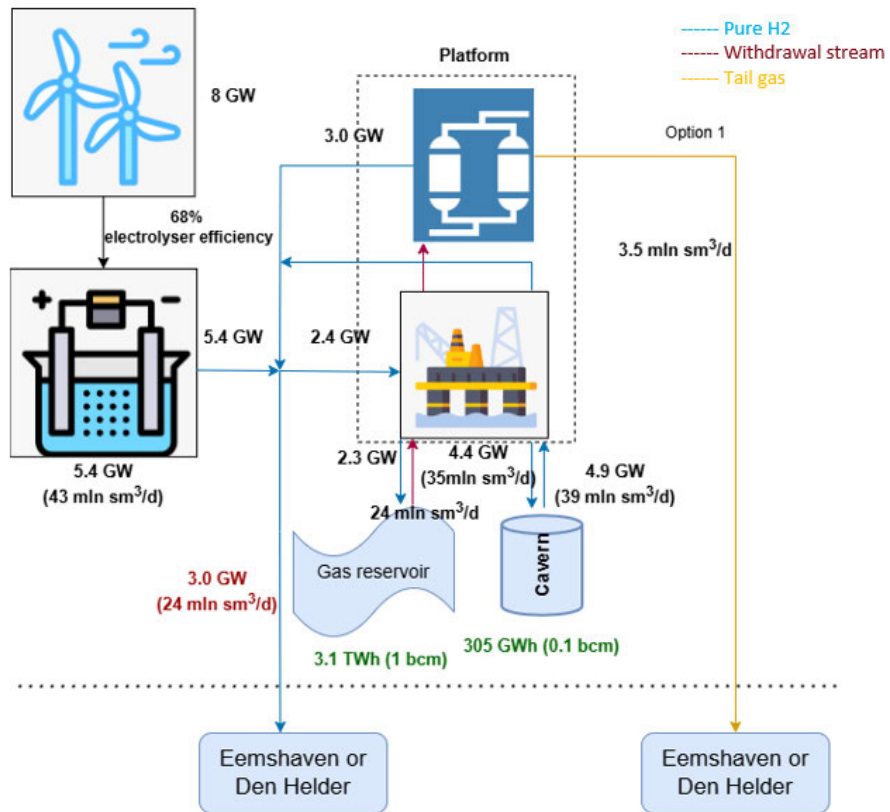


Figure 4.53: Schematic representation of offshore UHS using both salt caverns and depleted gas fields. Surface facilities for gas fields are more complex due to the need to manage tail gas produced during gas purification. Black numbers indicate peak rates, red shows the constant throughput rate, and green indicates total storage capacity.

5 Discussion

In the process of defining the storylines and developing the hub designs, we had to make a number of choices, the implications of which are relevant to discuss here. One choice concerned the “energy worlds” in which to root our storylines and hub designs. While initially we considered using the European-scale TYNDP scenarios (ENTSO, ENTSO-E, 2022), we ultimately decided to use the “Integrale Infrastructuur Verkenning 2030-2050 editie 2” (II3050-2) (Netbeheer Nederland, 2023) scenarios “National Leadership” (NAT) and “Decentralized Initiatives” (DEC). Our main reason for doing so was that these scenarios clearly differentiate between on- and offshore capacities, which would lead to hub designs (and associated design choices) that significantly differ in their levels of utilization of the North Sea, thus representing better the experienced uncertain bandwidth of future offshore energy development. In practice, however, when looking at the final hub designs, it can be observed that only for Hub North there is clear differentiation in design between the NSE5-NAT design (high level of utilization of offshore space, large wind capacity, significant hydrogen production) and the NSE5-DEC design (modest level of utilization of offshore space, with modest wind capacity and minor hydrogen production). What we experienced during the project was that as we were evaluating design choices for the hubs, e.g., in location, sizing and timing of wind farms (and wind search areas) and hydrogen production capacity to be developed, our choices were overtaken by policy and spatial planning decisions, mainly in the context of the PH-PNZ, PAWOZ, and VAWOZ programs. Especially for Hub West and Hub East this was the case, and this is why the differences in the NAT and DEC designs for those hubs are now minor (HUB West) to non-existent (Hub East).

Only for Hub North, there is clear differentiation in designs, which is directly related to the fact that until very recently (update of the PHPNZ, see below), the spatial planning process had not progressed beyond appointing wind farm search areas 6 and 7, i.e., no firm direction had been provided as to the expected capacities for wind and hydrogen, where these capacities would be likely built within that large area, and how they would be spatially integrated with other use functions while maintaining (if not strengthening) the ecological value of the area. This uncertainty allowed us to develop different designs for the NSE5-NAT and NSE5-DEC storylines that depict different levels of utilization of Hub North, designs that are nature-inclusive, in collaboration with WP 4 of NSE 5 (van der Heijden, et al., 2025), and that also leave space for other use functions (e.g., mining activities). Against this background, it is important here to highlight that the designs are the result of exploratory work, i.e., our aim was not to propose final (optimized) designs. Interestingly, in the recently published drafted version of the update of the “Partiële Herziening Programma Noordzee 2022-2027” of 2025 (PHPNZ25) (Ministerie van Infrastructuur en Waterstaat, 2025), we see proposals regarding capacities, design and spatial integration that align quite well with ours.

To answer the research questions stated in the introduction (Chapter 1) regarding the role and contribution of the hubs (and associated transport and storage infrastructure) in the overall energy system, we used different models to conduct scenario-based modelling studies. In this chapter we discuss the results and highlight the learnings.

A first set of learnings relates to the modelling of the energy production of the wind farms in the 3 hubs. In NSE5-DEC, the hubs supply 42% of the yearly electricity demand (364 TWh in

II3050-DEC) and 21% of yearly hydrogen demand (102 TWh in II3050-DEC), while in NSE5-NAT, they supply 43% of total electricity demand (433 TWh in II3050-NAT) and 19% of hydrogen demand (159 TWh in II3050-NAT). When we include the additional electricity generated by capacity outside of Hub North (in the areas around Klaverbank and Doggerbank) that must be built to reach the 2050 target of 70 GW in NSE5-NAT, then the total installed capacity in and around Hub North produces 60% of the yearly electricity demand of II3050-NAT, and 35% of hydrogen demand.

It was highlighted that this production is highly dependent on the meteorological year considered, as the difference in energy produced between a higher- and a lower-producing wind year can be ca. 15%. Another aspect that is very relevant is the impact of wake losses. In our NSE5-NAT design with 20GW installed wind power capacity in Hub North, only 50% of space is available when taking into account ecology and mining. Wind farms will be concentrated in two regions in the hub, and in close proximity to each other, which will result in significant wake losses. Our modelling results indicate that the full load hours (FLH) of wind farms in Hub North and Hub East can differ by 4-8% depending on wind farm location and power density (range 7-11MW/km² investigated). Furthermore, we noticed that the correlation between the wind profiles in the two hubs for the same (period of) hour(s) was not particularly high, probably because they are distanced by around 100 km. Differences between wind profiles could be even higher if wake losses across different wind areas were taken into account, which was out of scope of this study. This highlights the importance of providing location-specific profiles for wind farms. While comparing the results from our analysis with other studies, such as NSWPH or II3050, we noticed that some of the assumptions used for the calculation of wind energy production are often missing or incomplete. Examples of missing assumptions include the type of wind turbine used, the power density, the method for calculating wake losses and other losses (such as inter-array), the meteorological year considered, etc. This made the comparison with other studies, while similar in capacities, challenging. In fact, the comparison made with CorRES, which is one of the most complete datasets whose details are publicly available, and used by D3.1 of this programme (Blom, van Stralen, Eblé, Magan, & Hers, 2025), resulted in a difference in wind power production of up to 10% (CorRES with 3.16 MW/km² versus NSE 5 with 10 MW/km²). Some of the differences can be attributed to the type of models used for the wake losses, but also to the lower power densities than the ones defined in this project. Hence, we advocate for more transparency in the assumptions being made in future studies on this subject, especially because the effects can compound when adding other elements of the value chain, such as hydrogen production.

The transport scenarios provided a view on the effects of opting for larger pipelines (48 inches) compared to mostly re-using existing pipelines for hydrogen (24 and 36 inches). It can be seen from the analyses performed that the re-use of infrastructure comes with limitations if the NSE5-NAT ambitions are to be met: the pressure losses can reach up to 50 bar, and significant pressure fluctuations occur upstream, at the electrolyzer locations, and downstream, at the landing points (\approx 20 bar amplitude). While this is technically feasible in practice, it comes with significant compression requirements, and this level of pressure fluctuation may degrade the durability of the pipelines, impacting their lifetime. In addition, it would require complex control systems along the offshore-onshore connections. These are also results from a scenario where all actors are coordinated for supply-demand matching.

The assumption of coordination becomes more relevant if other elements of flexibility are present in the system (such as batteries or market incentives). Key pipeline sections that impact pressure losses are the sections with diameters of 24 inches that connect to AquaDuctus to enable import. This is illustrated by the results of the NSE5-DEC scenario, where the pressure losses are even higher than in NSE5-NAT, due to the higher imported flow from AquaDuctus in this storyline (25% larger than in NSE5-NAT). In the NOGAT pipes closer to this import connection, there are significant pressure drops, which also limit the applicability of this scenario in practice. A somewhat adjusted combination of newly built and re-used pipelines from what was presented here could strike the right balance between cost, durability and performance though.

The set of scenarios regarding onshore compression only, i.e., no offshore compression, provided similar conclusions than the ones derived from the transport scenarios. The re-use scenario was not feasible if 30 bar compression from the electrolyzers and the imports from AquaDuctus were considered. Only when these imports were not present, the DEC scenario was able to run, with around 10 bar of pressure drop and injection at 35 bar (= electrolyser output pressure). This is expected to be feasible for PEM systems in 2050, without a large penalty in their performance or their operational envelope. However, this scenario resulted in variability in the pipe connected to the electrolyzers of around 7 bar. The newly built scenario with NSE5-NAT (with extra capacity out of Hub North and AquaDuctus import) was feasible at 30 bar, i.e., without offshore compression, providing also a variation in pressure at the landing points of 5-8 bar. Large pressure drops were experienced along the east line running from wind area 7 to wind area 6, but the highest relative pressure drops of 6 Pa/m occurred in the pipe connecting to the landing point of Eemshaven. In D3.3 of NSE 5 (van Zoelen, Rob; Boer, Dina; Mahfoozi, Salar, 2025), represents a largest share of offshore hydrogen network costs, supporting the relevance of establishing further research in different compression and transport configurations.

The storage scenarios provided some non-intuitive results. Firstly, the pressure losses across the network increased for both storage locations (F8 and G17). This is a consequence of the operational strategy that was used. The requirement of delivering a certain flowrate to both landing points forces the flow to take a longer route than in the reference case on average. In fact, there is an increase in the west-east link utilization, due to the multiple cycles of charging and discharging the storage, and the enforcement of delivering flow at Den Helder. The pressure distribution at this landing point had a wider range (around 17-20 bar of differences depending on the specific hour and storage location, compared to the less than 10 bar differences for the reference case). For both locations, despite the higher-frequency dynamics associated with some hours without wind power, there was a clear seasonal pattern (for this meteorological year). This highlights that large-scale (underground) storages could well serve as a “bulk” storage (large volume with limited number of charge-discharge cycles), and that smaller power/molecule-based storage solutions could be used to compensate for (intra-)daily variations.

The offshore solar cases, while limited in scope, provided a qualitative estimation of the upper limit of this technology when operating in combination with offshore wind, by adding it in a 1:1 ratio of wind/solar capacity in the NSWPH blocks. Without looking at the cost structure of this solution, it gave an overview of the energy availability. This resulted in

significant improvements in supply/demand matching, but also on high curtailment levels, due to the congestion of the (assumed undersized) offshore infrastructure. A more thorough analysis, such as including power storage systems and more targeted inclusion of solar (e.g., in specific nodes with access to multiple electrolyzer blocks) could provide a better usage of this source. While the current/short-term future installed capacities of offshore solar are modest, it could become a viable source in specific applications.

In this report, the impact of different operational strategies was also analysed, and the effect of having grid-connected compared to off-grid hydrogen production in Hub North. Firstly, it was seen that in the NSWPH-block, where the ratio of wind power installed capacity to electrolyzers is 2:1, the number of hours using grid power is limited for the range of minimum electrolyser load considered (10-50%). For the most extreme case (50% minimum load), an 11% increase in the full load hours of the electrolyzer was observed, vs. only a 1% increase in FLH for 10% minimum load. It must be noted though that our analysis only focused on quantification of total energy produced (in the form of electricity and hydrogen), but not on the techno-economics associated with it. Grid tariffs could well become a blocker for strategies that rely heavily on use of grid power. Especially when the grid power is used infrequently, while tariffs are paid on reserved capacity and peak consumption, then the tariff component (in EUR/MWh of power consumed) can become a significant part of the cost structure. In addition, if the hydrogen is then sold to an off-taker, a distinction may have to be made between “green/non-green” hydrogen (such as Guarantees of Origin). These are elements that may complicate the operational strategies tested in this study.

If no grid power was to be used in this particular asset configuration, then a power storage system would have to be installed. Our analysis indicates that the energy storage capacity from such a power storage system would have to be around 1.5 times the capacity of the electrolyzer (e.g., 3 GWh of power storage required for a 2 GW electrolyzer with a 10% minimum load, covering 15-20 hours of not enough wind power) for the meteorological year considered (2015) to cover 90% of the moments with insufficient wind power (less than 10 shutdowns). However, we also found that the storage requirements greatly increase if no shutdowns are allowed at all, because there are some moments that require a storage capacity that is an order of magnitude higher. Following common definitions of short-duration (up to 4 hours at rated power) and long-duration (>10 hours at rated power) storage, it can be inferred that a combination of both short-term and medium-term could be potentially suitable, based on expected commercial solutions by 2040-2045 (TRL scaling and higher storage power densities). However, there are still a small number of moments (less than 10) during the year where the energy required is much higher (by a factor of around 5 times larger, 50-100 hours of not enough wind power). If no shutdowns at all are allowed, then long-duration storage or grid power would be required.

Another point of study tested was using two different strategies: equal wind power to the electrolyzer and the export cable versus the “NSE5 strategy”. The aim of this strategy was to absorb part of the fluctuations from wind power at the electrolyzer level, encouraging a more constant power delivery to shore. It was shown that more than 1000 extra hours of peak power delivery could be obtained with this method, with similar utilization factors of both the cable and the electrolyzer.

This latest argument brings up the question of *where should flexibility be applied/encouraged*. There are different levels: from the intermittent power production, to chemical/electrochemical conversion (such as hydrogen production), to transport (e.g., line pack), storage (electron/molecule-based) and on the off-taker side. In this work, the added value of encouraging flexibility has been studied at the conversion level offshore, via electrolysis, and via hydrogen storage offshore in different locations. It was shown that both of them, individually, can provide mechanisms to dampen some of the fluctuations, providing a more stable power and hydrogen delivery. There may also be trade-offs that provide to be more beneficial when *combining* these flexibility elements. As an example, establishing a different operational strategy in the wind farm/electrolyzer system depending on the hydrogen storage levels offshore and onshore. If scenarios such as the NSE5-NAT are to be fulfilled, there will be significant infrastructure challenges, and several flexibility elements may be needed to be synergized. This work does not enter into policy recommendations to increase the attractiveness of the business case of each part of these flexibility elements. Nevertheless, it can be qualitatively affirmed that an *alignment between the different stakeholders at early stages* to encourage the deployment of these technologies will be of high importance to provide security of supply of the different commodities as the capacities build up, the space is limited and the infrastructure challenges arise. In the next phase of the North Sea Energy programme, this could be addressed in the form of more detailed technical assessments of combining technologies that provide flexibility with wind energy and hydrogen production assets, as a stepping stone towards techno-economic optimization of use functions in (and around) the hubs. Additionally, synergies can be explored with (plans for) hubs being developed in other countries around the North Sea, and their coupling with onshore hubs (clusters) that are being developed under different decarbonization and energy system scenarios, with the aim to optimize the spatial integration of use functions at the level of the North Sea basin rather than at country level.

6 Conclusions and recommendations

6.1 Conclusions

In this workstream of WP 1 of NSE5, we developed designs for three NSE hubs (west, east and north) and presented them as spatial explicit blueprints that show how infrastructure for production, transport and storage of the 4 commodities (electricity, hydrogen, natural gas, and carbon dioxide) could develop in three phases until 2050. Hub designs have been made for two scenarios that differ in the level of utilization of the Dutch North Sea for producing renewable and low-carbon energy. The two scenarios, and the associated narratives for the phased development of the hubs, which we call “storylines”, can be seen as visions of how the future Dutch energy system, and the role of the hubs in that system, could evolve. In this section, the conclusions are linked with the research questions outlined in Chapter 1.

What areas in the hubs are (foreseen to be) developed for wind power, natural gas, hydrogen production and storage and CO₂ storage in the period between 2030-2050?

Our two storylines, named “NSE5-NAT” and “NSE5-DEC”, are rooted in the scenarios “National Leadership” (NAT) and “Decentralized Initiatives” (DEC) of the “Integrale Infrastructuur Verkenning 2030-2050 editie 2” (II3050-2) (Netbeheer Nederland, 2023), which presents four future scenarios for realizing a climate-neutral energy supply in 2050, with an associated narrative (also termed “storyline”). In NSE5-NAT (molecules-heavy), the North Sea plays a key role in supplying The Netherlands with clean energy to reach climate goals. It assumes that 70.3 GW offshore wind will be installed in 2050, which is in line with the 2050 ambition of the Dutch government. To realize that 70.3 GW capacity though, the speed at which wind farms are developed must increase significantly. In NSE5-NAT, offshore wind capacity must increase from 12 GW installed capacity in 2030 to 37 GW in 2040, i.e., an increase of 25 GW in 10 years, implying an average expansion rate of 2.5 GW/yr. In the period 2040-2050, 33 GW must then be additionally installed to reach 70 GW in 2050, at an expansion rate of 3.3 GW/yr. In comparison, the average expansion rate for realizing 12 GW in the period 2020-2030 was ~1 GW/yr. With clear signs today of lower appetite of wind farm developers to participate in tenders, and with spatial planning processes becoming more complex and time consuming, the ambition of the Dutch government to realize 70 GW offshore wind by 2050 becomes more and more challenging to meet.

How does the limited space in areas to be developed for offshore wind and hydrogen affect the capacities, spatial configuration and energy production of the hubs? How can they be developed in a way that maintains (if not strengthens) the ecological carrying capacity of the North Sea?

We find that of that 70.3 GW only 40.3 GW can be accommodated by the hubs. While in the “Partiële Herziening Programma Noordzee 2022-2027” of 2023 (Ministerie van Infrastructuur en Waterstaat, 2023) it is assumed that 20-28 GW offshore wind can be deployed in wind search areas 6 and 7 that together form our Hub North in NSE5, we can only accommodate max. 20 GW in our nature-inclusive design for NSE5-NAT. To strengthen the ecological carrying capacity of the North Sea, we reserve space for nature, in the form of an ecological corridor, and this leads to reduction of available space with 50%. This reduction is confirmed in the draft version of the update of the Partiële Herziening Programma Noordzee 2022-2027” published in April 2025 (Ministerie van Infrastructuur en Waterstaat, 2025), where 19

GW offshore wind is stated as the upper limit for wind search areas 6 and 7, to leave space for ecology and mining. Consequently, wind farms will be concentrated in two regions in the hub, and in close proximity to each other, which will result in wake losses in the range of 4-8% of full load hours for our designs depending on wind farm location and power density (range 7-11 MW/km² investigated). Our wake (proxy) model calculates lower full load hours compared to CorRES (Koivisto & Murcia Leon, Offshore wind generation time series for technology SP316 HH155 (PECD 2021 update), 2022), for the same meteorological year (2015) which is probably due to use of different wake models and/or different power densities assumed.

Hydrocarbon production is expected to remain relevant until (at least) the period 2045-2050 (Ministerie van Klimaat en Groene Groei, Element NL, and EBN, 2025), with a total potential of ~127 bcm¹³ (EBN forecast), of which 60% would come from the 3 hubs. Likewise, CO₂ storage is expected to reach 22 Mt/yr before 2040 in Hub West, with potential to increase further towards 40 Mt/yr afterwards by utilizing additional gas fields and/or aquifers for CO₂ storage. Considering that space must also be reserved for these mining activities, the space for offshore wind will further reduce in that region, unless we find innovative solutions that resolve the spatial conflicts.

Consequently, to realize the 70GW ambition, additional space must be found for 17GW of offshore wind. When looking at the North Sea today, however, available “free” space is limited to areas to the west and northwest of Hub North (wind search areas 6 and 7). In contrast, our “less ambitious” NSE5-DEC scenario (electrons-heavy) reaches 45GW offshore wind by 2050 and can probably be realized while reserving space for other uses, both in time, and from the perspective of available space. In that scenario, the North Sea plays a less prominent role in supplying The Netherlands with clean energy to reach climate goals.

What is the contribution of the hubs towards meeting the demand for electricity, hydrogen, natural gas and CO₂ storage in 2050?

Offshore hydrogen production is limited to Hub North (and areas to the west and northwest) in our designs, for which we assume it is connected to 50% of the offshore wind capacity (and to the substation), reaching 19.1GW electrolyser capacity in NSE5-NAT in 2050 (of which 10GW in Hub North) and 7.6GW in NSE5-DEC in 2050. By 2040, GW-scale offshore electrolysis must have matured to realize up to 5GW capacity, as an intermediate milestone towards realizing ~20GW by 2050, leaving a 7 year time window from start of operation of the 500MW demonstration project at the Ten Noorden van de Wadden wind farm to include learnings and up-scale to multi-GW scale modular roll-out.

In the NSE5-DEC storyline, the installed capacities in the 3 hubs produce 152 TWh of electricity, of which 34 TWh is consumed by electrolyzers to produce 21 TWh of hydrogen. In contrast, in the NSE5-NAT storyline, where installed capacities are higher, 187 TWh of electricity is produced in the hubs, of which 47 TWh is consumed to produce 30 TWh of hydrogen. In NSE5-DEC, the hubs supply 42% of the yearly electricity demand ((364 TWh in I13050-DEC) and 21% of yearly hydrogen demand (102 TWh in I13050-DEC), while in NSE5-

¹³ In the “Sectorakkoord gaswinning in de energietransitie” that was published in April 2025 (Ministerie van Klimaat en Groene Groei, Element NL, and EBN, 2025) the offshore potential is estimated at ~150 bcm.

NAT, they supply 43% of total electricity demand (433 TWh in I13050-NAT) and 19% of hydrogen demand (159 TWh in I13050-NAT). Furthermore, it can be observed that the additional electricity generated by capacity outside of Hub North (in the areas around Klaverbank and Doggerbank) that must be built to reach the 2050 target of 70 GW in NSE5-NAT is almost as large (75 TWh) as the electricity generated inside Hub North (88 TWh), and this accounts for an additional 17% of total yearly electricity demand of I13050-NAT. Of the 75 TWh, 38 TWh is consumed to produce 26 TWh of hydrogen. In total, the installed capacities in and around Hub North produce 60% of the yearly electricity demand of I13050-NAT, and 35% of hydrogen demand.

How do different operational strategies affect the utilization and need for flexibility of the offshore hydrogen production and transport infrastructure to absorb part of the wind power intermittency?

Platform-based electrolysis modules currently appear to be the most attractive option (North Sea Wind Power Hub Programme, 2024), with sizes of either 180MW (max. size that can be installed with cranes) or 500MW. Recently published designs by the NSWPH consortium assume modular set-ups of 4GW wind capacity with 2GW hydrogen production capacity (PEM) integrated, and a 2GW bidirectional connection to shore. In this grid-connected design, operating the electrolyzers with 10% minimum load leads to less than 2% use of grid electricity (from shore), while with 50% minimum load, the grid electricity consumption increased to 10%. If the electrolyzers were not connected to the grid, and (almost) continuous operation would be required, 10% minimum load could be achieved with a short-to-medium duration power storage solution (for a 1GW PEM electrolyzer, around 1.5GWh of energy to be delivered at moments with not enough wind power). Without a storage solution present, 200 shutdowns per year would have to be incurred, with the remark that this number is highly sensitive to the meteorological year considered. If fully continuous operation is required with zero shutdowns, then the energy storage capacity must increase dramatically, to 5-10 times the capacity of the electrolyzer, requiring long-duration storage capacity or access to the grid.

The operational strategy of the system wind farm-electrolyzer can also significantly affect how the flexibility is absorbed in different parts of the system. The tests with a “NSE5” operational strategy showed that a larger amount of stable power delivery (increased ≈ 1000 hours in a year) could be achieved compared to simply providing equal power to the electrolyzer and to shore, with similar utilization factors for the export cable and the electrolyzer.

How could the infrastructure for transporting electricity and hydrogen from the hubs to shore develop in time, and what role could existing (re-used) pipelines play?

To transport the hydrogen produced to shore, and allow for import (Denmark, Norway, UK), the capacity of the offshore hydrogen grid must reach ~ 20 GW by 2050 in our scenarios. We developed two designs that transport the hydrogen to landing points in the Eemshaven and Den Helder regions. One design assumes all new pipelines (48 inch), and the other design assumes reuse of sections of NGT and NOGAT with limited new pipelines (36 inch). Our model-based analysis shows that, under the assumptions made, newly built infrastructure for hydrogen transport with 48-inch diameters (vs. 36-inch for reuse) provides greater resilience for future energy needs, in particular for projected import and production beyond 2050. For the high-end offshore hydrogen production scenario (NSE5-NAT), the pressure

losses in the hydrogen network for the design with only newly built pipelines are around 3 bar, compared to around 50 bar for the design that incorporates significant reuse. Consequently, for the design based on newly built pipelines, the high-end hydrogen production scenario (NSE5-NAT) can be accommodated including extra out-of-hub production capacity and import without offshore compression, i.e., leveraging the 30 bar electrolyser outlet pressure. In contrast, for the design based on significant re-use, the case at 30 bar (with no offshore compression) was not feasible.

Offshore compression can only be avoided for the low-end hydrogen production scenario (NSE5-DEC) if no imports from AquaDuctus (nor extra production from outside of Hub North) is considered, and the electrolysers output hydrogen at 35 bar (probably feasible). In that scenario, the (much) lower amounts of hydrogen to be transported led to moderate pressure losses at the landing points of less than 10 bar.

Clearly, the high flowrates required in combination with (especially) some smaller-diameter pipeline sections limit the potential of the reuse-based design. In addition, the redundancy of the network is limited under these conditions. A different combination of reuse and newly built hydrogen pipelines from the one investigated here could strike the right balance between flexibility, resilience, future proofness, and investment cost though.

What is the potential role of offshore hydrogen storage in providing flexibility to maintain a stable and predictable hydrogen supply to shore?

Offshore hydrogen storage can play a role in reducing pressure fluctuations in the hydrogen network, by acting as a buffer to transform the inherently variable wind-based production into a constant flow to shore (use case). Examples of possible candidate salt structures (in license blocks F8, E17, and M2) and depleted gas fields (in license blocks G16, G17, K5 and K7) in and around Hub North were highlighted where sufficient hydrogen could be stored for the investigated use case (≈ 3 TWh storage capacity to transform a variable hydrogen production signal from 8 GW of electrolyser capacity into a ≈ 3 GW flow to shore year round).

Notional design studies for an offshore storage facility highlighted that for storage in gas fields, the transmissivity of the reservoir is a key parameter to be considered in selecting candidate fields. To limit the number of wells required to meet the performance criteria set by the use case, transmissivities (and well diameters) must be sufficiently high, which severely limits the number of “suitable” fields. Additionally, we realized that especially for storage in gas fields, the dimensions and weight of facilities for compression and gas cleaning would require very large offshore platforms to be built that are of similar size as some of the largest platforms in the world. When storing hydrogen in a (depleted) gas field, it mixes with the residual natural gas in the reservoir, and this must be separated from the hydrogen on withdrawal to bring the stored hydrogen back to specifications for injection into the hydrogen network. This separation step requires purification facilities (pressure-swing adsorption/PSA), and produces a sizeable mixed hydrogen-natural gas tail gas stream that comes out of the PSA at atmospheric pressure for which a solution must be found. It can either be transported to shore via a pipeline, or reinjected into a nearby reservoir, however, both solutions require recompression of the tail gas stream to either pipeline pressure (50 bar) or reservoir pressure (250-300 bar). Compression ratios would be in the order of 50-250, requiring a very large tail gas compressor with a large spatial footprint. Several cost analyses performed for developing offshore storage facilities for the selected use case indicate that

the total investment cost for a facility offshore can be 2-5 times higher than for an facility onshore.

Interestingly, in our simulations we observed that while hydrogen storage did allow for a more constant flow to shore, it did not necessarily lead to reduced pressure fluctuations or pressure losses. This was found to depend on the location of the storage and the operational strategy of the offshore/onshore grid. The largest pressure drop in the network at maximum hydrogen flowrate was found with a storage at G17 (57 bar) vs. 50 bar for the reference case without storage. A storage at F8 resulted in a 54 bar pressure loss. Increased losses were associated with additional flow through the pipeline connecting the west and east links. Furthermore, we noticed that the location of the storage influences the pressure at the landing point on the opposite side (G17-Eemshaven, F8-Den Helder), as the flow takes the shortest route to reach demand. Likewise, the pressure distribution at the landing points can get significantly affected by the charge/discharging events at the storage. In Eemshaven, F8 storage “controls” the rest of the network from far offshore. Conversely, G17 is too close to shore. For Den Helder, the higher utilization of the west-east link and the increased flowrates at certain times creates higher pressure losses and higher pressure fluctuations than in the reference case.

Clearly, the control strategy (fixed flowrate versus fixed pressure) and the coordination of the different actors (production, storage and transport) are key to optimize the operation of the offshore system. For example, with the operational strategy set (fixed flowrate), the Eemshaven landing point experienced an almost constant pressure delivery with the storage in F8 (Hub North). The case with G17 (Hub East) storage achieved a narrower pressure distribution than the reference case (around 12 bar of amplitude for G17, around 16 bar for the reference case). For the landing point at Den Helder, the peak-to-peak amplitude increased in both storage cases, highlighting that a different operational strategy would be needed if near-to-constant pressure is the aim.

6.2 Recommendations for future work

The following recommendations can be set based on the storylines and simulations developed:

Wake losses and spatial claims:

- No interactions between wind farms in the wake losses has been performed. If spatial claims provide additional constraints, power production could be lower than expected.
- No overplanting cases have been studied. This could further increase the power densities, decreasing the energy produced per wind turbine.

Supply/demand assumptions:

- The international context was not (fully) considered in this study. Simplifications were made, such as assuming that there would be constant imports from AquaDuctus. Modelling profiles for the different commodities across different countries in the North Sea would provide a better representation of the supply and demand matching and what flexibility options are needed.

Alignment with present/future wind tender criteria:

- Multi-stakeholder coordination can be a very influential assumption. Exploring scenarios where actors operate without these coordination and analysing its impact on flexibility could bring relevant results for policy-making (e.g., as seen in IJmuiden Ver Gamma tender criteria regarding curtailment/usage of power).
- The influence of different power storage models to tackle short and long-term flexibility has not been studied. This could open the room for more (semi) off-grid strategies for hydrogen production or power delivery (e.g., if ATR85 network code limitations for time-based and time-block transmission rights are present).

Alignment with other constraints (engineering, economic):

- No assumptions have been made in the different options regarding their cost and availability. A combined assessment of these could provide a more holistic perspective on the best pathways.

Combining scenarios:

- Most of the scenarios here explored one change with respect to a reference. However, as seen in the cases with hydrogen storage, it may be beneficial to explore cases with e.g., multiple storages.
- Similarly, a combination of newly built and re-use infrastructure could provide a good balance between cost, availability and performance.

7 References

- Aramis. (2021). *Aramis*. Retrieved from <https://www.aramis-ccs.com/>
- Arcadis, BRO, Delft, C., & Pondera. (2024, 02 09). *Programma VAWOZ 2031-2040*. Retrieved from <https://www.rvo.nl/sites/default/files/2024-03/Concept-notitie-reikwijdte-en-detailniveau-programma-VAWOZ-2031-2040.pdf>
- Blom, S., van Stralen, J., Eblé, L., Magan, I., & Hers, S. (2025). *North Sea Energy 5 D3.1: Public Value Assessment of Offshore System Integration*. North Sea Energy.
- Bot, E., & Kanev, S. (2020). Farmflow: Extensively validated and dedicated model for wind farm control. TNO.
- Bourgeois, B., Duclercq, L., Jannel, H., & Reveillere, A. (2022). *Life Cycle Cost Assessment of an underground storage site*. Hystories project. Retrieved from https://hystories.eu/wp-content/uploads/2022/05/Hystories_D7.2-1-Life-Cycle-Cost-Assessment-of-an-underground-storage-site.pdf
- Buijs, L., Venugopalan, S., Uritsky, V., Evertse, T., Saric, M., Skorikova, G., . . . van Cooten, Q. (2025). *North Sea Energy 5 D1.4: Technical Innovation*. North Sea Energy.
- Clark, C., & Varma, K. (2025). North Sea Energy 5 D1.3a: Overview of Subsea Pipeline Connection Options for Hydrogen Supply in the North Sea. North Sea Energy.
- de Borst, K., Looijer, M., Duff, S., Kuperus, E., & Vink, W. (2025). North Sea Energy 5 D1.3b: Offshore H2 storage salt caverns - Are they a viable alternative to onshore storage? North Sea Energy.
- Dighe, V. V., Fatou Gómez, J., Dussi, S., Poort, J., & Shoeibi Omrani, P. (2022). Digitalization of North Sea Energy Systems.
- EBN. (2023, 12 19). *Memo mijnbouwactiviteiten in windenergiegebied Doordewind/Doordewind-West*. Retrieved from <https://www.ebn.nl/wp-content/uploads/2024/12/2023-Memo-EBN-Mijnbouwactiviteiten-Doordewind.pdf>
- EBN. (2023, 12 19). *Memo mijnbouwactiviteiten in windenergiegebied Nederwiek (N & Z)*. Retrieved from <https://www.ebn.nl/wp-content/uploads/2024/12/2023-Memo-EBN-Mijnbouwactiviteiten-Nederwiek.pdf>
- EBN. (2023, 07 21). *Memo Mijnbouwactiviteiten in windzoekgebied 6/7* . Retrieved from <https://www.ebn.nl/wp-content/uploads/2024/12/2023-EBN-Memo-Mijnbouwactiviteiten-Zoekgebied-Windenergie-6-7.pdf>
- EBN. (2024, 04 19). *Mijnbouwactiviteiten in het windenergiegebied Lagelander N&Z*. Retrieved from <https://www.ebn.nl/wp-content/uploads/2024/12/2024-Memo-EBN-Mijnbouwactiviteiten-Lagelander.pdf>
- ENTSO-E. (2024, 01). *Sea-Basin ONDP Report - TEN_E Offshore Priority Corridor: Northern Seas Offshore Grids*. Retrieved from https://eepublicdownloads.blob.core.windows.net/public-cdn-container/tyndp-documents/ONDP2024/web_entso-e_ONDP_NS_240226.pdf
- ENTSOG, ENTSO-E. (2022, April). *TYNDP 2022 - Scenario Report - Version April 2022*. Retrieved from <https://2022.entsos-tyndp-scenarios.eu/>
- esdl. (n.d.). Retrieved from <https://www.esdl.nl/>
- ESDL. (2019). ESDL documentation.
- European Commission. (2019). *The European Green Deal - Striving to be the first climate-neutral continent*. Retrieved from https://commission.europa.eu/strategy-and-policy/priorities-2019-2024/european-green-deal_en

- European Commission. (2022). *REPowerEU - Affordable, secure and sustainable energy for Europe*. Retrieved from https://commission.europa.eu/strategy-and-policy/priorities-2019-2024/european-green-deal/repowereu-affordable-secure-and-sustainable-energy-europe_en
- European Commission. (2024, 06 13). *The Net-Zero Industry Act: Making the EU the home of clean technologies manufacturing and green jobs*. Retrieved from https://single-market-economy.ec.europa.eu/industry/sustainability/net-zero-industry-act_en
- European Commission. (2024). *The North Seas Energy Cooperation*. Retrieved from https://energy.ec.europa.eu/topics/infrastructure/high-level-groups/north-seas-energy-cooperation_en
- Fatou Gómez, J., Martín-Gil, A., & Dussi, S. (2025). PyDOLPHYN: Dynamic simulations and optimization of multi-energy assets. *Energy*.
- Gasunie. (2025, 03 13). *Petrogas and Gasunie investigate reuse of existing North Sea pipelines for hydrogen transport*. Retrieved from <https://www.gasunie.nl/en/news/petrogas-and-gasunie-investigate-reuse-of-existing-north-sea-pipelines-for-hydrogen-transport>
- Hancke, R., Bujlo, P., Holm, T., & Ulleberg, Ö. (2024). High-pressure PEM water electrolyser performance up to 180 bar differential pressure. *Journal of Power Sources*.
- Koivisto, M., & Murcia Leon, J. (2022, 05 03). Existing offshore wind generation time series (PECD 2021 update). Technical University of Denmark.
- Koivisto, M., & Murcia Leon, J. (2022). Offshore wind generation time series for technology SP316 HH155 (PECD 2021 update). Technical University of Denmark.
- Ministerie van Economische Zaken en Klimaat. (2022, 09 16). *Kamerbrief windenergie op zee 2030-2050*. Retrieved from <https://open.overheid.nl/documenten/ronl-b34f5ea2f405a4b9dbdf676288ace0736599264/pdf>
- Ministerie van Economische Zaken en Klimaat. (2023, 12 01). *Nationaal Plan Energiesysteem*. Retrieved from <https://www.rijksoverheid.nl/documenten/rapporten/2023/12/01/nationaal-plan-energiesysteem>
- Ministerie van Economische Zaken en Klimaat. (2024, 06 10). *Betreft Voortgang demonstratieprojecten waterstof op zee*. Retrieved from <https://open.overheid.nl/documenten/21547a28-9410-4fea-9931-2aa636fb423c/file>
- Ministerie van Economische Zaken en Klimaat. (2024, 06 06). *Energie Infrastructuur Plan Noordzee 2050*. Retrieved from <https://open.overheid.nl/documenten/857b868a-46d6-4484-a161-ae7d53571d39/file>
- Ministerie van Economische Zaken en Klimaat. (2024, 04 25). *Kamerbrief over Nij begun: op weg naar erkenning, herstel en perspectief*. Retrieved from *Kamerbrief over Nij begun: op weg naar erkenning, herstel en perspectief*
- Ministerie van Economische Zaken en Klimaat. (2024, 06 06). *Kamerbrief over totstandkoming van Energie Infrastructuur Plan Noordzee 2050*. Retrieved from <https://www.rijksoverheid.nl/documenten/kamerstukken/2024/06/06/energie-infrastructuur-plan-noordzee-2050>
- Ministerie van Economische Zaken en Klimaat. (2024, April 25). *Update aanvullende routekaart wind op zee*. Retrieved from <https://open.overheid.nl/documenten/a5b91671-5b23-45b5-aa0b-72439730a4dc/file>

- Ministerie van Economische Zaken en Klimaat. (2024, 04 25). *Update aanvullende routekaart wind op zee*. Retrieved from <https://open.overheid.nl/documenten/a5b91671-5b23-45b5-aa0b-72439730a4dc/file>
- Ministerie van Infrastructuur en Waterstaat. (2023, 05 17). *Partiële Herziening van het Programma Noordzee 2022-2027*. Retrieved from <https://www.rijksoverheid.nl/documenten/kamerstukken/2023/05/17/partiele-herziening-van-het-programma-noordzee-2022-2027>
- Ministerie van Infrastructuur en Waterstaat. (2025, 03 31). *Ontwerp Partiële Herziening Programma Noordzee 2022-2027*. Retrieved from <https://open.overheid.nl/documenten/53b6c8a3-9ccb-4038-a901-cad6ff4e7a4e/file>
- Ministerie van Klimaat en Groene Groei. (2025, 03 26). *Betreft Carbon, Capture and Storage*. Retrieved from <https://open.overheid.nl/documenten/f99f5e57-4bea-4945-8fb3-324efbab0c82/file>
- Ministerie van Klimaat en Groene Groei. (2025, 02 28). *Programma Aansluiting Wind op Zee (PAWOZ) – Eemshaven*. Retrieved from <https://www.rvo.nl/sites/default/files/2025-02/Ontwerpprogramma-PAWOZ-Eemshaven.pdf>
- Ministerie van Klimaat en Groene Groei, Element NL, and EBN. (2025, 04). *Sectorakkoord gaswinning in de energietransitie*. Retrieved from <https://open.overheid.nl/documenten/23b81a85-beb3-4fe8-9626-b8c8232dbdba/file>
- Murcia, J. P., Koivisto, M. J., Luzia, G., Olsen, B. T., Hahmann, A. N., Sørensen, P. E., & Als, M. (2022). Validation of European-scale simulated wind speed and wind generation time series. *Applied Energy*.
- Murcia, J. P., Koivisto, M. J., Luzia, G., Olsen, B. T., Hahmann, A. N., Sørensen, P. E., & Als, M. (2022). Validation of European-scale simulated wind speed and wind generation time series. *Applied Energy*.
- Netbeheer Nederland. (2023, 06 30). *Het energiesysteem van de toekomst: de I13050-scenario's*. Retrieved from https://www.netbeheernederland.nl/sites/default/files/Rapport_I13050_Scenario%2527s_280.pdf
- Netbeheer Nederland. (2023, 10 31). *Integrale infrastructuurverkenning 2030-2050 editie 2*. Retrieved from <https://www.rijksoverheid.nl/documenten/rapporten/2024/03/06/bijlage-integrale-infrastructuurverkenning-2030-2050-editie-2>
- NGT, NOGAT. (2023, 10). *Management Samenvatting - Hergebruik leidingen NGT & NOGAT voor waterstoftransport mogelijk voor 2030*. Retrieved from <https://noordgastransport.nl/content/uploads/2023/12/NGT-NOGAT-Hergebruik-scenarios-2020231017-Summary.pdf>
- Noordzeeloket. (2024, November). *Offshore wind energy*. Retrieved from <https://www.noordzeeloket.nl/en/functions-use/offshore-wind-energy/>
- North Sea Wind Power Hub Programme. (2024, 08). *North Sea Wind Power Hub*. Retrieved from <https://northseawindpowerhub.eu/>
- North Sea Wind Power Hub Programme. (2024, 09 16). *Offshore Energy Hubs: Blueprints with Offshore Electrolysis*. Retrieved from <https://northseawindpowerhub.eu/knowledge/offshore-energy-hubs-blueprints-with-offshore-electrolysis>

- Oceans of Energy; NWO-NIOZ; Deltares; Primo Marine; New Ground Law; Advanced Electromagnetics BV; TNO. (2025). SENSE Hub MOOI622002 Public Report Feb 2024 until Jan 2025 (M12-M24). TNO.
- Offshore TSO Collaboration. (2025, 04). Offshore TSO Collaboration - Expert Paper III - Joint Planning in Europe's Northern Seas - Supporting Europe's energy security and competitive growth through a regional approach to offshore grid development. Retrieved from <https://tennet-drupal.s3.eu-central-1.amazonaws.com/default/2025-04/Expert%20Paper%20III%20Offshore%20TSO%20Collaboration%20April%202025.pdf>
- Overlegorgaan Fisieke Leefomgeving. (2020, 06 19). *Het Akkoord voor de Noordzee*. Retrieved from <https://www.rijksoverheid.nl/documenten/rapporten/2020/06/19/bijlage-ofl-rapport-het-akkoord-voor-de-noordzee>
- Porthos. (2021). *Porthos, CO2 transport & storage*. Retrieved from <https://www.porthosco2.nl/en/>
- Rojer, J., Janssen, F., van der Klauw, T., & van Rooyen, J. (2024). Integral techno-economic design & operational optimization for district heating networks with a Mixed Integer Linear Programming strategy. *Energy*.
- Royal HaskoningDHV. (2024, 02 09). *Samenvattend Hoofdrapport MER Aramis - Aramis CO2 transportinfrastructuur*. Retrieved from <https://www.rvo.nl/sites/default/files/2024-09/Samenvattend-hoofdrapport-Aramis-fase-1.pdf>
- RVO. (2025, April 14). *Vergunningen windparken Ijmuiden Ver Gamma-A en Gamma-B, en Nederwiek I-A*. Retrieved from <https://www.rvo.nl/onderwerpen/windenergie-op-zee/ijmuiden-ver-gamma-nederwiek-i>
- Scheepers, M., Taminiau, F., Smekens, K., & Giraldo, J. (2025). Koolstofverwijdering in een duurzaam Nederlands energiesysteem - Nadere analyse van ADAPT en TRANSFORM scenario's . TNO.
- Taminiau, F., & van der Zwaan, B. (2022). The physical potential for dutch offshore wind energy. *Journal of Energy and Power Technology*.
- TenneT. (2022). *Offshore TSO Collaboration*. Retrieved from <https://www.tennet.eu/offshore-tso-collaboration>
- TenneT. (2025). *Grid maps*. Retrieved from <https://www.tennet.eu/grids-and-markets/grid-maps>
- Uritsky, V., & Mohanan Nair, J. (2025). *D6.3: Logistics*. North Sea Energy.
- van der Heijden, L., Emmanouil, A., Gerritsma, I., Rienstra, J., Versteeg, s., Schoon, B., . . . de Klerk, I. (2025). *North Sea Energy 5 D4.1: Nature-inclusive energy hubs: Methodology, design and comparative impact assessment for Hub North*. North Sea Energy.
- van der Linden, R., Octaviano, R., Bokland, H., & Busking, T. (2021). Security of Supply in Gas and Hybrid Energy Networks. *Energies*, 14(4), 792.
- van Gessel, S., Jaarsma, B., Groenenberg, R., Kleijweg, D., Juez-Larré, J., & van Klaveren, S. (2022). *Haalbaarheidsstudie offshore ondergrondse waterstofopslag*. TNO & EBN Rapport. Retrieved from <https://www.rijksoverheid.nl/documenten/rapporten/2022/07/01/22286281bijlage-1-haalbaarheidsstudie-offshore-ondergrondse-waterstofopslag>
- van Zoelen, R., Mahfoozi, S., Blom, S., & González-Aparicio, I. (2025). North Sea Energy 5 D3.4: White paper - Offshore Energy System Value and Business Cases: Aligning Project Decisions with Societal Objectives. North Sea Energy.
- van Zoelen, Rob; Boer, Dina; Mahfoozi, Salar. (2025). *D3.3: Business case assessment for the offshore value chain*. North Sea Energy.

- Westerhout, J. (2024). *Offshore Hydrogen Storage in a Depleted Gas Reservoir in the Dutch North Sea in Support of Offshore Green Hydrogen Production*. Delft University of Technology. Retrieved from <https://repository.tudelft.nl/record/uuid:11b770ac-fad8-4705-af39-c848ab66ee6a>
- Wijnant, I., van Uft, B., van Stratum, B., Barkmeijer, J., Onvlee, J., de Valk, C., . . . Stepek, A. (2019). *The Dutch Offshore Wind Atlas (DOWA): Description of the dataset*. Royal Netherlands Meteorological Institute, Ministry of Infrastructure and Water Management, De Bilt.
- Yousefi, S. H.-L. (2023). *A Comparative Study of Hydrogen/Natural Gas Storage in a Depleted Gas Field in the Netherlands Using Analytical and Numerical Modelling. SPE Europec featured at EAGE Conference and Exhibition* (p. D021S001R006). SPE.

Appendix A: Configuration of the MESIDO framework for the simulations

This appendix contains a detailed overview of the different assumptions taken to configure the MESIDO framework for the simulations. This includes the linearization of the models, using the electrolyzer as a specific example and the solver configuration.

A.1 MESIDO model linearization

The electrolyser linearization is based on the information regarding the factsheets from WP1 Technical Innovations, thus establishing a dynamic model in PyDOLPHYN with an approximate power consumption of 55 kWh/kg of hydrogen at nominal load, and a 10% minimum load factor. The efficiency curve of the PyDOLPHYN dynamic model has a parabolic shape, which is fitted in MESIDO with three points: power at the maximum efficiency, efficiency at the minimum load and the efficiency at the maximum load. From this fitted efficiency curve, we can obtain the hydrogen mass flowrate as a function of the input power, which corresponds to the blue curve in the left panel of Figure A.1. Since this curve is non-linear and MESIDO has an MILP problem formulation, we need to linearize this curve with a set of lines. For the current problem we chose a total of three lines to linearize the curve. With a set of binary constraints we force the output mass flowrate to be in the line closest to the non-linear curve. The right panel of A.1 shows that the NMAE between the PyDOLPHYN non-linear model and the linearized model is kept within 1.5%, where NMAE is defined as:

$$\text{NMAE} [\%] = \frac{\dot{m}_{\text{PyDOLPHYN}} - \dot{m}_{\text{MESIDO,LINEAR}}}{\dot{m}_{\text{PyDOLPHYN}}} \cdot 100$$

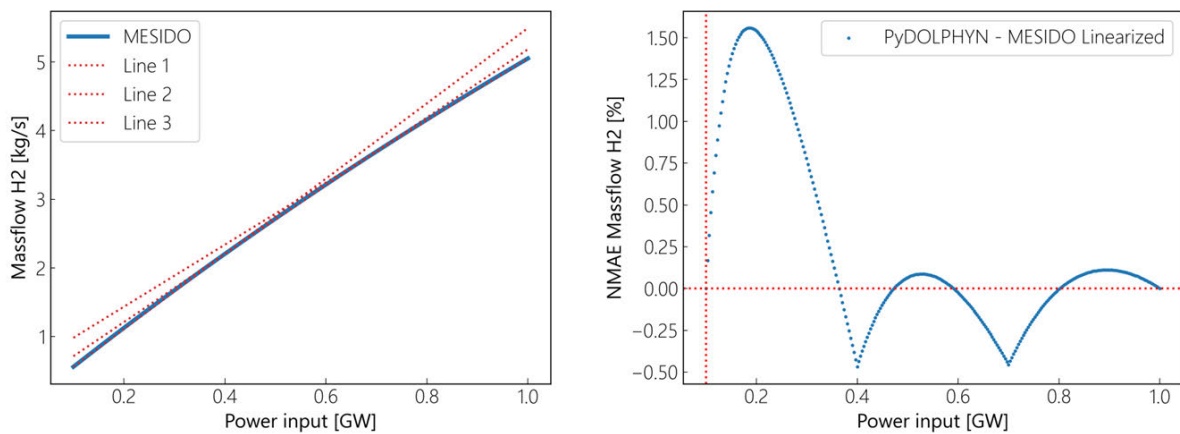


Figure A.1. Linearization of the MESIDO electrolyzer efficiency fitted curve (left) and Normalized Mean Absolute Error between the MESIDO linearized version and PyDOLPHYN (right), for a 1GW electrolyzer.

The pressure drop calculations performed on the pipelines are a linearization of the Darcy-Weisbach analytical equation. The pressure drop is a function the velocity, the pipe diameter and length, fluid density and the friction factor, which is in turn dependent on fluid and pipe properties as shown below:

$$\Delta p = \frac{f_D \cdot \rho \cdot L \cdot v^2}{2 \cdot D}$$

As fluid properties are dependent on the pressure, a reference pressure is selected at which the pressure drop equations are linearized. The provided fluid properties and pipe parameters result in a quadratic relation between the velocity and the pressure drop, which is made piecewise linear with the number of linear lines that can be selected (Figure A.2). This results in an error that ensures an overestimation of the pressure drop for pressures close to the reference pressure. The larger the number of linear lines that are selected, the smaller the absolute error becomes and particularly for small flowrates compared to their maximum flow rate, this can result in smaller relative errors.

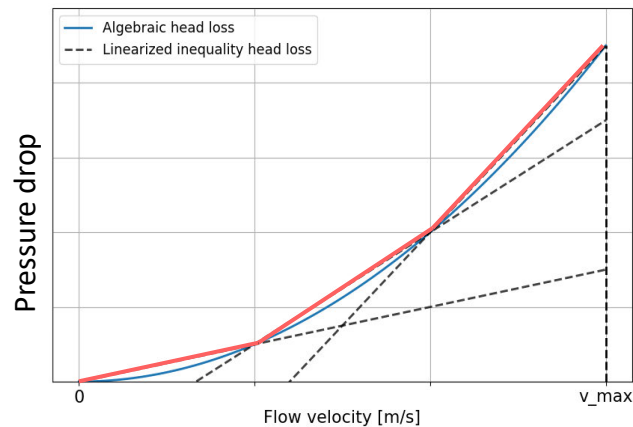


Figure A. 2. Linearization procedure of pressure drop in MESIDO (red linear lines) compared to the analytical solution (curved blue line), when the number of linearization lines is set to three.

A.2 MESIDO solver configuration

Objective function

MESIDO optimizations can be performed using goal programming and therefore, several goals can be prioritized consecutively. The first goal is defined as demand matching, where it ensures that for every demand asset the achieved demand fulfils/meets the required specific demand, irrespective of commodity, for demands that have a specified profile. MESIDO provides several options for the subsequent goals that can be used. Available options are for example, but not limited to, the maximization or minimization of specific assets' production capacity, or profile, or a minimization of costs are available. For the simulations in this project a cost related minimization goal is used. It consists out of an expense and revenue component which catered for via a 'marginal cost' attribute at the producer, consumer and conversion assets. At the producer assets these values are considered costs and for consumer and conversion assets it is considered as a revenue component. The cost, expense minus the revenue, is then minimized in the optimization. The marginal costs allows for prioritizing of how assets should be used, when no cost profiles are included.

The majority of the constraints in MESIDO are physics based. First of all, the equations for conservation of mass and energy are applied. These constraints ensure that the mass flow in and out of a pipe is the same and that the sum of the mass flow is zero at connection points, when also considering their direction. The conservation of energy can be described for instance for an electricity cable, power in should be equal to the sum of power out and the power losses (via voltage drops/losses). In addition to conservation of power at connections, it is also required that the voltage of all parts are the same and the current is summed to

zero, considering their direction, at the connections. Furthermore, the pressure equations are accounted for, by approximating the pressure drop relation by a piecewise linearized approach as explained in Section A.1. It also ensures that the pressure at the connections of all pipes and assets are equal.

Settings that are required for every simulation are dependent on the detail level of which assets and the system need to be modelled. Several settings are related to the pressure drop linearisations of the pipes; the reference pressure, to determine the fluid properties, the number of linearization lines and the maximum velocity for the pressure drop linearization. Furthermore the linearization strategy of electrolyzer needs to be selected, which in this project has been set to the described linearization strategy of Section A.1. Finally some more model or scenario specific settings need to be included, being the location where the pressure is fixed and in this case the ratio of flow between the two landing points. The latter one is prescribed by the demand profiles of the landing points. Typically assets have capacity and/or flow limitations, e.g. an electricity producer can produce up to an x amount of electrical power, or a hydrogen subsurface storage has maximum charging and/or discharging rate. Some assets can also have time dependent capacity related profiles, that are based on the maximum power that can be generated at a moment in time for example as a result of the windspeed. These profiles are incorporated as a time dependent upper limit for the power production of that asset, but they are not fixed to these exact values as there might also be occasions where curtailment is preferred or needed.

Table A.1: List of variables defined in MESIDO and their sources for the different assets.

Asset	Variable	Information source
Cable	Capacity (maximum power)	ESDL
Pipe	Diameter	ESDL
	Maximum velocity	Setting
	Maximum pressure drop	Maximum velocity, reference pressure, diameter
Windfarm	Capacity (maximum power)	ESDL
	Power profile (maximum power production for every timestep)	ESDL link to database
Electrolyzer	Capacity (maximum power)	ESDL
	Maximum Hydrogen outflow	Capacity multiplied with efficiency at max load
GasDemand	Demand capacity	ESDL
	Demand profile	ESDL link to database
GasImport	Import capacity	ESDL
GasStorage	Capacity	ESDL
	Maximum charge rate	ESDL
	Maximum discharge rate	ESDL



Figure B.1 shows an overview of the two scenarios tested in the validation activity. This validation was performed in an earlier stage of the project with transport scenarios relevant at that moment in time. Due to the timeline of this work and the further refining process of the transport scenarios in feedback with stakeholders, it was not possible to perform validation activities that exactly match the final scenarios.

For this activity, the first scenario (V1) comprises mostly re-use infrastructure, with 24-inch and 36-inch pipelines. This is a similar scenario to the re-use analysed in the Results Chapter (Chapter 4). The second validation case (V2) is a combination of re-use and new infrastructure. In this case, the new infrastructure has similarities with the new build case used as a reference for this report, but contains a higher degree of redundancy. Due to the timeline of this work and the further refining process of the transport scenarios in feedback with stakeholders, it was not possible to perform validation activities that exactly match the final scenarios. These cases were chosen in terms of MESIDO’s adaptability to solve either a network as complex as V2, or a simpler network V1 subjected to high flow parameters (flow rates, velocities, and pressure drops), where both cases were modelled at a pressure of 50 bar.

B.2 Results: Validation case 1 (V1)

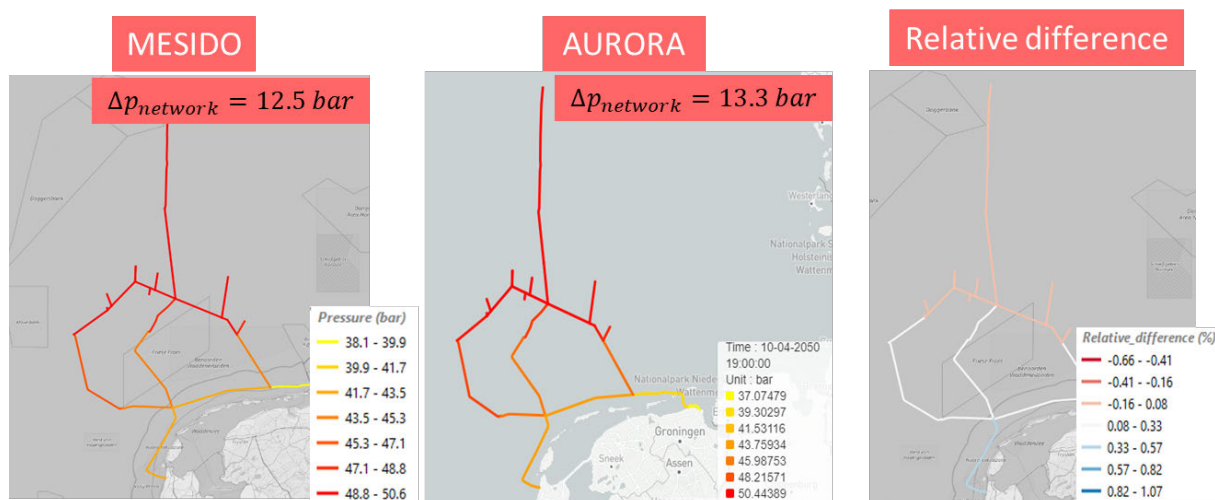


Figure B.2: Comparison of the pressure along the network for AURORA and MESIDO for the first validation case (V1).

The first validation case (V1) comprises mostly re-use infrastructure. Figure B.2Figure shows a comparison of the pressure distribution for both cases at the moment of maximum flow and pressure drop along the network (10-04-2050 19:00:00). It can be observed that the lowest pressures in the networks are experienced at the landing points, as expected, with a total pressure drop across the network of c.a. 13 bar. MESIDO is able to closely approximate the absolute pressure, with errors below 1.5%. With respect to the pressure drops, the relative error is around 6% along the network. Focusing on the landing points, the pressure drop error is around 3%. Due to the uncertainties present in the modelling of the network, such as material characteristics and imperfections, absence of intermediate control systems and idealized injection pressures, this is considered a satisfactory result.

Focusing in individual pipe segments, the linearization process and the errors incurred can be observed in Figure B.3. For the NGT segment, it is observed that the pressure loss for

MESIDO is more conservative (higher pressure loss) compared to AURORA at lower mass flowrates. The largest deviations occur at flowrates between 5 and 15 kg/s, and beyond 25 kg/s. The deviations are always below 0.2 bar for this segment comprising 80 km. For the NOGAT segment, the deviations in pressure losses are smaller on a relative basis, while being similar on an absolute basis to the NGT results.

Figure B.4 shows the flow and velocity for the moment of maximum pressure drop of the year. It can be observed that the results are very similar for both AURORA and MESIDO, with small differences which include the different solving of the physics and the control strategies (as MESIDO solves a supply/demand matching optimization problem, compared to solving the properties for the network of AURORA).

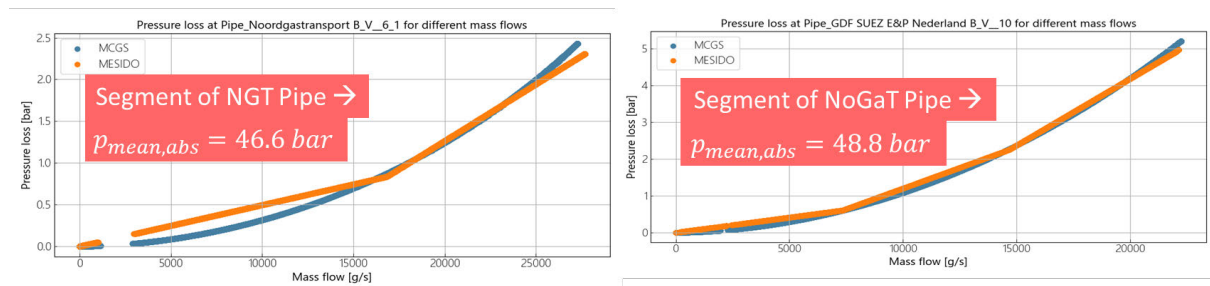


Figure B.3: Comparison of AURORA and MESIDO results for 2 pipe segments, corresponding to NGT (left) and NOGAT (right).

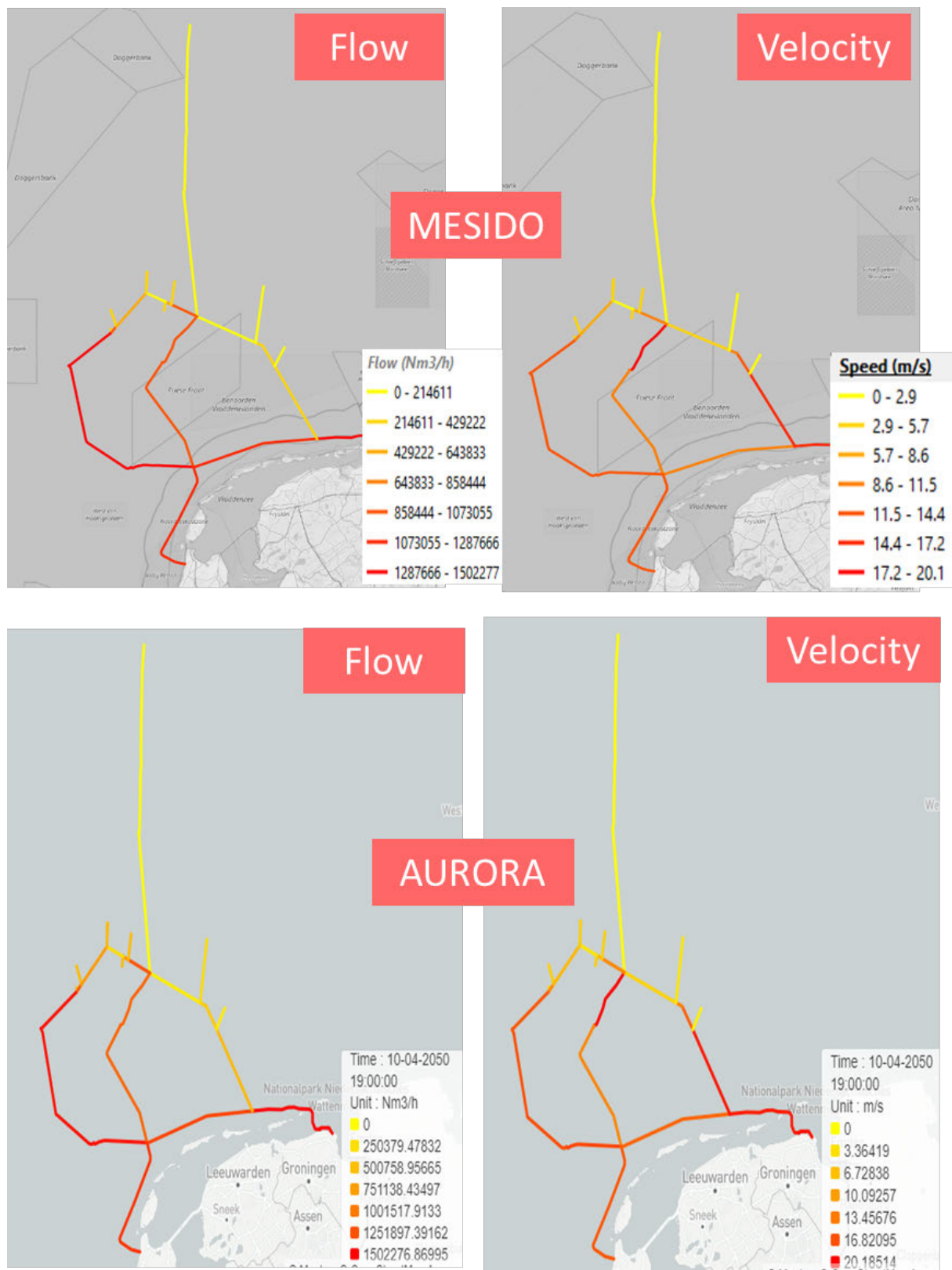


Figure B.4: Flow and velocity for MESIDO and AURORA at the moment of the maximum pressure drop of the year (10-04-2050 19:00:00).

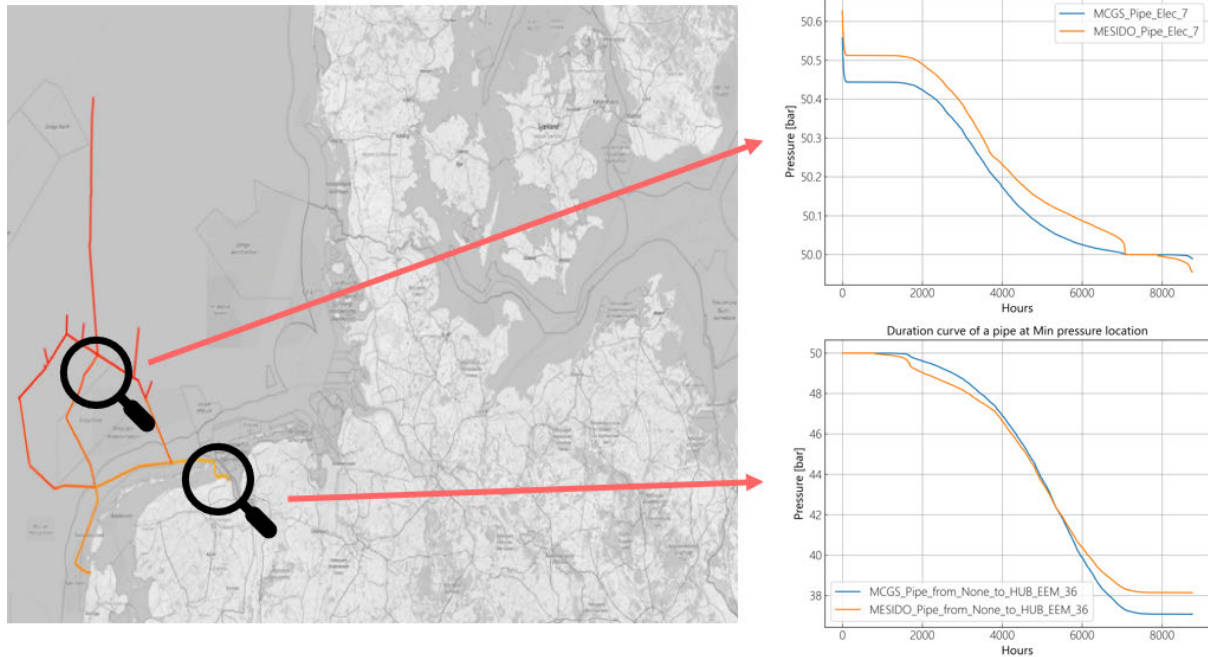


Figure B.5: Duration curves for the locations of maximum and minimum pressure on the network.

When looking at the locations of maximum and minimum pressure on the network, Figure B.5 shows that for the maximum pressure, the differences between both tools are below 0.2 bar across the majority of hours. For the location of the minimum pressure, there is a good match in the intermediate pressures, with larger discrepancies at the lower and upper ranges, as observed in the previous graphs. The load duration curves show a similar profile for MESIDO and Aurora, with a maximum difference of ca. 0.1 bar at the minimum pressure location and 1 bar at the maximum pressure location.

B.3 Results: Validation case 2 (V2)

For the second validation case, which includes a combination of re-used and newly built infrastructure, a similar pattern can be observed. This scenario included a network with larger capacities, resulting in lower flowrates and pressure drops. Figure B.6 shows the differences between both tools. While the relative differences in pressure losses (16% along the network) and landing point pressures (4%) are larger than in the previous cases, the absolute values of the differences are still small. The difference across the network is of around 0.4 bar. As in the previous case, the pipe segments subjected to lower velocities (see the right graph of Figure B.7) are subjected to the largest *relative* errors, with MESIDO overestimating the pressure losses in those occasions. The absolute differences are still lower than 0.2 bar across the different segments considered.

B.4 Conclusions of the validation activity

This validation activity shows that MESIDO, for the conditions considered, can represent the pressure losses with sufficient accuracy for the purposes considered. The absolute differences across the network were below 1 bar for V1, and 0.4 bar for V2. At the lower velocities the relative differences become more significant on a relative basis. However, at lower velocities the pressure drops are also smaller, and the absolute differences become

less relevant. If, for certain applications, a higher fidelity was necessary, increasing the number of segments of the linearization could provide it. That is associated with a higher computational cost, and was not deemed as necessary for this study.

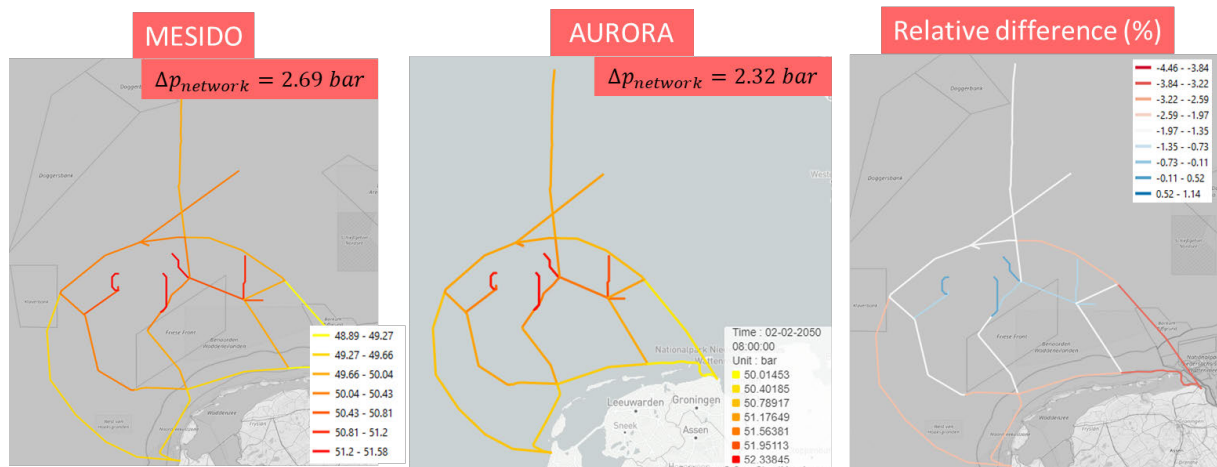


Figure B.6: Comparison of the pressure along the network for AURORA and MESIDO for the second validation case (V3).

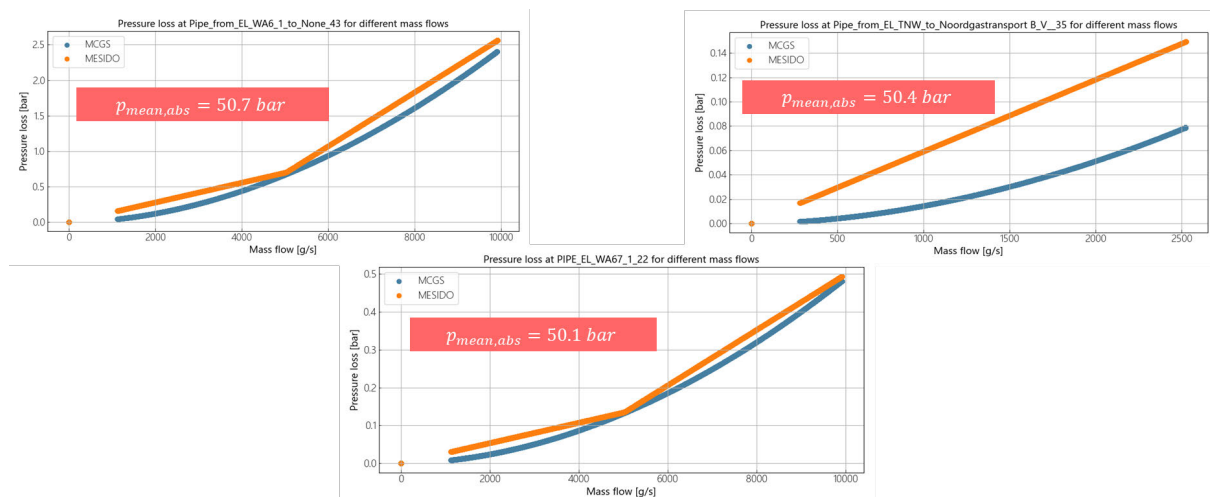


Figure B.7: Comparison between AURORA and MESIDO pressure losses for three different pipe segments.

In collaboration and appreciation to

Consortium members

TNO
Bureau Veritas
Total E&P Nederland
Shell Nederland
NAM
EBN
Nederlandse Gasunie
ONE-Dyas
DEME Dredging
Neptune Energy Netherlands (after ENI)
HINT Global
Noordgastransport
NOGAT
Peterson Offshore Group
Port of Den Helder
Port of Amsterdam
Groningen Seaports
Equinor Energy
ElementNL
Port of Rotterdam
SmartPort
Net Zero Technology Centre
Stichting Dutch Marine Energy Centre
BP Offshore Renewables
RWE Offshore Wind
Wintershall Carbon Management
Solutions (WDCMS)
Arcadis Nederland
Van Oord Offshore

Norce Norwegian Research Center

H2Sea
Aquaventus
MSG Sustainable Strategies
Stichting New Energy Coalition
TU Eindhoven
Deltares
Taqa Energy
Subsea7

Sounding Board members

Bluespring (Dutch Energy from Water
Association)
Energy Innovation NL – Topsector
Energie
Branche Organisatie Zeehavens
ECHT regie in transitie
IRO – The Association of Dutch Suppliers
in the Offshore Energy Industry
Jonge Klimaatbeweging
Ministerie Klimaat Groene Groei (KGG)
Nexstep
NLHydrogen
Noordzeeoverleg
De Nederlandse WindEnergie Associatie
(NWEA)
Stichting Natuur & Milieu
Stichting De Noordzee
Tennet TSO

North Sea Energy

offshore
system
integration